BEILSTEIN JOURNAL OF ORGANIC CHEMISTRY

Integrated multistep flow synthesis

Edited by Volker Hessel

Imprint

Beilstein Journal of Organic Chemistry
www.bjoc.org
ISSN 1860-5397
Email: journals-support@beilstein-institut.de

The *Beilstein Journal of Organic Chemistry* is published by the Beilstein-Institut zur Förderung der Chemischen Wissenschaften.

Beilstein-Institut zur Förderung der Chemischen Wissenschaften
Trakehner Straße 7–9
60487 Frankfurt am Main
Germany
www.beilstein-institut.de

BEILSTEIN JOURNAL OF ORGANIC CHEMISTRY

A concise flow synthesis of indole-3-carboxylic ester and its derivatisation to an auxin mimic

Marcus Baumann, Ian R. Baxendale* and Fabien Deplante

Full Research Paper

Open Access

Address:
Department of Chemistry, University of Durham, South Road, Durham, Durham, DH1 3LE, UK

Email:
Ian R. Baxendale* - i.r.baxendale@durham.ac.uk

* Corresponding author

Keywords:
flow chemistry; heterocycle; hydrogenation; indole; multistep

Beilstein J. Org. Chem. **2017,** *13,* 2549–2560.
doi:10.3762/bjoc.13.251

Received: 05 September 2017
Accepted: 16 November 2017
Published: 29 November 2017

This article is part of the Thematic Series "Integrated multistep flow synthesis".

Guest Editor: V. Hessel

Abstract

An assembled suite of flow-based transformations have been used to rapidly scale-up the production of a novel auxin mimic-based herbicide which was required for preliminary field trials. The overall synthetic approach and optimisation studies are described along with a full description of the final reactor configurations employed for the synthesis as well as the downstream processing of the reaction streams.

Introduction

Indoles are amongst the most important bioactive heterocyclic structures being commonly encountered in the amino acid tryptophan (**1**), the related neurotransmitter serotonin (**2**) as well as numerous complex alkaloid natural products and pharmaceuticals [1-4]. Indoles also play a significant role as phytohormones that promote and regulate the growth and development of plants. Indeed, four of the five endogenously synthesised auxins produced by plants contain the indole motif (Figure 1, structures **3**–**7**). As a consequence of their regulatory activity these structures have become prime targets for investigations into both enhancing plant growth as well as targeted plant growth inhibition generating new agrochemical herbicides [5]. A recent collaboration investigating the uptake and resulting distribution of synthetic indole-3-acetic acid analogues in broad leaf plant species (dicotyledons) required the preparation of structure **8** (Figure 1) at scale for extended field trials. Furthermore as weather patterns and environmental concerns impact significantly on the timing and ultimately the quantities of material required in such studies it was also deemed highly desirable to be able to produce material on demand using a flexible scale flow chemistry approach.

Since the report of the first synthetic access to indoles by Fischer in 1835 more than a dozen further unique indole syntheses have been reported showcasing the importance of developing new entries into these valuable structures [6]. However,

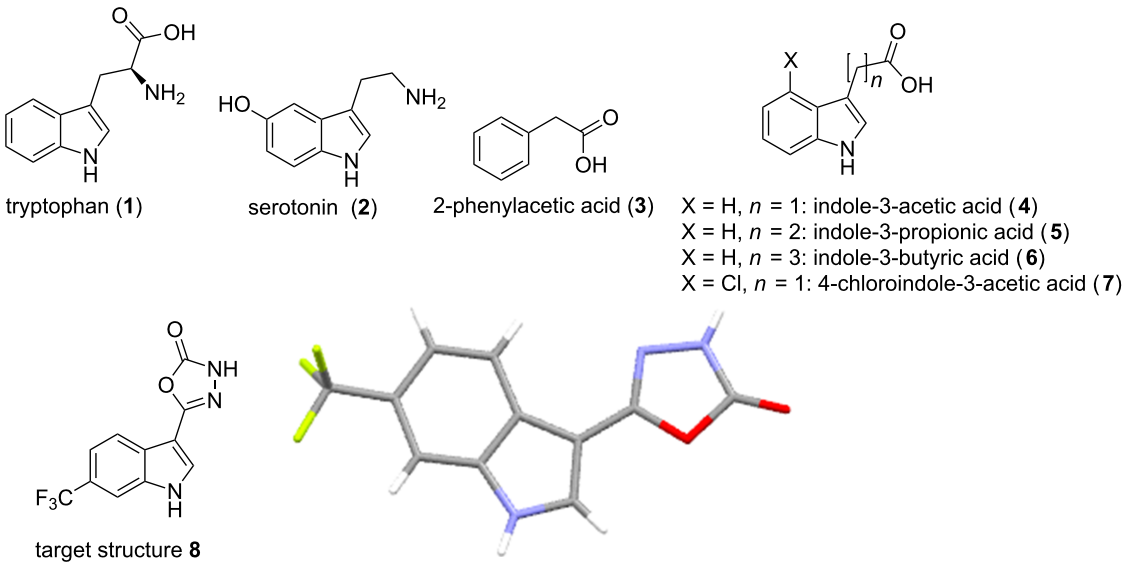

Figure 1: Natural indole containing molecules **1**–**7** of biological importance and synthetic auxin analogue **8** required at scale and X-ray structure.

common to the majority of these indole syntheses is the use of hazardous entities such as hydrazines (Fischer), diazonium species (Japp–Klingemann) or azides (Hemetsberger–Knittel) or the necessity to construct specifically functionalised precursors in a multistep sequence prior to indole ring formation [7]. In order to address these potential shortcomings we set out to develop a benign process relying on inexpensive substrates and non-toxic reagents that would rapidly deliver the desired indole in a readily scalable and continuous fashion.

Results and Discussion

In order to generate the core indole unit through a robust synthetic sequence we decided to investigate the treatment of a 2-chloronitrobenzene **9** with ethyl cyanoacetate (**10**) as the nucleophile in a base-mediated S_NAr reaction (Scheme 1). The resulting adduct **11** would then be subjected to heterogeneous hydrogenation conditions to produce the indole product **12** through a reductive cyclisation sequence. From the corresponding ester functionalised indole **12** we anticipated that condensation with hydrazine would furnish the corresponding acyl hydrazine **13** which could be cyclised to the desired product **8** through the action of a reactive carbonyl donor such as CDI (1,1′-carbonyldiimidazole) or triphosgene (bis(trichloromethyl)carbonate). This synthetic strategy presented various advantages as it relies on readily available substrates and reagents, creates small amounts of non-toxic byproducts

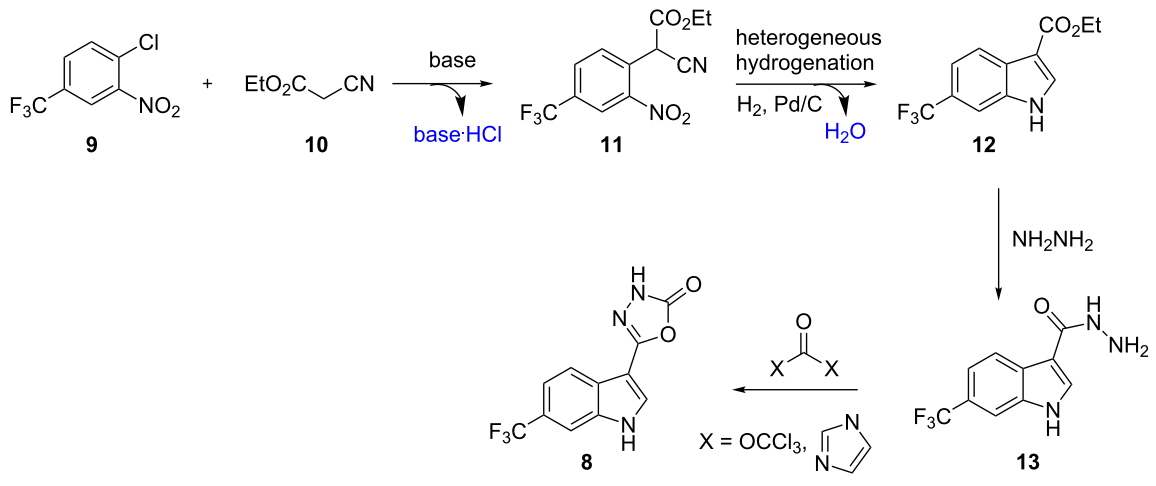

Scheme 1: Synthetic strategy towards desired indole product **8**.

(base·HCl, H_2O) and uses industrially favourable hydrogenation protocols in the key cyclisation step.

To commence the study we first conducted a comprehensive screening program to determine flow compatible conditions for the formation of compound **11** optimising for solvent, base, temperature and reagent stoichiometry – selected results are presented in Table 1.

Although DMF and MeCN were shown to be excellent solvents for the reaction (Table 1, entries 3–6, 10, 15–23, and 26) we encountered difficulties in efficiently extracting the product upon quenching the reactions (1 M HCl). EtOAc was promising and made extraction very easy but during the reactions small quantities of a dark red, sticky, precipitate were observed (Table 1, entry 12). This was considered problematic for processing in a meso flow reactor due to the potential for causing blockages. It was however found that the addition of between 10–20% v/v MeCN ensure a fully homogeneous solution and also allowed for simple aqueous extraction with good recovery (>90%). However, from the provisional results DCM stood out as the most viable solvent (Table 1, entries 7, 24 and 25) and allowed a 0.25 M solution of substrate **9** to be processed with TMG or DBU (2.5 equiv) and ethyl cyanoacetate (**10**, 1.1 equiv) at 50 °C in quantitative conversion.

Based upon these screening results we devised a simple flow set-up where two stock solutions were united at a simple T-mixing piece and subsequently directed into a heated flow coil reactor maintained at 50 °C (Scheme 2). The intensely red coloured solution (anion of the S_NAr adduct) [8] which quickly formed was quenched after the incubation period (35–108 min)

Table 1: Optimisation experiments for S_NAr with ethyl cyanoacetate (**10**).[a]

Entry	**9** [M]	**10** (equiv)	Solvent[b]	Base[c] (equiv)	Temp. (°C)	% Conv.
1	0.25	2	MeCN	Et_3N (5)	50	8
2	0.25	2	DCM	Et_3N (5)	40	3
3	0.25	2	DMF	Et_3N (5)	70	6
4	0.5	2	DMF	TMG (3)	40	98
5	0.75	2	DMF	TMG (3)	40	100[d]
6	0.25	1	DMF	TMG (3)	40	88
7	0.25	2	DCM	TMG (3)	40	100
8	0.25	2	EtOH	NaOEt (3)	40	–[e]
9	0.25	2	*t*-BuOH	KO*t*-Bu	40	44[d]
10	0.25	2	DMF	K_2CO_3 (5)	40	100[d]
11	0.25	2	THF	TMG (3)	50	55[d]
12	0.25	2	EtOAc	TMG (3)	50	90[d]
13	0.25	2	EtOAc/MeCN 5:1	TMG (2.5)	50	>98
14	0.25	2	EtOH	TMG (3)	50	64
15	0.25	2	MeCN	TMG (3)	50	100
16	0.25	1	MeCN	TMG (3)	50	90
17	0.25	1.5	MeCN	TMG (3)	50	100
18	0.25	1.2	MeCN	TMG (3)	50	100
19	0.25	1.1	MeCN	TMG (3)	50	100
20	0.25	1.1	MeCN	TMG (2)	50	87
21	0.25	1.1	MeCN	TMG (2.2)	50	94
22	0.25	1.1	MeCN	TMG (2.5)	50	100
23	0.25	1.1	MeCN	TMG (2.5)	40	96
24	0.25	1.1	DCM	TMG (2.5)	50	100
25	0.25	1.1	DCM	TMG (2.5)	40	89
26	0.5	1.1	DMF	TMG (2.5)	50	100
27	0.25	2	EtOAc/MeCN 5:1	TMG (2.5)	50	100

[a]All reactions were run in Biotage microwave vials being irradiated at the specified temperature for 1 hour. The organic phase was analysed after work-up by quenching with 1 M HCl (and extraction with EtOAc if required), drying over anhydrous Na_2SO_4 and solvent evaporation. Conversion to product was based upon calibrated LC. [b]Solvents were tested for full solubility of reagents and for the deprotonated ethyl cyanoacetate (**10**) prior to full testing. [c]It was determined that DBU (1,8-diazabicyclo[5.4.0]undec-7-ene) and TMG (1,1,3,3-tetramethylguanidine) could be used interchangeably without any effect on the yield or product purity, for clarity only the results with TMG are shown. [d]Solid formation occurred during the reaction. [e]Complex mixture generated including direct addition of the ethoxide anion.

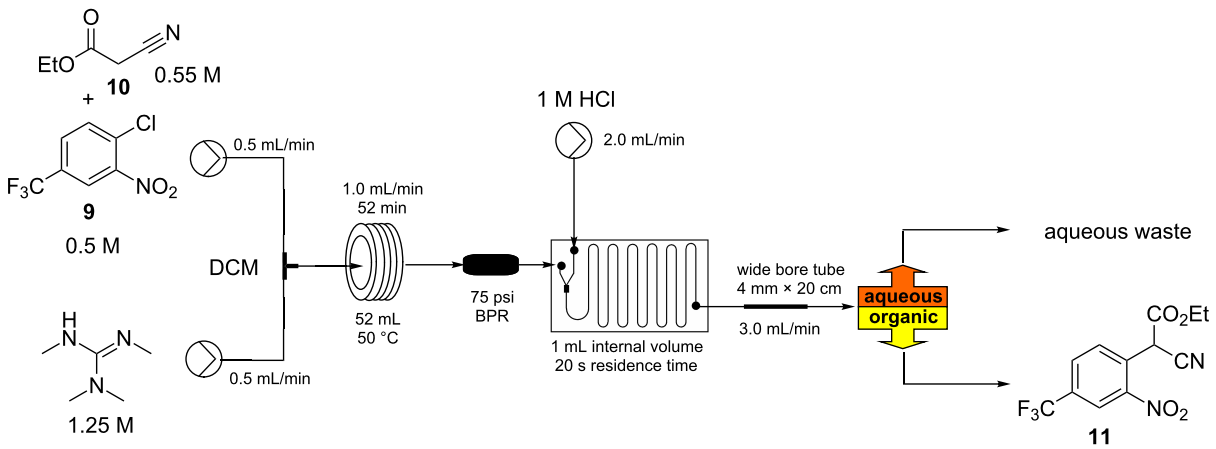

Scheme 2: Initial flow reactor setup for the synthesis of intermediate **11**.

using a third flow stream of hydrochloric acid (1 M) blended via a dedicated mixer chip before the combined mixture was phase separated.

To enable the phase separation we utilised a passive membrane system based upon a modified Biotage universal separator [9]. This enabled the heavier chlorinated phase to be removed from the lower connection and for the lighter aqueous phase to be decanted from an overflow positioned run-off. At flow rates of 0.5–1.2 mL/min emanating from the main reactor this unit performed reliably giving excellent quenching and separation. However, at higher flow rates issues were encountered with incomplete partitioning (some emulsion formation) of the biphasic mixture resulting in the loss of product containing material to the aqueous run off. This was determined to be a result of the high shear generated in the in-line mixing chip at the higher flow rates and the need for longer settling times of the heavily segmented flow. This issue could be overcome by directing the aqueous run off from the first separator into a second equivalent unit or by simply splitting the original quenched flow over two parallel separators. Although functional these approaches were not the optimum in design or utilisation of the separator components. We therefore also investigated the replacement of the problematic mixing chip with various configured T- and Y-connectors but this immediately gave other issues due to incomplete quenching which resulted in poor product recovery and associated contamination. A more straightforward approach proved to be to introduce a flow stratification zone prior to the separator which was achieved through the expedient introduction of a section of wider bore tubing (expanded from the reactor i.d. 1.6 mm → 4.0 mm × 20 cm) [10]. This enabled reactor throughput flow rates of up to 2.0 mL (for flow rates above 1.0 mL a second 52 mL flow coil was added to the system) to be successfully quenched inline and then successively handled by a single Biotage universal separator. In all cases the output from the main reactor showed quantitative conversion with only the product being isolated following solvent evaporation. At a flow rate of 1.8 mL/min from the reactor this gave a maximum throughput of 27 mmol/h operating at steady state.

Despite the versatility of the reactor its productivity was lower than we ideally wanted and unfortunately DCM proved to be an incompatible solvent with the following hydrogenation step. Although solvent swapping would have been possible we determined that when EtOAc was used as the solvent and diluted with EtOH in the presence of acetic acid as an additive this allowed for the successful reductive cyclisation to the indole. As a result we investigated the scaled synthesis of intermediate **11** in EtOAc. Having had previous success with handling slurries in flow using the Coflore, AM technology ACR device [11], we decided to utilise this equipment in the synthesis to overcome the issues encountered with solubility [12-14].

The starting materials were prepared as individual stock solutions in EtOAc and mixed sequentially, first the base and the ethyl cyanoacetate (**10**) being combined (note this was an exothermic process) before meeting a solution of the aryl chloride **9** and entering the ACR which was agitated at 8 Hz (Scheme 3).

In an attempt to intensify the process and with the specific aim of reducing the amount of solvent in order to maintain a viable working concentration in the subsequent reduction step (after dilution with EtOH) we undertook a series of concentration and flow rate optimisations. It was ultimately found that at a combined flow rate of 3 mL which equated to a residence time of approximately 30 min and a reactor temperature of 65 °C we were able to achieve a quantitative conversion of a 1.5 M solu-

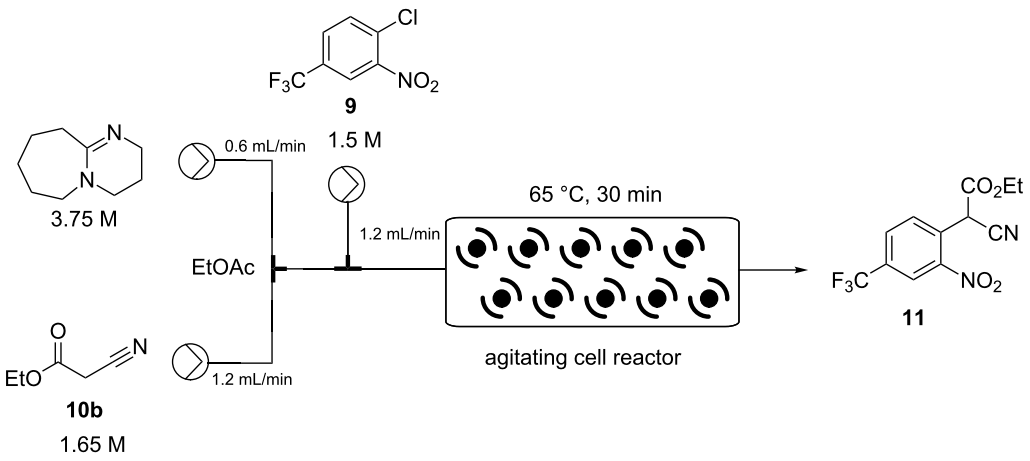

Scheme 3: Coflore ACR setup for the synthesis of intermediate **11**.

tion of substrate **9**. Under continuous operation the reactor output was a dark red suspension comprising approx. 10% solid by volume but was easily processed through the system even over extended periods of time (>14 h). This set-up gave a theoretical working throughput of 0.108 mol/h. Next, to facilitate the integrated quenching and work-up we added a static mixing element [15] at the confluence point of an aqueous solution of 2 M HCl delivered at a flow rate of 6 mL/min (Scheme 4). Evidence for effective quenching was immediately observed by the transformation of the dark red reaction mixture to a pale yellow biphasic solution which quickly phase separated upon collection. Confirmation of the successful quenching was obtained by ^{1}H NMR and LC analysis of the organic phase which indicated only the product **11** and trace amounts of ethyl cyanoacetate (**10**). Finally, manual separation followed by drying over Na_2SO_4 and solvent evaporation gave the desired product **11** in 94–96% yield, based upon 6 sampled aliquots of 20 min each processing time.

Several laboratory approaches to the automation of batch separation have been reported using machine vision systems [16,17], and inline detection devices employing optics [18] or inductive conductivity (impedance measurements) [19] to determine phase partitions. However, due to specific project time limitations we were constrained to use a more manual approach but would certainly incorporate such a labour saving device into a future development version. Our basic system used a simple batch collection vessel with two HPLC pumps with appropriately positioned inputs to remove independently the aqueous and organic phases. Occasional manual intervention allowed intermittent recalibration of the pumps to maintain working volumes and create a suitable phase segment for removal. Again, following evaporation of the solvent a high isolated yield of the target molecule **11** was attained in 93–97%.

The collected solution generated following aqueous quenching and separation contained 0.4 M product **11** which was further

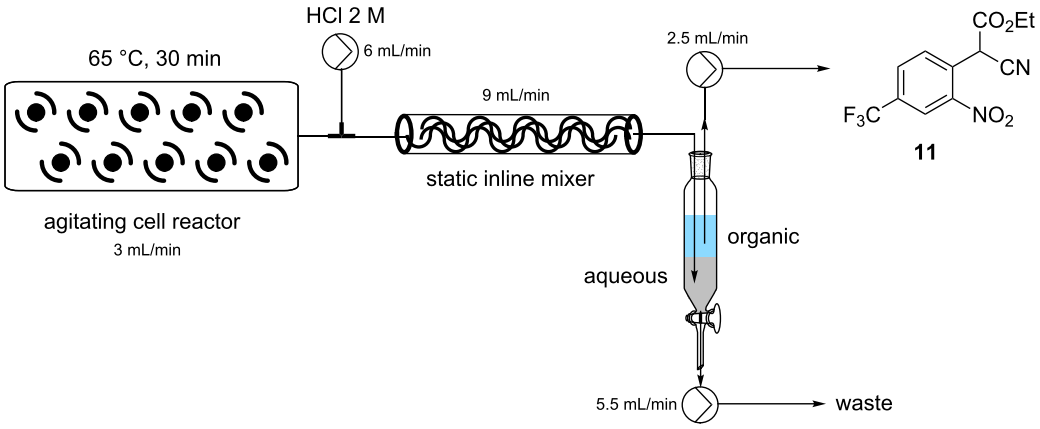

Scheme 4: Quenching and work-up of the reaction stream from the Coflore ACR for the synthesis intermediate **11**.

diluted with EtOH to furnish a 0.2 M stock solution for use in the next reductive cyclisation step. The reduction was performed using a ThalesNano H-cube system [20,21] operating in full hydrogen mode with a 10 mol % Pd/C catalyst cartridge. At a flow rate of 0.4 mL/min and a temperature of 50 °C full conversion to the indole product **12** was achieved (Table 2, entry 1). When the flow rate was raised to 0.8–1 mL/min complete consumption of the starting material was observed but a mixture of products was isolated (Table 2, entries 2 and 3). Careful analysis of the composition indicated the presence of the desired product (**12**, 62%) along with two other compounds (Figure 2), which following chromatographic isolation, were assigned as the amino indole (**14**, 29%) and the *N*-hydroxyamino indole (**15**, 9%). As expected these latter two products resulting from incomplete reduction were obtained in greater amounts as the flow rate was further increased along with an increasing proportion of the hydroxyaminoindole **15**. This correlates with previous literature findings employing catalysed hydrogenation [22-26] or stoichiometric metal (zinc or indium) mediated reduction and is consistent with a stepwise reduction mechanism (Scheme 5) [27-29]. It is evident from the sequence that several equivalents of hydrogen are necessary for full reduction and as a result a higher concentration (pressure) of hydrogen would be beneficial (Table 2, entries 4–10). We also noted that according to the mechanism protonation of the anilino nitrogen could be beneficial in promoting the reduction steps as well as aiding in the loss of water (**16** and **18**) and ammonia (**20**). We therefore screened a series of acid catalysts which highlighted acetic acid (10–30 mol %) as the optimum additive (Table 2, entries 11–14). Stronger acids or higher loading of acid often resulted in the generation of high internal pressures and in certain cases the formation of precipitates was noted requiring premature termination of the run and a safe shutdown. Using acetic acid and limiting the acid concentration (10 mol %) whilst working at a higher internal pressure (15 bar) enabled stable and continuous operation permitting the flow rate to be raised to 1.3 mL/min whilst ensuring a >98% conversion to the desired indole **12** (Table 2, entries 15–18) [30,31]. This translated into a throughput of 15.6 mmol/h (3.7 g/h product). The final product could be easily isolated in 93% yield as an off white solid by solvent evaporation and trituration with 9:1 hexane/Et_2O. This purification removed both residual acetic acid and, if present, small traces of byproducts.

In the next sequence we looked at telescoping the final two steps of the process; substitution of the ethoxy group by hydrazine and then ring formation to the 3*H*-[1,3,4]oxadiazol-2-one unit [32,33].

In this procedure a 0.95 M THF solution of compound **12** was united with a solution of hydrazine (1.0 M in THF) and directed into a heated flow coil to be superheated at 100 °C (Scheme 6).

Table 2: Selected optimisation experiments for reductive cyclisation to compound **12**.[a]

Entry	AcOH (mol %)	Temp. (°C)	Pressure (bar)	Flow rate (mL/min)	Product composition ratio **11**:**12**:**14**:**15**
1	0	50	0	0.4	0:100:0:0
2	0	50	0	0.8	0:62:29:9
3	0	50	0	1.0	10:30:40:20
4	0	50	5	0.8	0:86:11:3
5	0	50	10	0.8	0:95:5:0
6	0	50	15	0.8	0:99:1:0
7	0	50	15	1.2	0:77:18:5
8	0	40	5	0.8	4:43:19:34
9	0	60	5	0.8	0:83:12:5
10	0	70	5	0.8	3:46:23:9[b]
11	5	50	0	0.8	0:80:17:3
12	10	50	0	0.8	0:93:6:1
13	20	50	0	0.8	0:95:4:1
14	50	50	0	0.8	0:94:5:0
15	10	50	15	1.1	0:99:1:0
16	10	50	15	1.2	0:100:0:0
17	10	50	15	1.3	0:98:2:0
18	10	50	15	1.4	0:89:8:3

[a]Reaction concentration of **11** was 0.2 M in EtOH/EtOAc 50:50 v/v. Composition analysis was performed by LC–MS against isolated standards. [b]An additional product of almost double the mass of **12** was observed in the LC–MS but this material could not be isolated. The catalyst cartridge rapidly lost activity and could not be regenerated through washing.

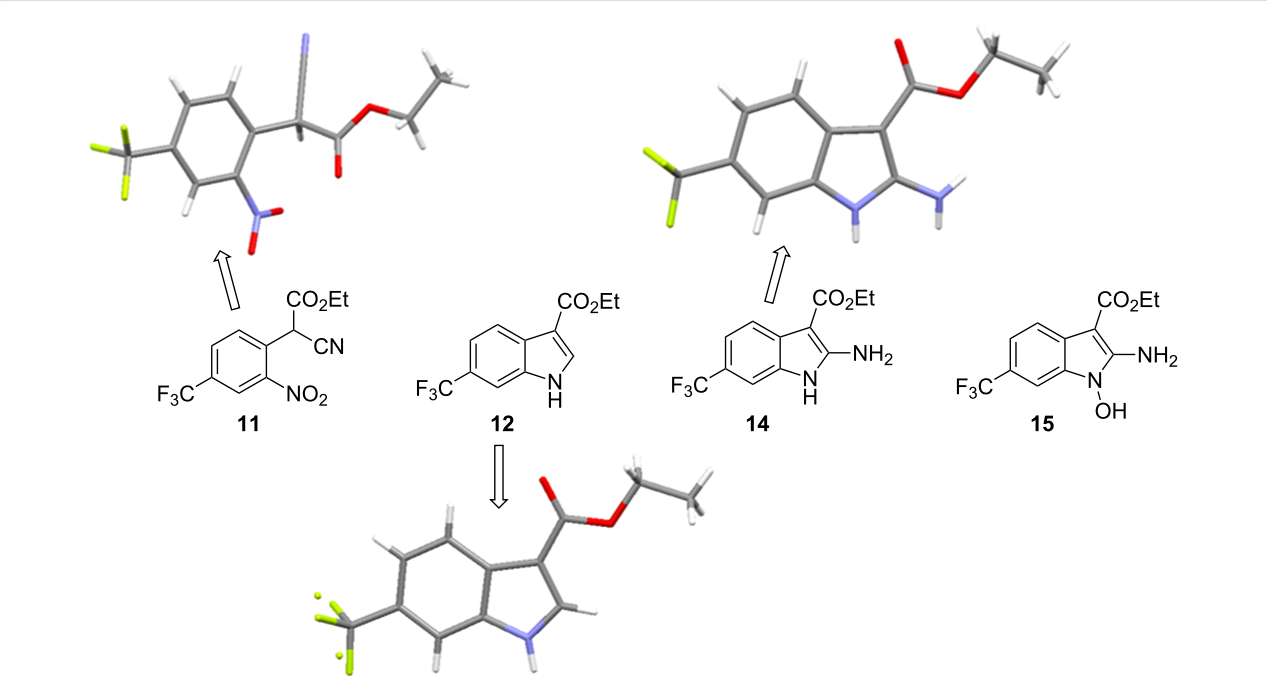

Figure 2: X-ray structure of intermediate **11**, and reductive cyclisation products **12** and **14**, assigned structure of byproduct **15**.

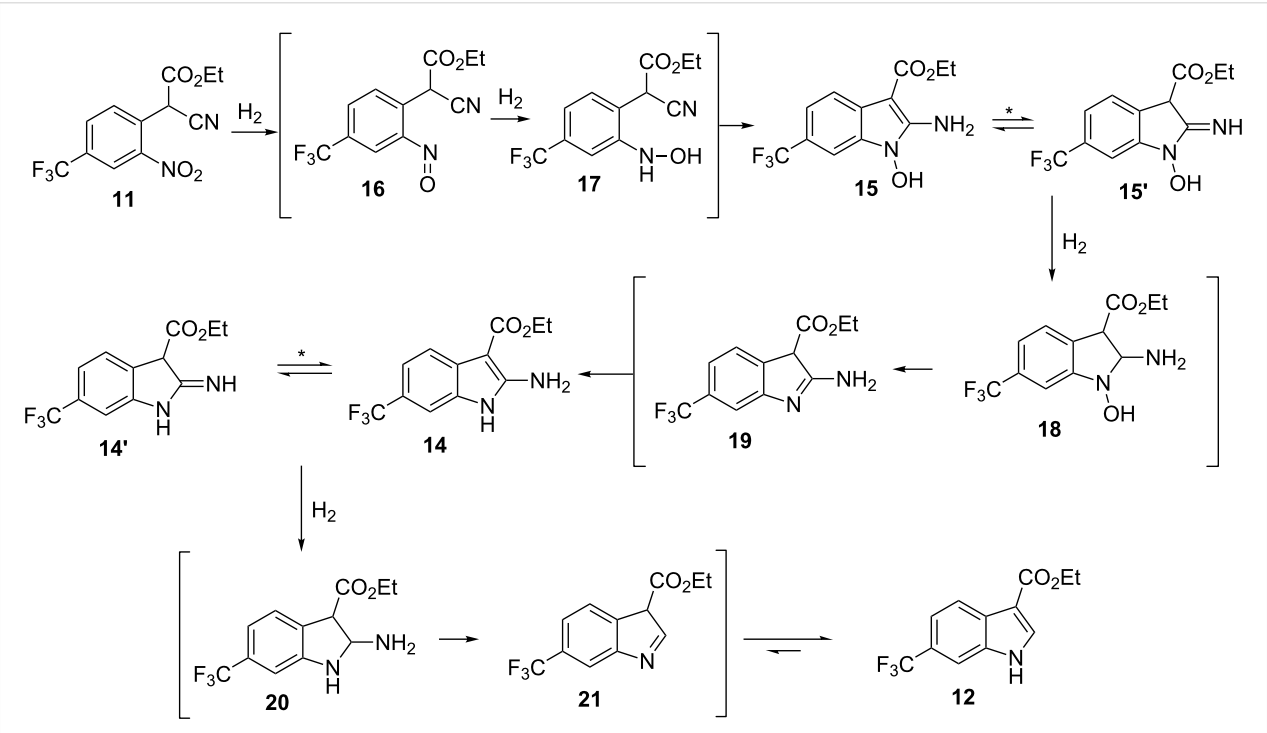

Scheme 5: Stepwise reduction of intermediate **11** under hydrogenation conditions. * Indicates potential tautomeric structure. Species in parentheses are proposed transient intermediates.

A residence time of 40 min allowed full conversion to the corresponding acyl hydrazine **13** which was directly intercepted with a further input stream containing CDI (1.1 M in THF) and heated at 75 °C for an additional 26 min in a second flow coil. This furnished the final product **8** in quantitative conversion with the product stream being readily purified by passage

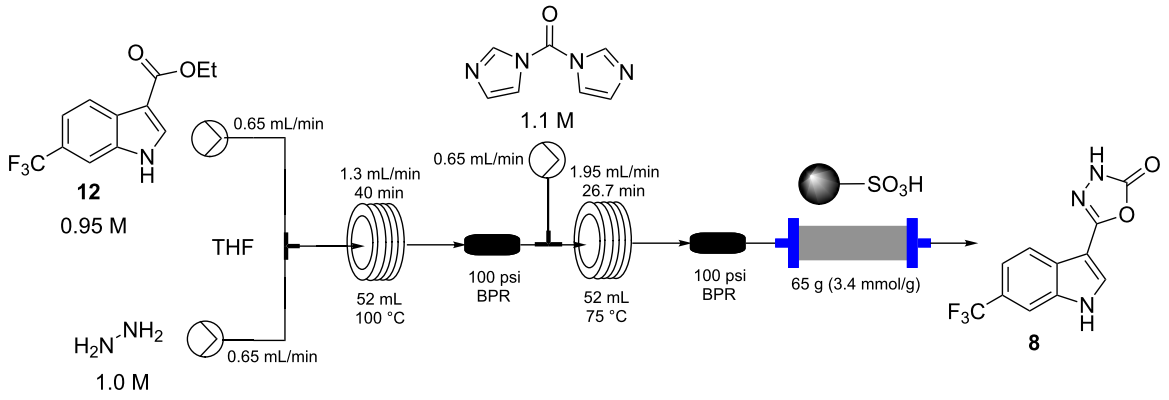

Scheme 6: Flow sequence for the construction of product **8**.

through a scavenging cartridge of QP-SA (a sulfonic acid functionalised polymer). The product **8** was obtained after solvent evaporation as a yellow solid (94%) but required recrystallization from DCM to give a white amorphous powder of high purity in 82% yield.

A series of attempts to employ dimethyl carbonate as a replacement reagent for CDI in the final step failed under a range of conditions as did trials to directly utilise (methoxycarbonyl)hydrazide (CAS 6294-89-9) in the previous acyl hydrazine forming step. However, we found that triphosgene (0.4 equiv) could be successfully used in the latter cyclisation process [34-37]. Using a similar reactor assembly as per Scheme 6 the triphosgene (0.8 M in $CHCl_3$) was combined with the solution of intermediate **13** and passed through a heated (55 °C) flow coil and then through a packed bed scavenging cartridge containing QP-DMA (*N*,*N*-dimethylbenzylamine polystyrene). Following solvent evaporation this gave the product as an off white solid in 91% isolated yield. In practice this approach proved far superior to the previously employed CDI cyclisation providing higher overall yields and improved quality product direct from the reactor. Indeed, the final product **8** was of sufficient purity for direct application allowing on demand and scalable production from a stable intermediate **12** in less than 2 h from reactor start-up.

Conclusion

Using the procedures outlined we have been able to rapidly assembly the desired target molecule **8** through a flexible workflow generating sufficient material for on-going field trials. Obviously in the context of our currently assembled route the reductive cyclisation to the indole unit **12** is the process limiting step (Scheme 7). However, several options including commercially available larger scale flow apparatus for performing such flow hydrogenations are available (i.e., H-Cube Mid [38], FlowCAT [39]) [40,41]. However, as intermediate **12** was shown to be a highly stable structure, in practice, this created a convenient staging point to generate intermediate holding

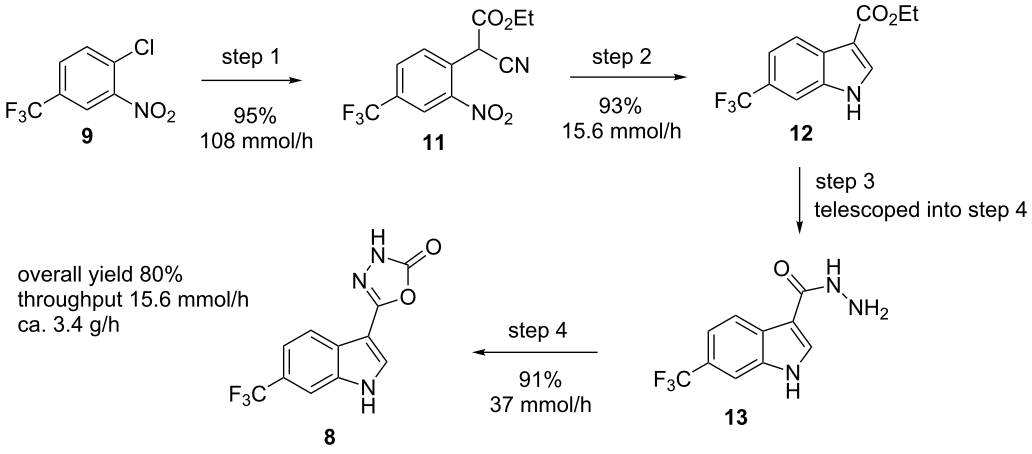

Scheme 7: Assembled process for flow synthesis of product **8** with yields and throughputs.

batches of material for subsequent on demand processing. Overall we envisage this laboratory scale design to offer several opportunities for further development enabling quick up regulation of production in the future.

Experimental

Material and methods

Unless otherwise stated, all solvents, substrates and reagents were used as purchased without further purification.

^{1}H NMR spectra were recorded on Bruker Avance-400 instruments and are reported relative to residual solvent: $CHCl_3$ (δ 7.26 ppm), DMSO (δ 2.50 ppm). ^{13}C NMR spectra were recorded on the same instruments and are reported relative to $CHCl_3$ (δ 77.16 ppm) or DMSO (δ 39.52 ppm). Data for ^{1}H NMR are reported as follows: chemical shift (δ ppm) (multiplicity, coupling constant (Hz), integration). Multiplicities are reported as follows: s = singlet, d = doublet, t = triplet, q = quartet, p = pentet, m = multiplet, br. s = broad singlet, app = apparent. Data for ^{13}C NMR are reported in terms of chemical shift (δ ppm) and multiplicity (C, CH, CH_2 or CH_3). Data for ^{19}F NMR were recorded on the above instruments at a frequency of 376 MHz using $CFCl_3$ as external standard. For all compounds DEPT-135, COSY, HSQC, and HMBC were run and used in the structural assignment. IR spectra were recorded neat (ATR sampling) with the intensities of the characteristic signals being reported as weak (w, <20% of tallest signal), medium (m, 20–70% of tallest signal) or strong (s, >70% of tallest signal). Low and high-resolution mass spectrometry was performed using the indicated techniques on instruments equipped with Acquity UPLC and a lock-mass electrospray ion source. For accurate mass measurements the deviation from the calculated formula is reported in ppm. Melting points were recorded on an automated melting point system with a heating rate of 1 °C/min and are uncorrected. Microwave optimisation reactions were performed in a Biotage® Initiator+ microwave system.

Flow reactions were preformed using the pumping system of a Vapourtec R-Series modular flow chemistry system [42]. Heating for the 52 mL flow coils was provided using a Polar Bear Plus unit [43].

Ethyl 2-cyano-2-(2-nitro-4-(trifluoromethyl)phenyl)acetate (11) [44]**:**

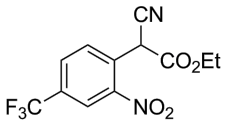

chemical formula: $C_{12}H_9F_3N_2O_4$
exact mass: 302.0514

Process 1 (DCM): Two stock solutions in DCM were prepared. Solution A: TMG (1.25 M, 2.5 equiv) and solution B: a mixture of 4-chloro-3-nitrobenzotrifluoride (0.5 M, 1.0 equiv) and ethyl cyanoacetate (0.55 M, 1.1 equiv). The two stock solutions were pumped (0.65 mL/min each channel) direct from their respective reservoirs to combine at a PEEK T-piece and were then directed through a FEP flow coil (52 mL maintained at 50 °C using a Polar Bear Plus reactor – Cambridge Reactor Design). The system pressure was controlled using a 75 psi inline back pressure regulator. The flow stream was quenched by mixing with a solution of hydrochloric acid (1 M) at a flow rate of 2 mL/min within a glass microreactor (1 mL, Little Things Factory). The biphasic mixture was passed into a section of wide bore FEP tubing (4 mm i.d × 20 cm length) and on into a modified Biotage Universal Separator (Biotage) allowing separation of the organic and aqueous fluidic flows. The organic layer was dried (Na_2SO_4) and the solvent evaporated to yield the title compound in 94–96%.

Process 2 (EtOAc): Three EtOAc stock solutions were prepared. Solution A: DBU (3.75 M, 2.5 equiv), solution B: ethyl cyanoacetate (1.65 M, 1.1 equiv), and solution C: 4-chloro-3-nitrobenzotrifluoride (1.5 M, 1.0 equiv). Stock solutions A (0.6 mL/min) and B (1.2 mL/min) were pumped from their respective reservoirs and combined at a PEEK T-piece. The combined flow was then combined at a second PEEK T-piece with solution C (1.2 mL/min) and the flow directed into the Coflore ACR (spring inserts). The ACR was agitated at 8 Hz and heated at 65 °C. The flow stream was quenched by mixing with a solution of hydrochloric acid (2 M) at a flow rate of 6 mL/min using a inline static mixing element (Esska [15]). The biphasic mixture was passed into a collection vessel. The input lines for two Knauer K120 HPLC pumps were positioned to draw independently the aqueous and organic phases. The organic layer was collected and dried (Na_2SO_4) and the solvent evaporated to yield the title compound. The product was isolated in 93–97% yield.

^{1}H NMR (400 MHz, chloroform-*d*) δ 8.51 (dt, *J* = 2.0, 0.6 Hz, 1H), 8.12–7.86 (m, 2H), 5.79 (s, 1H), 4.35 (q, *J* = 7.2 Hz, 2H), 1.37 (t, *J* = 7.2 Hz, 3H); ^{13}C NMR (101 MHz, $CDCl_3$) δ 162.8 (C), 147.6 (C), 133.3 (q, *J* = 35 Hz, C), 132.4 (CH), 131.0 (q, *J* = 4 Hz, CH), 128.9 (C), 123.7 (q, *J* = 4 Hz, CH), 122.2 (q, *J* = 273 Hz, C), 113.8 (C), 64.4 (CH_2), 41.2 (CH), 13.9 (CH_3); ^{19}F NMR (376 MHz, $CDCl_3$) δ −63.2; IR (neat) ν/cm^{-1}: 3092 (w), 2925 (w), 1732 (m), 1537 (m), 1502 (m), 1357 (m), 1324 (s), 1257 (s), 1182 (s), 1138 (s), 1090 (s), 1012 (m), 866 (m), 825 (m), 698 (m); LC–MS (TOF$^+$) 302.1 (M + H); HRMS (ESI) *m*/*z*: calcd for $C_{12}H_8N_2O_4F_3$, 301.0436; found, 301.0452 (Δ = 5.3 ppm); melting range: 60.5–61.6 °C; X-ray crystal data: CCDC 1572810.

Ethyl 6-(trifluoromethyl)-1*H*-indole-3-carboxylate (12) [23]**:**

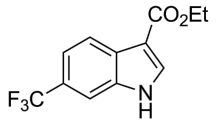

chemical formula: $C_{12}H_{10}F_3NO_2$
exact mass: 257.0664

A 0.2 M solution of compound **11** in a 1:1 mixture of EtOAc/EtOH with 10 mol % AcOH was passed through a ThalesNano H-cube at 1.3 mL/min containing a 10 mol % Pd/C heated at 50 °C and pressurised at 15 bar. The solvent was removed under reduced pressure and the residue triturated with 9:1 hexane/Et_2O. The product was isolated in 93% yield. ^{1}H NMR (400 MHz, DMSO-d_6) δ 12.33 (s, 1H), 8.31 (d, J = 3.0 Hz, 1H), 8.18 (dd, J = 8.5, 0.9 Hz, 1H), 7.83 (dt, J = 1.7, 0.9 Hz, 1H), 7.49 (dd, J = 8.5, 1.7 Hz, 1H), 4.31 (q, J = 7.1 Hz, 2H), 1.34 (t, J = 7.1 Hz, 3H); ^{13}C NMR (101 MHz, DMSO-d_6) δ 164.4 (C), 135.8 (d, J = 3 Hz, CH), 128.7 (C), 125.4 (q, J = 273 Hz, C), 123.3 (q, J = 34 Hz, C), 121.75 (CH), 118.0 (q, J = 4 Hz, CH), 117.6 (C), 110.3 (q, J = 4 Hz, CH), 107.5 (C), 59.8 (CH_2), 14.9 (CH_3); ^{19}F NMR (376 MHz, DMSO-d_6) δ −59.3; IR (neat) ν/cm^{-1}: 3196 (m), 1667 (s), 1514 (m), 1440 (m), 1328 (s), 1228 (s), 1191 (m), 1160 (s), 1117 (s), 1055 (s), 826 (m), 745 (m), 674 (m), 615 (m), 524 (m); LC–MS (TOF$^+$) 258.1 (M + H); HRMS (ESI) *m*/*z*: calcd for $C_{12}H_{11}NO_2F_3$, 258.0742; found, 258.0753 (Δ = 4.3 ppm); melting range: 197.3–200.0 °C; X-ray crystal data: CCDC 1572811.

Ethyl 2-amino-6-(trifluoromethyl)-1*H*-indole-3-carboxylate (14) [45]**:**

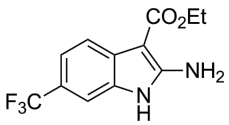

chemical formula: $C_{12}H_{11}F_3N_2O_2$
exact mass: 272.0773

^{1}H NMR (400 MHz, DMSO-d_6) δ 10.90 (br s, 1H), 7.68 (d, J = 8.0 Hz, 1H), 7.44 (s, 1H), 7.27 (d, J = 8.0 Hz, 1H), 7.00 (s, 2H), 4.26 (q, J = 7.2 Hz, 2H), 1.33 (t, J = 7.2 Hz, 3H); ^{13}C NMR (101 MHz, DMSO-d_6) δ 165.9 (C), 155.3 (C), 132.5 (C), 130.5 (C), 126.0 (CF_3, q, J = 271 Hz), 119.8 (C), 118.1 (CH, q, J = 31 Hz), 117.6 (CH, q, J = 4 Hz), 106.9 (CH, q, J = 4 Hz), 84.5 (C), 58.8 (CH_2), 15.1 (CH_3); ^{19}F NMR (376 MHz, DMSO-d_6) δ −58.6; IR (neat) ν/cm^{-1}: 3496 (m), 3344 (m), 1645 (m), 1619 (s), 1555 (m), 1506 (s), 1379 (m), 1325 (s), 1230 (m), 1152 (s), 1099 (s), 1070 (s), 1052 (s), 856 (m), 812 (s), 671 (m), 530 (m); LC–MS (TOF$^+$) 273.1 (M + H); HRMS (ESI) *m*/*z*: calcd for $C_{12}H_{12}N_2O_2F_3$, 273.0851; found, 273.0860 (Δ = 3.3 ppm); melting range: >140 °C (decomposition); X-ray crystal data: CCDC 1572812.

Ethyl 2-amino-1-hydroxy-6-(trifluoromethyl)-1*H*-indole-3-carboxylate (15) [25]**:**

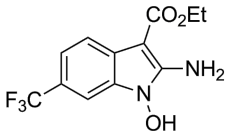

chemical formula: $C_{12}H_{11}F_3N_2O_3$
exact mass: 288.0722

^{1}H NMR (400 MHz, DMSO-d_6) δ 11.55 (br s, 1H), 7.75 (d, J = 8.2 Hz, 1H), 7.36 (s, 1H), 7.33 (d, J = 8.2 Hz, 1H), 4.26 (q, J = 7.2 Hz, 2H), 1.33 (t, J = 7.2 Hz, 3H); ^{13}C NMR (101 MHz, DMSO-d_6) δ 165.3 (C), 151.9 (C), 131.5 (C), 125.8 (CF_3, q, J = 272 Hz), 125.7 (C), 120.0 (C, q, J = 32 Hz), 118.4 (CH), 118.1 (CH, q, J = 2 Hz), 103.7 (CH, q, J = 4 Hz), 80.4 (C), 58.9 (CH_2), 15.2 (CH_3); ^{19}F NMR (376 MHz, DMSO-d_6) δ −58.7; IR (neat) ν/cm^{-1}: 3266 (br), 3113 (br), 2981 (m), 1748 (s), 1696 (s), 1632 (m), 1441 (s), 1323 (s), 1254 (m), 1223 (m), 1172 (s), 1120 (s), 1060 (s), 879 (m), 824 (m), 668 (m); LC–MS (TOF$^+$) 289.1 (M + H); HRMS (ESI) *m*/*z*: calcd for $C_{12}H_{12}N_2O_3F_3$, 289.0800; found, 289.0805 (Δ = 1.7 ppm); melting range: decomposition >145 °C.

6-(Trifluoromethyl)-1*H*-indole-3-carbohydrazide (13):

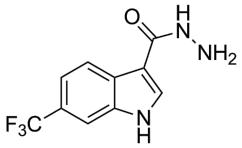

chemical formula: $C_{10}H_8F_3N_3O$
exact mass: 243.0619

Two stock solutions in THF were prepared. Solution A: hydrazine (1.00 M, 1.05 equiv) and solution B containing compound **11** (0.95 M, 1.0 equiv). The two stock solutions were pumped (0.65 mL/min each channel) from their respective reservoirs to combine at a PEEK T-piece and were then directed through a FEP flow coil (52 mL maintained at 100 °C using a Polar Bear Plus reactor – Cambridge Reactor Design, residence time 40 min). A 100 psi inline back pressure regulator was positioned prior to the exit. Collection of the reactor output allowed isolation of the title compound in 81% isolated yield following column silica chromatography (DCM/MeOH 9:1). ^{1}H NMR (400 MHz, DMSO-d_6) δ 11.42 (br. s, 1H), 9.33 (s, 1H), 8.33 (d, J = 8.4 Hz, 1H), 8.19 (s, 1H), 7.89–7.70 (m, 1H), 7.41 (dd, J =

8.4, 1.7 Hz, 1H), 2.95 (br. s, 2 H); ^{13}C NMR (101 MHz, DMSO-d_6) δ 164.9 (C), 135.3 (C), 130.5 (CH), 129.2 (C), 125.6 (q, J = 272 Hz, C), 122.8 (q, J = 31 Hz, C), 122.2 (CH), 117.0 (q, J = 4 Hz, CH), 109.8 (C), 109.8 (q, J = 4 Hz, CH); ^{19}F NMR (376 MHz, DMSO-d_6) δ −59.0; IR (neat) ν/cm^{-1}: 2900–3300 (broad), 3116 (m), 1615 (m), 1519 (m), 1376 (m), 1331 (s), 1238 (m), 1142 (m), 1096 (s), 1049 (s), 960 (m), 916 (m), 866 (s), 816 (s), 662 (s); LC–MS (TOF$^+$) 244.1 (M + H); HRMS (ESI) m/z: calcd for $C_{10}H_9N_3OF_3$, 244.0698; found, 244.0700 (Δ = 0.8 ppm); melting range: >220 °C (decomposition).

5-(6-(Trifluoromethyl)-1*H*-indol-3-yl)-1,3,4-oxadiazol-2(3*H*)-one (8):

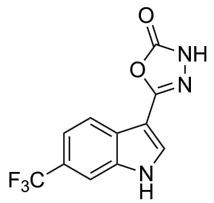

chemical formula: $C_{11}H_6F_3N_3O_2$
exact mass: 269.0412

Stage 1: Two stock solutions in THF were prepared. Solution A: hydrazine (1.00 M, 1.05 equiv) and solution B containing compound **11** (0.95 M, 1.0 equiv). The two stock solutions were pumped (0.65 mL/min each channel) from their respective reservoirs to combine at a PEEK T-piece and were then directed through a FEP flow coil (52 mL maintained at 100 °C using a Polar Bear Plus reactor – Cambridge Reactor Design, residence time 40 min). A 100 psi inline back pressure regulator was added to control the system pressure.

Stage 2 (CDI): The reactor stream was further combined with a input of CDI (1.1 M, 1.1 equiv) in THF (0.65 mL/min). The unifided flow was directed through a second FEP flow coil (52 mL heated at 75 °C using a Polar Bear Plus reactor – Cambridge Reactor Design, residence time 26.7 min). A 75 psi inline back pressure regulator was positioned at the exit of the coil reactor to control the system pressure. A scavenging cartridge of QP-SA (65 g, 3.4 mmol/g loading) was placed in the flow path of the exiting solution. The reactor output was collected and the solvent was evaporated under reduced pressure allowing isolation of title compound **8** in 82% yield following recrystalisation from DCM.

Alternative stage 2 (triphosgene): The reactor stream was further combined with a input of triphosgene (0.8 M, 0.4 equiv) in THF (0.325 mL/min). The unified flow was directed through a second FEP flow coil (52 mL heated at 55 °C using a Polar Bear Plus reactor – Cambridge Reactor Design, residence time 32 min). A 75 psi inline back pressure regulator was positioned at the exit of the coil reactor to control the system pressure. A scavenging cartridge of QP-DMA (70 g, 2.4 mmol/g loading) was placed in the flow path of the exiting solution. The reactor output was collected and the solvent was evaporated under reduced pressure and enabling isolation of the title compound **8** in 91% yield as an off white solid.

^{1}H NMR (400 MHz, DMSO-d_6) δ 12.35 (br. s, 1H), 12.29 (br. s, 1H), 8.23 (d, J = 1.4 Hz, 1H), 8.09 (d, J = 8.4 Hz, 1H), 7.85 (m, 1H), 7.50 (dd, J = 8.4, 1.4 Hz, 1H); ^{13}C NMR (101 MHz, DMSO-d_6) δ 154.6 (C), 152.4 (C), 135.8 (C), 131.0 (CH), 126.8 (C), 125.3 (C, q, J = 272 Hz), 123.7 (C, q, J = 30 Hz), 121.4 (CH), 117.7 (CH, q, J = 4 Hz), 110.2 (CH, q, J = 5 Hz), 100.9 (C); ^{19}F NMR (376 MHz, DMSO-d_6) δ −59.3; IR (neat) ν/cm^{-1}: 3344 (br), 2820 (br), 1750 (s), 1628 (s), 1507 (m), 1455 (m), 1332 (s), 1224 (m), 1160 (m), 1100 (s), 1052 (s), 977 (m), 915 (m), 920 (m), 751 (m), 738 (s), 619 (s);· LC–MS (TOF$^+$) 270.3 (M + H); HRMS (ESI) m/z: calcd for $C_{11}H_7N_3O_2F_3$, 270.0490; found, 270.0497 (Δ = 2.6 ppm); melting range: decomposition >220 °C; X-ray crystal data: CCDC 1572809.

Supporting Information

Supporting Information File 1

Reproductions of ^{1}H and ^{13}C NMR spectra for the reported compounds.
[http://www.beilstein-journals.org/bjoc/content/supplementary/1860-5397-13-251-S1.pdf]

Acknowledgements

We gratefully acknowledge financial support from the Royal Society (MB and IRB) and the Engineering School École Centrale de Marseille (FD).

ORCID® iDs

Marcus Baumann - https://orcid.org/0000-0002-6996-5893
Ian R. Baxendale - https://orcid.org/0000-0003-1297-1552
Fabien Deplante - https://orcid.org/0000-0002-9516-8396

References

1. Kaushik, N. K.; Kaushik, N.; Attri, P.; Kumar, N.; Kim, C. H.; Verma, A. K.; Choi, E. H. *Molecules* **2013,** *18,* 6620–6662. doi:10.3390/molecules18066620
2. *Heterocyclic Scaffolds II: Reactions and Applications of Indoles;* Gribble, G. W., Ed.; *Topics in Heterocyclic Chemistry*, Vol. 26; Springer, 2010. doi:10.1007/978-3-642-15733-2
3. Knölker, H.-J. *The Alkaloids. Chemistry and Biology;* Academic Press, 2014; Vol. 74.
4. Baumann, M.; Baxendale, I. R.; Ley, S. V.; Nikbin, N. *Beilstein J. Org. Chem.* **2011,** *7,* 442–495. doi:10.3762/bjoc.7.57

5. Ferro, N.; Bredow, T.; Jacobsen, H.-J.; Reinard, T. *Chem. Rev.* **2010,** *110,* 4690–4708. doi:10.1021/cr800229s
6. Fischer, E.; Jourdan, F. *Ber. Dtsch. Chem. Ges.* **1883,** *16,* 2241–2245. doi:10.1002/cber.188301602141
7. Taber, D. F.; Tirunahari, P. K. *Tetrahedron* **2011,** *67,* 7195–7210. doi:10.1016/j.tet.2011.06.040
8. Stazi, F.; Maton, W.; Castoldi, D.; Westerduin, P.; Curcuruto, O.; Bacchi, S. *Synthesis* **2010,** *19,* 3332–3338. doi:10.1055/s-0030-1257871
9. Kitching, M. O.; Dixon, O. E.; Baumann, M.; Baxendale, I. R. *Eur. J. Org. Chem.* **2017**. doi:10.1002/ejoc.201700904
10. Assmann, N.; Ładosz, A.; von Rohr, P. R. *Chem. Eng. Technol.* **2013,** *36,* 921–936. doi:10.1002/ceat.201200557
11. A Coflore ACR lab flow reactor was employed (http://www.amtechuk.com/lab-scale-acr/).
12. Filipponi, P.; Gioiello, A.; Baxendale, I. R. *Org. Process Res. Dev.* **2016,** *20,* 371–375. doi:10.1021/acs.oprd.5b00331
13. Filipponi, P.; Baxendale, I. R. *Eur. J. Org. Chem.* **2016,** 2000–2012. doi:10.1002/ejoc.201600222
14. Browne, D. L.; Deadman, B. J.; Ashe, R.; Baxendale, I. R.; Ley, S. V. *Org. Process Res. Dev.* **2011,** *15,* 693–697. doi:10.1021/op2000223
15. Two linked static mixers of PMS 4 – FEP tubing with integrated Teflon Elements (i.d. 6.4 mm, o.d. 9 mm, Length 263 mm with 36 elements available from Esska.co.uk Item No.: 304330060924) were used.
16. Hu, D. X.; O'Brien, M.; Ley, S. V. *Org. Lett.* **2012,** *14,* 4246–4249. doi:10.1021/ol301930h
17. Fitzpatrick, D. E.; Ley, S. V. *React. Chem. Eng.* **2016,** *1,* 629–635. doi:10.1039/C6RE00160B
18. http://www.optek.com/en/process-control-solutions/chemical/Phase-Separation.asp (accessed Aug 29, 2017).
19. http://www.modcon.co.il/wp-content/uploads/cmdm/3679/1434967608_AN_0411_CONDInd_phase_separation.pdf (accessed Aug 29, 2017).
20. Bryan, M. C.; Wernick, D.; Hein, C. D.; Petersen, J. V.; Eschelbach, J. W.; Doherty, E. M. *Beilstein J. Org. Chem.* **2011,** *7,* 1141–1149. doi:10.3762/bjoc.7.132
21. Jones, R. V.; Godorhazy, L.; Varga, N.; Szalay, D.; Urge, L.; Darvas, F. *J. Comb. Chem.* **2006,** *8,* 110–116. doi:10.1021/cc050107o
22. Belley, M.; Sauer, E.; Beaudoin, D.; Duspara, P.; Trimble, L. A.; Dubé, P. *Tetrahedron Lett.* **2006,** *47,* 159–162. doi:10.1016/j.tetlet.2005.10.165
23. Belley, M.; Scheigetz, J.; Dubé, P.; Dolman, S. *Synlett* **2001,** 222–225. doi:10.1055/s-2001-10784
24. Walkington, A.; Gray, M.; Hossner, F.; Kitteringham, J.; Voyle, M. *Synth. Commun.* **2003,** *33,* 2229–2233. doi:10.1081/SCC-120021501
25. Xing, R.; Tian, Q.; Liu, Q.; Li, L. *Chin. J. Chem.* **2013,** *31,* 263–266. doi:10.1002/cjoc.201200834
26. Choi, I.; Chung, H.; Park, J. W.; Chung, Y. K. *Org. Lett.* **2016,** *18,* 5508–5511. doi:10.1021/acs.orglett.6b02659
27. Kalir, A.; Pelah, Z. *Isr. J. Chem.* **1966,** *4,* 155–159. doi:10.1002/ijch.196600025
28. Munshi, K. L.; Kohl, H.; De Souza, N. J. *J. Heterocycl. Chem.* **1977,** *14,* 1145–1146. doi:10.1002/jhet.5570140704
29. Bensen, D.; Finn, J.; Lee, S. J.; Chen, Z.; Lam, T. T.; Li, X.; Trzoss, M.; Jung, M.; Nguyen, T. B.; Lightsone, F.; Tari, L. W.; Zhang, J.; Aristoff, P.; Phillipson, D. W.; Wong, S. E. Tricylic gyrase inhibitors. WO Patent WO2012125746 (A1), Sept 20, 2012.
30. Raucher, S.; Koolpe, G. A. *J. Org. Chem.* **1983,** *48,* 2066–2069. doi:10.1021/jo00160a026
31. Tischler, A. N.; Lanza, T. J. *Tetrahedron Lett.* **1986,** *27,* 1653–1656. doi:10.1016/S0040-4039(00)84339-7
32. Farghaly, A.-R.; Haider, N.; Lee, D.-H. *J. Heterocycl. Chem.* **2012,** *49,* 799–805. doi:10.1002/jhet.864
33. Zhang, M.-Z.; Mulholland, N.; Beattie, D.; Irwin, D.; Gu, Y.-C.; Chen, Q.; Yang, G.-F.; Clough, J. *Eur. J. Med. Chem.* **2013,** *63,* 22–32. doi:10.1016/j.ejmech.2013.01.038
34. Yamada, N.; Kataoka, Y.; Nagaami, T.; Hong, S.; Kawai, S.; Kuwano, E. *J. Pestic. Sci. (Tokyo, Jpn.)* **2004,** *29,* 205–208. doi:10.1584/jpestics.29.205
35. Kumar, D.; Vemula, S. R.; Cook, G. R. *Green Chem.* **2015,** *17,* 4300–4306. doi:10.1039/C5GC01028D
36. Zampieri, D.; Mamolo, M. G.; Laurini, E.; Fermeglia, M.; Posocco, P.; Pricl, S.; Banfi, E.; Scialino, G.; Vio, L. *Bioorg. Med. Chem.* **2009,** *17,* 4693–4707. doi:10.1016/j.bmc.2009.04.055
37. Jansen, M.; Rabe, H.; Strehle, A.; Dieler, S.; Debus, F.; Dannhardt, G.; Akabas, M. H.; Lüddens, H. *J. Med. Chem.* **2008,** *51,* 4430–4448. doi:10.1021/jm701562x
38. http://thalesnano.com/h-cube-midi (accessed Aug 29, 2017).
39. http://www.helgroup.com/reactor-systems/hydrogenation-catalysis/flowcat/ (accessed Aug 29, 2017).
40. Mallia, C. J.; Baxendale, I. R. *Org. Process Res. Dev.* **2016,** *20,* 327–360. doi:10.1021/acs.oprd.5b00222
41. Cossar, P. J.; Hizartzidis, L.; Simone, M. I.; McCluskey, A.; Gordon, C. P. *Org. Biomol. Chem.* **2015,** *13,* 7119–7130. doi:10.1039/C5OB01067E
42. https://www.vapourtec.com/ (accessed Aug 29, 2017).
43. http://www.cambridgereactordesign.com/polarbearplus/index.html (accessed Aug 29, 2017).
44. Konishi, K.-i.; Nishiguchi, I.; Hirashima, T. *Chem. Express* **1986,** *1,* 287–290.
45. Yang, X.; Fu, H.; Qiao, R.; Jiang, Y.; Zhao, Y. *Adv. Synth. Catal.* **2010,** *352,* 1033–1038. doi:10.1002/adsc.200900887

License and Terms

BEILSTEIN JOURNAL OF ORGANIC CHEMISTRY

Latest development in the synthesis of ursodeoxycholic acid (UDCA): a critical review

Fabio Tonin and Isabel W. C. E. Arends*

Review

Open Access

Address:
Department of Biotechnology, Delft University of Technology, Van der Maasweg 9, 2629 HZ Delft, The Netherlands

Email:
Isabel W. C. E. Arends* - I.W.C.E.Arends@tudelft.nl

* Corresponding author

Keywords:
bile acids; biotransformation; hydroxysteroid dehydrogenases; production process; UDCA

Beilstein J. Org. Chem. **2018,** *14,* 470–483.
doi:10.3762/bjoc.14.33

Received: 30 October 2017
Accepted: 05 February 2018
Published: 20 February 2018

This article is part of the Thematic Series "Integrated multistep flow synthesis".

Guest Editor: V. Hessel

Abstract

Ursodeoxycholic acid (UDCA) is a pharmaceutical ingredient widely used in clinics. As bile acid it solubilizes cholesterol gallstones and improves the liver function in case of cholestatic diseases. UDCA can be obtained from cholic acid (CA), which is the most abundant and least expensive bile acid available. The now available chemical routes for the obtainment of UDCA yield about 30% of final product. For these syntheses several protection and deprotection steps requiring toxic and dangerous reagents have to be performed, leading to the production of a series of waste products. In many cases the cholic acid itself first needs to be prepared from its taurinated and glycilated derivatives in the bile, thus adding to the complexity and multitude of steps involved of the synthetic process. For these reasons, several studies have been performed towards the development of microbial transformations or chemoenzymatic procedures for the synthesis of UDCA starting from CA or chenodeoxycholic acid (CDCA). This promising approach led several research groups to focus their attention on the development of biotransformations with non-pathogenic, easy-to-manage microorganisms, and their enzymes. In particular, the enzymatic reactions involved are selective hydrolysis, epimerization of the hydroxy functions (by oxidation and subsequent reduction) and the specific hydroxylation and dehydroxylation of suitable positions in the steroid rings. In this minireview, we critically analyze the state of the art of the production of UDCA by several chemical, chemoenzymatic and enzymatic routes reported, highlighting the bottlenecks of each production step. Particular attention is placed on the precursors availability as well as the substrate loading in the process. Potential new routes and recent developments are discussed, in particular on the employment of flow-reactors. The latter technology allows to develop processes with shorter reaction times and lower costs for the chemical and enzymatic reactions involved.

Introduction

Ursodeoxycholic acid (UDCA), is applied in the pharmaceutical industry (Figure 1) [1]. As reported in several papers published in the 90's, UDCA solubilizes cholesterol gallstones [2,3], it improves the liver function in cholestatic diseases [4-8] and it significantly decreases cholesterol saturation in the bile [8-10]. In terms of pharmacology, it is considered to be better

than chenodeoxycholic acid (CDCA) in the treatment against biliary calculus, since it possesses high efficacy and total absence of side effects [11].

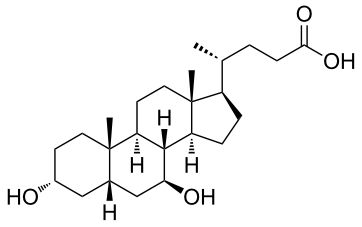

Figure 1: Chemical structure of UDCA.

UDCA is commonly produced by transformation of cholic acid (CA), which is the most abundant and least expensive bile acid available. Because of the molecular complexity of bile acids, the chemical modification requires several protection and deprotection steps, resulting in an overall yield of about 30% [12-15]. For that reason, research has been performed on the development of more selective procedures which involve less reaction steps. In particular, microbial transformations [16-19] or chemoenzymatic procedures [20,21] employing CA, CDCA or lithocholic acid (LCA) as starting material have been studied.

This minireview summarises different aspects to be addressed and hurdles to be taken in the development of a selective and sustainable process for the production of UDCA. Different chemical, chemoenzymatic and enzymatic routes will be considered. In addition, the precursors availability as well as the substrate loading in the process and the requisites for potential new routes will be discussed. Furthermore, the potential benefits of a flow reactor setup for this multistep synthesis will be discussed.

Review

Precursor availability

Bile acids

The most important active ingredients of bile are the bile acids. Together with their salts, they allow the emulsification of lipids, a fundamental step for their absorption and digestion. Bile acids are 24-carbon containing 5β-steroids. Their structure contains multiple hydroxy substituents: the position and the stereochemistry of these OH groups influence the solubility and biochemical properties of the compounds. In CA, for example, the OH groups on the steroidal ring are all in α-position with respect to the ring plane, defining a structure in which the molecule has a polar and an apolar surface. For this reason, these molecules and their derivatives are defined as amphipathic. Bile acids are considered very important molecules for their ability to form micelles in an aqueous environment [22].

Bile acids biosynthesis takes place in the liver starting from cholesterol: 17 enzymes are involved in the production of these molecules. The final products are the so-called primary bile acids: CDCA and CA [23]. Subsequently, these bile acids can be modified by intestinal bacteria to form the secondary bile acids as, for example, deoxycholic acid (DCA), LCA and UDCA. Secondary bile acids can be subsequently resorbed and returned to the liver where they are re-secreted in a process known as enterohepatic circulation.

In mammals, bile acids are secreted as conjugated molecules with glycin or taurine (Figure 2), forming the so called bile salts, with slightly different properties (p*K*a, solubility) in comparison to the corresponding free acids [24,25]. These bile salts also lead to an increased retention in the intestine.

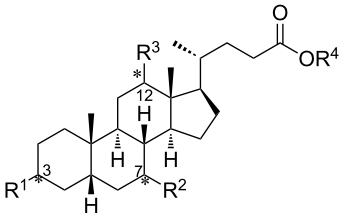

compound name	abbrev.	R^1	R^2	R^3	R^4
cholic acid	CA	α-OH	α-OH	α-OH	H
chenodeoxycholic acid	CDCA	α-OH	α-OH	H	H
deoxycholic acid	DCA	α-OH	H	α-OH	H
dehydrocholic acid	DHCA	keto	keto	keto	H
lithocholic acid	LCA	α-OH	H	H	H
ursocholic acid	UCA	α-OH	β-OH	α-OH	H
ursodeoxycholic acid	UDCA	α-OH	β-OH	H	H
glycocholate	–	α-OH	α-OH	α-OH	glycine
glycochenodeoxycholate	–	α-OH	α-OH	H	glycine
taurocholate	–	α-OH	α-OH	α-OH	taurine
taurochenodeoxycholate	–	α-OH	α-OH	H	taurine

Figure 2: Chemical structures of bile acids and salts.

The only economically viable resource of bile acids is the bovine bile, which must be extracted at the time of slaughter.

In slaughterhouses, the bovine gallbladder is recovered during the processing of the meat and from a single cow, around 230 mL of bile can be obtained. The commercial prize of bile is in the range of 0.1–0.4 $/L. Bile acids represent roughly 0.7% (w/w) of the bile [26].

In order to extract and purify the different bile acids, bile is frozen and lyophilized: from 100 mL of bile 8 g of dry powder can be obtained. From these about 6.9 g of 90% pure bile acids can be obtained [27]. Cholesterol, cholesterol esters, triglyc-

erides and free fatty acids are selectively extracted with organic solvents from aqueous buffers at different pHs. Then, the bile acids were separated from inorganic salts by extraction of the dry residue with absolute ethanol. The major components of the obtained mixture are the primary bile acids (CA and CDCA), secondary bile acids (DCA and LCA) and bile salts like taurocholic acid and glycocholic acid (derivatives of CA), taurochenodeoxycholic acid and glycochenodeoxycholic acid (derivatives of CDCA) and other conjugated salts of their 7-α-dehydroxylated derivatives [27].

CA

3α,7α,12α-Trihydroxy-5β-cholan-24-oic acid, also named cholic acid (CA, Figure 2), is one of the primary bile acids. It is almost insoluble in water, but soluble in methanol, ethanol and acetic acid. Differently from the acid, the sodium salt of CA is much more soluble in water at pH > 8.0 [28,29]. Salts of CA are called cholates. From the 3D structure of CA is it possible to observe an hydrophilic and an hydrophobic face, giving to CA its characteristic surfactant properties. CA is sold as a treatment for children and adults affected by bile acids synthesis disorders. Because of its abundance in bovine bile, CA is the precursor for UDCA.

CDCA

3α,7α-Dihydroxy-5β-cholan-24-oic acid, also known as CDCA (Figure 2), is a primary bile acid in human, but represents only 2.7% (w/w) of total bovine bile salts [30]: this is the main reason why it is not used as precursor for the preparation of UDCA.

CDCA can be used to treat gallstones avoiding, unlike CA, the downregulation of the cholesterol-7-α-hydroxylase, that represent the rate-limiting step in bile acid synthesis [31]. It can be metabolized by bacteria in the colon to form the secondary bile acid known as LCA [32].

LCA and other bile acids

LCA, also known as 3α-hydroxy-5β-cholan-24-oic acid (Figure 2), is a secondary bile acid. It is produced by bacteria in the colon from CDCA trough the dehydroxylation of the C7 functional group of the steroid framework. Low percentages of other secondary bile acids and related keto derivatives can be found in the bile. The solubility properties, interactions and metabolisms are related to the position and stereochemistry of the hydroxy groups attached to the steroid ring. A general structure with the names of several bile acids is reported in Figure 2.

Deconjugation

Free bile acids can be obtained from the corresponding bile amides (with glycine and taurine) through a deconjugation step. Chemically, the reaction is an hydrolysis of the amide derivatives, that can be carried out at high temperature in alkaline environment. This reaction requires large amounts of sodium hydroxide (30%) and high temperatures (120 °C) for extremely long times (8–12 hours). Few enzymes (acylases, EC: 3.5.1) have been reported to hydrolyse glycinates and taurinates to the corresponding carboxylic acid. Recently, Pedrini et al. [33] have isolated and characterized a cholylglycine hydrolase from *Xanthomonas maltophilia* CBS 827.97: this enzyme completely hydrolyses glycine and taurine conjugates in 20 minutes at 50 °C. Unfortunately the protein sequence of this enzyme is not reported, making recombinant expression and its industrial use impossible. A second enzyme, isolated in *Lactobacillus plantarum* and recombinantly expressed in *E. coli*, was reported by Christiaens et al. [34]: this enzyme shows almost the same properties of the one described above but with lower activities (the specific activities of *X. maltophilia* and *L. plantarum* acylases on glycocholic acid as substrate are 100 U/mg and 3.42 U/mg, respectively).

From a biocatalytic point of view, other acylases and the well-known lipases can be used to achieve the same reaction. Few literature reports can be found on the promiscuous amidase activity of wild-type or engineered lipases [35,36], but no one have tested their activities on bile salts.

Conclusions on the precursor availability

Natural UDCA is a very expensive pharmaceutical active ingredient since, to date, it can only be obtained by isolation from bear bile (practice used in traditional Chinese medicine) [37]. Alternatively, it can be produced by chemical transformation of CA and CDCA from the cheaper bovine bile. Nowadays, the transformation process is not yet optimized in terms of costs and environmental impact [20]. CA is the main constituent of bovine bile and is the main precursor for the synthesis of UDCA.

One of the main problems regarding the availability of precursors for the synthesis of UDCA is the direct relation with meat industries. The major manufacturers of bovine meat are in newly industrialised countries, in particular south America (Brasil) and India. Reports on Ecuadorian slaughterhouses [26,38-40], point out that in some cases there is a lack of adequate technical conditions and hygienic protocols, leading to environmental pollution and the need to include sanitary procedures in the processing of bile acids.

Alternative sources of sterols can be found in eukaryotic microorganisms like yeast and algae [41]. However, technological and scientific knowledge on these metabolic pathways are still in an early stage, and will not be included in this review.

C12 Dehydroxylation

Chemical dehydroxylation

UDCA can be obtained by a multistep chemical synthesis starting from CA. Two main steps are involved: the dehydroxylation at C12 and the epimerization of the 7-OH group.

In order to achieve chemical dehydroxylation, firstly CA has to be oxidized in position C12 to the corresponding ketone, after which Wolff–Kishner reduction can be applied. This whole sequence comprises 5 steps [13]. After the protection of the carboxylic group by acid-catalyzed esterification (quantitative yield), the 3- and 7-OH groups are protected selectively with acetic anhydride and pyridine (yield 92%). The 12-OH group is oxidized with CrO_3 (yield 98%) and, after a deprotection step in alkaline environment, the formed ketone group can be removed by a Wolff–Kishner reaction yielding CDCA (yield 82%). The overall yield of the dehydroxylation step is around 65%.

Wolff–Kishner reduction

The Wolff–Kishner reaction is widely used by chemists to remove carbonyl moieties yielding unsubstituted alkyl chains. The reaction requires two steps: the hydrazine first reacts with the ketone forming a hydrazone; The addition of a strong base and heat then promote a rearrangement with the elimination of N_2 yielding the desired alkyl chain (Figure 3). This reaction is applied to the synthesis of UDCA in order to remove the carbonyl group at C12.

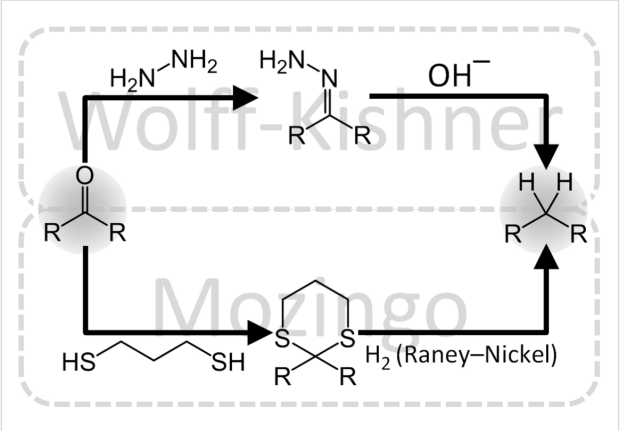

Figure 3: Comparison between Wolff–Kishner and Mozingo reduction. Notably the overall chemical reaction is the same for both cases.

The use of hydrazine is a disadvantage in terms of safety (explosive risk) and economic costs (it should be used in excess relative to substrate). Several modifications of the Wolff–Kishner reaction can be found in literature: i.e., the Huang–Minlon modification, that consists of removing the unreacted hydrazine after the first step by distillation [42]. This results in higher yield and partial recovery of the unreacted hydrazine. In order to reduce the explosive risk, different hydrazine derivatives have been discovered and tested (e.g., methyl hydrazinocarboxylate, [43]). Other reports have demonstrated the feasibility of this reaction in a flow-system, avoiding the large excess of hydrazine, giving high yields in a more rapid reaction [44]. In this field, flow reactors offer benefits in terms of mass and heat transfer, both enhanced by the geometry of the reactor. Furthermore, the possibility to have a continuous production and to easily perform multiple modular reactions, leads to the improved scalability of these systems. In addition, a microwave-assisted Wolff–Kishner reduction has been examined with good results in a 30 seconds reaction [45]. Another option is the production of hydrazine in situ, using chemical methods. Also enzymatic activities towards hydrazine have been discovered [46], however, not enough optimized to be applicable.

A Wolff–Kishner alternative: the Mozingo reduction

The Mozingo reduction effects the same reaction as Wolff–Kishner, albeit under neutral conditions (Figure 3). It involves two steps: firstly, the carbonyl compound is converted into a dithioketal by adding a dithiol. The mechanism for this step is analogous to the mechanism for ketal or acetal formation except sulphur replaces oxygen as the nucleophile attacking the carbonyl group.

In a second step, the dithioketal is reduced to the corresponding methylene compound by hydrogenolysis in presence of Raney Nickel (actually used for the hydrogenation of fatty acids). In comparison to the Wolff–Kishner reaction, the use of hydrazine is replaced by the use of hydrogen gas, which can be seen as a double-bladed knife. The reduction step can also be performed with $NaBH_4$ or other reductants. At the moment, a complete and clear reaction mechanism has not been well identified yet.

There is one report that suggests the application of this reaction for the synthesis of UDCA (yield 95%) [47]. The major problem related to this reaction is the very characteristic odor of ethanedithiol which is compared by many people to rotten cabbage. Ideally, there is the possibility of using other types of less volatile compounds but no reports thereof have been found.

12α-Hydroxysteroid dehydrogenase

12α-Hydroxysteroid dehydrogenases (12α-HSDH) are particularly interesting for the selective oxidation of the 12-hydroxy group of CA (Figure 4). These enzymes belong to the family of oxidoreductases with NAD^+ or $NADP^+$ as electron acceptor.

This oxidation is a mandatory step for removing the OH functionality at C12. In all the chemoenzymatic routes reported by Eggert et al. [20], the carbonyl group resulting from the oxida-

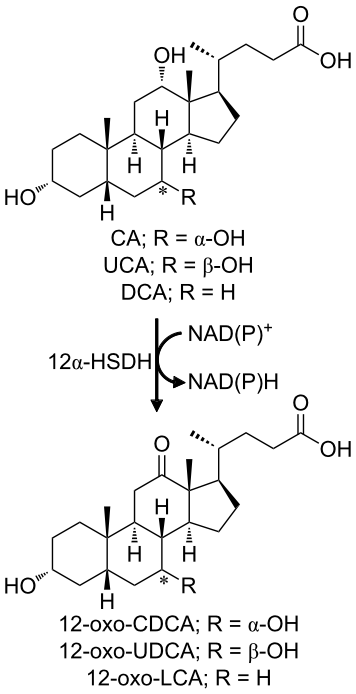

Figure 4: Reaction catalysed by the 12α-HSDH; the 12-OH group of CA or UCA is oxidized yielding 12-oxo-CDCA or 12-oxo-UDCA, respectively, with the concomitant reduction of one molecule of $NAD(P)^+$.

tion of the 12-OH group was subsequently reduced by the Wolff–Kishner reaction (see above). The few cases showing a dehydroxylation in position C12 by bacteria are reported in the next paragraph. The $NADP^+$-dependent 12α-HSDHs activity (Table 1, [48-51]) is spread among the strains of the genus *Clostridium* (e.g., *Clostridium leptum* [48] and *Clostridium* group P strain C 48–50 [49,52]). Furthermore, on the other side, the NAD^+-dependent 12α-HSDHs activity was observed and reported in *Eubacterium lentum* and *Clostridium perfringens* [50,51]. A NAD^+ dependent process for the production of 12-oxo-CDCA was patented in 2006 [53].

Biocatalytic C12 dehydroxylation

In contrast to the reports on the epimerization of CA and CDCA with enzymes (see below "Enzymes for the production of UDCA from CDCA"), the dehydroxylation of CA remains an undiscovered field for microbiologists and biochemists. To our knowledge, the only evidence of a bacterial-catalysed 12α-dehydroxylation was reported by Edenharder in 1983 [54]. He found eight strains of the *Bacteroides* genus that specifically dehydroxylate CA to CDCA. However, no other studies have been carried out concerning this topic. A method for the production of 12-dehydro steroids by the action of 12-dehydroxylase producing microorganism (*Clostridium perfringens* ATCC 19574) was patented in 1976 [55]. However, the presence and the expression of a protein that can catalyse this reaction were never confirmed in other papers.

The putative molecular mechanism for the C12 dehydroxylation is still unknown: it can resemble the dehydroxylation mechanism described for position C7 [56-58] (Supporting Information File 1, Figure S1). Interestingly all the genes catalysing that reaction where clustered in the BAI operon and, by analogy, it can be possible to design a biochemical pathway that specifically acts on C12 (see postulated sequence of steps in Supporting Information File 1, Figure S2). The reaction sequence can be divided in 3 steps: firstly, the substrate is oxidized by a specific alcohol dehydrogenase and an ene-reductase-like enzyme. Then dehydration occurs, catalysed by a specific dehydratase. The dehydrated product is then reduced through a 3-step-cascade reaction (catalysed by 3 different enzymes) giving the final dehydroxylated product.

7-OH epimerization: shift the equilibrium

Chemical epimerization of CDCA into UDCA

The second step of UDCA synthesis from CA, is the epimerization of the 7-OH group. Chemically, the 7α-OH group of CDCA, obtained by dehydroxylation of CA (see above "C12 dehydroxylation"), is selectively oxidized in the presence of sodium bromate [59] (yield 88%), *N*-bromosuccinimide [13,15] (ungiven yield) or 1-hydroxy-1,2-benziodoxol-3(1*H*)-one 1-oxide [60] (yield 90%) and subsequently reduced with metallic sodium in presence of imidazole and 1-propanol (yield 80%) yielding the 7β-OH epimer (UDCA) as imidazole salt. Notably, the regiospecific oxidoreduction of the 7α-OH group is achieved using weak oxidants: this behavior can be explained by the peculiar conformation of CDCA (the 7α-OH group is surrounded by alkyl chains, generating an hydrophobic environment that favors oxidation to the ketone, which is not the case

Table 1: Summary of reported 12α-HSDH. The given activity is based on CA as substrate.

microbial source	ref.	cofactor	specific activity	sequence
Clostridium leptum	[48]	$NADP^+$	3.3 U/mg	/
Clostridium group P.	[49]	$NADP^+$	128 U/mg	GenBank: HC036073.1
Eubacterium lentum	[50]	NAD^+	0.5 U/mg	/
Clostridium perfringens	[51]	NAD^+	/	/

for the other epimer). These data are supported by a density functional calculation or rather the differential change in electron density due to an infinitesimal change in the number of electrons [61]. The overall yield of the epimerization step is around 70% [12,15,62].

A further purification step is necessary for the preparation of free UDCA: it can be easily obtained with sequential esterification, extraction and hydrolysis (yield 91%). The theoretical yield of the whole process fluctuates around 30 to 40%.

Enzymes for the production of UDCA from CDCA

The enzymatic transformation of CDCA into UDCA can be obtained using different combinations of biocatalysts that act specifically on the 7-OH group of hydroxysteroids. In order to find the right combination of enzymes and the optimum reaction conditions, different aspects (enzymatic activities, equilibrium of the reaction, inhibition of enzymes by substrate and products and their stabilities) have to be assessed.

A list of enzymes that can be used for the transformation of CDCA is presented in the next paragraphs.

7α-Hydroxysteroid dehydrogenases (7α-HSDH)

These enzymes are able to oxidise specifically the α-hydroxy group at C7 together with the concomitant reduction of NAD^+ or $NADP^+$ (Figure 5). All of them are part of the group of the short chain dehydrogenases/reductases (SDR), showing a molecular weight around 30 kDa and a homodimeric or homotetrameric quaternary structure.

Reported 7α-HSDHs were isolated from both aerobic and anaerobic bacteria: the state of art, together with the cofactor dependence and the specific activities, are summarized in Table 2 [33,63-70]. Examples of processes for the selective oxidation of bile acids, their salts or derivatives were patented [71,72].

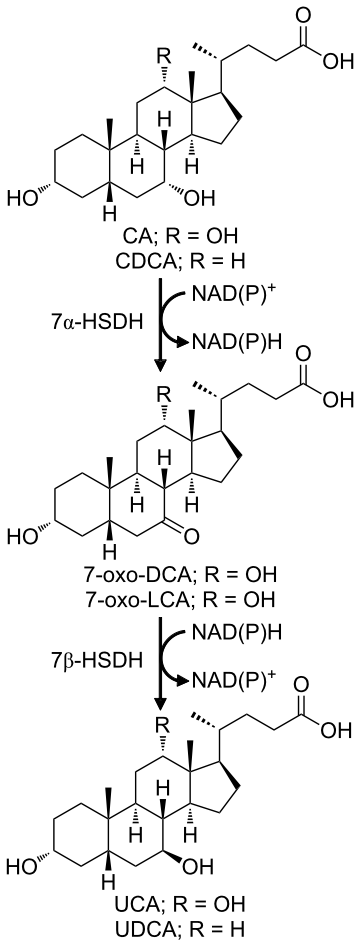

Figure 5: Epimerization reaction catalysed by the 7α-HSDH and 7β-HSDH; the 7α-OH group of CA (R = OH) or CDCA (R = H) is firstly oxidized by the 7α-HSDH yielding 7-oxo-DCA or 7-oxo-LCA, respectively. Subsequently, the keto group is reduced by the 7β-HSDH giving the final products UCA or UDCA.

In addition to these reported biotransformations, many additional 7α-HSDHs have been discovered and reported over the past years. About 500 entries can be found in Reference sequence

Table 2: Summary of reported 7α-HSDH. The given activity is on chenodeoxycholic acid as substrate.

microbial source	ref.	cofactor	specific activity	sequence
Clostridium sordelii	[63]	$NADP^+$	1.1 U/mg	GenBank: AAA53556.1
Eubacterium scindens	[64]	$NADP^+$	338 U/mg	GenBank: AAB61151.1
Clostridium absonum	[65]	$NADP^+$	59 U/mg	GenBank: JN191345.1
Clostridium difficile	[66]	$NADP^+$	8.5 U/mg	Genbank: YP 001086529
Escherichia coli	[67]	NAD^+	190 U/mg	GenBank: KXH01569.1
Pseudomonas sp. B-0831	[68]	NAD^+	941 U/mg	GenBank: D50325.1
Bacteroides fragilis	[69]	NAD^+	351 U/mg	GenBank: OGX95366.1
Xanthomonas maltophilia	[33]	NAD^+	70 U/mg	/
Comamonas testosteroni	[70]	/	/	/

(RefSeq) database at NCBI [73] typing "7-alpha-hydroxysteroid dehydrogenase".

7β-Hydroxysteroid dehydrogenases (7β-HSDH)

Unlike their homologues, only few examples of bioconversion with 7β-HSDH have been reported in literature (Table 3, [33,65,74-77], Figure 5): one $NADP^+$-dependent dehydrogenase from *Clostridium absonum* [65] was used in two different processes for the production of UDCA [78,79]. The $NADP^+$-dependent enzyme from *Eubacterium aerofaciens* shows a significantly lower specific activity [74] and another $NADP^+$-dependent enzyme was isolated from *Ruminococcus gnavus* [75]. In order to increase the activity and stability of 7β-HSDHs, protein engineering studies were carried out, as described in literature by Weuster-Botz et al. [77] and Zheng et al. [76]. Up till now, *Xanthomonas maltophilia* 7β-HSDH (33 U/mg) represents the only isolated NAD^+-dependent enzyme [33]. Unfortunately its protein sequence has not been reported.

Biocatalytic processes

Both microorganisms and purified enzymes have been applied for the fully biocatalytic epimerization of the 7-OH group. Several examples reported in literature are summarized in Table 4 [80-85].

The use of whole-cell conversion offers both advantages and disadvantages: wild-type microorganisms are normally difficult to grow, especially if the enzyme expression is related to anaerobic conditions. In addition the pathogenicity of these microorganisms represents a problem for their use in the pharmaceutical industry; additional steps of purification and control of sterility are necessary to obtain a safe product for the market. Otherwise, the circumvention of protein isolation and production makes it cheaper than their free-enzyme analogues.

In this way, the use of lyophilized whole-cell containing recombinant HSDHs can represent a solution in the reduction of catalyst costs, maintaining a reasonable safety. This approach was followed by Braun et al. and Sun et al. obtaining the 12-oxo-UDCA with a yield of 99.5% using engineered *E. coli* cells [86,87]. In comparison to the systems that employed purified enzymes (see below), this approach allows higher substrate loading (70–100 mM).

Several enzymatic systems have been proposed in the literature, together with cofactor regeneration systems. As general rule, the oxidative and reductive steps are coupled with a related regeneration system. In this way, the equilibrium of the reaction can be pushed to the production of UDCA. An overview of

Table 3: Summary of reported 7β-HSDH. The given activity is based on 7-oxo-LCA as substrate.

microbial source	ref.	cofactor	specific activity	sequence
Clostridium absonum	[65]	$NADP^+$	65 U/mg	GenBank: JN191345.1
Eubacterium aereofaciens	[74]	$NADP^+$	30 U/mg	GenBank: ZP0177306.1
Ruminococcus gnavus	[75]	$NADP^+$	23 U/mg	GenBank: ZP02041813
Collinsella aerofaciens	[77]	$NADP^+$	15 U/mg	GenBank: WP006236005
Collinsella aerofaciens	[77]	$NADP^+$	21 U/mg	Engineered[a]
Ruminococcus torques	[76]	$NADP^+$	8.6 U/mg	GenBank: WP015528793
Ruminococcus torques	[76]	$NADP^+$	46.8 U/mg	Engineered[b]
Xanthomonas maltophilia	[33]	NAD^+	33 U/mg	/

[a]G39A variant of the 7β-HSDH from *Collinsella aerofaciens*; [b]T198V/V207M variant of the 7β-HSDH from *Ruminococcus torques*.

Table 4: Summary of reported whole-cell transformations with wild type microorganisms. Epimerization yields of CDCA to UDCA are given.

microorganism	ref.	yield (%)
Colinsiella aerofaciens	[80]	–
Clostridium absonum	[81]	75%
E. coli + *Bacteroides fragilis*	[82]	25–30%
Colinsiella aerofaciens + *Bacteroides fragilis*	[82]	95%
mixed culture	[83]	–
Clostridium limosum	[84]	55–60% (75–80%[a])
Stenotrophomonas maltophilia	[85]	27% (80%[b])

[a]Reported yield of epimerization of CA to ursocholic acid; [b]reported yield of epimerization of 12-oxo-CDCA to 12-oxo-UDCA.

reported enzymatic and chemoenzymatic cascades is summarized in Table 5 and Figure 6 [12,33,78,86-94].

From the comparison of the different routes, it can be observed that higher productions are obtained when the Wolff–Kishner reaction is carried out in the late stage. The typical substrate loading in systems employing purified enzymes is in the range of 10–15 mM. This disadvantage is partially compensated by the reuse of the biocatalysts through the employment of membrane reactors [12,78] or the immobilization of enzymes [93].

Table 5: Summary of reported chemoenzymatic transformations with purified enzymes.

reaction pathway	ref.	conversion yield (%)	productivity (g L^{-1} d^{-1})
DHCA→12-oxo-UDCA	[12]	85%	7.0
	[86]	95%	9.6
	[87]	99%	40.1
	[88]	95%	55.6
	[89]	99%	7.3
CA→UDCA	[90]	70%	1.8
CA→12-oxo-UDCA	[78]	88%	8.0
	[91]	73%	24.1
CDCA→UDCA	[33]	82%	0.02
	[92]	100%	47.2
	[93]	100%	88.5
	[94]	63%	3.0

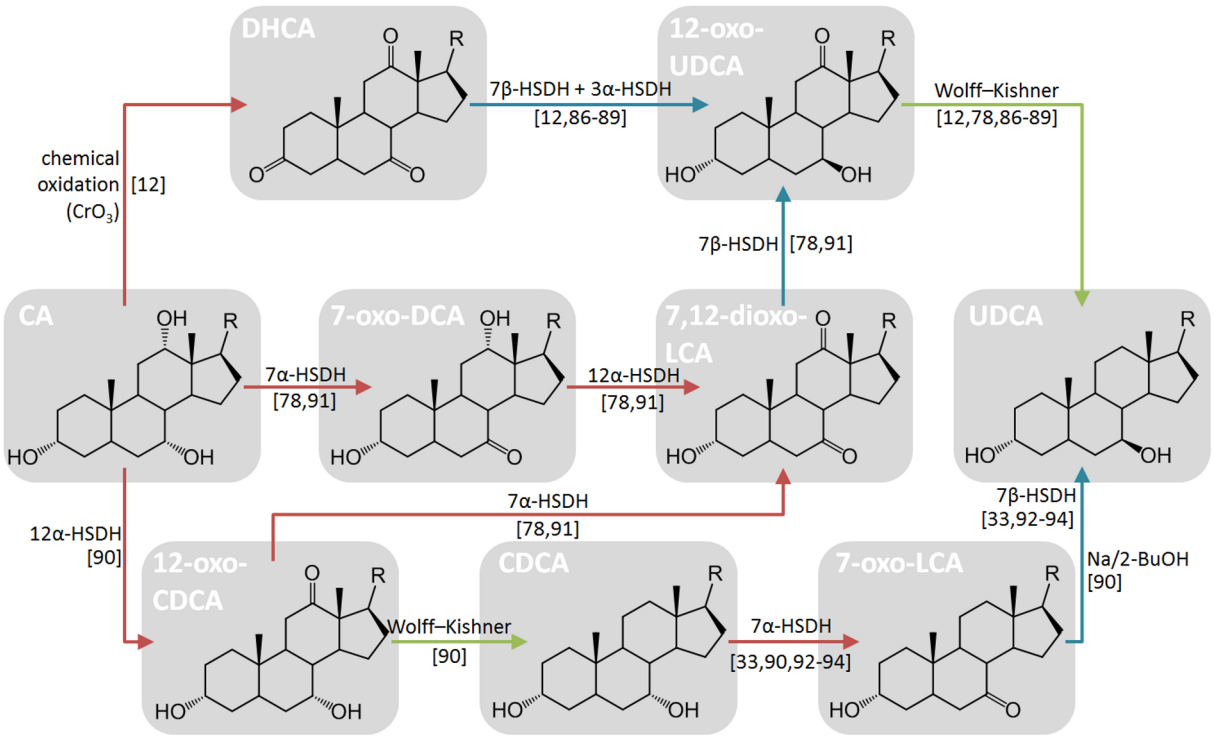

Figure 6: Overview of the chemoenzymatic process for the production of UDCA from CA: The oxidation, reduction and dehydroxylation reactions are highlighted with a red, blue and green arrow, respectively. Names of compounds are indicated in the box. The general stereoinformation of steroid scaffold is shown in Figure 2. R = 4-pentanoic acid.

The first system shows high stability (enzymes in the membrane reactor have a half-life of 1–2 weeks) and the biocatalysts can be reused for eight cycles of conversions. On the other hand, immobilized enzymes show a higher productivity (88.5 vs 8 g L^{-1} d^{-1}) despite the fact that the half-life (23 h) is lower and the biocatalyst can be reused for only five cycles of conversions.

In order to reduce the mechanical stress that might inactivate the immobilized enzymes, the flow-system represents a valid technology. The packed-bed reactor set up by Zheng et al. partially solved this problem, achieving full conversion of CDCA into UDCA for at least 12 hours. This represents an improvement compared to the use of the same biocatalysts under batch conditions. This particular flow-system consists of two modular column reactors (Figure 7): firstly, CDCA is oxidized to 7-oxo-LCA by an immobilized NAD^+-dependent 7α-HSHS (first reactor column); afterwards, 7-oxo-LCA is reduced to UDCA by an immobilized $NADP^+$-dependent 7β-HSDH (second reactor column). The cofactors are individually regenerated in each column by the co-immobilized enzymes, lactate dehydrogenase (LDH) and glucose dehydrogenase (GDH), respectively.

The decoupling of the 2 reactions is an elegant way to spin the equilibrium but, in every catalytic cycle, the co-substrates used to regenerate the cofactor have to be added in great surplus, leading to additional costs and additional problems in the downstream process. The most used enzymes for the cofactor regeneration are glucose dehydrogenase (glucose to glucuronic acid), lactate dehydrogenase (pyruvate to lactate), glutamate dehydrogenase (α-ketoglutarate to glutamate) and formate dehydrogenase (formate to CO_2). In particular, the last enzyme is interesting because formate is cheap and, because of the gaseous nature of CO_2 as product, the equilibrium of the reaction is entropically favoured.

Pedrini et al. in 2006 [33] reported the successful epimerization of CDCA to UDCA using a redox-neutral cascade reaction, with two NAD^+-dependent dehydrogenases. In this way the requirement of external systems for cofactor regeneration was circumvented and UDCA was obtained with a final yield of 75%. Interestingly, the addition of 2-hexanol led to an increase of NADH available for the reduction of 7-oxo-LCA and a final yield of 82% was observed. According to the authors, the presence of another alcohol dehydrogenase in the partially-purified enzyme preparation increases the amount of NADH for the 7-oxo-LCA reduction.

To conclude, it is difficult to denote the "best" route for the 7-OH epimerization. All the processes mentioned, demonstrate reasonable yield and high selectivity. A redox-neutral cascade seems most elegant, but in order to fully understand and push the equilibrium of the reaction, a full biochemical characterization and a deep knowledge of the kinetics and stability of the involved enzymes is required.

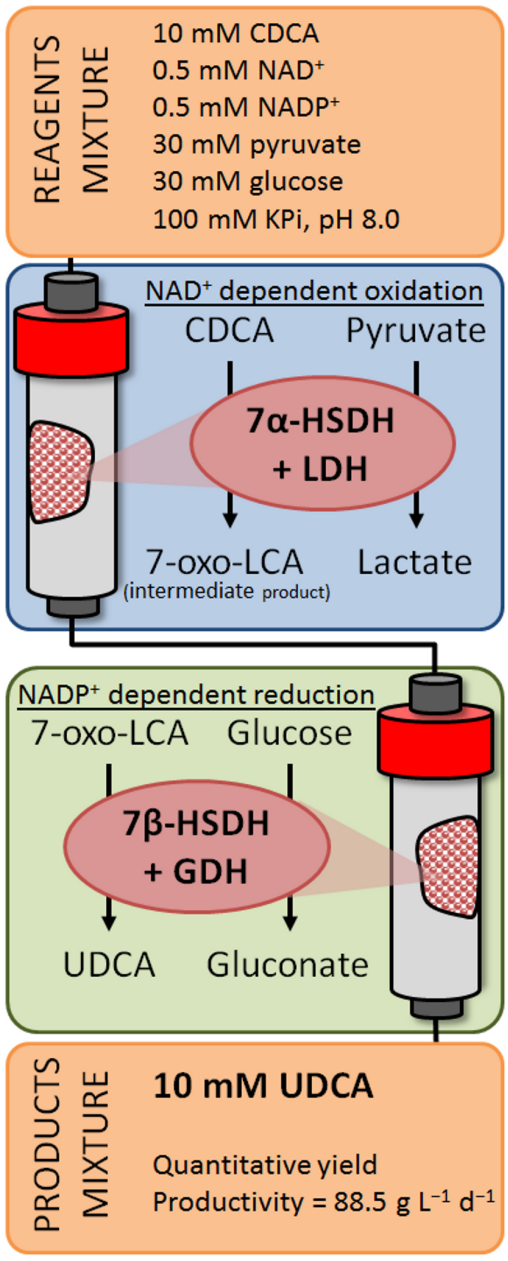

Figure 7: Schematic representation of the flow reactor for the continuous conversion of CDCA to UDCA [93].

Other ways to obtain 7-OH epimerization

Other chemical routes for the production of UDCA have been patented and published: for example, Dangate et al. [60] pro-

posed a chemical route where the order of the two steps (C12 dehydroxylation and C7 epimerization) is reverted and the specific oxidation of 7- and 12-OH group can be achieved without any protection step (yield 53%).

Another interesting chemoenzymatic way to obtain the epimerization of the 7-OH group consists is the removal of the functionality and the subsequent rehydroxylation with a specific final chiral configuration. Both steps can be performed by enzymes and/or microorganisms: Sawada et al. [95] reported that a fungal strain (*Fusarium equiseti* M41) was able to introduce a 7β-hydroxy group into LCA by hydroxylation forming UDCA directly.

Later, many other microorganisms with a 7β-hydroxylating activity were discovered in strains of actinobacteria and filamentous fungi [96,97]. The key-enzyme in that pathway is a P450-like enzyme that catalyses the specific and irreversible 7β-hydroxylation. On this topic, a recent work by Kollerov et al. [98] describes several DCA modifying filamentous fungi strains (mostly ascomycetes and zygomycetes): the highest 7β-hydroxylase activity level was found in *Fusarium merismoides* VKM F-2310.

The possibility to access that kind of chemical and chemoenzymatic reactions pave the way for the design of other unexplored routes for the production of UDCA (example in Figure 8).

In addition, other reported enzymes can eventually play a role in the cascade reaction synthesis of UDCA. For example the 3α-HSDHs [51,99] catalyze the oxidoreduction of the 3α-OH groups to the corresponding ketones and the well-known laccase-TEMPO system [100] can be used for the unselective oxidation of CA to dehydrocholic acid (DHCA).

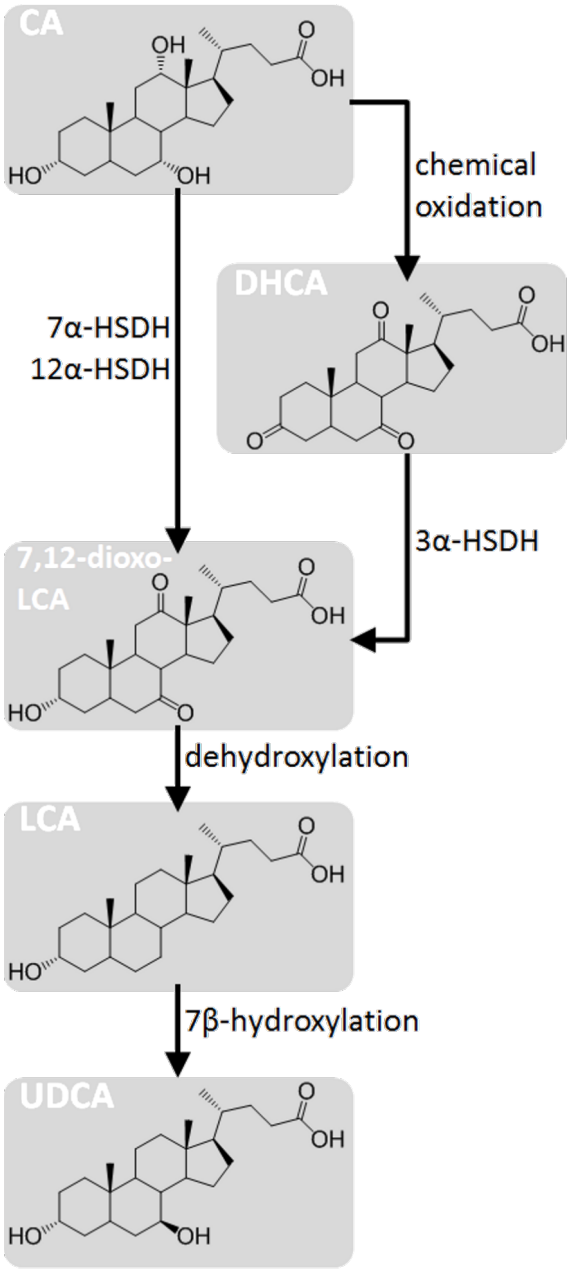

Figure 8: Chemoenzymatic pathways for the formation of UDCA from CA that profit by the C7 hydroxylation activity described by Sawada et al. [95]. CA can be transformed to 7,12-dioxo-LCA trough specific oxidation of 7α-OH and 12α-OH with a 7α-HSDH and 12α-HSDH, respectively. Alternatively, 7,12-dioxo-LCA can be obtained by chemically oxidizing (e.g., with CrO_3) all the hydroxy groups, yielding DHCA and then reducing the 3-oxo group to 3α-OH by a 3α-HSDH. LCA can be obtained from 7,12-dioxo-LCA through dehydroxylation by Wolff–Kishner or Mozingo reduction. Finally, UDCA can be obtained from LCA by 7β-hydroxylation. The general stereoinformation of the steroid scaffold is shown in Figure 2.

Solvent and substrate loading considerations in processing

For an economically and environmentally sustainable process volumetric productivities have to be considered. In other words substrate loadings cannot be too low. While it does not represent a problem in chemical synthesis (UDCA, CDCA and CA are pretty soluble in alcohols like methanol and ethanol), the water-based environment required by enzymes is an obstacle in the development of a biocatalytic process.

In comparison to CA, the solubility of CDCA and UDCA at pH 8.0 (typically used for HSDHs) is lower (around 25 mM) [101], and it could be increased when adding methanol or ethanol as co-solvent. In addition, at higher concentrations than the critical micelles concentration (CMC), bile acids tend to form micelles: this phenomenon, due to the amphipathic structure of these molecules, is limiting the availability of free hydroxysteroids in solution. The reported CMCs of bile acids

are in the range of 5–15 mM [101-104]. Accordingly, the addition of co-solvents increases the CMC of bile acids and the availability of monomers in solution. Notably, HSDHs are relatively stable and active in 10–20% methanol. Moreover, the immobilization of the enzyme can provide a higher stability to the protein and makes the system work also at higher concentrations of co-solvent [105]. However, working with a diluted solution, produce a large amount of wastewater that had to be treated.

Another option is represented by biphasic systems: In these cases, the organic phase works as reservoir of reagents and products. This methodology is widely used in biocatalysis to solve solubility issues. Unfortunately, the solubility of hydroxysteroids in non-alcoholic organic solvents (e.g., ethers, alkanes, dichloromethane, chloroform) is not very high (e.g., the reported solubility values for CDCA and CA in chloroform are 7.6 and 14.4 mM, respectively [102]). Several attempts to carry out hydroxysteroid transformations in biphasic systems were reported [106-108]: good conversions and an increase of reaction rates were observed for 7-OH and 3-OH epimerizations. In these cases the reactions were carried out at final concentrations of substrate in the range of 10–20 mM, the usual substrate loading in monophasic systems.

Of no lesser importance, the increased amount of substrates and products up to relevant concentrations for industrial application can inhibit the enzymes used in the biocatalytic process. Several examples are reported in literature about substrate or product inhibition of HSDHs. Protein engineering could help to solve or lowering the effect of these issues, leading to the optimization of the biocatalyst for industrial applications. In addition, the use of flow-reactors can be beneficial to diminish substrate and product inhibition by controlling the contact time.

In conclusion, the increase of the substrate loading is one of the main challenges in the development of an efficient biocatalytic system for the production of UDCA form CA. More research is needed to address this aspects.

Conclusion

The organic synthesis of CDCA and UDCA starting from taurinated and glycinated cholic acid is a long process, complicated and risky due to the nature and toxicity of the reagents used, the costs of disposal of large amounts of sodium hydroxide, chromium salts and organic solvents, and the purification processes necessary to eliminate byproducts formed at each step of reaction involved. All this extends the time, increases costs and decreases production yields. Therefore, research nowadays is geared towards more economical synthesis methods that are waste-free and safe to operate.

An approach that bears great promise is the biotransformation with non-pathogenic, easy-to-manage microorganisms, and their enzymes. Several chemical, chemoenzymatic and enzymatic routes have been proposed for the production of UDCA. In view of sustainability, instead of pursuing a step-wise approach, an integrated one-pot or one-flow reaction, involving highly selective enzymatic steps would be preferred.

When a multi-enzyme system is employed, the different enzyme activities, pH optima, cross reactions and inhibitions have to be taken into account in order to reach high product yields [109-111]. Furthermore, when a combination of chemical and enzymatic steps is employed special attention has to be paid to the compatibility: the combination of enzymatic and chemical transformation steps is the main task to achieve in order to obtain high yields of UDCA.

Nowadays, the most promising system for the biocatalytic production of UDCA are flow-reactors. They can be used for the setup of continuous working systems, lowering the quantity of catalyst needed and the time of each reaction. This technology was recently employed by Zheng et al. [93] leading to high yields (99%) and productivity (88.5 g L^{-1} d^{-1}) for the epimerization of CDCA to UDCA. However, the employed enzymes have different cofactor specificities, leading to the consumption of stoichiometric amounts of sacrificial substrates (pyruvate and glucose). In addition, substrate loadings in the latter process are still modest (10 mM). Therefore, there is much room for improvement and further studies are needed to design a truly sustainable integrated process for the production of UDCA.

Abbreviations

CA, cholic acid; CDCA, chenodeoxycholic acid; DCA, deoxycholic acid; DHCA, dehydrocholic acid; LCA, lithocholic acid; UCA, ursocholic acid; UDCA, ursodeoxycholic acid; HSDH, hydroxysteroid dehydrogenase; LDH, lactate dehydrogenase; GDH, glucose dehydrogenase.

Supporting Information

Supporting Information features Figure S1 relative to the C7 dehydroxylation mechanism of hydroxysteroids and Figure S2 relative to the postulated biochemical pathway for the C12 dehydroxylation.

Supporting Information File 1

Supporting Figures S1 and S2.
[https://www.beilstein-journals.org/bjoc/content/supplementary/1860-5397-14-33-S1.pdf]

Acknowledgements

This work was done as part of the ONE-FLOW project (https://one-flow.org) that has received funding from the European Union's FET-Open research and innovation actions (proposal 737266 - ONE-FLOW). We thank Linda Otten, Duncan McMillan and all the BOC group of TU Delft for the scientific discussions.

References

1. Ikegami, T.; Matsuzaki, Y. *Hepatol. Res.* **2008,** *38,* 123–131. doi:10.1111/j.1872-034X.2007.00297.x
2. Crosignani, A.; Battezzati, P. M.; Setchell, K. D. R.; Invernizzi, P.; Covini, G.; Zuin, M.; Podda, M. *Dig. Dis. Sci.* **1996,** *41,* 809–815. doi:10.1007/BF02213140
3. Salen, G.; Colalillo, A.; Verga, D.; Bagan, E.; Tint, G.; Shefer, S. *Gastroenterology* **1980,** *78,* 1412–1418.
4. Colombo, C.; Setchell, K. D. R.; Podda, M.; Crosignani, A.; Roda, A.; Curcio, L.; Ronchi, M.; Giunta, A. *J. Pediatr.* **1990,** *117,* 482–489. doi:10.1016/S0022-3476(05)81103-5
5. Colombo, C.; Crosignani, A.; Assaisso, M.; Battezzati, P. M.; Podda, M.; Giunta, A.; Zimmer-Nechemias, L.; Setchell, K. D. R. *Hepatology (Hoboken, NJ, U. S.)* **1992,** *16,* 924–930. doi:10.1002/hep.1840160412
6. Colombo, C.; Battezzati, P. M.; Podda, M.; Bettinardi, N.; Giunta, A. *Hepatology (Hoboken, NJ, U. S.)* **1996,** *23,* 1484–1490. doi:10.1002/hep.510230627
7. Combes, B.; Carithers, R. L.; Maddrey, W. C.; Lin, D.; McDonald, M. F.; Wheeler, D. E.; Eigenbrodt, E. H.; Muñoz, S. J.; Rubin, R.; Garcia-Tsao, G.; Bonner, G. F.; West, A. B.; Boyer, J. L.; Luketic, V. A.; Shiffman, M. L.; Mills, A. S.; Peters, M. G.; White, H. M.; Zetterman, R. K.; Rossi, S. S.; Hofmann, A. F.; Markin, R. S. *Hepatology (Hoboken, NJ, U. S.)* **1995,** *22,* 759–766. doi:10.1002/hep.1840220311
8. Podda, M.; Zuin, M.; Battezzati, P. M.; Ghezzi, C.; De Fazio, C.; Dioguardi, M. L. *Gastroenterology* **1989,** *96,* 222–229. doi:10.1016/0016-5085(89)90784-1
9. Thistle, J. L. *Semin. Liver Dis.* **1983,** *3,* 146–156. doi:10.1055/s-2008-1040680
10. Ward, A.; Brogden, R. N.; Heel, R. C.; Speight, T. M.; Avery, G. S. *Drugs* **1984,** *27,* 95–131. doi:10.2165/00003495-198427020-00001
11. Roda, E.; Bazzoli, F.; Labate, A. M. M.; Mazzella, G.; Roda, A.; Sama, C.; Festi, D.; Aldini, R.; Taroni, F.; Barbara, L. *Hepatology (Hoboken, NJ, U. S.)* **1982,** *2,* 804–810. doi:10.1002/hep.1840020611
12. Carrea, G.; Pilotti, A.; Riva, S.; Canzi, E.; Ferrari, A. *Biotechnol. Lett.* **1992,** *14,* 1131–1134. doi:10.1007/BF01027015
13. Hofmann, A. F. *Acta Chem. Scand.* **1963,** *17,* 173–186. doi:10.3891/acta.chem.scand.17-0173
14. Kanazawa, T.; Shimazaki, A.; Sato, T.; Hoshino, T. *Nippon Kagaku Zasshi* **1955,** *76,* 297–301. doi:10.1246/nikkashi1948.76.297
15. Fieser, L. F.; Rajagopalan, S. *J. Am. Chem. Soc.* **1950,** *72,* 5530–5536. doi:10.1021/ja01168a046
16. Sutherland, J. D.; Macdonald, I. A.; Forrest, T. P. *Prep. Biochem.* **1982,** *12,* 307–321. doi:10.1080/00327488208065679
17. Prabha, V.; Ohri, M. *World J. Microbiol. Biotechnol.* **2006,** *22,* 191–196. doi:10.1007/s11274-005-9019-y
18. Midtvedt, T.; Norman, A. *Acta Pathol. Microbiol. Scand.* **1967,** *71,* 629–638. doi:10.1111/j.1699-0463.1967.tb05183.x
19. Mahato, S. B.; Garai, S. *Steroids* **1997,** *62,* 332–345. doi:10.1016/S0039-128X(96)00251-6
20. Eggert, T.; Bakonyi, D.; Hummel, W. *J. Biotechnol.* **2014,** *191,* 11–21. doi:10.1016/j.jbiotec.2014.08.006
21. Bortolini, O.; Medici, A.; Poli, S. *Steroids* **1997,** *62,* 564–577. doi:10.1016/S0039-128X(97)00043-3
22. Mukhopadhyay, S.; Maitra, U. *Curr. Sci.* **2004,** *87,* 1666–1683.
23. Hofmann, A. F. *Arch. Intern. Med.* **1999,** *159,* 2647–2658. doi:10.1001/archinte.159.22.2647
24. Fini, A.; Roda, A. *J. Lipid Res.* **1987,** *28,* 755–759.
25. Bonar-Law, R. P.; Davis, A. P. *Tetrahedron* **1993,** *49,* 9829–9844. doi:10.1016/S0040-4020(01)80185-X
26. Maldonado Rodríguez, M. E. Biotrasformazioni di Acidi Biliari. Ph.D. Thesis, Università degli Studi di Ferrara, Italy, 2013.
27. Ahrens, E. H.; Craig, L. C. *J. Biol. Chem.* **1952,** *195,* 763–778.
28. Carey, M. C. *Hepatology (Hoboken, NJ, U. S.)* **1984,** *4,* 66S–71S. doi:10.1002/hep.1840040812
29. Fossati, E.; Polentini, F.; Carrea, G.; Riva, S. *Biotechnol. Bioeng.* **2006,** *93,* 1216–1220. doi:10.1002/bit.20753
30. Washizu, T.; Tomoda, I.; Kaneko, J. J. *J. Vet. Med. Sci.* **1991,** *53,* 81–86. doi:10.1292/jvms.53.81
31. Iser, J. H.; Sali, A. *Drugs* **1981,** *21,* 90–119. doi:10.2165/00003495-198121020-00002
32. Carey, M. C. *N. Engl. J. Med.* **1975,** *293,* 1255–1257. doi:10.1056/NEJM197512112932412
33. Pedrini, P.; Andreotti, E.; Guerrini, A.; Dean, M.; Fantin, G.; Giovannini, P. P. *Steroids* **2006,** *71,* 189–198. doi:10.1016/j.steroids.2005.10.002
34. Christiaens, H.; Leer, R.; Pouwels, P.; Verstraete, W. *Appl. Environ. Microbiol.* **1992,** *58,* 3792–3798.
35. Nakagawa, Y.; Hasegawa, A.; Hiratake, J.; Sakata, K. *Protein Eng., Des. Sel.* **2007,** *20,* 339–346. doi:10.1093/protein/gzm025
36. Torres-Gavilán, A.; Castillo, E.; López-Munguía, A. *J. Mol. Catal. B: Enzym.* **2006,** *41,* 136–140. doi:10.1016/j.molcatb.2006.06.001
37. Feng, Y.; Siu, K.; Wang, N.; Ng, K.-M.; Tsao, S.-W.; Nagamatsu, T.; Tong, Y. *J. Ethnobiol. Ethnomed.* **2009,** *5,* 2. doi:10.1186/1746-4269-5-2
38. Delgado, H.; Cedeño, C.; de Oca, N.; Villoch, A. *Rev. Salud Anim.* **2015,** *37,* 1–9.
39. Delgado, D.; Roque, P.; Cedeño, P.; Villoch, C. *Rev. Salud Anim.* **2015,** *37,* 69–78.
40. Delgado, H.; Cedeño, C.; Villoch, A.; Dueñas, R. *Rev. Salud Anim.* **2015,** *37,* 198–202.
41. Volkman, J. *Appl. Microbiol. Biotechnol.* **2003,** *60,* 495–506. doi:10.1007/s00253-002-1172-8
42. Huang-Minlon, B. Y. *J. Am. Chem. Soc.* **1949,** *71,* 3301–3303. doi:10.1021/ja01178a008
43. Cranwell, P. B.; Russell, A. T.; Smith, C. D. *Synlett* **2016,** *27,* 131–135. doi:10.1055/s-0035-1560805
44. Newman, S. G.; Gu, L.; Lesniak, C.; Victor, G.; Meschke, F.; Abahmane, L.; Jensen, K. F. *Green Chem.* **2014,** *16,* 176–180. doi:10.1039/C3GC41942H
45. Parquet, E.; Lin, Q. *J. Chem. Educ.* **1997,** *74,* 1225. doi:10.1021/ed074p1225

46. Dietl, A.; Ferousi, C.; Maalcke, W. J.; Menzel, A.; de Vries, S.; Keltjens, J. T.; Jetten, M. S. M.; Kartal, B.; Barends, T. R. M. *Nature* **2015,** *527,* 394–397. doi:10.1038/nature15517
47. Sato, Y.; Ikekawa, N. *J. Org. Chem.* **1959,** *24,* 1367–1368. doi:10.1021/jo01091a623
48. Harris, J. N.; Hylemon, P. B. *Biochim. Biophys. Acta, Lipids Lipid Metab.* **1978,** *528,* 148–157. doi:10.1016/0005-2760(78)90060-7
49. Braun, M.; Lünsdorf, H.; Bückmann, A. F. *Eur. J. Biochem.* **1991,** *196,* 439–450. doi:10.1111/j.1432-1033.1991.tb15835.x
50. Macdonald, I. A.; Jellett, J. F.; Mahony, D. E.; Holdeman, L. V. *Appl. Environ. Microbiol.* **1979,** *37,* 992–1000.
51. Macdonald, I. A.; Meier, E. C.; Mahony, D. E.; Costain, G. A. *Biochim. Biophys. Acta, Lipids Lipid Metab.* **1976,** *450,* 142–153. doi:10.1016/0005-2760(76)90086-2
52. Aigner, A.; Gross, R.; Schmid, R. D.; Braun, M.; Mauer, S. Novel 12 alpha-hydroxysteroid dehydrogenase, production and use thereof. US Patent 20110091921 A1, April 21, 2011.
53. Fossati, E.; Carrea, G.; Riva, S.; Polentini, F. Process for the selective oxydation of cholic acid. Eur. Patent EP 1731618 A1, Dec 13, 2006.
54. Edenharder, R. *J. Steroid Biochem.* **1984,** *21,* 413–420. doi:10.1016/0022-4731(84)90304-2
55. Saltzman, W. H. Synthesis of steroids. U.S. Patent US 3954562 A, May 4, 1976.
56. Wells, J. E.; Hylemon, P. B. *Appl. Environ. Microbiol.* **2000,** *66,* 1107–1113. doi:10.1128/AEM.66.3.1107-1113.2000
57. Ridlon, J. M.; Kang, D.-J.; Hylemon, P. B. *Anaerobe* **2010,** *16,* 137–146. doi:10.1016/j.anaerobe.2009.05.004
58. Ridlon, J. M.; Harris, S. C.; Bhowmik, S.; Kang, D.-J.; Hylemon, P. B. *Gut Microbes* **2016,** *7,* 22–39. doi:10.1080/19490976.2015.1127483
59. Ferrari, M.; Zinetti, F. Process for preparing high purity ursodeoxycholic acid. WO Patent WO 2014020024 A1 06/02/2014.
60. Dangate, P. S.; Salunke, C. L.; Akamanchi, K. G. *Steroids* **2011,** *76,* 1397–1399. doi:10.1016/j.steroids.2011.07.009
61. Parr, R. G.; Yang, W. *J. Am. Chem. Soc.* **1984,** *106,* 4049–4050. doi:10.1021/ja00326a036
62. Samuelsson, B. *Acta Chem. Scand.* **1960,** *14,* 17–20. doi:10.3891/acta.chem.scand.14-0017
63. Coleman, J. P.; Hudson, L. L.; Adams, M. J. *J. Bacteriol.* **1994,** *176,* 4865–4874. doi:10.1128/jb.176.16.4865-4874.1994
64. Baron, S. F.; Franklund, C. V.; Hylemon, P. B. *J. Bacteriol.* **1991,** *173,* 4558–4569. doi:10.1128/jb.173.15.4558-4569.1991
65. Ferrandi, E. E.; Bertolesi, G. M.; Polentini, F.; Negri, A.; Riva, S.; Monti, D. *Appl. Microbiol. Biotechnol.* **2012,** *95,* 1221–1233. doi:10.1007/s00253-011-3798-x
66. Bakonyi, D.; Hummel, W. *Enzyme Microb. Technol.* **2017,** *99,* 16–24. doi:10.1016/j.enzmictec.2016.12.006
67. Yoshimoto, T.; Higashi, H.; Kanatani, A.; Lin, X. S.; Nagai, H.; Oyama, H.; Kurazono, K.; Tsuru, D. *J. Bacteriol.* **1991,** *173,* 2173–2179. doi:10.1128/jb.173.7.2173-2179.1991
68. Ueda, S.; Oda, M.; Imamura, S. *Int. J. Biol. Macromol.* **2004,** *4,* 33–38.
69. Bennett, M. J.; McKnight, S. L.; Coleman, J. P. *Curr. Microbiol.* **2003,** *47,* 475–484. doi:10.1007/s00284-003-4079-4
70. Ji, W.; Chen, Y.; Zhang, H.; Zhang, X.; Li, Z.; Yu, Y. *Microbiol. Res.* **2014,** *169,* 148–154. doi:10.1016/j.micres.2013.07.009
71. Monti, D.; Ferrandi, E. E.; Riva, S.; Polentini, F. New process for the selective oxidation of bile acids, their salts or derivatives. WO Patent WO 2012131591 A1, Oct 4, 2012.
72. Gupta, A.; Tschentscher, A.; Bobkova, M. Process for the enantioselective reduction and oxidation, respectively, of steroids. U.S. Patent US 20090280525 A1, Nov 12, 2009.
73. O'Leary, N. A.; Wright, M. W.; Brister, J. R.; Ciufo, S.; Haddad, D.; McVeigh, R.; Rajput, B.; Robbertse, B.; Smith-White, B.; Astashyn, D. A.-A. A.; Batretdin, A.; Bao, Y.; Blinkova, O.; Brover, V.; Chetvernin, V.; Choi, J.; Cox, E.; Ermolaeva, O.; Farrell, C. M.; Goldfarb, T.; Gupta, T.; Haft, D.; Hatcher, E.; Hlavina, W.; Joardar, V. S.; Kodali, V. K.; Li, W.; Maglott, D.; Masterson, P.; McGarvey, K. M.; Murphy, M. R.; O'Neill, K.; Pujar, S.; Rangwala, S. H.; Rausch, D.; Riddick, L. D.; Schoch, C.; Shkeda, A.; Storz, S. S.; Sun, H.; Thiaud-Nissen, F.; Tolstoy, I.; Tully, R. E.; Vatsan, A. R.; Wallin, C.; Webb, D.; Wu, W.; Landrum, M. J.; Kimchi, A.; Tatusova, T.; DiCuccio, M.; Kitts, P.; Murphy, T. D.; Pruitt, K. D. *Nucleic Acids Res.* **2015,** *44,* D733–D745. doi:10.1093/nar/gkv1189
74. Liu, L.; Aigner, A.; Schmid, R. D. *Appl. Microbiol. Biotechnol.* **2011,** *90,* 127–135. doi:10.1007/s00253-010-3052-y
75. Lee, J.-Y.; Arai, H.; Nakamura, Y.; Fukiya, S.; Wada, M.; Yokota, A. *J. Lipid Res.* **2013,** *54,* 3062–3069. doi:10.1194/jlr.M039834
76. Zheng, M.-M.; Chen, K.-C.; Wang, R.-F.; Li, H.; Li, C.-X.; Xu, J.-H. *J. Agric. Food Chem.* **2017,** *65,* 1178–1185. doi:10.1021/acs.jafc.6b05428
77. Hummel, W.; Bakonyi, D. 7-beta-hydroxysteroid dehydrogenase mutants and process for the preparation of ursodeoxycholic acid. WO Patent WO 2016016213 A1, Feb 4, 2016. ; .
78. Bovara, R.; Carrea, G.; Riva, S.; Secundo, F. *Biotechnol. Lett.* **1996,** *18,* 305–308. doi:10.1007/BF00142949
79. Monti, D.; Ottolina, G.; Carrea, G.; Riva, S. *Chem. Rev.* **2011,** *111,* 4111–4140. doi:10.1021/cr100334x
80. Macdonald, I. A.; Hutchison, D. M. *J. Steroid Biochem.* **1982,** *17,* 295–303. doi:10.1016/0022-4731(82)90203-5
81. Sutherland, J. D.; Macdonald, I. A. *J. Lipid Res.* **1982,** *23,* 726–732.
82. Macdonald, I.; Rochon, Y.; Hutchison, D.; Holdeman, L. *Appl. Environ. Microbiol.* **1982,** *44,* 1187–1195.
83. Hirano, S.; Masuda, N. *J. Lipid Res.* **1982,** *23,* 1152–1158.
84. Sutherland, J. D.; Holdeman, L. V.; Williams, C. N.; Macdonald, I. A. *J. Lipid Res.* **1984,** *25,* 1084–1089.
85. Medici, A.; Pedrini, P.; Bianchini, E.; Fantin, G.; Guerrini, A.; Natalini, B.; Pellicciari, R. *Steroids* **2002,** *67,* 51–56. doi:10.1016/S0039-128X(01)00136-2
86. Braun, M.; Sun, B.; Anselment, B.; Weuster-Botz, D. *Appl. Microbiol. Biotechnol.* **2012,** *95,* 1457–1468. doi:10.1007/s00253-012-4072-6
87. Sun, B.; Kantzow, C.; Bresch, S.; Castiglione, K.; Weuster-Botz, D. *Biotechnol. Bioeng.* **2013,** *110,* 68–77. doi:10.1002/bit.24606
88. Bakonyi, D.; Wirtz, A.; Hummel, W. *Z. Naturforsch., B: Chem. Sci.* **2012,** *67,* 1037–1044. doi:10.5560/ZNB.2012-0165
89. Liu, L.; Braun, M.; Gebhardt, G.; Weuster-Botz, D.; Gross, R.; Schmid, R. D. *Appl. Microbiol. Biotechnol.* **2013,** *97,* 633–639. doi:10.1007/s00253-012-4340-5
90. Giovannini, P. P.; Grandini, A.; Perrone, D.; Pedrini, P.; Fantin, G.; Fogagnolo, M. *Steroids* **2008,** *73,* 1385–1390. doi:10.1016/j.steroids.2008.06.013
91. Monti, D.; Ferrandi, E. E.; Zanellato, I.; Hua, L.; Polentini, F.; Carrea, G.; Riva, S. *Adv. Synth. Catal.* **2009,** *351,* 1303–1311. doi:10.1002/adsc.200800727

92. Zheng, M.-M.; Wang, R.-F.; Li, C.-X.; Xu, J.-H. *Process Biochem. (Oxford, U. K.)* **2015,** *50,* 598–604. doi:10.1016/j.procbio.2014.12.026
93. Zheng, M.-M.; Chen, F.-F.; Li, H.; Li, C.-X.; Xu, J.-H. *ChemBioChem* **2017,** in press. doi:10.1002/cbic.201700415
94. Ji, Q.; Tan, J.; Zhu, L.; Lou, D.; Wang, B. *Biochem. Eng. J.* **2016,** *105,* 1–9. doi:10.1016/j.bej.2015.08.005
95. Sawada, H.; Kulprecha, S.; Nilubol, N.; Yoshida, T.; Kinoshita, S.; Taguchi, H. *Appl. Environ. Microbiol.* **1982,** *44,* 1249–1252.
96. Carlström, K.; Kirk, D.; Sjövall, J. *J. Lipid Res.* **1981,** *22,* 1225–1234.
97. Kollerov, V. V.; Monti, D.; Deshcherevskaya, N. O.; Lobastova, T. G.; Ferrandi, E. E.; Larovere, A.; Gulevskaya, S. A.; Riva, S.; Donova, M. V. *Steroids* **2013,** *78,* 370–378. doi:10.1016/j.steroids.2012.12.010
98. Kollerov, V. V.; Lobastova, T. G.; Monti, D.; Deshcherevskaya, N. O.; Ferrandi, E. E.; Fronza, G.; Riva, S.; Donova, M. V. *Steroids* **2016,** *107,* 20–29. doi:10.1016/j.steroids.2015.12.015
99. Möbus, E.; Maser, E. *J. Biol. Chem.* **1998,** *273,* 30888–30896. doi:10.1074/jbc.273.47.30888
100. Arends, I. W. C. E.; Li, Y.-X.; Ausan, R. A.; Sheldon, R. A. *Tetrahedron* **2006,** *62,* 6659–6665. doi:10.1016/j.tet.2005.12.076
101. Igimi, H.; Carey, M. C. *J. Lipid Res.* **1980,** *21,* 72–90.
102. Cabral, D. J. In *Physical chemistry of bile, Compr. Physiol.;* Small, D. M., Ed.; John Wiley & Sons, 2010.
103. Carey, M. C.; Small, D. M. *Arch. Intern. Med.* **1972,** *130,* 506–527. doi:10.1001/archinte.1972.03650040040005
104. Hisadome, T.; Nakama, T.; Itoh, H.; Furusawa, T. J. *Gastroenterol. Jpn.* **1980,** *15,* 257–263.
105. Khmelnitsky, Y. L.; Levashov, A. V.; Klyachko, N. L.; Martinek, K. *Enzyme Microb. Technol.* **1988,** *10,* 710–724. doi:10.1016/0141-0229(88)90115-9
106. Riva, S.; Bovara, R.; Zetta, L.; Pasta, P.; Ottolina, G.; Carrea, G. *J. Org. Chem.* **1988,** *53,* 88–92. doi:10.1021/jo00236a018
107. Bovara, R.; Canzi, E.; Carrea, G.; Pilotti, A.; Riva, S. *J. Org. Chem.* **1993,** *58,* 499–501. doi:10.1021/jo00054a039
108. Monti, D.; Ferrandi, E. E.; Riva, S.; Polentini, F. Process for the selective reduction of bile acids, their salts or derivatives, in a biphasic system. WO Patent WO 2013179210 A2, Dec 5, 2013.
109. Ricca, E.; Brucher, B.; Schrittwieser, J. H. *Adv. Synth. Catal.* **2011,** *353,* 2239–2262. doi:10.1002/adsc.201100256
110. Oroz-Guinea, I.; García-Junceda, E. *Curr. Opin. Chem. Biol.* **2013,** *17,* 236–249. doi:10.1016/j.cbpa.2013.02.015
111. Riva, S.; Fessner, W.-D. *Cascade Biocatalysis Integrating Stereoselective and Environmentally Friendly Reactions;* John Wiley & Sons, 2014.

License and Terms

BEILSTEIN JOURNAL OF ORGANIC CHEMISTRY

Continuous multistep synthesis of 2-(azidomethyl)oxazoles

Thaís A. Rossa[1,2], Nícolas S. Suveges[3], Marcus M. Sá[2], David Cantillo[*1,4] and C. Oliver Kappe[*1,4]

Full Research Paper

Open Access

Address:
[1]Institute of Chemistry, University of Graz, NAWI Graz, Heinrichstrasse 28, 8010 Graz, Austria, [2]Departamento de Química, Universidade Federal de Santa Catarina, Florianópolis 88040-900, SC, Brazil, [3]Chemistry Institute, Federal University of Rio de Janeiro, Rio de Janeiro, RJ, Brazil 22941-909, and [4]Research Center Pharmaceutical Engineering GmbH (RCPE), Inffeldgasse 13, 8010 Graz, Austria

Email:
David Cantillo[*] - david.cantillo@rcpe.at; C. Oliver Kappe[*] - oliver.kappe@uni-graz.at

* Corresponding author

Keywords:
azirines; continuous flow; heterocycles; oxazoles; process integration; vinyl azides

Beilstein J. Org. Chem. **2018,** *14,* 506–514.
doi:10.3762/bjoc.14.36

Received: 22 November 2017
Accepted: 08 February 2018
Published: 23 February 2018

This article is part of the Thematic Series "Integrated multistep flow synthesis".

Guest Editor: V. Hessel

Abstract

An efficient three-step protocol was developed to produce 2-(azidomethyl)oxazoles from vinyl azides in a continuous-flow process. The general synthetic strategy involves a thermolysis of vinyl azides to generate azirines, which react with bromoacetyl bromide to provide 2-(bromomethyl)oxazoles. The latter compounds are versatile building blocks for nucleophilic displacement reactions as demonstrated by their subsequent treatment with NaN_3 in aqueous medium to give azido oxazoles in good selectivity. Process integration enabled the synthesis of this useful moiety in short overall residence times (7 to 9 min) and in good overall yields.

Introduction

Oxazoles are an important class of five-membered aromatic heterocycles containing one oxygen and one nitrogen atom in their structures. The oxazole moiety is relatively stable and is found widely in nature [1-3]. Naturally occurring oxazoles include compounds with antibiotic or antimicrobial properties such as pimprinine [4] or phenoxan [5] (Figure 1a). Also many synthetic active pharmaceutical ingredients (API) contain the oxazole as an active moiety [1-3]. Oxaprozin, for example, is an important non-narcotic, non-steroidal anti-inflammatory drug [6,7]. Sulfamoxole is a broad-spectrum antibiotic for the treatment of bacterial infections (Figure 1b) [8]. In addition, ongoing studies show the potential of amino and amido-oxazoles to act as fluorescent dipeptidomimetics (Figure 1c) [9]. Due to their diene character, oxazoles find also use as intermediates in the synthesis of other organic scaffolds such as furans and pyridines, via cycloaddition/retro-cycloaddition

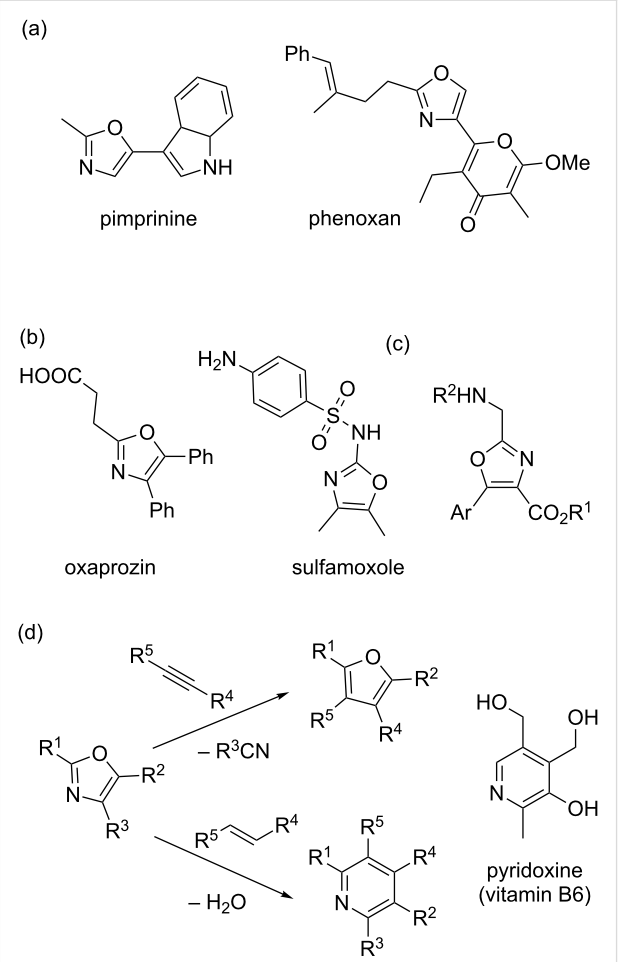

Figure 1: Examples of naturally occurring oxazoles (a); some drugs containing oxazole as the active moiety (b); general structure of fluorescent dipeptidomimetics derived from trisubstituted oxazoles (c); reactivity of the oxazole system as an azadiene (d).

tandem processes (Figure 1d) [10-13]. A classical example is the preparation of pyridoxine (a form of vitamin B6) using this approach [14,15].

There are several methods for the preparation of oxazoles described in the literature. These include ring-closure reactions of diazocarbonyl compounds with amides or nitriles [16], α-haloketones and amides [17-19], cyanohydrins and aldehydes (Fischer synthesis) [20,21], or oxidative additions of α-methylene ketones to nitriles [22,23]. An alternative approach consists of the ring expansion of azirines, which can be prepared from vinyl azides **1**, by the reaction with carbonyl compounds. Substituted 2-acylazirines rearrange to oxazoles in the presence of bases [24-26]. In addition the light-mediated synthesis of oxazoles from azirines and aldehydes also has been described by Lu and Xiao [27]. Hassner and Fowler described the reaction of azirines **2** with acyl chlorides with formation of intermediate adduct **3** to give oxazoles **4** in polar solvents (Scheme 1) [28,29]. In the latter reaction amide **5** was formed as a side-product and the aziridine intermediate **3** was stable and could be isolated when the reaction was carried out in non-polar solvents.

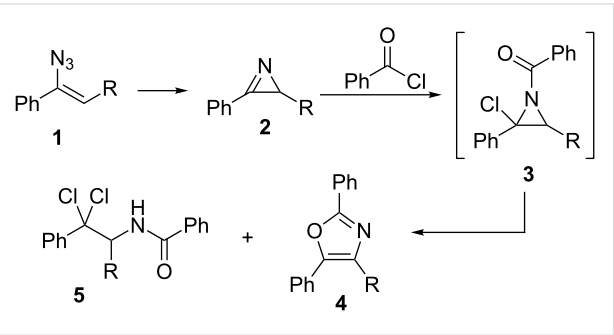

Scheme 1: Synthesis of oxazoles **4** by addition of acyl chlorides to azirines **2**, as described by Hassner et al. [28,29].

In particular, 2-(halomethyl)oxazoles **6** are a class of compounds rather underexplored, even though they are frequently key intermediates in the total synthesis of natural products [30-32]. Recently, Patil and Luzzio reported the preparation of a wide range of 2-substituted derivatives **7** by a simple nucleophilic halide displacement from 2-chloromethyl-4,5-diaryloxazoles, illustrating their usefulness (Scheme 2) [33]. In a related work, Luzzio et al. described the synthesis of 1,4-disubstituted triazoles **8** through click reaction between 2-azidomethyl-4,5-diaryloxazoles and alkynes in the presence of a copper(I) catalyst (Scheme 2). The authors were able to synthesize an array of small-molecule peptidomimetics that inhibited *Porphyromonas gingivalis* biofilm formation [34].

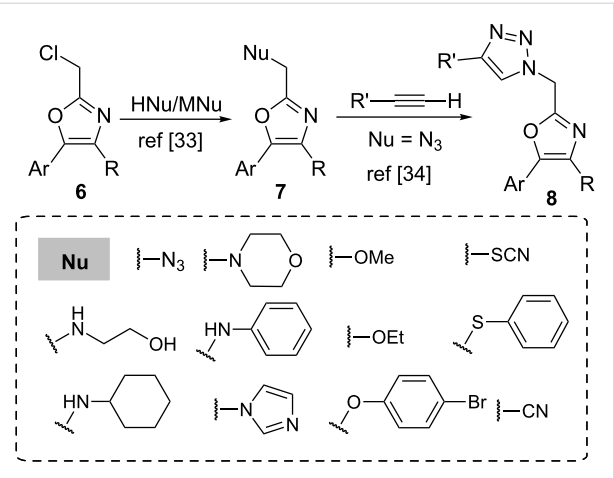

Scheme 2: Preparation of 2-functionalized oxazoles **7** from 2-(chloromethyl)oxazoles **6** and their application to the synthesis of peptidomimetics **8**.

Important drawbacks observed in the generation of compounds of type **7** include the instability of the halide intermediate **6**,

which might be difficult to isolate due decomposition reactions, as well as selectivity issues during the generation of the oxazole ring. It has been shown that problems associated with unstable intermediates or reagents can be overcome with the use of continuous-flow chemistry. Continuous-flow processing has demonstrated to be an ideal tool for the development of uninterrupted multistep reactions [35-37]. The integration of several sequential steps can be readily achieved through a continuous addition of reagent streams, quenching, liquid–liquid extraction, or even filtration stages, thus avoiding the handling of unstable intermediates [35-37].

In this article we present an integrated continuous-flow procedure for the preparation of 2-(azidomethyl)oxazoles **7** starting from vinyl azides through an azirine intermediate (Scheme 3). The process starts with the generation of the azirine from the vinyl azide by thermolysis. Formation of azirines from vinyl azides by photolysis and thermolysis in continuous flow has been previously described [38,39]. The azirine intermediate is then reacted with a 2-haloacyl halide at room temperature, to form the 2-(halomethyl)oxazole moiety. Subsequent reaction with an aqueous stream containing NaN_3 then leads to the formation of the desired 2-(azidomethyl)oxazole. The optimization of each reaction step and the integration to a fully continuous process are described in detail.

Results and Discussion

Thermolysis of the vinyl azide and oxazole formation. Batch optimization

The reaction conditions for the thermolysis of the vinyl azide and the subsequent ring expansion of the intermediate azirine to form the oxazole ring were initially optimized in batch. For these experiments, vinyl azide **1a** was used as a model substrate. The small-scale batch thermolyses were carried out using sealed 1.5 mL vials heated in an aluminum platform. A 0.5 M solution of substrate **1a** was prepared using acetone as the solvent. The experiments were carried out placing 0.5 mL of the solution in the vial, which was sealed with a crimp-cap. The reactions were performed at three different temperatures (130–150 °C, Table 1). Notably, at 150 °C a very fast (1 min) and clean reaction (>99% purity by HPLC–UV analysis) was achieved.

Table 1: Batch optimization of the thermolysis of vinyl azide **1a**.[a]

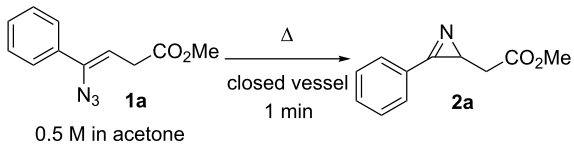

entry	temp. (°C)	conv. (%)[b]	purity (%)[b]
1	130	88	>99
2	140	97	>99
3	150	>99	>99

[a]Conditions: **1a** in acetone (0.5 M), 0.5 mL solution in a 1.5 mL vial.
[b]Determined by HPLC peak area integration at 254 nm.

Next, the formation of 2-(bromomethyl)oxazole **6a** from azirine **2a** was also optimized under batch conditions. All reactions were carried out under an argon atmosphere using a 0.5 M solution of the substrate **2a** in acetone. In general, the addition of the reagents was performed at 0 °C in an ice-bath followed by stirring the reaction mixture at room temperature. When triethylamine (TEA) or *N,N*-diisopropylethylamine (DIPEA) were used as the base a solid formed after a few minutes in the reaction mixture (Table 2, entries 1–4), probably their corresponding ammonium bromide salts. Yet, good purities were achieved employing both bases and the incomplete conversions were ascribed to the presence of water in the reaction mixture. For this reason, further transformations were carried out in acetone dried over molecular sieves (3 Å). Using 1,5-diazabi-

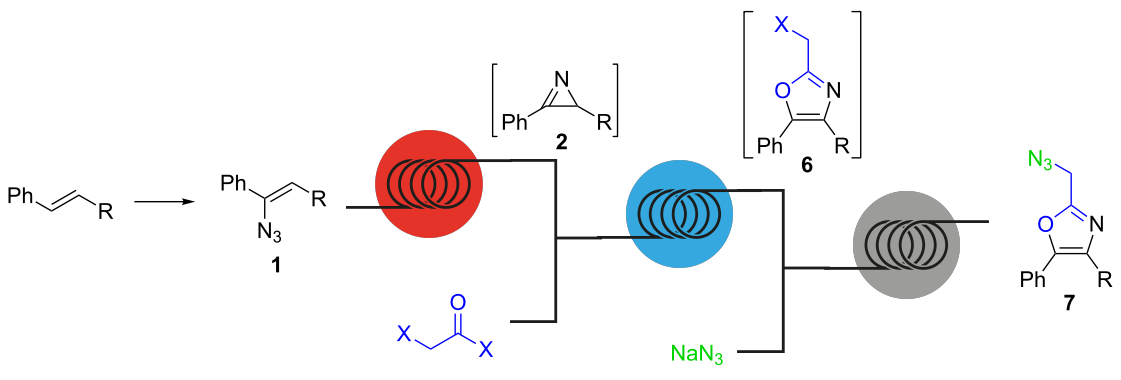

Scheme 3: Integrated continuous-flow synthesis of 2-(azidomethyl)oxazoles **7**.

Table 2: Optimization of the reaction conditions for the generation of oxazole **6a** from azirine **2a**.[a]

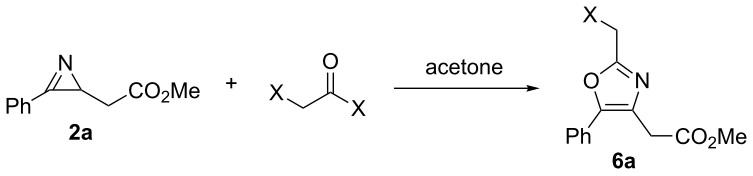

entry	halide equiv	X	base (equiv)	time (min)	temp.	conv. (%)[b]	purity (%)[b]
1[c]	1.1	Br	TEA (1.1)	3	0 °C to rt	90	82
2[c]	1.1	Br	TEA (1.1)	30	0 °C to rt	94	77
3[c]	1.2	Br	DIPEA (1.1)	3	0 °C to rt	66	76
4[c]	1.2	Br	DIPEA (1.1)	30	0 °C to rt	76	77
5	1.1	Br	DBN (1.1)	3	0 °C to rt	>99	74
6	1.1	Br	DBN (1.1)	30	0 °C to rt	>99	70
7	1.1	Cl	DBN (1.1)	10	0 °C to rt	92	79
8[d]	1.1	Br	DBN (1.1)	5	0 °C to rt	>99	75
9[d]	1.1	Br	DBN (1.1)	5	−10 °C	>99	73
10[e]	1.1	Br	DBN (1.1)	4	rt	>99	81
11	1.1	Br	–	1	rt	>99	77
12	1.0	Br	–	1	rt	>99	79
13	1.3	Br	–	1	rt	>99	80

[a]Conditions: 0.50 mL solution of **2a** in acetone (0.5 M) was mixed with 0.50–0.65 mL of a solution of the acyl halide in acetone (0.5 M), followed by addition of the base (0.275 mmol). [b]Determined by HPLC (254 nm) peak area integration. [c]Formation of insoluble solid during the reaction. [d]Base added after 3 min of reaction. [e]Substrate added after 1 min of reaction.

cyclo[4.3.0]non-5-ene (DBN) as the base (Table 2, entry 5) full conversion of the azirine **2a** was observed after 3 min reaction time. In this case the oxazole **6a** was formed with 74% purity and no formation of solids was observed. At longer reaction time (30 min) a slight decrease in purity could be detected, probably due to slow decomposition of **6a** (Table 2, entry 6). The reaction with chloroacetyl chloride instead of the bromo derivative delivered the corresponding (chloromethyl)oxazole with similar selectivity, the reaction was slower though, with 92% conversion being achieved after 10 min (Table 2, entry 7). The adjustment of other parameters such as the order of added reactants or variation in temperature showed little influence on the outcome of the reaction (Table 2, entries 8–10). Notably, oxazole **6a** was also formed in the absence of base (Table 2, entries 11–13). This was probably due to the weak basic character of the oxazole moiety itself, producing the oxazole hydrobromide. Finally, the variation of the amount of bromoacetyl bromide had no significant effect on the outcome of the reaction (Table 2, entries 12 and 13).

To identify the reaction byproducts formed during the coupling of azirine **2a** and bromoacetyl bromide, the reaction was performed on a 3 mmol scale. The reaction mixture was quenched with $NaHCO_3$ solution, extracted with ethyl acetate and concentrated under reduced pressure. The ^{1}H NMR analysis of the crude product mixture revealed three major side products. Purification by column chromatography permitted the separation and isolation of each component (Scheme 4), which were characterized by ^{1}H NMR, ^{13}C NMR and low-resolution mass spectroscopy. In agreement with the observations by Hassner et al. [28,29], dibromoamide **5a** and its hydrolysis product **9a** were obtained in addition to ketoester **10a**. The distribution profile

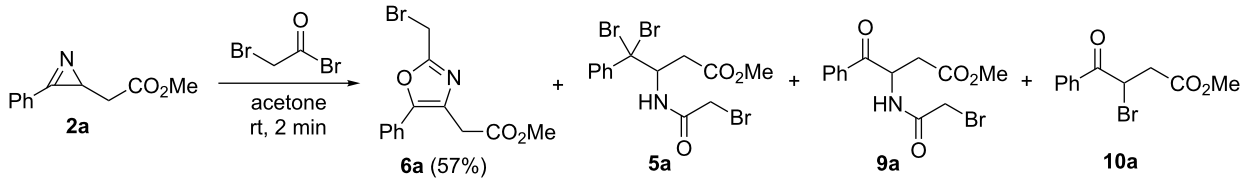

Scheme 4: Side products generated during the reaction of azirine **2a** with bromoacyl bromide at room temperature.

calculated by ^{1}H NMR peak integration revealed a composition of 76% product **6a**, and side products in 7% (**5a**), 10% (**9a**) and 7% (**10a**), respectively. The oxazole **6a** was isolated as yellow solid (mp 76.3–78.1 °C) in 57% yield.

The optimization of the reaction conditions for the nucleophilic halide displacement with sodium azide were also evaluated in batch. A one-pot procedure starting from the azirine (without isolation of the 2-(bromomethyl)oxazole) was utilized to simulate the conditions of an integrated process. Thus, azirine **2a** was reacted with bromoacetyl bromide in a 1.5 mL vial using the conditions stated in Figure 2 (1.1 equiv bromide added at 0 °C, cf. Table 2, entry 5) in dry acetone for 3 min. Then, DBN was added to neutralize the acidic medium, followed by a 2.5 M aqueous solution of NaN_3 (1.1 equiv) and the resulting mixture was stirred at room temperature. A conversion of 89% to **7a** from bromo oxazole **6a** with a selectivity of 74% was achieved after 30 min (Figure 2).

Subsequently, the amount of NaN_3 was increased to 1.3 equiv to enhance the reaction rate. During the formation of the 2-(bromomethyl)oxazoles **6** addition of a base is not required (see Table 2, entries 11–13). However, neutralization of the resulting oxazole hydrobromide is required prior to the addition of NaN_3 in order to avoid the generation of hydrazoic acid. Taking this into account, we decided to replace DBN by less expensive DIPEA for the subsequent reactions. Using both substrates **2a** and **2b**, it was observed that after 5 min of reaction at rt, the conversion of bromo oxazoles **6** into azido oxazoles **7** was up to 92% (Table 3, entries 1 and 4). When the reaction temperature was increased from rt to 50 °C, good conversions were achieved after 5 min reaction for both for the model substrate **2a** and the azirine **2b** (Table 3, entries 2 and 5). NaN_3 was not fully soluble in the reaction mixture (after mixing with the acetone medium), which would be problematic for the later translation to flow conditions. Diluting the NaN_3 solution from 2.5 M to 1.5 M (and therefore adding a larger volume of the solution to obtain the same excess of the reagent) resulted in fully homogeneous conditions suitable for flow processing (Table 3, entry 3).

Continuous-flow experiments

Azirine formation. With the optimal conditions for the three reaction steps in hand, we translated the process to continuous-flow conditions. For that purpose, individual continuous-flow reactors for each step were setup, the reaction conditions re-optimized when necessary, and finally all the steps integrated in a single continuous stream.

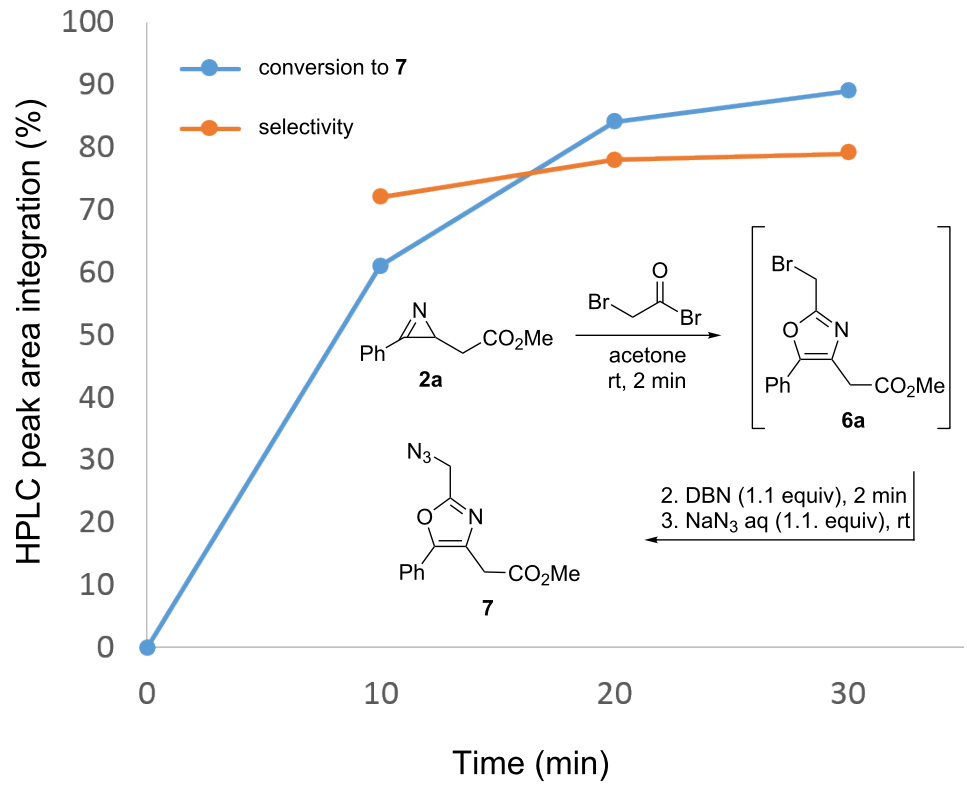

Figure 2: HPLC monitoring of the formation of 2-(azidomethyl)oxazole **7a**.

Table 3: Batch optimization of the generation of 2-(azidomethyl)oxazoles **7a** and **7b**.[a]

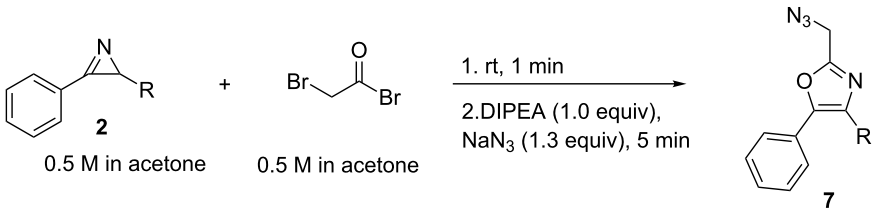

entry	R	NaN_3 conc. (M)	temp. (°C)[b]	conv. (%)[c,d]	purity (%)[d]
1	CH_2CO_2Me (**2a**)	2.5	rt	84	80
2	CH_2CO_2Me (**2a**)	2.5	50 °C	95	69
3	CH_2CO_2Me (**2a**)	1.5	50 °C	97	74
4	H (**2b**)	2.5	rt	92	69
5	H (**2b**)	2.5	50 °C	97	67

[a]Conditions: 0.4 mL of a 0.5 M solution of azirine in acetone, bromoacetyl bromide injected as a 0.5 M solution. [b]Temperature for the reaction with NaN_3. [c]Conversion for the nucleophilic displacement step. [d]Determined by HPLC (254 nm) peak area integration.

The thermolysis of vinyl azide **1** was performed in a continuous flow reactor consisting of a perfluoroalkoxy (PFA) coil (0.5 mL, 0.8 mm i.d.) immersed in a silicon bath at 150 °C. The vinyl azide solution in acetone was introduced into the reactor by a syringe pump (Syrris) with variable flow rates (Table 4) to obtain different residence times. The system was pressurized using a back-pressure regulator (BPR, Upchurch) at 17 bar (250 psi). The reaction mixture was cooled by immersing a second section of the coil reactor in an ice bath, to avoid damage of the BPR by the hot reaction mixture and evaporation of the solvent after the pressure release. Notably, flow rates had to be reduced with respect to those calculated for a residence time of 1 min for the generation of azirine **2a**, probably due to an expansion of the reaction mixture from the N_2 generation, which reduced the actual residence time within the coil (Table 4, entries 1 and 2). Using the same flow setup azirines **2b** and **2c** were also successfully generated from the corresponding vinyl azides (Table 4, entries 3–5).

The continuous-flow setup was then extended by incorporating a second reagent feed with a stream containing the bromoacetyl bromide solution (0.5 M in acetone, Figure 3). A vessel was placed between the two reaction zones to release the N_2 generated during the azirine formation, which was maintained under argon atmosphere. Using this system, the crude reaction mixture obtained from the first reaction zone, containing the azirine in acetone, was directly pumped into the second reaction zone (500 µL/min), mixed with the bromoacetyl bromide stream in a T-mixer, and reacted at 30 °C in a PFA tubing (1 mL volume). Using a flow rate of 500 µL/min in the feed containing the bromoacetyl bromide solution – corresponding to 1.0 equiv of the bromide with respect to the starting vinyl azide – both

Table 4: Continuous-flow generation of azirines **2** by thermolysis of vinyl azides **1**.[a]

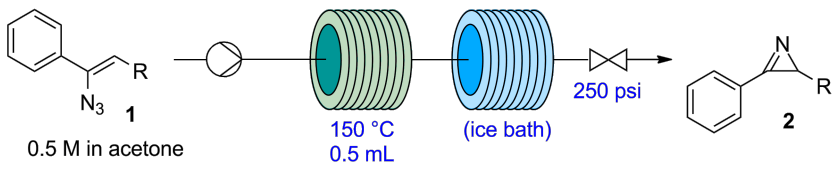

entry	R	flow rate (µL/min)[b]	time (min)	conv. (%)[c]	purity (%)[c]
1	CH_2CO_2Me (**2a**)	500	1	98	100
2	CH_2CO_2Me (**2a**)	250	2	100	100
3	H (**2b**)	250	2	91	92
4	H (**2b**)	167	3	95	94
5	CH_2OH (**2c**)	500	1	100	94

[a]Conditions: 0.5 M substrate in acetone, 5 mL reaction mixture (2.5 mmol) collected from the reactor output. [b]Theoretical residence time calculated from the flow rate and reactor volume. [c]Determined by HPLC (254 nm) peak area integration.

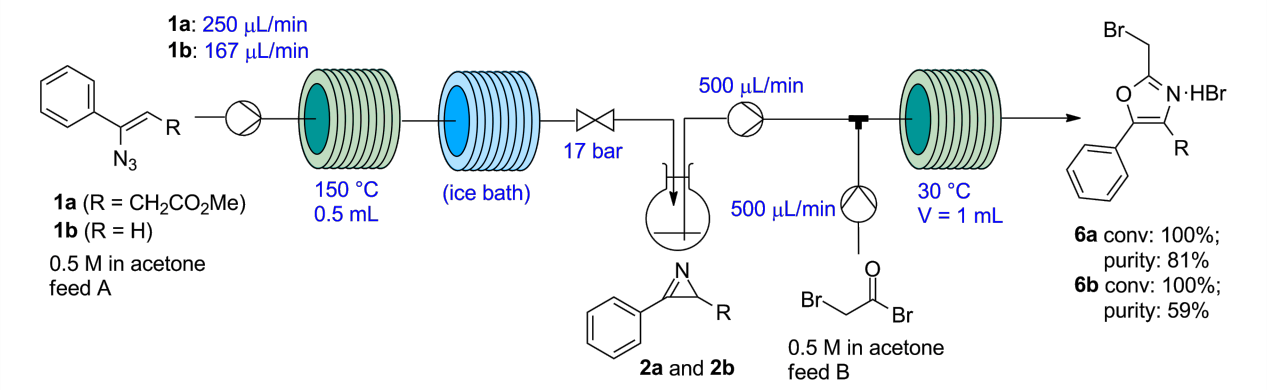

Figure 3: Continuous sequential thermolysis of vinyl azides **1** and ring expansion of azirines **2** with bromoacetyl bromide to give 2-(bromomethyl)oxazoles **6**.

oxazoles **6a** and **6b** were obtained in full conversion, with 81% and 59% purity (HPLC). Unfortunately, the oxazoles could not be precipitated as hydrobromide salts even after cooling at −20 °C and adding petroleum ether as co-solvent. The work-up consisted in extraction with aqueous $NaHCO_3$, evaporation of the organic phase, and purification of the residue by column chromatography. Relatively poor isolated yields (42% and 35% for compounds **6a** and **6b**, respectively) were achieved due to decomposition of the products during isolation. The decomposition of the 2-(bromomethyl)oxazoles inside the column was apparent, both when silica or neutral alumina were used as stationary phase.

Decomposition of 2-(bromomethyl)oxazoles **6** was successfully avoided by further integrating into the continuous-flow reactor the final nucleophilic halide displacement step with NaN_3. The resulting 2-(azidomethyl)oxazole derivatives **7** presented higher stability and could be isolated without decomposition. Thus, two additional reagents streams were added to the flow setup (Figure 4) containing an aqueous solution of NaN_3 (1.5 M) and DIPEA, respectively. The three streams were mixed in a cross mixer before entering a coil reactor at 50 °C (PFA tubing, 6 mL). While the vinyl azide thermolysis reactor zone was pressurized at 250 psi (17 bar), for this reactor zone 75 psi (5 bar) sufficed. Using this continuous-flow setup, azido oxazoles **7a** and **7b** were prepared from vinyl azides **1a** and **1b** in a three-step sequence (azirine was not isolated, the solution of the generated azirine was directly employed in the reaction described above). After reaction, 2-(azidomethyl)oxazoles **7a** and **7b** were purified by column chromatography, giving a three-step overall yield of 60% and 50%, respectively.

The vinyl azide **1c** was also subjected to the conditions described above. However, the reaction could not be completed due to solid generation in the second reactor zone (likely the hydrobromide salt of the oxazole). The reactor clogging could not be avoided either by sonication of the tubing or increasing the temperature to 50 °C. Thus, the reaction was performed em-

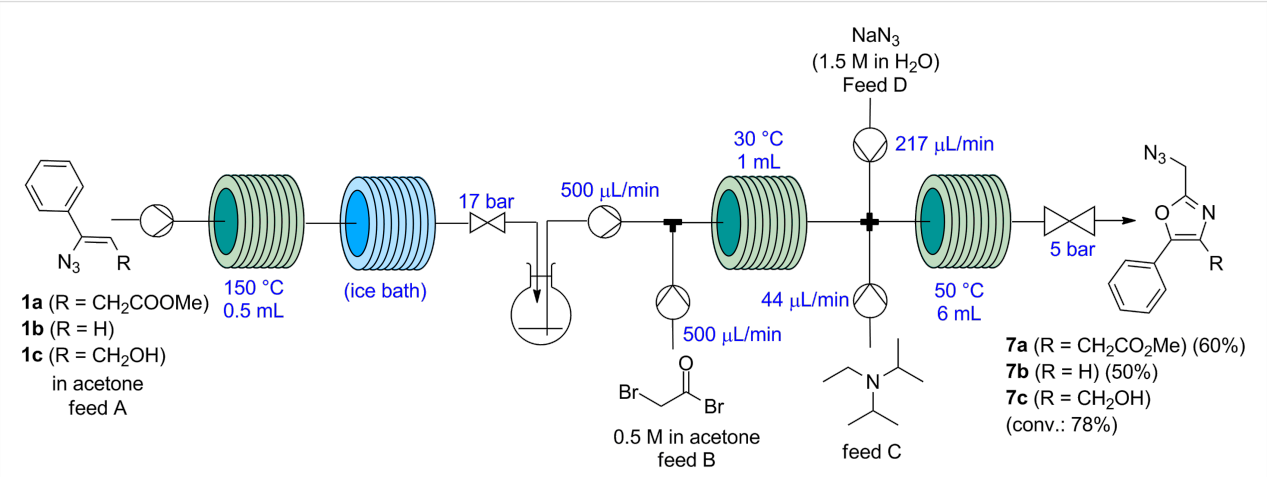

Figure 4: Continuous-flow three-step sequential synthesis of 2-(azidomethyl)oxazoles **7a–c** from vinyl azides **1a–c**. Yields refer to isolated yields.

ploying a 0.25 M solution of substrate **1c**. Under diluted conditions the reaction mixture remained fully homogeneous but no full conversion from bromo oxazole **6c** to azido oxazole **7c** was achieved (78%), which prevented the formation of the final product in a pure form.

Conclusion

We have developed a continuous-flow protocol for the preparation of 2-(azidomethyl)oxazoles. The procedure consists of a three-step sequential synthesis combining an initial thermolysis of the starting vinyl azide to form an azirine intermediate, followed by reaction with bromoacetyl bromide to generate the oxazole moiety, and a final nucleophilic halide displacement with NaN_3 to give the desired product. After optimization of all individual steps in batch and continuous-flow mode, the complete sequence has been integrated in a single continuous-flow reactor, in which the vinyl azide is fed as substrate and the final 2-(azidomethyl)oxazole is formed and collected from the reactor output. The process avoids the isolation and handling of the unstable 2-(bromomethyl)oxazole intermediates, thus circumventing decomposition problems. The continuous reactor has been tested for three different vinyl azide substrates. Good results were obtained for compounds **7a** and **7b**, while for **7c** dilution was necessary to avoid clogging of the reactor.

Supporting Information

Supporting Information File 1

Experimental procedures and copies of the NMR spectra for all isolated compounds.
[https://www.beilstein-journals.org/bjoc/content/supplementary/1860-5397-14-36-S1.pdf]

Acknowledgements

C.O.K acknowledges the Science without Borders program (CNPq, CAPES) for a “Special Visiting Researcher” fellowship. T.A.S. and N.S.S. are grateful to CAPES (Coordenação de Aperfeiçoamento de Pessoal de Nível Superior, Brazil) for fellowships. Special thanks are due to CEBIME (Laboratorio Central de Biologia Molecular e Estrutural, UFSC, Brazil) for providing the mass spectra.

ORCID® iDs

Thaís A. Rossa - https://orcid.org/0000-0001-9851-447X
C. Oliver Kappe - https://orcid.org/0000-0003-2983-6007

References

1. Ibrar, A.; Khan, I.; Abbas, N.; Farooq, U.; Khan, A. *RSC Adv.* **2016,** *6,* 93016–93047. doi:10.1039/C6RA19324B
2. Hassner, A.; Fischer, B. *Heterocycles* **1993,** *35,* 1441–1465. doi:10.3987/REV-92-SR(T)6
3. Yeh, V. S. C. *Tetrahedron* **2004,** *60,* 11995–12042. doi:10.1016/j.tet.2004.10.001
4. Naik, S. R.; Harindran, J.; Varde, A. B. *J. Biotechnol.* **2001,** *88,* 1–10. doi:10.1016/S0168-1656(01)00244-9
5. Kunze, B.; Jansen, R.; Pridzun, L.; Jurkiewicz, E.; Hunsmann, G.; Höfle, G.; Reichenbach, H. *J. Antibiot.* **1992,** *45,* 1549–1552. doi:10.7164/antibiotics.45.1549
6. Greenblatt, D. J.; Matlis, R.; Scavone, J. M.; Blyden, G. T.; Harmatz, J. S.; Shader, R. I. *Br. J. Clin. Pharmacol.* **1985,** *19,* 373–378. doi:10.1111/j.1365-2125.1985.tb02656.x
7. Wang, R.; Dasgupta, A.; Ward, M. M. *Ann. Rheum. Dis.* **2016,** *75,* 1152–1160. doi:10.1136/annrheumdis-2015-207677
8. Crawford, P. F.; Crawley, K. R.; Tucker, H. A. *J. New Drugs* **1961,** *1,* 279–283.
9. Chowdhury, S. R.; Chauhan, P. S.; Dedkova, L. M.; Bai, X.; Chen, S.; Talukder, P.; Hecht, S. M. *Biochemistry* **2016,** *55,* 2427–2440. doi:10.1021/acs.biochem.6b00102
10. Boger, D. L. *Chem. Rev.* **1986,** *86,* 781–793. doi:10.1021/cr00075a004
11. Turchi, I. J.; Dewar, M. J. S. *Chem. Rev.* **1975,** *75,* 389–437. doi:10.1021/cr60296a002
12. Levin, J. I.; Laakso, L. M. Oxazole Diels–Alder Reactions. *Oxazoles: Synthesis, Reactions, and Spectroscopy, Part A;* John Wiley & Sons, Inc.: Hoboken, NJ, USA, 2003; pp 417–472. doi:10.1002/0471428035.ch3
13. Blond, G.; Gulea, M.; Mamane, V. *Curr. Org. Chem.* **2016,** *20,* 2161–2210. doi:10.2174/1385272820666160216000401
14. Firestone, R. A.; Harris, E. E.; Reuter, W. *Tetrahedron* **1967,** *23,* 943–955. doi:10.1016/0040-4020(67)85043-9
15. Dumond, Y. R.; Gum, A. G. *Molecules* **2003,** *8,* 873–881. doi:10.3390/81200873
16. Bresciani, S.; Tomkinson, N. C. O. *Heterocycles* **2014,** *89,* 2479–2543. doi:10.3987/REV-14-808
17. Bredereck, H.; Gompper, R. *Chem. Ber.* **1954,** *87,* 700–707. doi:10.1002/cber.19540870514
18. Gompper, R.; Christmann, O. *Chem. Ber.* **1959,** *92,* 1944–1949. doi:10.1002/cber.19590920829
19. Ritson, D. J.; Spiteri, C.; Moses, J. E. *J. Org. Chem.* **2011,** *76,* 3519–3522. doi:10.1021/jo1025332
20. Fischer, E. *Ber. Dtsch. Chem. Ges.* **1896,** *29,* 205–214. doi:10.1002/cber.18960290143
21. Ingham, B. H. *J. Chem. Soc.* **1927,** 692–700. doi:10.1039/JR9270000692
22. Kotani, E.; Kobayashi, S.; Adachi, M.; Tsujioka, T.; Nakamura, K.; Tobinaga, S. *Chem. Pharm. Bull.* **1989,** *37,* 606–609. doi:10.1248/cpb.37.606
23. Ishiwata, Y.; Togo, H. *Tetrahedron* **2009,** *65,* 10720–10724. doi:10.1016/j.tet.2009.09.109
24. Ning, Y.; Otani, Y.; Ohwada, T. *J. Org. Chem.* **2017,** *82,* 6313–6326. doi:10.1021/acs.joc.7b00904
25. Brahma, S.; Ray, J. K. *J. Heterocycl. Chem.* **2008,** *45,* 311–317. doi:10.1002/jhet.5570450203
26. Sauers, R. R.; Hagedorn, A. A., III; Van Arnum, S. D.; Gomez, R. P.; Moquin, R. V. *J. Org. Chem.* **1987,** *52,* 5501–5505. doi:10.1021/jo00234a001
27. Zeng, T.-T.; Xuan, J.; Ding, W.; Wang, K.; Lu, L.-Q.; Xiao, W.-J. *Org. Lett.* **2015,** *17,* 4070–4073. doi:10.1021/acs.orglett.5b01994
28. Fowler, F. W.; Hassner, A. *J. Am. Chem. Soc.* **1968,** *90,* 2875–2881. doi:10.1021/ja01013a026

29. Hassner, A.; Burke, S. S.; I, J. C. *J. Am. Chem. Soc.* **1975,** *97,* 4692–4700. doi:10.1021/ja00849a035
30. Smith, A. B., III; Minbiole, K. P.; Freeze, S. *Synlett* **2001,** 1739–1742. doi:10.1055/s-2001-18096
31. Linder, J.; Blake, A. J.; Moody, C. J. *Org. Biomol. Chem.* **2008,** *6,* 3908–3916. doi:10.1039/b810855b
32. Kuntiyong, P.; Lee, T. H.; Kranemann, C. L.; White, J. D. *Org. Biomol. Chem.* **2012,** *10,* 7884–7899. doi:10.1039/c2ob25766a
33. Patil, P. C.; Luzzio, F. A. *Tetrahedron Lett.* **2016,** *57,* 757–759. doi:10.1016/j.tetlet.2016.01.016
34. Patil, P. C.; Tan, J.; Demuth, D. R.; Luzzio, F. A. *Bioorg. Med. Chem.* **2016,** *24,* 5410–5417. doi:10.1016/j.bmc.2016.08.059
35. Wegner, J.; Ceylan, S.; Kirschning, A. *Adv. Synth. Catal.* **2012,** *354,* 17–57. doi:10.1002/adsc.201100584
36. McQuade, D. T.; Seeberger, P. H. *J. Org. Chem.* **2013,** *78,* 6384–6389. doi:10.1021/jo400583m
37. Ahmed-Omer, B.; Barrow, D. A.; Wirth, T. *ARKIVOC* **2011,** *iv,* 26–36. doi:10.3998/ark.5550190.0012.404
38. Cludius-Brandt, C.; Kupracz, L.; Kirschning, A. *Beilstein J. Org. Chem.* **2013,** *9,* 1745–1750. doi:10.3762/bjoc.9.201
39. Cantillo, D.; Gutmann, B.; Kappe, C. O. *Org. Biomol. Chem.* **2016,** *14,* 853–857. doi:10.1039/C5OB02425K

License and Terms

BEILSTEIN JOURNAL OF ORGANIC CHEMISTRY

High-yielding continuous-flow synthesis of antimalarial drug hydroxychloroquine

Eric Yu‡, Hari P. R. Mangunuru‡, Nakul S. Telang, Caleb J. Kong, Jenson Verghese, Stanley E. Gilliland III, Saeed Ahmad, Raymond N. Dominey and B. Frank Gupton*

Full Research Paper

Open Access

Address:
Department of Chemistry and Department of Chemical and Life Science Engineering, Virginia Commonwealth University, 601 W. Main St., Richmond, VA 23220, USA

Email:
B. Frank Gupton* - bfgupton@vcu.edu

* Corresponding author ‡ Equal contributors

Keywords:
antimalarial; API manufacturing; flow chemistry; hydrogenation; hydroiodic acid; hydroxychloroquine

Beilstein J. Org. Chem. **2018,** *14,* 583–592.
doi:10.3762/bjoc.14.45

Received: 04 November 2017
Accepted: 14 February 2018
Published: 08 March 2018

This article is part of the Thematic Series "Integrated multistep flow synthesis".

Guest Editor: V. Hessel

Abstract

Numerous synthetic methods for the continuous preparation of fine chemicals and active pharmaceutical ingredients (API's) have been reported in recent years resulting in a dramatic improvement in process efficiencies. Herein we report a highly efficient continuous synthesis of the antimalarial drug hydroxychloroquine (HCQ). Key improvements in the new process include the elimination of protecting groups with an overall yield improvement of 52% over the current commercial process. The continuous process employs a combination of packed bed reactors with continuous stirred tank reactors for the direct conversion of the starting materials to the product. This high-yielding, multigram-scale continuous synthesis provides an opportunity to achieve increase global access to hydroxychloroquine for treatment of malaria.

Introduction

Our research group has been focused on the development of new synthetic methods for the preparation of a variety of active pharmaceutical ingredients for global health applications by employing the principles of process intensification [1-3]. In 2016, estimated 212 million cases of malaria, including 429,000 fatalities, were reported worldwide, with the majority of these cases occurring in sub-Saharan Africa and Southern Asia [4]. The malaria epidemic is particularly difficult to control due to the multidrug resistant nature of the malaria parasite *Plasmodium falciparum*. Hydroxychloroquine (**1**) is an antimalarial drug developed for both treatment and prevention of the disease in response to the widespread malaria resistance to chloroquine (**2**, Figure 1) [5,6].

Additionally, hydroxychloroquine (**1**, HCQ) is an effective non-steroidal drug with anti-inflammatory activity for the treatment of rheumatoid arthritis (RA) in patients with cardiovascular disease [7-9]. The World Health Organization has identified

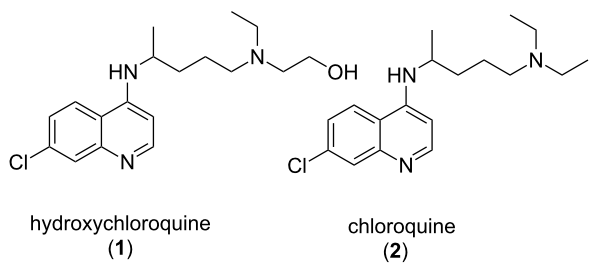

Figure 1: Commercially available antimalarial drugs.

HCQ (**1**) as an essential antimalarial medication for a basic healthcare system, but global access to HCQ (**1**) has been hindered by high manufacturing costs of the API. Thus, the development of cost effective synthetic strategies to increase the global access to this important global health drug is of great importance. Effective strategies for accomplishing such objectives often include identifying more cost effective starting materials and reagents, simplifying the synthetic route in terms of reducing the total number of steps as well as reducing the cost and improving the efficiency of individual steps.

Flow chemistry methodologies have been increasingly investigated in recent years in the pharmaceutical industry for multistep preparations of highly-complex natural products and APIs [10-19]. Advantages include precise control of key reaction parameters such as heat and pressure, improved heat and mass transfer capabilities for better thermal control, enhanced selection of kinetically controlled products to potentially maximize conversion, smaller equipment footprint, and increased safety profiles when working with hazardous materials and reaction conditions [20]. These advantages often result in flow processes being significantly more efficient, as well as less costly, when compared to batch processes.

HCQ (**1**) is currently produced via the batch method shown in Scheme 1. Therefore, continuous-flow chemistry approaches to synthesizing HCQ (**1**) offer a great potential to maximize the efficiency, and thus significantly reduces the overall manufacturing costs of this important medicine.

The commercial HCQ synthesis employs a key intermediate, 5-(ethyl(2-hydroxyethyl)amino)pentan-2-one (**6**), which is a major cost driver in the process. The protection–deprotection strategy of chloro-ketone starting material **3** used in the commercial route (Scheme 1a) [21] has been targeted as a significant opportunity for optimization. While the recent improved route (Scheme 1b) by Li and co-workers [21] eliminates the protection–deprotection steps, its use of a complex multi-transition-metal-catalyst system to achieve direct S_N2 substitution of the chlorine on **3** by amine **7**, is sub-optimal [22,23]. With these issues in mind, we carried out a retrosynthetic analysis (Scheme 2) in which **10**, an iodo analogue to the starting material **3**, could be generated in a single step via a decarboxylative ring-opening of α-acetyl butyrolactone **8**. The iodo analogue **10** could then be used without isolation to prepare compound **6**.

It is well known that the direct one-step reductive amination of **6** to give **12** can be accomplished by simple heterogeneous reduction with H_2/Raney-nickel [24]. However, THF is employed in all of our prior flow steps and is a poor choice as a solvent for the reductive amination step due to limited solubility of ammonia in THF. H_2/Raney-nickel reductions are often carried out in alcoholic media where much higher concentrations of ammonia are achievable but would require a solvent exchange. There are many reports of continuous-flow chemistry methods for reductive amination of ketones [25-31]; however, such processes typically require soluble reductants such as diisobutylaluminium hydride (DIBAL-H), superhydrides, or supported borohydride species [32-36]. Although these ap-

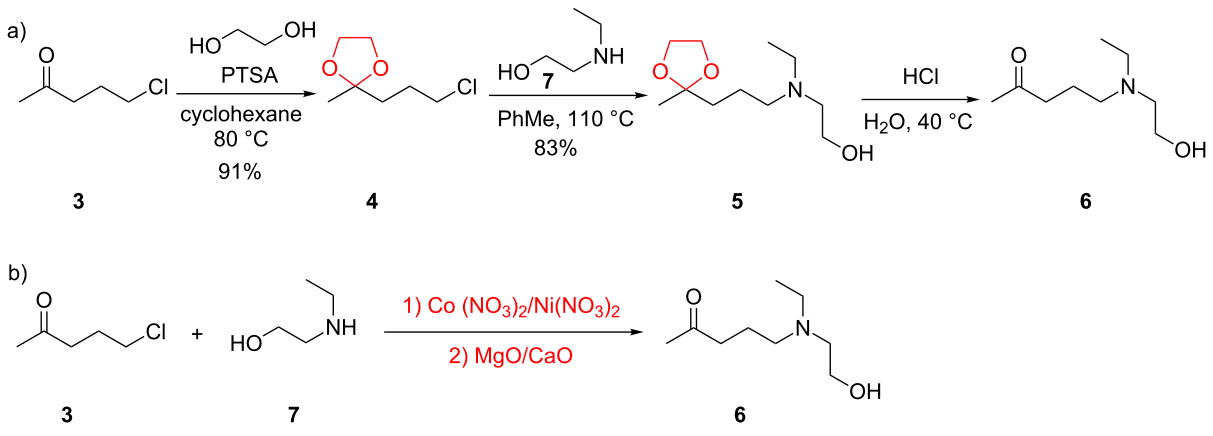

Scheme 1: Current batch syntheses of the key intermediate 5-(ethyl(2-hydroxyethyl)amino)pentan-2-one (**6**).

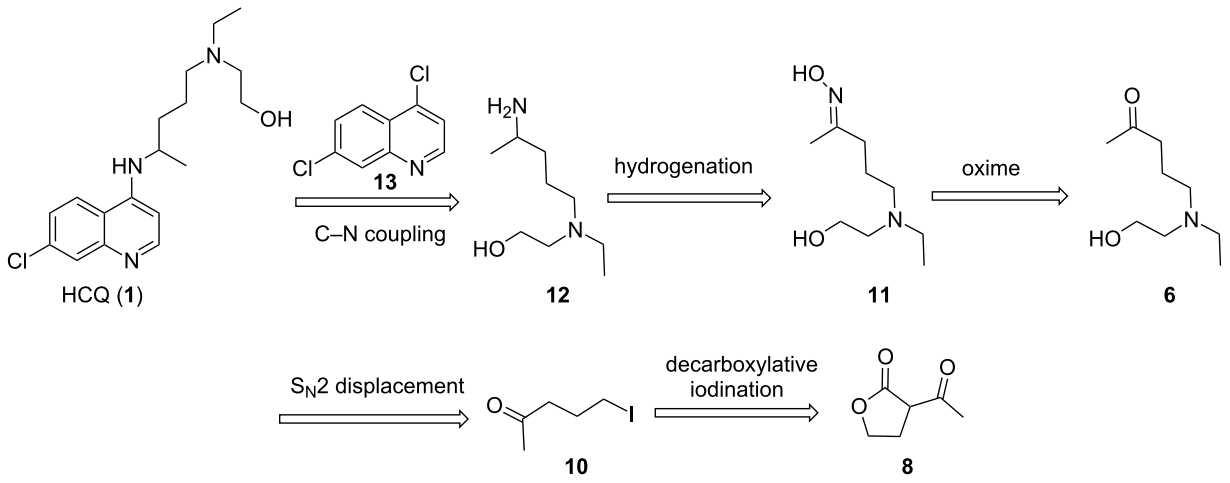

Scheme 2: Retrosynthetic strategy to hydroxychloroquine (**1**).

proaches are effective, they are significantly more costly than using simple heterogeneous reduction with H_2/Raney-nickel. Therefore, we explored an alternate strategy: simple conversion of the ketone group of **6** to oxime **11,** followed by reduction to give 5-(ethyl(2-hydroxyethyl)amino)-2-aminopentane (**12**). We have found H_2/Raney-nickel efficiently reduces **11** to **12** with THF as the solvent in a continuous stirred tank reactor (CSTR).

The last step requires the reaction of **12** with 4,7-dichloroquinoline (**13**) which when used neat takes 24–48 hours at 120–140 °C to give 75–80% yield of HCQ (**1**) [37]. We have found that this step can be accelerated by employing K_2CO_3/triethylamine, to facilitate the formation of **1**, resulting in a comparable yield in less than 6 hours. Thus, we have integrated the continuous preparation of reaction with our new efficient continuous-flow synthesis of **12** with the final step by using a CSTR to accommodate the longer reaction time required to produce HCQ (**1**).

Results and Discussion

Initial optimization efforts to prepare **6** (Scheme 1) revealed poor reactivity of starting material **3**, so we pursued the iodo analogue of **3**, 5-iodopentan-2-one (**10**) as an alternative. By optimizing the reaction concentration, we have also shown that (see Table S1 in Supporting Information File 1) **10** reacts rapidly and cleanly with **7** under flow conditions to give **6** in high yield (>80%). Furthermore, we have developed and optimized a continuous synthesis of **10** (Table 1), wherein hydroiodic acid is reacted with neat 3-acetyldihydrofuran-2(3*H*)-one (**8**) to provide a rapid route to **10** which is significantly higher in yield than in previously reported syntheses [38,39]. Initial results using diluted hydroiodic acid (20–40%) provided only modest conversion to product over a range of temperatures (Table 1, entries 1–5); however, the use of 55% hydroiodic acid (Table 1, entries 6–8) was found to give near quantitative conversion. The reaction profile was monitored using GC–MS and ^{1}H NMR – no intermediates were observed under these conditions. Optimization of the flow rate with 55% hydroiodic acid (Table 1, entries 6–8) revealed that a flow rate of 1.0 mL min^{-1} (t_R = 5 min) gave an isolated yield of 89%.

Due to the need to use an excess of hydroiodic acid it is important to remove its excess from the eluting reaction stream before telescoping into the next step in flow. The product stream containing crude **10** was mixed in-line with methyl *tert*-butyl ether (MTBE) and saturated $NaHCO_3$ before phase separation using a hydrophobic, membrane-based separator (Zaiput) [40] (Scheme 3) to afford purified **10** in the organic phase. A loss of 5–10% of product to the water layer was observed, however, this was deemed adequate as it prevented the need for a complete work-up step in batch.

In the next step **6** was reacted with hydroxylamine, which was facilitated by passing through a packed-bed of K_2CO_3 to give oxime **11** (Table 2). As was seen with the reaction to produce **6** (Table S1 in Supporting Information File 1), reactant concentrations also had a dramatic effect on the oxime formation. A series of experiments were conducted to optimize the continuous formation of **11**. Reaction yields were modest at lower reactant concentrations across several temperatures and residence times (Table 2). Conversion to **11** increased when reactant concentrations were increased (9% at 0.1 M to 72% at 1 M, Table 2, entries 1–6). Optimization of the flow rate with 1 M concentrations of each reactant (Table 2, entries 6–8) showed that a flow rate of 1.0 mL min^{-1} (t_R = 20 min) was optimal, giving an isolated yield of 78% (Table 2, entry 7).

Table 1: Optimization of the flow process for the synthesis of **10**.

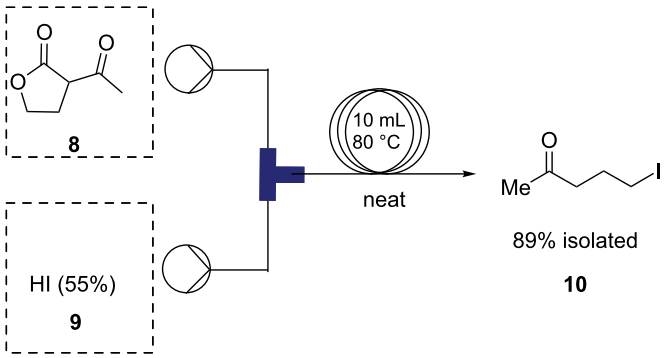

entry	HI [aqueous %]	temp (°C)	t_R = min	pressure (bar)	conv.[a] (%)
1	20	r.t.	5	1.5	5
2	20	40	5	2.0	31
3	20	80	5	2.0	34
4	40	80	5	2.0	43
5	40	80	5	2.5	46
6	55	80	5	3.0	98 (89%)[b]
7	55	80	2.5	3.0	91
8	55	80	10	3.0	92

[a]Conversion determined by GC–MS and ^{1}H NMR. [b]Isolated yield.

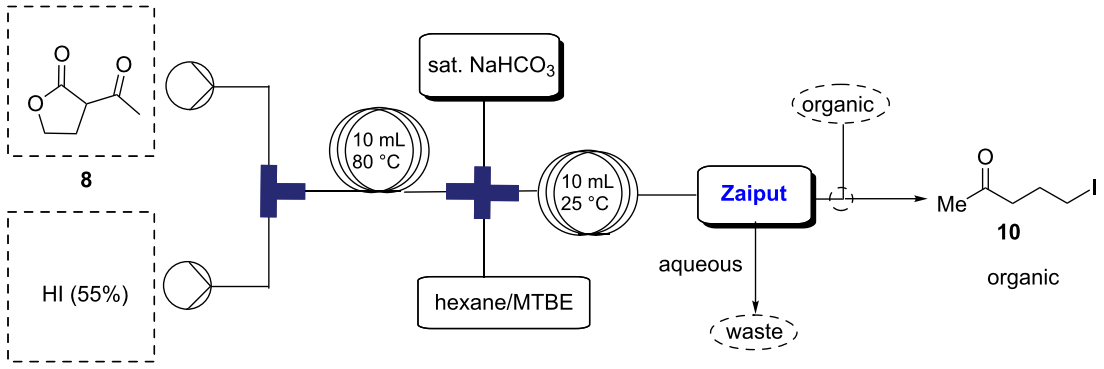

Scheme 3: Schematic representation for continuous in-line extraction of **10**.

The reductive amination of **11** performed in the first generation batch process was carried out using Raney-nickel at 80 °C and 10 bar hydrogen pressure for 4–6 h [21-24]. In order to perform this step in a continuous fashion, a continuous stirred tank reactor [25,41] was employed (Table 3). Materials were delivered to the CSTR vessel through an HPLC pump and were reacted under hydrogen pressure with mechanical stirring. The dip tube in the CSTR was outfitted with a fritted metal filter, allowing for retention of the heterogeneous catalyst within the CSTR vessel. Optimization of this CSTR-based flow process (Table 3) showed near quantitative yields of **12** over a broad range of oxime **11** reactant concentrations. An optimum residence time was determined to be 4 hours.

After optimizing the individual steps up to compound **12** the entire reaction was telescoped into a continuous reaction process that convert **10** and **6** into **12** (Scheme 4) with an overall isolated yield of 68% for compound **12**.

With an optimized continuous process for producing the key intermediate **12** in-hand the reaction conditions for the conver-

Table 2: Schematic representation for the continuous telescoped process to synthesize **11**.

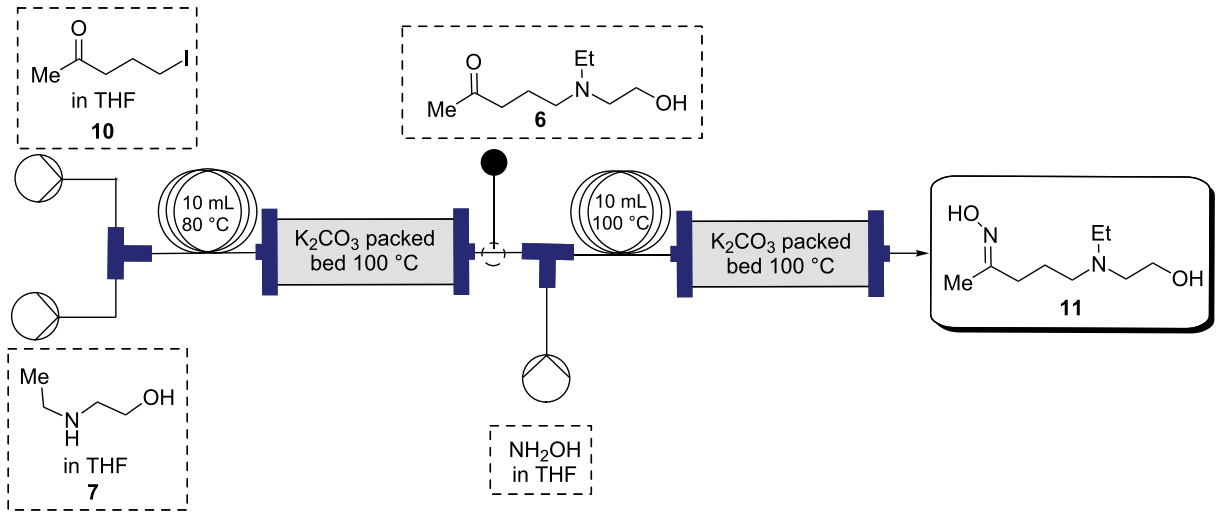

entry	concentration[a]	temp (°C)	t_R = min	conv. of **11** (%)[b]
1	0.1 M	100	10	9
2	0.2 M	100	10	16
3	0.4 M	100	10	34
4	0.6 M	100	10	37
5	0.8 M	100	10	62
6	1.0 M	100	10	72
7	1.0 M	100	20	85 (78)[c]
8	1.0 M	100	40	76

[a]Concentration of **10** , **7** and hydroxylamine. [b]Conversion determined by GC–MS and ^{1}H NMR. [c]Isolated yield.

sion of **12** to HCQ (**1**) were examined. In the commercial process this step is carried out in batch under neat reactant conditions and requires a relatively long reaction time of 24–48 h [42-44]. In order to convert this step to a flow chemistry method, we selected to employ a CSTR (Table 4). This final step, transforming **13** and **12** into **1**, was first investigated in batch to optimize the conditions before implemented in a CSTR.

Process optimization for the final step started with the screening of the effect of solvents and base(s) on the yield of HCQ (**1**). Screening of different polar–protic and non-protic solvents (see Table S2 in Supporting Information File 1) demonstrated that ethanol is the most effective for this transformation. During the screening of bases, the pK_a of the amine and alcohol groups present in compound **12** were given careful consideration in order to minimize C–O bond formation (Table 4). NaOH or KOH in ethanol gave low (<40%) conversion, whereas using K_2CO_3 in ethanol gave 82% conversion to HCQ (Table 4, entry 3). Attempts with organic bases (Table 4, entries 5 and 6) resulted in only moderate conversions to the desired product; however, using a 1:1 mixture of K_2CO_3/Et_3N (1:1) resulted in 88% conversion (Table 4, entry 6) to **1**, with corresponds to an isolated yield of 78%.

Conclusion

In summary, we have developed a high-yielding continuous-flow process for the synthesis of hydroxychloroquine (**1**, HCQ) by optimizing continuous-flow methods for the synthesis of key intermediates **6** and **12**. Additionally, we have developed and optimized flow-chemistry conditions for performing reductive amination of **11** using Raney-nickel as catalyst in a continuous stirring tank reactor (CSTR) for the synthesis of compound **12**, and have incorporated it into a fully continuous telescoped process for the synthesis of **12** from lactone **8** and amino-ethanol **7**. Feeding the output stream containing **12** from the above CSTR into a second CSTR in which **12** is converted to HCQ (**1**) provides a completely continuous-flow process for producing HCQ (**1**) from readily available starting materials. This efficient process has the potential to increase the global access to this strategically important antimalarial drug. We are currently working to demonstrate that this fully integrated continuous-flow process for the synthesis of HCQ (**1**) can be scaled to commercial operations.

Table 3: Optimization of the flow process for the reductive amination of **12** using a CSTR.

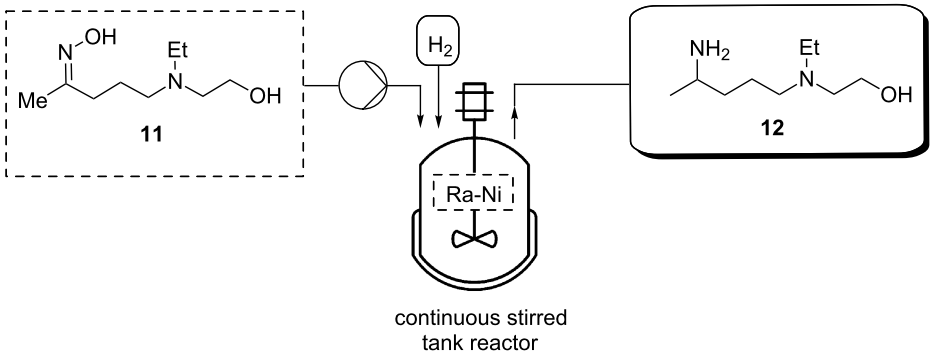

entry	oxime [concentration]	temp. (°C)	pressure (bar)	t_R = hours	conv. of **12** (%)[a]
1	0.05 M	80	10	4	94%
2	0.25 M	80	10	4	96%
3	0.5 M	80	10	4	97%
4	2.0 M	80	10	4	98% (89%)[b]
5	2.0 M	80	10	2	56%
6	2.0 M	80	10	1	46%

[a]Conversion determined by GC–MS and ^{1}H NMR. [b]Isolated yield.

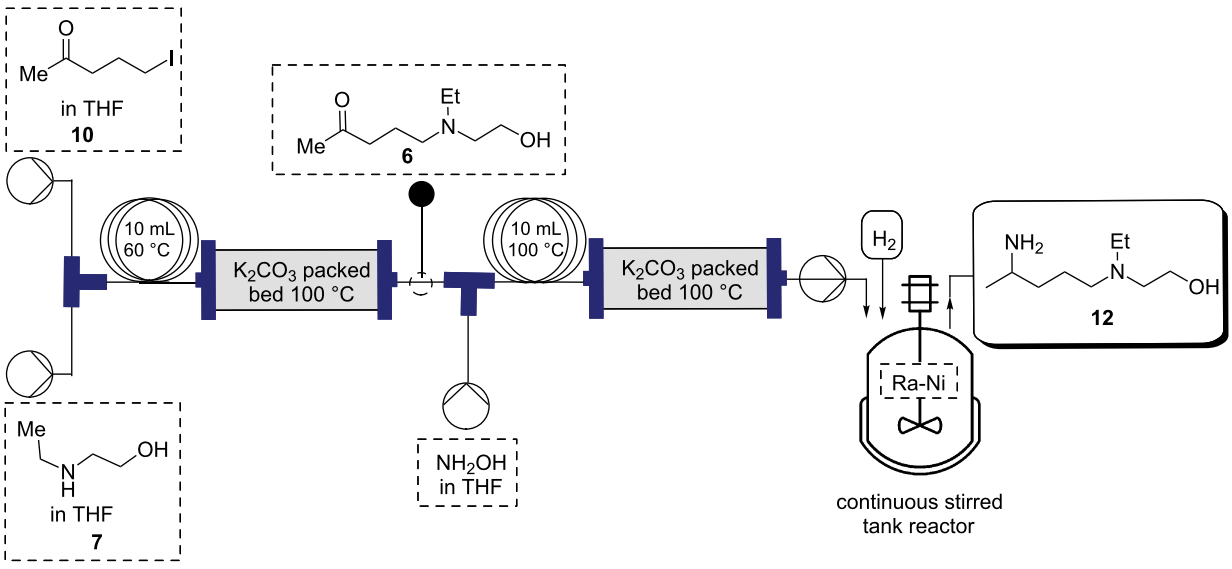

Scheme 4: Optimization of the flow process for the synthesis of **12**.

Experimental

General information

All reactions for the preparation of substrates were performed in standard, dry glassware under an inert atmosphere of nitrogen or argon unless otherwise described. All starting materials and reagents were purchased from commercial sources and were used as received unless otherwise noted. ^{1}H and ^{13}C NMR spectra were recorded using 600 MHz spectrometers. Chemical shift (δ) values are given in ppm, and coupling constants (*J*) are given in Hz. The 7.26 ppm resonance of residual $CHCl_3$ (or 0 ppm of TMS) for proton spectra and the 77.23 ppm resonance of $CDCl_3$ for carbon spectra were used as internal references. Continuous-flow experiments were carried out using the E-series flow reactor instrument purchased from Vapourtec Ltd.

Table 4: Optimization of the reaction conditions for the preparation of hydroxychloroquine (**1**).[a]

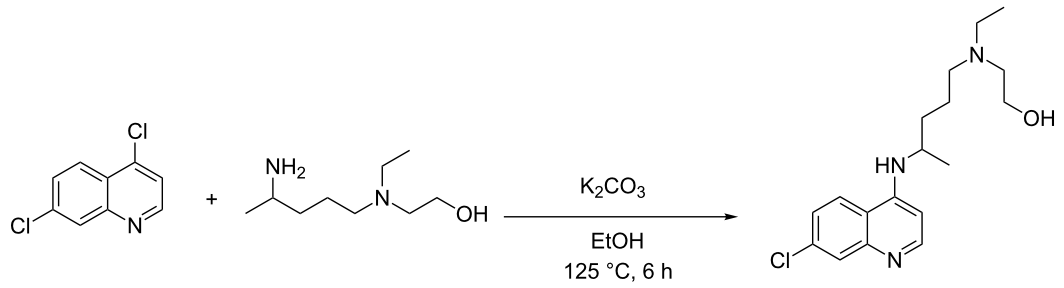

13 **12** **1**

entry	base	solvent	temp. (°C)	conv. to **1** (%)[b]
1	NaOH	EtOH	125	30
2	KOH	EtOH	125	35
3	K_2CO_3	EtOH	125	82
4	Et_3N	EtOH	125	61
5	DIPEA	EtOH	125	55
6	K_2CO_3/Et_3N	EtOH	125	88 (78)[c]

[a]Reaction conditions: 4,7-dichloroquinoline (**13**, 1.0 equiv), base (1.0 equiv), amine **12** (1.2 equiv). [b]Conversion determined by HPLC and ^{1}H NMR, [c]Isolated yield.

PFA tubing (1/16 OD × 1 mm ID) was used for all reactor coils in flow experiments. Most of the reagents and starting materials were purchased from commercial sources and used as received. All HPLC chromatograms were recorded on an Agilent Technologies 1260 Infinity instrument with a Poroshell 120 EC-C18 column (4.6 × 50 mm, 2.7 micron). Continuous flow hydrogenation was performed using a FlowCAT instrument.

Synthesis of 5-iodopentan-2-one (**10**)

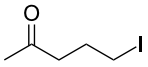

10

Two solutions, 2-acetylbutyrolactone (**8**, 1.176 mL, 10.35 mmol, 1.0 equiv) and hydroiodic acid (55% aqueous solution) were pumped at 1.0 mL min^{-1} using peristaltic pumps through a 10 mL coil (residence time, t_R = 5 min) at 80 °C. The completion of the reaction was monitored using GC–MS. Complete consumption of starting material was observed. The reaction mixture was cooled to room temperature and sodium hydrogencarbonate was added until neutralized at pH 7. The crude mixture was extracted with hexanes/MTBE and the combined organic phase was dried over anhydrous sodium sulfate and evaporated in vacuo to dryness yielding the desired product as a light brown liquid (14.72 g, 89%). ^{1}H NMR (600 MHz, $CDCl_3$) δ 3.22 (t, *J* = 6.9 Hz, 2H), 2.59 (t, *J* = 6.9 Hz, 2H), 2.17 (s, 3H), 2.06 (quin, *J* = 7.0 Hz, 2H); ^{13}C NMR (125 MHz, $CDCl_3$) δ 207.4, 44.0, 30.3, 27.2, 6.7. Spectra were obtained in accordance with those previously reported [3].

Synthesis of 5-(ethyl(2-hydroxyethyl)amino)pentan-2-one (**6**)

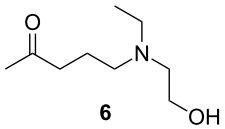

6

Telescope of compound 6: Prior to the start of the experiment, the flow reactor unit was rinsed with dry THF and flushed with nitrogen gas. At room temperature, the stock solutions of 5-iodopentan-2-one (**10**, 1.0 M) and 2-(ethylamino)ethan-1-ol (**7**) in THF solution (1.0 M) were streamed in at 0.5 mL min^{-1} via a T-piece into a 10 mL reactor coil (t_R = 10 min) and passed through a packed bed reactor of potassium carbonate at 100 °C. The output solution was collected and quenched with a saturated solution of ammonium chloride. The aqueous phase was extracted by DCM (3 × 50 mL) and the organic layers were combined, dried over sodium sulfate, and evaporated in vacuo to give a light brown liquid (14.05 g, 86%). ^{1}H NMR (600 MHz, $CDCl_3$) δ 3.53 (t, *J* = 5.2 Hz, 2H), 2.58 (m, 3H), 2.53 (m, 2H), 2.45 (t, *J* = 6.7 Hz, 4H), 2.59 (t, *J* = 6.9 Hz, 2H), 2.17 (s, 3H), 2.07 (quin, *J* = 7.0 Hz, 2H); ^{13}C NMR (125 MHz, $CDCl_3$) δ 208.9, 58.6, 55.0, 52.4, 47.2, 41.3, 30.0, 21.2, 11.7.

Spectra were obtained in accordance with those previously reported [38,39].

Synthesis of (*E*)-5-(ethyl(2-hydroxyethyl)amino)-pentan-2-one oxime (**11**)

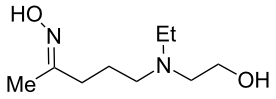

11

Flow: Prior to the start of the experiment, the flow reactor unit was rinsed with dry THF and flushed with nitrogen gas. At room temperature, the stock solutions of 5-iodopentan-2-one (**10**, 1.0 M) and 2-(ethylamino)ethan-1-ol (**7**) in THF solution (1.0 M) were streamed in at 0.5 mL min^{-1} via a T-piece into a 10 mL reactor coil (t_R =10 min) and passed through a packed bed reactor of potassium carbonate. The output solution was streamlined with hydroxylamine (1.0 M) at 1.0 mL min^{-1} via a T-piece into a 10 mL reactor coil (t_R =10 min) and passed through a packed bed reactor of potassium carbonate at 100 °C. The reaction mixture was then concentrated in vacuo, taken up in dichloromethane (3 × 20 mL) and concentrated under reduced pressure to yield **11** as light brown liquid. The crude product was used in the next step without further purification.

Synthesis of 2-((4-aminopentyl)(ethyl)amino)ethan-1-ol (**12**)

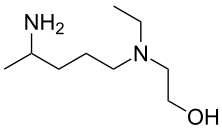

12

Flow: The synthesis of compound **12** was performed in a HEL continuous stirred tank reactor (CSTR) with a reaction volume of 150 mL. The reaction vessel was first charged with Raney-nickel (1.0 g). The Raney-nickel catalyst was retained in the CSTR by the 2 µm metal filter frit on the dip tube of the exit stream. The reaction mixture, consisting of compound **11** (0.05–2.0 M) in THF, was pumped by a HPLC pump set at a flow rate of 0.6–2.5 mL min^{-1} into the reaction vessel. The reaction pressure was set to 10 bar of hydrogen supplied by hydrogen gas (ultrahigh purity) at a flow rate of 0.5 mL min^{-1}. The reaction temperature was set to 80 °C which was controlled by a thermocouple positioned in the reaction mixture. The reaction was stirred with mechanical stirring (750 rpm) to provide proper mixing. Two thermocouples were used to control the reaction volume in the reactor by setting a level control of −3 °C. The lower thermocouple constantly measured and controlled the reaction temperature and the upper thermocouple measured the temperature at approximately 150 mL reactor volume. When the two thermocouples were within 3 °C, the level control 'opened' the exit stream dip tube to allow products to exit the reactor, or 'closed' the exit stream dip tube to allow the reactor to fill when the temperature difference between the two thermocouples was greater than 3 °C. The product was collected after a full reaction volume of material (150 mL) had passed through the CSTR indicating that steady-state was reached. The reaction was monitored by liquid chromatography and ^{1}H NMR. The reaction mixture was filtered through a celite pad and dried under reduced pressure. The solution was extracted with water (10 mL) and dichloromethane (3 × 20 mL). The organic layers were combined, washed with brine and dried over sodium sulfate and evaporated in vacuo. The resulting oil was fractionally distilled to give a colorless liquid (16.83 g, 84%). ^{1}H NMR (600 MHz, $CDCl_3$) δ 3.53 (t, *J* =5.3 Hz, 2H), 2.89 (sx, *J* = 6.4 Hz, 1H), 2.57 (t, *J* = 5.5 Hz, 2H), 2.55 (t, *J* = 7.0 Hz, 2H), 2.45 (t, *J* = 7.0 Hz, 2H), 1.55–1.44 (m, 2H), 1.36–1.27 (m, 2H), 1.22 (t, *J* = 7.1 Hz, 2H), 1.07 (d, *J* = 7.1 Hz, 2H), 1.00 (t, *J* = 7.1 Hz, 2H); ^{13}C NMR (125 MHz, $CDCl_3$) δ 58.2, 54.9, 53.2, 46.9, 46.7, 36.6, 23.8, 22.4, 10.6. Spectra were obtained in accordance with those previously reported [38,39].

Synthesis of 2-((4-((7-chloroquinolin-4-yl)amino)-pentyl)(ethyl)amino)ethan-1-ol (**1**)

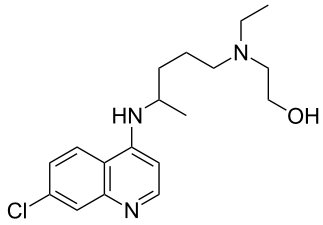

1

Batch: In a CSTR reactor, to a mixture of 4,7-dichloroquinoline (200 mg, 1.0 mmol), compound **12** (208 mg, 1.2 mmol), triethylamine (0.069 mL, 0.5 mmol, 0.5 equiv) and potassium carbonate (69 mg, 0.5 mmol, 0.5 equiv) was added ethanol (1.0 mL). The ethanol was distilled off from the reaction mixture and kept under nitrogen atmosphere (15 psi). The reaction was left at 125 °C in the nitrogen atmosphere for 6 h. After cooling, the mixture was transferred into a separatory funnel using 1 M aqueous sodium hydroxide (5 mL) and dichloromethane (2 × 20 mL). The organic phases were separated and the aqueous phase was re-extracted with dichloromethane (2 × 10 mL). The organic layers were combined and dried over sodium sulfate and evaporated in vacuo. The crude material was purified using flash chromatography with DCM/Et_3N/MeOH 95:3:2 to give a white solid (0.263 g, 78%). ^{1}H NMR (600 MHz, $CDCl_3$) δ 8.48 (d, *J* = 5.4 Hz, 1H), 7.93 (d, *J* = 5.4

Hz, 1H), 7.70 (d, J = 9.2 Hz, 1H), 7.34 (dd, J = 8.8, 7.3 Hz, 1H), 6.39 (d, J = 5.4 Hz, 1H), 4.96 (d, J = 7.5 Hz, 1H), 3.70 (sx, J = 6.8 Hz, 1H), 3.55 (m, 2H), 2.57 (m, 5H), 2.49 (m, 2H), 1.74–1.62 (m, 1H), 1.65–1.53 (m, 3H), 1.31 (d, J = 6.9 Hz, 3H), 1.24 (d, J = 7.2 Hz, 2H); ^{13}C NMR (125 MHz, $CDCl_3$) δ 152.2, 149.5, 149.2, 135.0, 129.0, 125.4, 121.2, 117.4, 99.4, 58.6, 54.9, 53.18, 48.5, 47.9, 34.5, 24.1, 20.6, 11.9. Spectra were obtained in accordance with those previously reported [38,39].

Supporting Information

Supporting Information File 1

Additional experimental descriptions and NMR spectra.
[https://www.beilstein-journals.org/bjoc/content/supplementary/1860-5397-14-45-S1.pdf]

Acknowledgements

This work was supported by The Defense Advanced Research Projects Agency (DARPA) (W911NF-16-2-0023). We thank all members of the two teams (Prof. B. Frank Gupton and Prof. Thomas Roper) for their discussions and kind help.

ORCID® iDs

Eric Yu - https://orcid.org/0000-0001-6051-8969
Hari P. R. Mangunuru - https://orcid.org/0000-0002-5038-9654
Nakul S. Telang - https://orcid.org/0000-0002-9781-4830
Stanley E. Gilliland III - https://orcid.org/0000-0002-5335-0886

References

1. Verghese, J.; Kong, C. J.; Rivalti, D.; Yu, E. C.; Krack, R.; Alcázar, J.; Manley, J. B.; McQuade, D. T.; Ahmad, S.; Belecki, K.; Gupton, B. F. *Green Chem.* **2017,** *19,* 2986–2991. doi:10.1039/C7GC00937B
2. Kong, C. J.; Fisher, D.; Desai, B. K.; Yang, Y.; Ahmad, S.; Belecki, K.; Gupton, B. F. *Bioorg. Med. Chem.* **2017,** *25,* 6203–6208. doi:10.1016/j.bmc.2017.07.004
3. Martin, A. D.; Siamaki, A. R.; Belecki, K.; Gupton, B. F. *J. Flow Chem.* **2015,** *5,* 145–147. doi:10.1556/JFC-D-15-00002
4. World Health Organization. WHO Malaria Report 2016. Geneva, 2016; http://www.who.int/malaria/publications/world-malaria-report-2016/report/en/.
5. Surrey, A.-R.; Hammer, H. F. *J. Am. Chem. Soc.* **1950,** *72,* 1814–1815. doi:10.1021/ja01160a116
6. Bailey, D. M. *J. Med. Chem.* **1969,** *12,* 184–185. doi:10.1021/jm00301a055
7. Pavelka, K., Jr.; Sen, K. P.; Pelísková, Z.; Vácha, J.; Trnavský, K. *Ann. Rheum. Dis.* **1989,** *48,* 542–546. doi:10.1136/ard.48.7.542
8. Hage, M. P.; Al-Badri, M. R.; Azar, S. T. *Ther. Adv. Endocrinol. Metab.* **2014,** *5,* 77–85. doi:10.1177/2042018814547204
9. Poorvashree, J.; Suneela, D. *Drug Delivery Transl. Res.* **2017,** *7,* 709–730. doi:10.1007/s13346-017-0420-5
10. Belecki, K.; Gupton, B. F. Continuous Processing in Drug Discovery. *Green Chemistry Strategies for Drug Discovery;* The Royal Society of Chemistry, 2015; pp 127–150. doi:10.1039/9781782622659-00127
11. Baumann, M.; Baxendale, I. R. *Beilstein J. Org. Chem.* **2015,** *11,* 1194–1219. doi:10.3762/bjoc.11.134
12. Baxendale, I. R.; Brocken, L.; Mallia, C. J. *Green Process. Synth.* **2013,** *2,* 211–230. doi:10.1515/gps-2013-0029
13. Opalka, S. M.; Park, J. K.; Longstreet, A. R.; McQuade, D. T. *Org. Lett.* **2013,** *15,* 996–999. doi:10.1021/ol303442m
14. Alonso, N.; Miller, L. Z.; Muñoz, J. d. M.; Alcázar, J.; McQuade, D. T. *Adv. Synth. Catal.* **2014,** *356,* 3737–3741. doi:10.1002/adsc.201400243
15. McQuade, D. T.; Seeberger, P. H. *J. Org. Chem.* **2013,** *78,* 6384–6389. doi:10.1021/jo400583m
16. Poechlauer, P.; Colberg, J.; Fisher, E.; Jansen, M.; Johnson, M. D.; Koenig, S. G.; Lawler, M.; Laporte, T.; Manley, J.; Martin, B.; Kearney-McMullan, A. *Org. Process Res. Dev.* **2013,** *17,* 1472–1478. doi:10.1021/op400245s
17. Poechlauer, P.; Manley, J.; Broxterman, R.; Gregertsen, B.; Ridemark, M. *Org. Process Res. Dev.* **2012,** *16,* 1586–1590. doi:10.1021/op300159y
18. Britton, J.; Raston, C. L. *Chem. Soc. Rev.* **2017,** *46,* 1250–2171. doi:10.1039/C6CS00830E
19. Plutschack, M. B.; Pieber, B.; Gilmore, K.; Seeberger, P. H. *Chem. Rev.* **2017,** *117,* 11796–11893. doi:10.1021/acs.chemrev.7b00183
20. Gutmann, B.; Cantillo, D.; Kappe, C. O. *Angew. Chem., Int. Ed.* **2015,** *54,* 6688–6728. doi:10.1002/anie.201409318
21. You, H.; Liu, Y.; Ning, F.; Zheng, Z.; Yu, Q.; Niu, X.; Li, C. CN104803859A, 2015.
22. Glenn, J. S.; Pham, E. A. Use of chloroquine and clemizole compounds for treatment of inflammatory and cancerous conditions PCT. Int. Appl. WO2017004454 A1, Jan 5, 2017.
23. Min, Y. S.; Cho, H.-S.; Mo, K. W. New preparation of hydroxychloroquine. PCT Int. Appl. WO 2010027150 A2, March 11, 2010.
24. Ashok, K.; Dharmendra, S.; Snajay, N.; Sanjay, B.; Atul, J. An improved process for the preparation of 7-chloro-4-(5-*N*-ethyl-*N*-2-hydroxyethylamine)-2-pentyl]aminoquinoline and its intermediates. WO2005/062723, July 14, 2005.
25. Continuous flow chemistry catalytic reactions with FlowCAT. http://www.helgroup.com/reactor-systems/hydrogenation-catalysis/flowcat/.
26. Jensen, R. K.; Thykier, N.; Enevoldsen, M. V.; Lindhardt, A. T. *Org. Process Res. Dev.* **2017,** *21,* 370–376. doi:10.1021/acs.oprd.6b00441
27. Falus, P.; Boros, Z.; Hornyánszky, G.; Nagy, J.; Darvas, F.; Ürge, L.; Poppe, L. *Tetrahedron Lett.* **2011,** *52,* 1310–1312. doi:10.1016/j.tetlet.2011.01.062
28. Chi, Y.; Zhou, Y.-G.; Zhang, X. *J. Org. Chem.* **2003,** *68,* 4120–4122. doi:10.1021/jo026856z
29. Hoffmann, S.; Seayad, A. M.; List, B. *Angew. Chem., Int. Ed.* **2005,** *44,* 7424–7427. doi:10.1002/anie.200503062
30. Kitamura, M.; Lee, D.; Hayashi, S.; Tanaka, S.; Yoshimura, M. *J. Org. Chem.* **2002,** *67,* 8685–8687. doi:10.1021/jo0203701
31. Kadyrov, R.; Riermeier, T. H. *Angew. Chem., Int. Ed.* **2003,** *42,* 5472–5474. doi:10.1002/anie.200352503
32. Abdel-Magid, A. F.; Carson, K. G.; Harris, B. D.; Maryanoff, C. A.; Shah, R. D. *J. Org. Chem.* **1996,** *61,* 3849–3862. doi:10.1021/jo960057x
33. Gilmore, K.; Vukelić, S.; McQuade, D. T.; Koksch, B.; Seeberger, P. H. *Org. Process Res. Dev.* **2014,** *18,* 1771–1776. doi:10.1021/op500310s

34. Webb, D.; Jamison, T. F. *Org. Lett.* **2012,** *14,* 568–571. doi:10.1021/ol2031872
35. Fan, X.; Sans, V.; Yaseneva, P.; Plaza, D. D.; Williams, J.; Lapkin, A. *Org. Process Res. Dev.* **2012,** *16,* 1039–1042. doi:10.1021/op200373m
36. Kirschning, A.; Monenschein, H.; Wittenberg, R. *Angew. Chem., Int. Ed.* **2001,** *40,* 650–679. doi:10.1002/1521-3773(20010216)40:4<650::AID-ANIE6500>3.0.CO;2-C
37. Blaney, P. M.; Byard, S. J.; Carr, G.; Ellames, G. J.; Herbert, J. M.; Peace, J. E.; Smith, D. I.; Michne, W. F.; Sanner, M. S. *Tetrahedron: Asymmetry* **1994,** *5,* 1815–1822. doi:10.1016/0957-4166(94)80090-1
38. Cornish, C. A.; Warren, S. *J. Chem. Soc., Perkin Trans. 1* **1985,** 2585–2598. doi:10.1039/P19850002585
39. Münstedt, R.; Wannagat, U.; Wrobel, D. *J. Organomet. Chem.* **1984,** *264,* 135–148. doi:10.1016/0022-328X(84)85139-6
40. Hamlin, T. A.; Lazarus, G. M. L.; Kelly, C. B.; Leadbeater, N. E. *Org. Process Res. Dev.* **2014,** *18,* 1253–1258. doi:10.1021/op500190j
41. Chapman, M. R.; Kwan, M. H. T.; King, G.; Jolley, K. E.; Hussain, M.; Hussain, S.; Salama, I. E.; Niño, C. G.; Thompson, L. A.; Bayana, M. E.; Clayton, A. D.; Nguyen, B. N.; Turner, N. J.; Kapur, N.; Blacker, A. J. *Org. Process Res. Dev.* **2017,** *21,* 1294–1301. doi:10.1021/acs.oprd.7b00173
42. Xiao, H.; Tong, R.; Liao, Z.; Chuan, J.; Zhang, L.; Zhang, Y.; Bian, Y. Hydroxychloroquine linolenate and synthesis method thereof. CN103772277 A, May 7, 2014.
43. Sleightholm, R.; Yang, B.; Yu, F.; Xie, Y.; Oupický, D. *Biomacromolecules* **2017,** *18,* 2247–2257. doi:10.1021/acs.biomac.7b00023
44. Ansari, A. M.; Craig, J. C. *J. Chem. Soc., Perkin Trans. 2* **1994,** 1731–1733. doi:10.1039/P29940001731

License and Terms

BEILSTEIN JOURNAL OF ORGANIC CHEMISTRY

Heterogeneous Pd catalysts as emulsifiers in Pickering emulsions for integrated multistep synthesis in flow chemistry

Katharina Hiebler[1], Georg J. Lichtenegger[1], Manuel C. Maier[1], Eun Sung Park[2], Renie Gonzales-Groom[2], Bernard P. Binks[*2] and Heidrun Gruber-Woelfler[*1]

Full Research Paper

Open Access

Address:
[1]Institute of Process and Particle Engineering, Graz University of Technology, Inffeldgasse 13/III, 8010 Graz, Austria and [2]School of Mathematics and Physical Sciences, University of Hull, Hull HU6 7RX, UK

Email:
Bernard P. Binks[*] - b.p.binks@hull.ac.uk; Heidrun Gruber-Woelfler[*] - woelfler@tugraz.at

* Corresponding author

Keywords:
compartmentalisation; heterogeneous catalysis; multistep flow chemistry; palladium; Pickering emulsions

Beilstein J. Org. Chem. **2018,** *14,* 648–658.
doi:10.3762/bjoc.14.52

Received: 03 November 2017
Accepted: 27 February 2018
Published: 19 March 2018

This article is part of the Thematic Series "Integrated multistep flow synthesis".

Guest Editor: V. Hessel

Abstract

Within the “compartmentalised smart factory” approach of the ONE-FLOW project the implementation of different catalysts in “compartments” provided by Pickering emulsions and their application in continuous flow is targeted. We present here the development of heterogeneous Pd catalysts that are ready to be used in combination with biocatalysts for catalytic cascade synthesis of active pharmaceutical ingredients (APIs). In particular, we focus on the application of the catalytic systems for Suzuki–Miyaura cross-coupling reactions, which is the key step in the synthesis of the targeted APIs valsartan and sacubitril. An immobilised enzyme will accomplish the final product formation via hydrolysis. In order to create a large interfacial area for the catalytic reactions and to keep the reagents separated until required, the catalyst particles are used to stabilise Pickering emulsions of oil and water. A set of Ce–Sn–Pd oxides with the molecular formula $Ce_{0.99-x}Sn_xPd_{0.01}O_{2-\delta}$ (x = 0–0.99) has been prepared utilising a simple single-step solution combustion method. The high applicability of the catalysts for different functional groups and their minimal leaching behaviour is demonstrated with various Suzuki–Miyaura cross-coupling reactions in batch as well as in continuous flow employing the so-called “plug & play reactor”. Finally, we demonstrate the use of these particles as the sole emulsifier of oil–water emulsions for a range of oils.

Introduction

Palladium (Pd) catalysis has been established as a key component in the toolbox of organic chemists. Reactions that are catalysed by palladium benefit from the remarkable versatility and functional-group tolerance of the transition metal as well as the ability to control the reaction selectivity [1-3]. Pd catalysts have been implemented in the synthesis of various active pharmaceu-

tical ingredients (APIs), natural products and agrochemicals amongst others [4]. In particular, Pd-catalysed C–C cross-coupling reactions have become indispensable in many modern synthetic protocols both in the laboratory and on an industrial scale. A highly important representative of this class of transformation is the Suzuki–Miyaura reaction [5,6], involving the coupling of aryl halides with phenylboronic acids yielding the corresponding biphenyls as product [7]. The biphenyl unit is a common structural motif in various pharmaceutically active agents and plays a crucial role in the binding affinity and the oral bioavailability of diverse APIs [8], including antihypertensive [9] and antitumour agents [10]. Advantages of the Suzuki–Miyaura coupling are mild reaction conditions, commercial availability of a large number of boronic acids and simple product purification [7]. Concerning the transition metal source for C–C cross-coupling reactions, homogeneous and heterogeneous Pd catalysts are utilised.

The employment of a variety of different ligands such as phosphines, amines and carbenes allows precise tuning of the properties of homogeneous Pd catalysts, which led to significant improvements in turn over number (TON), reaction rates, enantioselectivity as well as catalyst robustness and lifetime. Apart from that, ligand-free Pd catalysts are also known in the literature [11,12]. However, homogeneous Pd catalysis often requires catalyst loadings in the order of mol % to achieve effective coupling and suffers from catalyst re-use and recycling problems [11,13]. Furthermore, concerning the synthesis of pharmaceuticals, tedious purification steps need to be performed in order to remove residual metals. Considering these drawbacks of homogeneous catalysis, easily recoverable and recyclable heterogeneous Pd catalysts are much more attractive with respect to ecological and economical aspects [13]. One possibility to prepare heterogeneous transition metal catalysts is to immobilise palladium directly on a solid support such as activated carbon [14], zeolites [15], modified silica [16-18] or molecular sieves [19] to name but a few. Another option is the complexation of palladium by ligands which are covalently bound to the support material [12]. One example of such a catalyst was reported by our group using a bis(oxazoline) ligand bonded to 3-mercaptopropyl-functionalised silica [20]. Alternatively, the use of unsupported Pd nanoparticles or encapsulated Pd complexes are strategies to realise heterogeneous palladium catalysis [21]. Immobilisation of catalytic systems on solid supports can mitigate a lot of problems of homogeneous catalysts, for example, it allows a straightforward removal of the catalyst from the reaction system. However, most heterogeneous approaches require more drastic reaction conditions in comparison to their homogeneous counterparts, which often introduce undesirable leaching effects [17,20,22,23]. Consequently, the synthesis and application of unprecedented nonleaching heterogeneous palladium catalysts for cross-coupling reactions have been investigated intensively and vigorous efforts are made to implement them in industrial synthesis [11,13,20].

The idea of the so-called “compartmentalised smart factory” within the ONE-FLOW project [24] is to go a step further and combine different kinds of chemo- and biocatalysts in one “compartment". For this approach and to keep the reagents separated until required, the catalysts are contained within Pickering emulsions of oil and water phases. Emulsions are thermodynamically unstable mixtures of two immiscible liquids, e.g., oil and water, with typical droplet sizes in the micron range. Traditionally, emulsions have been kinetically stabilised by molecular species including surfactants, polymers or proteins all of which possess water-liking groups and oil-liking groups enabling them to adsorb to freshly created oil–water interfaces preventing to some extent coalescence between neighbouring droplets [25]. So-called Pickering emulsions, however, are stabilised solely by solid colloidal particles which can adsorb to droplet interfaces forming a protective layer endowing the emulsion with extremely high stability to coalescence [26]. Examples of suitable particles include silica, alumina, metals, polymers and proteins of different sizes and shapes. One of the key factors influencing the effectiveness of a particle to act as an emulsifier is its wettability normally quantified by the contact angle θ the particle makes with the oil–water interface (through water). For relatively hydrophilic particles, $\theta < 90°$ and preferred emulsions are oil-in-water (o/w). For relatively hydrophobic particles, $\theta > 90°$ and water-in-oil (w/o) emulsions are preferred [27]. Particles of intermediate wettability are well held at a fluid interface as the energy required to remove them can be several thousand kT (k is Boltzmann constant, T is temperature); such particles are deemed irreversibly adsorbed under quiescent conditions. As summarised recently [28], the two liquids may be oil and water, two immiscible oils or even two immiscible water phases and different particles need to be designed in each case to impart stabilisation of dispersed drops in a continuous phase. In 2010, Crossley et al. [29] put forward the idea that catalyst particles may both act simultaneously as an emulsifier in Pickering emulsions and serve as the catalyst in which water-soluble reactants and oil-soluble reactants react at the oil–water interface populated by catalyst particles. They deposited metallic Pd onto carbon nanotube–inorganic oxide hybrid nanoparticles and used them in emulsions for the hydrodeoxygenation of a phenolic compound and the hydrogenation and etherification of an aldehyde. The advantages of such a system include a high interfacial area for reaction, the ultrastability of emulsion drops during reaction and easy recovery of the catalyst particles and products as emulsions may be rendered unstable subsequently. A mini-review of the area of Pickering emulsion interfacial catalysis appeared in 2015 [30].

In this work an outlook on the planned realisation of the integrated multistep continuous flow synthesis of valsartan and sacubitril within the frame of the ONE-FLOW project is given. The compounds are well known as APIs in a combination drug for the treatment of hypertension and chronic heart failure (Entresto®, Novartis) [31-35]. A preliminary scheme of the planned synthetic route is shown in Figure 1. As can be seen, the key step of our processes is the formation of the biaryl unit via a Suzuki–Miyaura cross-coupling reaction. To provide solid Pd catalysts with a high potential for the planned approaches, a set of Ce–Sn–Pd oxides with the molecular formula $Ce_{0.99-x}Sn_xPd_{0.01}O_{2-\delta}$ (x = 0–0.99; δ indicates the oxygen vacancies in the crystal lattice of the oxides, the values for delta are rather small, thus the value for oxygen is ≈2, [36,37]) is tested for that approach. The tolerance of the catalysts towards different functional groups and their minimal leaching which has already been demonstrated with various Suzuki–Miyaura cross-coupling reactions in batch as well as in continuous flow employing the so-called plug & play reactor [38], is summarised. In this work we present for the first time the use of these particles as the sole emulsifier of oil–water emulsions for a range of oils.

Results and Discussion

Metal oxide-supported ionic palladium catalysts

Synthesis

The heterogeneous Ce–Sn–Pd compounds were synthesised using the solution combustion technique according to Baidya et al. [39] with slight modifications [37]. The benefits of this single-step method are the simplicity of the procedure, the usage of nontoxic and inexpensive precursors and that several grams of material can be obtained within hours. To study the influence of the amounts of Ce and Sn on the catalytic behaviour, five mixed oxides with the molecular formula $Ce_{0.99-x}Sn_xPd_{0.01}O_{2-\delta}$ (x = 0, 0.20, 0.495, 0.79 and 0.99) were synthesised and attained in quantitative amounts (>99%). The obtained solids can be used directly for characterisation as well as for the activity tests.

Characterisation

The Ce–Sn–Pd catalysts were analysed using different state-of-the-art methods. Details of the characterisation were published recently [37]. Here, only the most important characteristics are summarised. The obtained X-ray diffraction (XRD) profiles proved the nanocrystallinity of the catalyst particles, which either show single phase cubic, tetragonal or a more amorphous cubic/tetragonal mixed phase structure depending on the content of Sn. As far as palladium substitution in the lattice is concerned, XRD and X-ray photoelectron spectroscopy (XPS) analysis approved the predominant cationic nature of incorporated palladium (Pd^{2+}) and revealed only minor amounts of metallic Pd. Brunauer–Emmett–Teller (BET) measurements showed that the specific surface areas of the five catalysts range from 27–98 m^2/g. Particle sizes of ≈10–100 µm were measured with a monomodal size distribution for the cerium-rich catalysts and a polymodal distribution for catalysts rich in tin.

Suzuki–Miyaura coupling reactions

Batch reactions

The catalytic activity of the synthesised catalysts in the Suzuki–Miyaura reaction was investigated using phenylboronic acid **3** in combination with various bromoarenes **4a–e**, featuring *ortho*- and *para*-substitution of electron donating as well as electron withdrawing functional groups, as coupling partners (Scheme 1). Concerning the targeted synthesis of **1**, aryl halide **4e** was of special interest as the cyano group is known to be convertible to the *ortho*-tetrazole moiety [9] present in the API. Based on prior optimisation studies [37], reactions were performed in EtOH/H_2O 7:3 (v/v) at 75 °C using K_2CO_3 as inor-

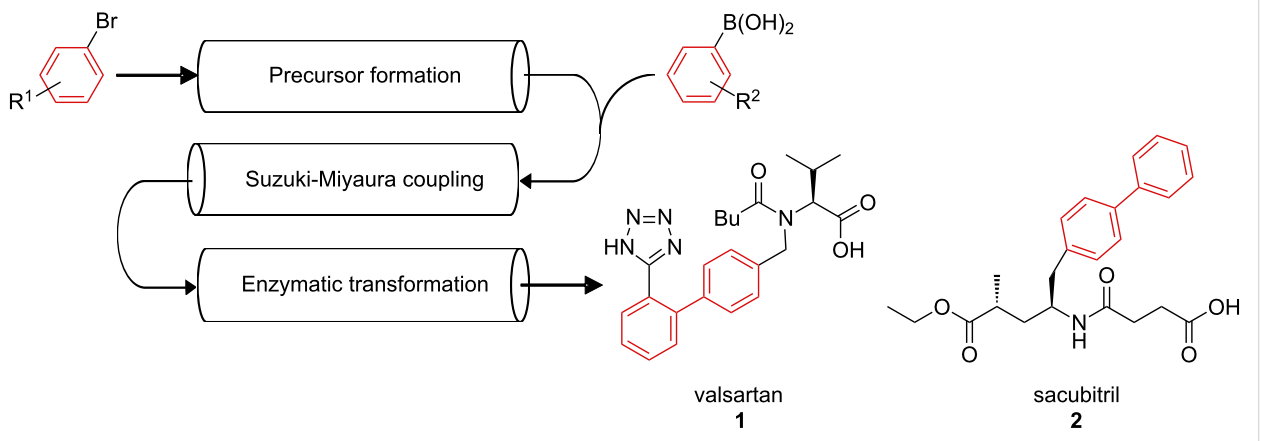

Figure 1: Targeted integrated multistep synthesis of valsartan (**1**) and sacubitril (**2**).

ganic base. Phenylboronic acid as well as K_2CO_3 were added in 50% molar excess relative to the corresponding aryl bromide, whereas a catalyst amount corresponding to 0.05 mol % of Pd was used. The reaction progress was monitored by high-performance liquid chromatography (HPLC).

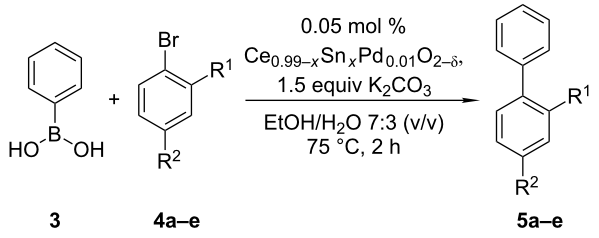

Scheme 1: Suzuki–Miyaura coupling of phenylboronic acid **3** with various bromoarenes **4a–e** (**a**: R^1 = H, R^2 = CH_3; **b**: R^1 = H, R^2 = OH; **c**: R^1 = H, R^2 = $COOCH_3$; **d**: R^1 = H, R^2 = CF_3; **e**: R^1 = CN, R^2 = H).

In general, the catalysts with tin proportions of 0.20, 0.79 and 0.99 proved to be most effective in the desired transformations with exceptional high activities (turn over frequency, TOF > 12,000 h^{-1}) in all tested Suzuki–Miyaura cross-coupling reactions. While *para*-substituted bromoarenes were converted quantitatively within a reaction time of 2 h with an order of 4-bromoacetophenone (**4c**) ≥ 4-bromobenzotrifluoride (**4d**) > 4-bromotoluene (**4a**) > 4-bromophenol (**4b**), the coupling of 2-bromobenzonitrile (**4e**) required the 4-fold amount of catalyst to reach full conversion. *p*-Bromobenzenes containing electron-withdrawing substituents showed higher reactivity than bromobenzenes containing electron-donating groups. When $Ce_{0.495}Sn_{0.495}Pd_{0.01}O_{2-\delta}$ was employed as catalyst, however, the catalytic activity was found to be significantly lower and the binary oxide $Ce_{0.99}Pd_{0.01}O_{2-\delta}$ showed to be least efficient for the explored Suzuki–Miyaura couplings. Regarding the selectivity of the catalysts in the selected cross-coupling reactions, no bromoarene-deriving side products (dehalogenation product Ar' and bromoarene homocoupling product Ar'Ar') could be detected. However, both boronic acid homocoupling (ArAr) and boronic acid oxidation (ArOH) occurred to a small extent as indicated by HPLC. As the side product formation mainly occurs when the bromoarene coupling partner gets depleted, highest reaction selectivity (up to 99.5% [37]) can be achieved by termination of the transformation just at the moment of full conversion.

In conclusion, $Ce_{0.99-x}Sn_xPd_{0.01}O_{2-\delta}$ (x = 0–0.99) proved to be very active catalysts for Suzuki–Miyaura reactions. Based on the experimental results, the tin and cerium content of the catalysts respectively do not seem to be directly connected to their catalytic activity. Nevertheless, there are indications that the surface area and the particle size distribution play a role in the catalytic performance of the palladium substituted metal oxides. In view of the aimed application of the Pd metal oxides for targeted API synthesis, the obtained results are very promising although the relevant transformation needed higher catalyst amounts.

Recyclability and metal leaching

In the context of heterogeneous catalysis it is essential to investigate the actual nature of the catalysts during the reaction as well as the reusability and stability of the catalytic active compounds. To assess the reusability of the heterogeneous catalysts, the Pd-substituted metal oxides were subjected to Suzuki–Miyaura couplings of 4-bromotoluene with phenylboronic acid in five subsequent reactions, i.e., after one reaction was finished, the particles were separated from the solution via filtration, washed, dried and reused for a new reaction with new substrates. Although during the filtration and drying steps catalyst loss could not be prevented, a high degree of recyclability was established and only a minor decrease of mass specific catalyst activity was observed [37].

As far as palladium leaching is concerned, ICP–MS measurements revealed 0.06–0.14 mg/L Pd in the reaction solution after the 3rd reaction run [37]. This finding is in accordance with the theory that the actual catalyst of the coupling reaction is leached palladium and supports a reaction mechanism via homogeneous catalysis. For the purpose of elucidating the homo- or heterogeneous nature of synthesised catalysts in more detail, further studies including a hot filtration test and catalyst poisoning [40,41] were performed [37]. In summary, the obtained results confirm a palladium release and capture mechanism. The synthesised heterogeneous metal oxides act as pre-catalysts, which slowly release minimal amounts of active palladium into solution. However, as levels of leached Pd are below the regulatory limits for orally administered pharmaceuticals [41], the mixed metal oxides have high potential as heterogeneous catalysts for the synthesis of APIs, such as **1** and **2**.

Suzuki–Miyaura reactions in continuous flow

After the applicability and versatility of the palladium substituted cerium tin oxides was confirmed in batch, the aim was to implement the catalysts in a continuous flow setup, which is also suitable for the multistep synthesis of **1** and **2**. Therefore, the so-called plug & play reactor, a versatile device featuring both exchangeable reaction segments and modules for heating/cooling and mixing [38], was employed to test the activity and stability of the catalysts in continuous flow. In the plug & play reactor the reaction media flow through 1 mm tubes embedded in channels filled with heating/cooling media, ensuring both, enhanced mixing and rapid heat transfer. Commercially available HPLC columns filled with catalyst particles serve as fixed-

bed reactors and contribute to the high versatility of the device. With this approach, gas–solid, liquid–solid as well as gas–liquid–solid reactions can be realised within the upper performance limits of 200 °C and 40 bar [38].

The performance of the plug & play reactor in terms of continuous Suzuki–Miyaura cross coupling was investigated using phenylboronic acid (**3**) in combination with different *ortho*- and *para*-substituted bromoarenes in aqueous ethanolic mixtures employing K_2CO_3 as base [38]. Monitoring of the reaction progress via inline UV–vis spectroscopy as well as offline HPLC analysis [38] led to the result that after an initial induction phase (≈30 min) a stable process was achieved, forming the respective products in high yields (up to 99%) for more than 30 h with excellent selectivity without catalyst deactivation [42]. As expected, increasing the catalyst amount and residence time by use of three sequential fixed bed reactors enhanced product formation and conversions >90% were obtained. Furthermore, analysis of the crystalline product by means of ICP–MS confirmed only trace amounts of leached cerium (≈1 mg/kg final product), tin (≈0.2 mg/kg product) and palladium (≈1 mg/kg product). In addition to that, direct product isolation via integrated crystallisation was successfully implemented as a continuous downstream protocol [42].

Concluding, the plug & play reactor is a highly versatile device, which is applicable for different kinds of heterogeneously catalysed reactions. The results obtained strongly indicate the high potential for realising other reactions of interest to produce pharmaceutical and fine chemical intermediates in continuous flow, including the multistep synthesis of valsartan (**1**) and sacubitril (**2**). In addition to the approach with the compartmentalised catalysts in Pickering emulsions and thus the usage of one HPLC column filled with catalytic active compounds, the setup is optimal to employ multiple columns filled with different types of catalysts. Furthermore, the implementation of other functionalised materials, e.g., solid-supported scavengers for leached metals, is straightforward.

Size reduction of catalyst particles

As mentioned before, the as synthesised catalyst particles have particle diameters in the range of 10–100 µm. Since the stabilisation of micron-sized Pickering emulsion droplets requires particle sizes <1 µm, a decrease of particle size was necessary. For that purpose, a Resch PM10 planet ball mill equipped with metal balls (d = 8 mm, 500 rpm, 10 min milling time) was used for dry milling of powdered $Ce_{0.495}Sn_{0.495}Pd_{0.01}O_{2-\delta}$ and wet milling (suspension in water) of $Ce_{0.20}Sn_{0.79}Pd_{0.01}O_{2-\delta}$, respectively. These two catalysts were chosen since they showed the highest activities for Suzuki–Miyaura couplings in batch [37] and continuous flow [38]. After milling, the coarse and fine fractions of the particles were separated via sedimentation. For this purpose, 2 g of catalyst were suspended in 1 L water, the particles were de-aggregated by ultrasonic treatment and left to sediment. After a sedimentation time of 35 min, the upper half of the suspension was removed with a pipette and fractions were dried in a muffle furnace (120 °C until dryness, then at 350 °C overnight). Table 1 and Figure 2 indicate that for both catalysts 90% of the particles in the separated fines fractions are

Table 1: x_{90} and specific surface area of the catalysts after milling and separation *via* sedimentation.

Catalyst	x_{90} [µm]	BET surface area [$m^2\ g^{-1}$]
$Ce_{0.495}Sn_{0.495}Pd_{0.01}O_{2-\delta}$	2.84	28
$Ce_{0.20}Sn_{0.79}Pd_{0.01}O_{2-\delta}$	4.20	58

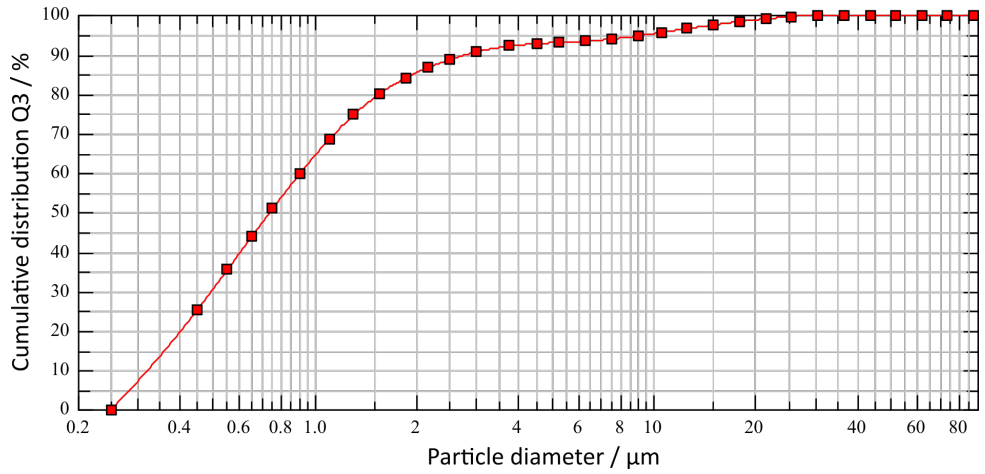

Figure 2: Particle size distribution of $Ce_{0.495}Sn_{0.495}Pd_{0.01}O_{2-\delta}$ after size reduction via milling and separation via sedimentation in water.

<5 µm (= x_{90}) in diameter. The overall yield for this particle fraction was 20%, but future work will concentrate on the optimisation of this step. Microscopic pictures indicate spherical particle shape. The density of the particles, also important for the usage of the particles as stabilisers in Pickering emulsions, was determined to be 5.97 g/cm^3 for $Ce_{0.495}Sn_{0.495}Pd_{0.01}O_{2-\delta}$ and 5.38 g/cm^3 for $Ce_{0.20}Sn_{0.79}Pd_{0.01}O_{2-\delta}$.

Implementation of the catalyst particles in Pickering emulsions

For simplicity, we have investigated emulsions containing equal volumes of water (Milli-Q) and oil with catalyst particles first dispersed in water using an ultrasonic probe (Jencons Vibra-Cell, 5 min, 130 W). The oils chosen are the aliphatic alkane octane (Sigma, >99%, density 0.699 g/cm^3), the cyclic alkane cyclohexane (Fisher Scientific, >99%, density 0.774 g/cm^3) and the aromatic oil toluene (VWR Chemicals, >99%, density 0.865 g/cm^3). Emulsions were prepared using a rotor-stator homogeniser (IKA T25 digital Ultra-Turrax) with a stator diameter of 8 mm for 1 min at 10,000 rpm at room temperature. Emulsion type was established using the drop test (addition of a drop of emulsion to either water or oil). The stability of emulsions to gravity-induced creaming or coalescence was assessed by monitoring the position of the water–emulsion or oil–emulsion interfaces respectively. Microscopy images of the emulsions were recorded using an Olympus BX53 microscope with GXCAM-U318 camera attached and GXCapture-T software.

Catalyst $Ce_{0.495}Sn_{0.495}Pd_{0.01}O_{2-\delta}$

Being relatively hydrophilic mixed oxides, both types of catalysts formed in water suspensions with discrete particles, at least at low concentration (0.05 wt %) (see Figure 3).

Emulsions of all the oils are o/w in which their stability to both creaming and coalescence as well as their average droplet size depend markedly on particle concentration. As an example, the appearance of cyclohexane-in-water emulsions with time for three selected particle concentrations can be seen in Figure 4. This pattern of behaviour is followed with the other two oils also. For particle concentrations in water between 0.01 and

Figure 4: Photos of vessels containing cyclohexane-in-water emulsions stabilised by particles of $Ce_{0.495}Sn_{0.495}Pd_{0.01}O_{2-\delta}$ at concentrations in water of 0.03 wt % (upper), 0.30 wt % (middle) and 1.0 wt % (lower) at different times since preparation. A is the aqueous dispersion of particles, B is after addition of oil but before emulsification.

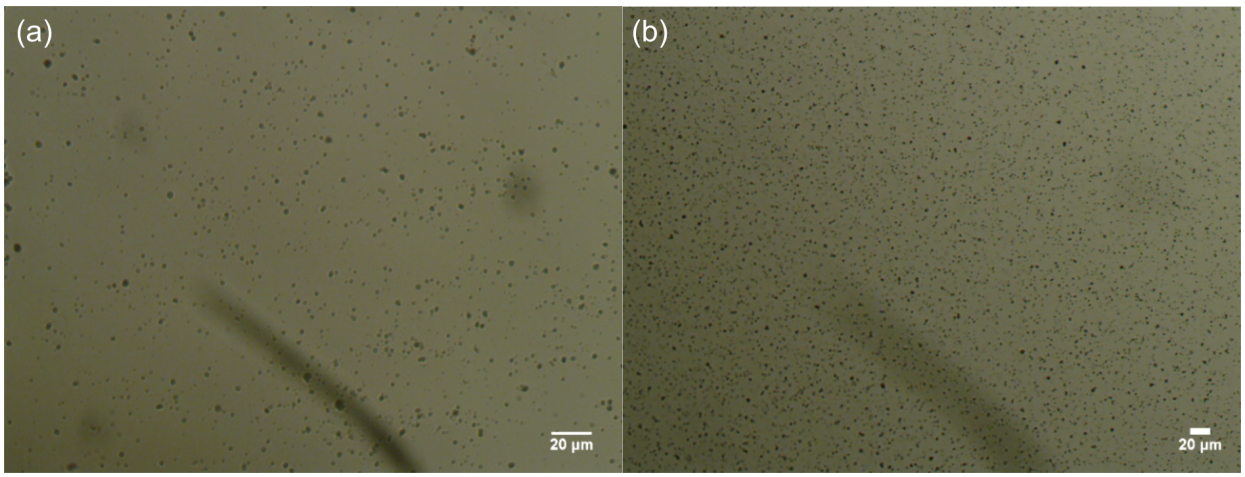

Figure 3: Optical microscope images of fresh aqueous dispersions, 0.05 wt %, of (a) $Ce_{0.495}Sn_{0.495}Pd_{0.01}O_{2-\delta}$ and (b) $Ce_{0.20}Sn_{0.79}Pd_{0.01}O_{2-\delta}$ particles.

0.10 wt % (upper in Figure 4), reasonably stable emulsions to coalescence are formed although they exhibit creaming with the separation of a lower serum from which nonadsorbed particles sediment. Although the initial oil volume fraction in emulsions is 0.5 (t = 0), that in creamed emulsions after 1 day reaches as high as 0.7–0.8. Such excellent stability to coalescence in high internal phase emulsions is due to the particle layer on droplet interfaces acting as a barrier to drop fusion. Between 0.20 and 0.50 wt % (middle), although an emulsion forms initially, it rapidly coalesces until complete phase separation in some cases. At and above 1.0 wt % (lower), emulsions can be re-stabilised to some extent although visible oil drops (mm-sized) develop within the cream.

For the stable emulsions at low particle concentrations, optical microscopy reveals the presence of catalyst particles around oil droplets in water, Figure 5. Roughly, an increase in particle concentration results in increased coverage of droplets by particles. Since around 50% of the particles are sub-micron in size, however, a fraction of droplet interfaces may be coated in these particles which are of a size smaller than the resolution limit of the microscope. By contrast, the larger sized particles appear aggregated at droplet interfaces. The variation in the average oil droplet diameter with particle concentration is given in Figure 6 (top). Relatively small drops (between 70 and 150 μm) exist below 0.1 wt %, drops as large as 5 mm exist at 0.3 wt % after which the drop size decreases progressively to around 1 mm at 2 wt %. For emulsion stability with respect to coalescence, we define a parameter f_o = (vol. free oil at time t/vol. oil initially). Likewise, the stability to creaming is given by f_w = (vol. free water at time t/vol. water initially). Values of both parameters can vary from 0 (completely stable) to 1 (complete phase separation). After one month, the variation of f_o and f_w with particle concentration is given in Figure 6 (bottom). Up to 0.1 wt %, creaming is extensive and although some coalescence ensues, the residual emulsions remain stable for at least six months. Coalescence is then very extensive at 0.2, 0.3 and 0.5 wt % and mm-sized drops are formed in the early stages. Our first hypothesis was that the sudden increase in emulsion instability at higher particle concentrations may be due to particle aggregation in water prior to emulsification. Such large particle aggregates of high density would be weakly retained at the oil–water interfaces offering little protection to the coalescence between drops. However, a more detailed look at the particle size in water at different particle concentrations (Figure 7) as well as the unexpected results of the zeta potential and the pH value at different particle concentrations (Figure 8) are an indication that

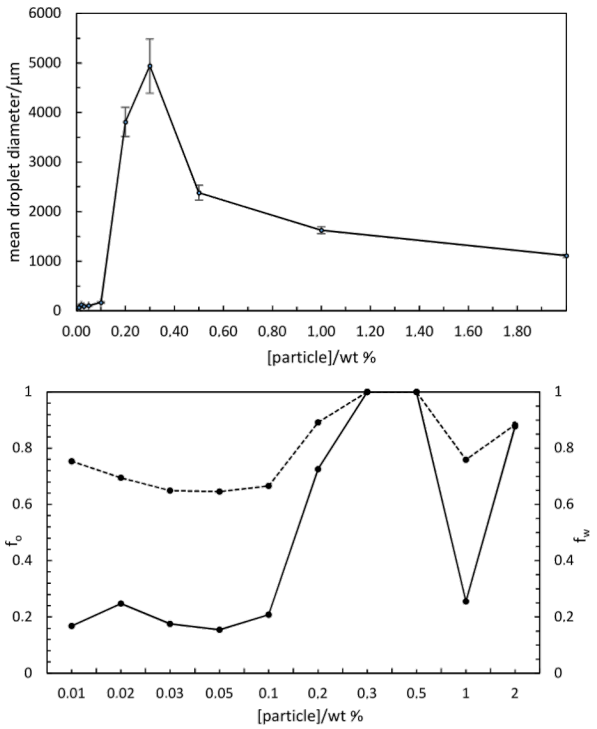

Figure 6: (top) Mean emulsion droplet diameter after 30 min as a function of particle concentration for system in Figure 4; (bottom) variation of f_o (solid line) and f_w (dashed line) after one month with particle concentration for emulsions in Figure 4 (note nonlinear scale).

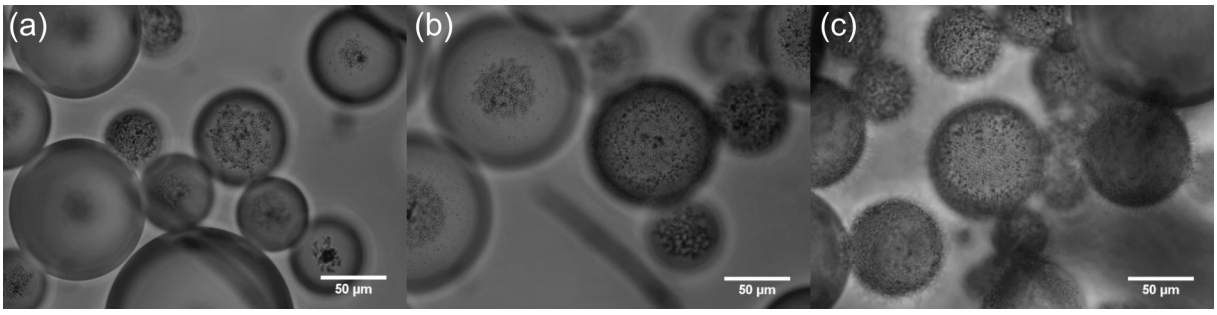

Figure 5: Optical microscopy images of cyclohexane-in-water emulsions of Figure 4 after one month for particle concentrations of (a) 0.02 wt %, (b) 0.05 wt % and (c) 0.10 wt %.

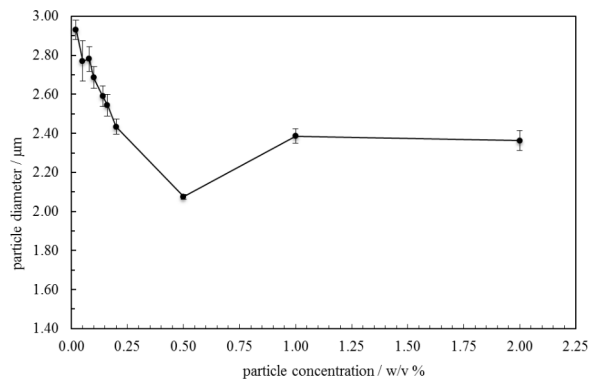

Figure 7: Mean particle diameter in aqueous dispersions as a function of $Ce_{0.495}Sn_{0.495}Pd_{0.01}O_{2-\delta}$ concentration. Particle size measurements were carried out with a Mastersizer 2000 laser diffraction granulometer with the dispersion unit Hydro2000SM(A).

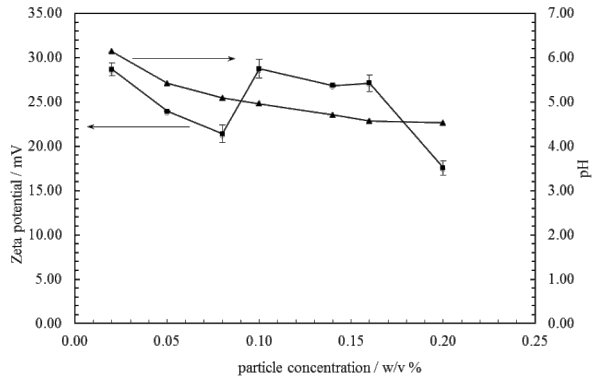

Figure 8: Variation of the zeta potential and pH value of aqueous dispersions of $Ce_{0.495}Sn_{0.495}Pd_{0.01}O_{2-\delta}$ particles versus particle concentration. Zeta potentials were measured using the Malvern Zetasizer Nanoseries. pH values were determined at room temperature using a Jenway 3510 pH meter.

other effects, such as possible reactions of the particles with water, are the reason for the instability of the emulsions at higher concentrations.

Similar trends were found with octane and toluene as the oil phase with the most stable emulsions to coalescence and creaming appearing around ≤0.05 wt % particles (Figure 9).

Catalyst $Ce_{0.20}Sn_{0.79}Pd_{0.01}O_{2-\delta}$

For these particles of larger mean size and with a higher Sn content, surprisingly no stable emulsion was possible using cyclohexane as oil for particle concentrations in water between 0.01 and 2.0 wt % with complete phase separation occurring within 2 h. For octane, emulsion stability to coalescence increased progressively with particle concentration up to 0.2 wt %. The average droplet size however increased from around 60 µm to 150 µm in this range (Figure 10). It is worth noting that relatively stable emulsions (f_o = 0.2 after one month) also exist at 0.3 and 0.5 wt % particles where very large oil drops form (4–6 mm), a feature not possible using surfactants as emulsifier. Densely packed catalyst particles around oil drops can be seen in Figure 10 enabling high stability. Similar trends in behaviour are also found in toluene-in-water emulsions, Figure 11.

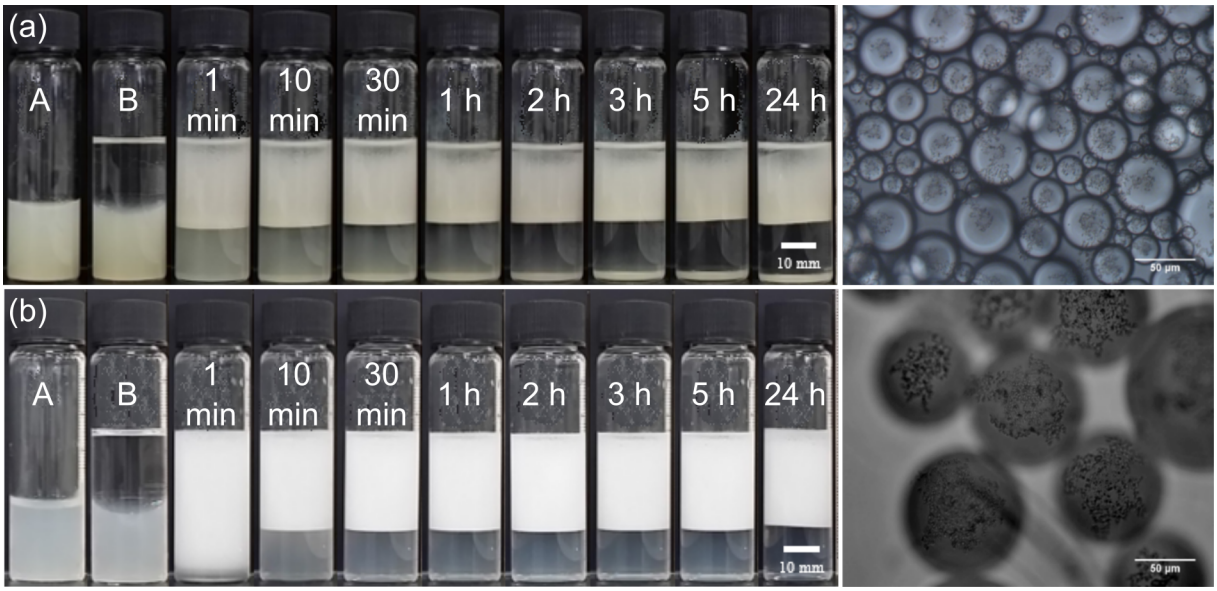

Figure 9: (a) Appearance of octane-in-water emulsions with time at 0.05 wt % of $Ce_{0.495}Sn_{0.495}Pd_{0.01}O_{2-\delta}$ (left) and optical microscope image after 1 week (right); (b) Appearance of toluene-in-water emulsions with time at 0.01 wt % $Ce_{0.495}Sn_{0.495}Pd_{0.01}O_{2-\delta}$ (left) and optical microscope image after 1 week (right).

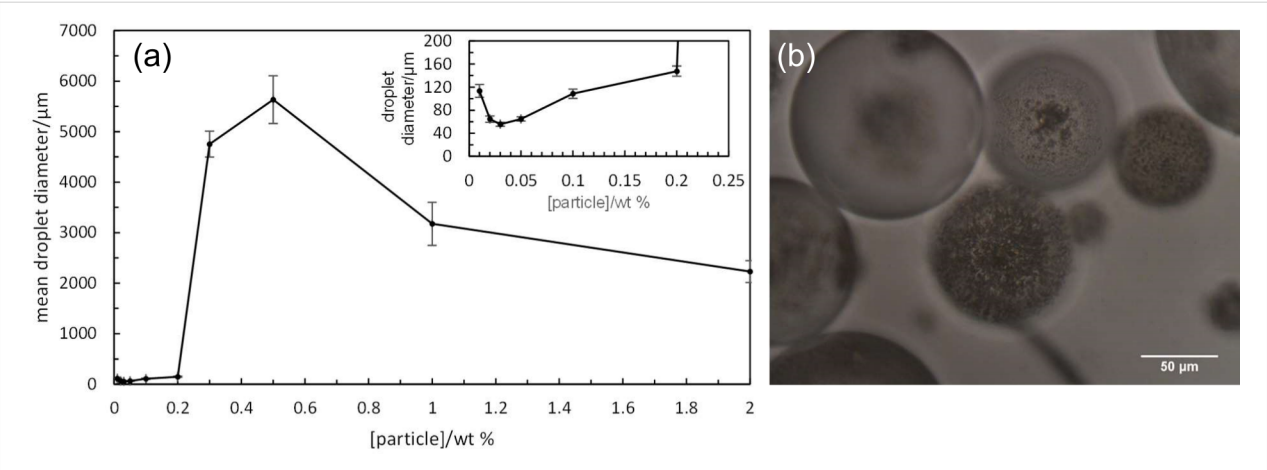

Figure 10: (a) Variation of droplet diameter with particle concentration for octane-in-water emulsions stabilised by $Ce_{0.20}Sn_{0.79}Pd_{0.01}O_{2-\delta}$ particles after one month, (b) optical microscope image of the emulsion at 0.2 wt % particles.

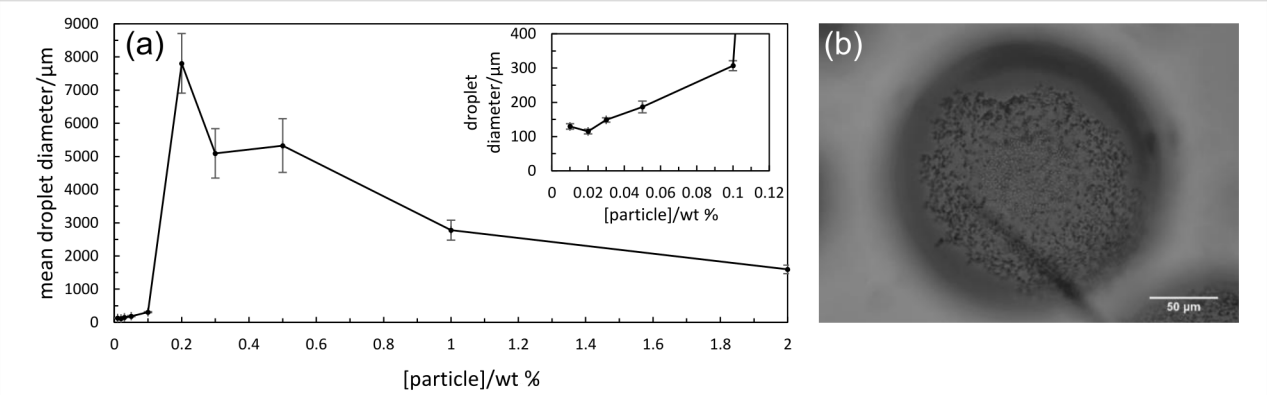

Figure 11: (a) Variation of droplet diameter with particle concentration for toluene-in-water emulsions stabilised by $Ce_{0.20}Sn_{0.79}Pd_{0.01}O_{2-\delta}$ particles after one month, (b) optical microscope image of the emulsion at 0.1 wt % particles.

Conclusion

In this work we present a set of heterogeneous Ce–Sn–Pd oxide catalysts that can be used as stabilisers of Pickering emulsions. The catalysts were demonstrated to be very efficient and versatile for Suzuki–Miyaura reactions. The presence of low amounts of dissolved Pd indicates a release/capture mechanism with the synthesised metal oxides acting as pre-catalysts, which slowly release trace amounts of catalytically active Pd into solution. Considering the application of the palladium catalysts in a continuous flow setup, recyclability as well as stability of the catalysts was substantiated and levels of leached Pd in the reaction mixture were determined to be below the critical limit for oral pharmaceuticals. Furthermore, the palladium catalysts proved to be stable for more than 30 h in continuous flow using the so-called plug & play reactor. Since this device can feature multiple HPLC columns, it can also be used for multistep synthesis as planned for the APIs valsartan and sacubitril. In addition, successful implementation of heterogeneous Pd catalysts in Pickering emulsions is a first promising step towards the aimed combination of chemo- and biocatalysis for the continuous formation of valsartan and sacubitril via multistep catalytic cascade reactions.

Finally, it could be shown that the two sets of Pd-containing particles act as sole emulsifiers of various oils in stabilising oil-in-water emulsions. Emulsions stable to coalescence for at least six months can be prepared at low particle concentrations (<0.1 wt %).

Future approaches will concentrate on the applicability of the Pickering emulsions for multistep reactions as well as on the proposed procedure for the synthesis of valsartan and sacubitril.

Acknowledgements

The authors kindly acknowledge the funding by the H2020-FETOPEN-2016-2017 programme of the European Commission (Grant agreement number: 737266-ONE FLOW).

ORCID® iDs

Katharina Hiebler - https://orcid.org/0000-0001-9964-2027
Manuel C. Maier - https://orcid.org/0000-0003-4441-7353
Eun Sung Park - https://orcid.org/0000-0002-4941-2319
Bernard P. Binks - https://orcid.org/0000-0003-3639-8041
Heidrun Gruber-Woelfler - https://orcid.org/0000-0002-6917-4442

References

1. Selander, N.; Szabó, K. J. *Chem. Rev.* **2011,** *111,* 2048–2076. doi:10.1021/cr1002112
2. Beletskaya, I. P.; Cheprakov, A. V. *Chem. Rev.* **2009,** *100,* 3009–3066. doi:10.1021/cr9903048
3. Wu, X.-F.; Anbarasan, P.; Neumann, H.; Beller, M. *Angew. Chem., Int. Ed.* **2010,** *49,* 9047–9050. doi:10.1002/anie.201006374
4. Torborg, C.; Beller, M. *Adv. Synth. Catal.* **2009,** *351,* 3027–3043. doi:10.1002/adsc.200900587
5. Suzuki, A. *J. Organomet. Chem.* **2002,** *653,* 83–90. doi:10.1016/S0022-328X(02)01269-X
6. Miyaura, N.; Suzuki, A. *Chem. Rev.* **1995,** *95,* 2457–2483. doi:10.1021/cr00039a007
7. Kotha, S.; Lahiri, K.; Kashinath, D. *Tetrahedron* **2002,** *58,* 9633–9695. doi:10.1016/S0040-4020(02)01188-2
8. Magano, J.; Dunetz, J. R. *Chem. Rev.* **2011,** *111,* 2177–2250. doi:10.1021/cr100346g
9. Goossen, L. J.; Melzer, B. *J. Org. Chem.* **2007,** *72,* 7473–7476. doi:10.1021/jo701391q
10. Hung, H.-Y.; Ohkoshi, E.; Goto, M.; Bastow, K. F.; Nakagawa-Goto, K.; Lee, K.-H. *J. Med. Chem.* **2012,** *55,* 5413–5424. doi:10.1021/jm300378k
11. Nicolaou, K. C.; Bulger, P. G.; Sarlah, D. *Angew. Chem., Int. Ed.* **2005,** *44,* 4442–4489. doi:10.1002/anie.200500368
12. Lichtenegger, G. J.; Gruber-Wölfler, H. *Chim. Oggi* **2015,** *33* (4), 12–18.
13. Farina, V. *Adv. Synth. Catal.* **2004,** *346,* 1553–1582. doi:10.1002/adsc.200404178
14. Hagiwara, H.; Shimizu, Y.; Hoshi, T.; Suzuki, T.; Ando, M.; Ohkubo, K.; Yokoyama, C. *Tetrahedron Lett.* **2001,** *42,* 4349–4351. doi:10.1016/S0040-4039(01)00748-1
15. Djakovitch, L.; Koehler, K. *J. Am. Chem. Soc.* **2001,** *123,* 5990–5999. doi:10.1021/ja001087r
16. Crudden, C. M.; McEleney, K.; MacQuarrie, S. L.; Blanc, A.; Sateesh, M.; Webb, J. D. *Pure Appl. Chem.* **2007,** *79,* 247–260. doi:10.1351/pac200779020247
17. MacQuarrie, S.; Nohair, B.; Horton, J. H.; Kaliaguine, S.; Crudden, C. M. *J. Phys. Chem. C* **2010,** *114,* 57–64. doi:10.1021/jp908260j
18. Webb, J. D.; MacQuarrie, S.; McEleney, K.; Crudden, C. M. *J. Catal.* **2007,** *252,* 97–109. doi:10.1016/j.jcat.2007.09.007
19. Mehnert, C. P.; Weaver, D. W.; Ying, J. Y. *J. Am. Chem. Soc.* **1998,** *120,* 12289–12296. doi:10.1021/ja971637u
20. Gruber-Woelfler, H.; Radaschitz, P. F.; Feenstra, P. W.; Haas, W.; Khinast, J. G. *J. Catal.* **2012,** *286,* 30–40. doi:10.1016/j.jcat.2011.10.013
21. Lee, D.-H.; Choi, M.; Yu, B.-W.; Ryoo, R.; Taher, A.; Hossain, S.; Jin, M.-J. *Adv. Synth. Catal.* **2009,** *351,* 2912–2920. doi:10.1002/adsc.200900495
22. Glasnov, T. N.; Findenig, S.; Kappe, C. O. *Chem. – Eur. J.* **2009,** *15,* 1001–1010. doi:10.1002/chem.200802200
23. Cantillo, D.; Kappe, C. O. *ChemCatChem* **2014,** *6,* 3286–3305. doi:10.1002/cctc.201402483
24. ONE-FLOW Research Project: Catalyst Cascade Reactions in 'One-Flow' within a Compartmentalized, Green-Solvent 'Digital Synthesis Machinery' – End-to-End Green Process Design for Pharmaceuticals. Work programme: EU proposal 737266 - ONE-FLOW. https://one-flow.org/.
25. Binks, B. P., Ed. *Modern Aspects of Emulsion Science;* The Royal Society of Chemistry: Cambridge, 1998.
26. Pickering, S. U. *J. Chem. Soc., Trans.* **1907,** *91,* 2001–2021. doi:10.1039/CT9079102001
27. Binks, B. P. *Curr. Opin. Colloid Interface Sci.* **2002,** *7,* 21–41. doi:10.1016/S1359-0294(02)00008-0
28. Binks, B. P. *Langmuir* **2017,** *33,* 6947–6963. doi:10.1021/acs.langmuir.7b00860
29. Crossley, S.; Faria, J.; Shen, M.; Resasco, D. E. *Science* **2010,** *327,* 68–72. doi:10.1126/science.1180769
30. Pera-Titus, M.; Leclercq, L.; Clacens, J.-M.; De Campo, F.; Nardello-Rataj, V. *Angew. Chem., Int. Ed.* **2015,** *54,* 2006–2021. doi:10.1002/anie.201402069
31. Vilela-Martin, J. F. *Drug Des., Dev. Ther.* **2016,** *10,* 1627–1639. doi:10.2147/DDDT.S84782
32. Lau, S.-H.; Bourne, S. L.; Martin, B.; Schenkel, B.; Penn, G.; Ley, S. V. *Org. Lett.* **2015,** *17,* 5436–5439. doi:10.1021/acs.orglett.5b02806
33. Aalla, S.; Gilla, G.; Bojja, Y.; Anumula, R. R.; Vummenthala, P. R.; Padi, P. R. *Org. Process Res. Dev.* **2012,** *16,* 682–686. doi:10.1021/op3000306
34. Pandarus, V.; Desplantier-Giscard, D.; Gingras, G.; Béland, F.; Ciriminna, R.; Pagliaro, M. *Org. Process Res. Dev.* **2013,** *17,* 1492–1497. doi:10.1021/op400118f
35. Wang, G.-x.; Sun, B.-p.; Peng, C.-h. *Org. Process Res. Dev.* **2011,** *15,* 986–988. doi:10.1021/op200032b
36. Guo, M.; Lu, J.; Wu, Y.; Wang, Y.; Luo, M. *Langmuir* **2011,** *27,* 3872–3877. doi:10.1021/la200292f
37. Lichtenegger, G. J.; Maier, M.; Hackl, M.; Khinast, J. G.; Gössler, W.; Griesser, T.; Kumar, V. S. P.; Gruber-Woelfler, H.; Deshpande, P. A. *J. Mol. Catal. A: Chem.* **2017,** *426,* 39–51. doi:10.1016/j.molcata.2016.10.033
38. Lichtenegger, G. J.; Tursic, V.; Kitzler, H.; Obermaier, K.; Khinast, J. G.; Gruber-Wölfler, H. *Chem. Ing. Tech.* **2016,** *88,* 1518–1523. doi:10.1002/cite.201600013
39. Baidya, T.; Gupta, A.; Deshpandey, P. A.; Madras, G.; Hegde, M. S. *J. Phys. Chem. C* **2009,** *113,* 4059–4068. doi:10.1021/jp8060569
40. Richardson, J. M.; Jones, C. W. Assessing Catalyst Homogeneity/Heterogeneity via Application of Insoluble Metal Scavengers: Application to Heck and Suzuki Reactions. In *Catalysis of Organic Reactions;* Prunier, M. L., Ed.; CRC Pres: Boca Raton, FL, 2009; pp 193–202.
41. Richardson, J. M.; Jones, C. W. *J. Catal.* **2007,** *251,* 80–93. doi:10.1016/j.jcat.2007.07.005
42. Lichtenegger, G. J.; Maier, M.; Khinast, J. G.; Gruber-Wölfler, H. *J. Flow Chem.* **2016,** *6,* 244–251. doi:10.1556/1846.2016.00021

License and Terms

BEILSTEIN JOURNAL OF ORGANIC CHEMISTRY

Biocatalytic synthesis of the Green Note *trans*-2-hexenal in a continuous-flow microreactor

Morten M. C. H. van Schie[1], Tiago Pedroso de Almeida[1], Gabriele Laudadio[2], Florian Tieves[1], Elena Fernández-Fueyo[3], Timothy Noël[*2], Isabel W. C. E. Arends[1] and Frank Hollmann[*1]

Letter

Open Access

Address:
[1]Department of Biotechnology, Delft University of Technology, Van der Maasweg 9, 2629 HZ Delft, The Netherlands, [2]Department of Chemical Engineering and Chemistry, Micro Flow Chemistry & Process Technology, Eindhoven University of Technology, Den Dolech 2, 5612 AZ Eindhoven, The Netherlands and [3]Centro de Investigaciones Biológicas, CSIC, Madrid, Spain

Email:
Timothy Noël[*] - t.noel@tue.nl; Frank Hollmann[*] - f.hollmann@tudelft.nl

* Corresponding author

Keywords:
alcohol oxidase; alcohol oxidation; aldehyde; flow chemistry

Beilstein J. Org. Chem. **2018,** *14,* 697–703.
doi:10.3762/bjoc.14.58

Received: 20 October 2017
Accepted: 15 March 2018
Published: 26 March 2018

This article is part of the Thematic Series "Integrated multistep flow synthesis".

Guest Editor: V. Hessel

Abstract

The biocatalytic preparation of *trans*-hex-2-enal from *trans*-hex-2-enol using a novel aryl alcohol oxidase from *Pleurotus eryngii* (*Pe*AAOx) is reported. As O_2-dependent enzyme *Pe*AAOx-dependent reactions are generally plagued by the poor solubility of O_2 in aqueous media and mass transfer limitations resulting in poor reaction rates. These limitations were efficiently overcome by conducting the reaction in a flow-reactor setup reaching unpreceded catalytic activities for the enzyme in terms of turnover frequency (up to 38 s^{-1}) and turnover numbers (more than 300000) pointing towards preparative usefulness of the proposed reaction scheme.

Introduction

trans-2-Hexenal is well-known as a major component of the Green Notes of fruits and vegetables such as apples, strawberries, cherries and more. It is widely used in the flavour and fragrance industry as fresh flavour ingredient in foods and beverages.

One attractive access to *trans*-2-hex-2-enal is the oxidation of the corresponding allylic alcohol to the aldehyde. Though at first sight an oxidation of primary alcohols to the corresponding aldehydes does not appear to be a major challenge, the methods of the state-of-the-art are mostly plagued by undesired side reactions [1]. Also some of the stoichiometric oxidants used are questionable from an environmental and/or toxicological point of view and therefore are not compatible with consumer products such as Green Notes. Therefore, we turned our attention to biocatalytic oxidation methods. For clean conver-

sion of primary alcohols to aldehydes principally two biocatalytic approaches are available (Scheme 1) [2-5]. Alcohol dehydrogenases catalyse the reversible oxidation of alcohols in a Meerwein–Ponndorf–Verley-type of reaction (Scheme 1A). The poor thermodynamic driving force of this reaction, however, necessitates significant molar surpluses of the stoichiometric oxidant (such as acetone). This not only negatively influences the environmental impact of the reaction [6] but also complicates downstream processing. Furthermore, the nicotinamide cofactor (even if used in catalytic amounts only) causes additional costs.

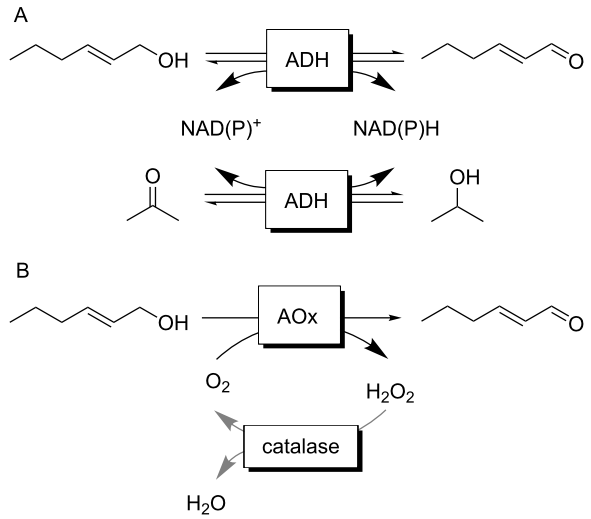

Scheme 1: Enzymatic reaction schemes for the selective oxidation of *trans*-hex-2-enol. A: Alcohol dehydrogenase (ADH)-catalysed oxidation producing stoichiometric amounts of NAD(P)H, which needs to be recycled in situ; the overall reaction is reversible requiring surpluses of the cosubstrate (e.g., acetone) to shift the overall equilibrium to the side of *trans*-hex-2-enal. B: Envisioned aerobic oxidation using alcohol oxidases (AOx). H_2O_2 is formed as byproduct and dismutated by catalase into H_2O and O_2.

Therefore, we concentrated on alcohol oxidase-catalysed reaction schemes (Scheme 1B. Oxidases utilise O_2 as terminal electron acceptor for the oxidation reaction yielding H_2O_2 as sole byproduct. The latter can be disproportionated easily by using catalase (Scheme 1B). Furthermore, O_2 reduction adds sufficient thermodynamic driving force to the reaction to make it essentially irreversible.

The benefits of using O_2, however, also come with the disadvantage of its very poor solubility in aqueous media (ca. 0.25 mM at room temperature). Hence, in the course of an oxidation reaction dissolved O_2 is consumed rapidly and diffusion of O_2 into the reaction medium can easily become overall rate-limiting. The O_2 diffusion rate into the reaction medium directly correlates with the interfacial area between aqueous medium and the gas phase. Large interfacial surface areas can be achieved via heterogeneous intake, by bubbling, stirring, etc. Soluble enzymes, however, are often rather unstable under these conditions, possibly owing to the mechanical stress leading to irreversible inactivation of the biocatalyst [7,8]. Methods of bubble-free aeration have been described in the literature to alleviate the inactivation issue described above [9-12].

The continuous-flow microreactor technology has emerged as a safe and scalable way to approach oxidation reactions [13,14]. Due to its small dimensions, hazardous reactions can be easily controlled, owing to the large surface-to-volume ratio which can minimise hot-spot formation and allows for control over mixing and heating phenomena [15,16]. Furthermore, a well-defined gas–liquid regime can be easily maintained [17,18]. High mass-transfer coefficients are generally the consequence of small vortices induced by the segmented flow regime. This flow pattern guarantees an enhanced contact between the two phases and provides a uniform gas concentration in the liquid segment.

Therefore, it is not very astonishing that also the biocatalysis community is showing interest in flow chemistry. Several biocatalytic processes have been reported in flow reactors [19], mostly advocating easier process intensification in combination with enzyme immobilization [20-23]. Also the higher oxygen-transfer rates in flow reactions compared to batch reactions have been emphasised by several groups. Here, reactor designs ranging from simple flow reactors, tube-in-tube reactors [24], agitated tube reactors [25,26] and continuous agitated cell reactors [27] have been reported.

Encouraged by these contributions, we asked ourselves whether a slug-flow approach may combine mechanically less demanding conditions with high O_2-transfer rates thereby enabling efficient and robust oxidase-catalysed oxidation reactions.

Results and Discussion

Selection and characterisation of the biocatalyst

As biocatalyst for this study we focussed on the recombinant aryl alcohol oxidase from *Pleurotus eryngii* (*Pe*AAOx) [28-31]. Especially the availability as recombinant enzyme (enabling future at-scale production and protein engineering) and its promising activity on allylic alcohols make *Pe*AAOx a promising starting point. Commercially available alcohol oxidases from *Pichia pastoris* and *Candida boidinii* showed no significant activity for the substrate under the same conditions. As *trans*-2-hex-enol had not been reported as substrate for

*Pe*AAOx we evaluated its catalytic properties, particularly the substrate concentration-dependency of the enzymatic oxidation. Initial rate measurements (performed in 1 mL cuvettes) revealed a Michaelis–Menten dependency of the enzyme activity (Figure 1). Apparent K_M and k_{cat} values of approximately 1 mM and 22 s^{-1} were estimated, respectively. These values are in the same order of magnitude as those for benzyl alcohol substrates reported previously [29]. The slightly decreasing enzyme activity at elevated substrate concentrations may be an indication for a slight substrate inhibition. Performing these initial rate measurements in the presence of varying product concentrations showed a pronounced product inhibition (Supporting Information File 1, Figure S2, vide infra).

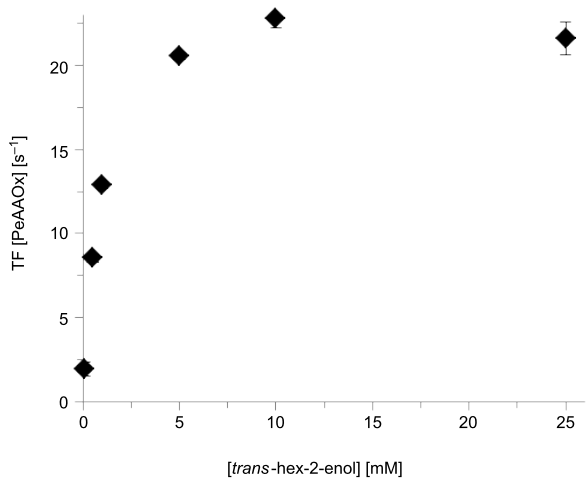

Figure 1: Michaelis–Menten kinetics of the *Pe*AAOx-catalysed oxidation of *trans*-hex-2-enol. Conditions: 50 mM KP_i buffer (pH 7, 30 °C), [*trans*-hex-2-enol]$_0$ = 3 mM, [*Pe*AAOx] = 0.044 μM, [horseradish peroxidase] = 500 U mL^{-1}, [ABTS] = 2 mM.

Continuous-flow reactor enzymatic oxidation

Next, we performed the *Pe*AAOx-catalysed oxidation of *trans*-hex-2-enol in a slug-flow reactor setup (Supporting Information File 1, Figure S1 and Figures S9–S11). In a first set of experiments we systematically varied the residence time of the reaction mixture in the flow reactor (and thereby the reaction time, Figure 2).

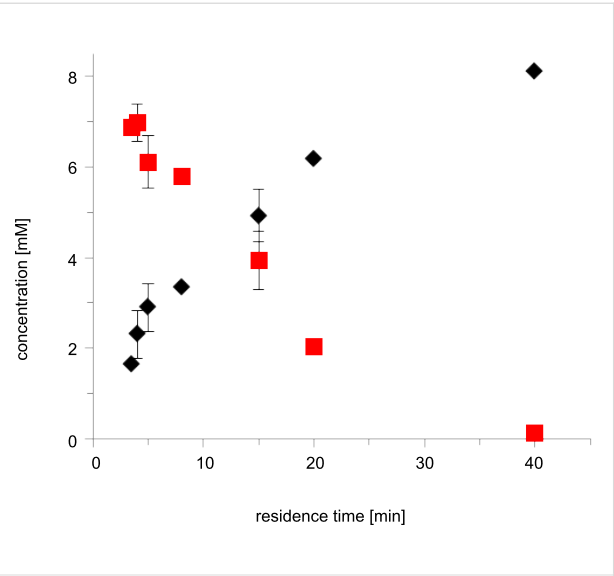

Figure 2: The influence of the residence time on the conversion of *trans*-hex-2-enol (red squares) to *trans*-2-hexenal (black diamonds) in a flow reactor. Conditions: 3 mL flow reactor, 50 mM KP_i buffer (pH 7, 30 °C), [*trans*-hex-2-enol]$_0$ = 10 mM, [*Pe*AAOx] = 0.25 μM, [catalase] = 600 U mL^{-1}.

A full conversion of the starting material into the desired *trans*-hex-2-enal was observed at residence (reaction) times of approximately 40 min corresponding to a turnover number (TN) for the biocatalysts of 32400 and an average turnover frequency (TF) of 13.5 s^{-1}. Even more interestingly, at higher flow rates apparent TF of up to 38 s^{-1} (RT = 5 min) were observed. This value exceeds the previously determined k_{cat}(*Pe*AAOx) (Figure 1) significantly. We attribute this observation to an increased oxygen-transfer rate at high flow rates. In the case of the 5 minutes residence time this corresponds to an O_2-transfer rate of roughly 0.25 mM min^{-1}. Similarly high values could be obtained previously only under mechanically demanding reaction conditions or using surfactant-stabilised emulsions [7]. Varying the ratio of gas to liquid had no significant effect on the overall rate of the reaction (Table 1).

Table 1: Effect of variation of the gas-to-liquid ratio on the rate of the *Pe*AAOx-catalysed aerobic oxidation of *trans*-hex-2-enol.

ratio (liquid:gas)	liquid flow [mL min^{-1}]	gas flow [mL min^{-1}]	residence time [min]	[product] [mM]
1:1	0.20	0.20	15	5.48 (± 0.01)
1:3	0.10	0.30	15	5.18 (± 0.32)
1:5	0.067	0.333	16	4.99 (± 0.49)

Conditions: 3 mL flow reactor, 50 mM KP_i buffer (pH 7, 30 °C), [*trans*-2-hexen-1-ol]$_0$ = 10 mM, [*Pe*AAOx] = 0.25 μM, [catalase] = 600 U mL^{-1}.

Within the experimental error, the conversion in all experiments was identical indicating that even at a comparably low volumetric ratio of 1:1 the O_2 availability was already sufficient not to be overall rate-limiting.

It is worth mentioning here that under batch reaction conditions, similar progression curves were only attainable under mechanically very demanding conditions (i.e., very vigorous stirring and bubbling of O_2 directly into the reaction mixture, Supporting Information File 1, Figure S3). These conditions also caused a significant evaporation of the substrate at higher substrate concentration (Supporting Information File 1, Figure S4), which was much less the case in the flow-reaction setup.

From an economical point-of-view the catalyst performance in terms of turnover number (TN) is of utmost importance as it directly correlates with the cost-contribution of the catalyst to the production costs [32-34]. Therefore we evaluated the TN attainable for *Pe*AAOx in the flow setup (Figure 3). For this lower *Pe*AAOx concentrations as well as significantly increased residence times were applied. The increased residence times were achieved by decreasing the flow rates and using a longer flow reactor (6 mL volume instead of 3 mL).

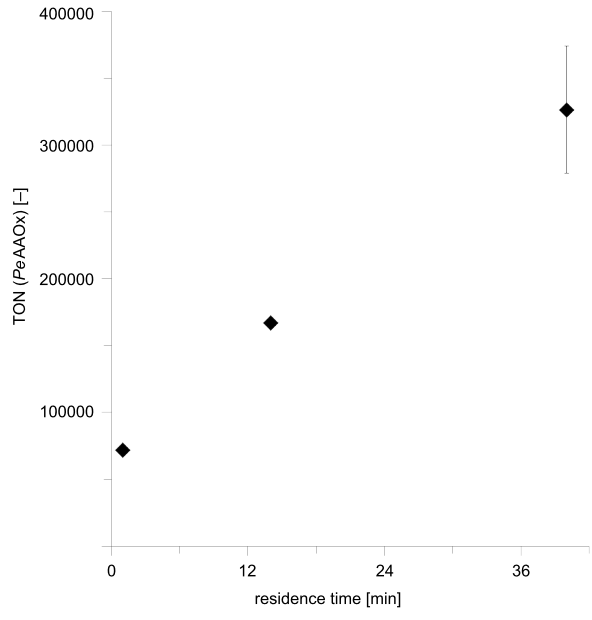

Figure 3: Increasing the *Pe*AAOx turnover numbers (TN) by increasing the residence time. Conditions: 6 mL flow reactor, 50 mM KP_i buffer (pH 7, 30 °C), [*trans*-hex-2-enol]$_0$ = 40 mM, [*Pe*AAOx] = 0.02 µM, [catalase] = 600 U mL^{-1}. The TN value was calculated based on the GC yield of every run. The TN was obtained by dividing the product concentration (as determined chromatographically) by the biocatalyst concentration.

Pleasingly, already in these first experiments a TN for the enzyme of more than 300000 was observed at long residence times. This also underlines the robustness of the enzyme under the flow conditions. Compared to Figure 2 somewhat lower TFs for *Pe*AAOx were observed here, which again can be attributed to a lower O_2-transfer rate at lower flow rates. The quasi-linear relationship shown in Figure 3 also suggests that even higher TN may be attainable – however at the expense of longer reaction times. Therefore, further investigations will focus on identifying conditions satisfying the demand for high TNs and short reaction times. Encouraged by these results, we also tried a semi-preparative scale reaction using 5 g L^{-1} (50 mM) substrate loading in a total of 50 mL with 0.75 µM *Pe*AAOx. As a result, 90% conversion was achieved after 18 h of total reaction time (roughly 80 minutes of residence time in the 6 mL reactor). The product was purified chromatographically resulting in 200 mg of pure *trans*-hex-2-enal (as determined by NMR) in 81% isolated yield thereby demonstrating the preparative potential of the proposed reaction setup.

Conclusion

Alcohol oxidase-catalysed oxidation of alcohols to aldehydes bears a significant potential for preparative biocatalysis. The reaction is independent from expensive and instable nicotinamide cofactors (and the corresponding cosubstrates/coproducts as well as possible regeneration enzymes) and produces only water as byproduct. These advantages, however, are counteracted by the generally low reaction rates caused by the poor O_2 availability. Flow chemistry is a promising technique to provide the aqueous reaction mixture with O_2 needed for the oxidation. It enables high O_2 transfer rates while avoiding enzyme robustness issues frequently observed with 'traditional' aeration methods.

Future developments in our laboratories will concentrate on the characterisation, extension and preparative demonstration of this powerful combination of oxidase catalysis and flow chemistry.

Experimental

General

Turnover numbers (TN) and turnover frequencies (TF) reported in this manuscript were calculated based on Equation 1 and Equation 2.

$$\mathrm{TN}\,[-] = \frac{c(\mathrm{product})}{c(\mathrm{PeAAOx})} \quad (1)$$

$$\mathrm{TF}\,[\mathrm{s}^{-1}] = \frac{\mathrm{TN}}{\text{reaction time}} \quad (2)$$

Production of *Pe*AAOx

E. coli cultivation

For the production, activation and purification of *Pe*AAOx, a slightly modified literature protocol was used [28]. Pre-cultures of LB media containing 100 μg mL^{-1} of ampicillin were inoculated with *E. coli* W3110 containing pFLAG1-AAO and incubated overnight at 37 °C and 180 rpm. Overexpression was carried out in 5 L flasks with 1 L of TB medium supplemented with 100 μg mL^{-1} of ampicillin. The medium was inoculated with the pre-culture to an OD of 0.05 and grown at 37 °C and 180 rpm. At an OD_{600} of 0.8, 1 mM isopropyl β-D-thiogalactopyranoside (IPTG) was added and the cultures were incubated for additional 4 h at 37 °C and 180 rpm. The bacterial pellets, obtained after harvesting the cells, were re-suspended in a total volume of 40 mL 50 mM Tris/HCl buffer, pH 8.0, containing 10 mM EDTA and 5 mM dithiothreitol (DTT).

Refolding

The re-suspended cells were disrupted by incubation with 2 mg mL^{-1} lysozyme for 1 h at 4 °C. Afterwards, 0.1 mg mL^{-1} DNase, 1 mM $MgCl_2$ and 0.1 mM PMSF were added followed by sonication. The insoluble fraction was collected by centrifugation (30 min at 15,000 rpm and 4 °C), re-suspended and washed three times with 20 mL 20 mM Tris/HCl buffer, pH 8.0, containing 10 mM EDTA and 5 mM DTT using a potter homogenizing device. The pellets obtained after centrifugation (15 min at 15,000 rpm and 4 °C) were solubilized in a total volume of 30 mL 20 mM Tris/HCl buffer, pH 8.0, containing 2 mM EDTA, 50 mM DTT and 8 M urea. After incubation on ice for 30 min, the solution was cleared by centrifugation (15 min at 15,000 rpm and 4 °C). The obtained supernatant was used as stock solution for the in vitro refolding.

The *Pe*AAOx was solubilized using 150 μg mL^{-1} protein in 20 mM Tris/HCl buffer, pH 9.0, containing 2.5 mM GSSG, 1 mM DTT, 0.02 mM FAD, 34% glycerol and 0.6 M urea at 4 °C for 80 h. After the incubation for *Pe*AAOx activation/refolding, the refolding mixture was concentrated to 100 mL and the buffer exchanged against 10 mM sodium phosphate buffer, pH 5.5 by diafiltration (DV 20) and subsequently concentrated using an Amicon Ultra 15 mL centrifugal filter (MWCO 10 kDa). After centrifugation (overnight at 15,000 rpm and 4 °C), the soluble fraction was further purified using anion-exchange chromatography.

Purification

The concentrated *Pe*AAOx solution was purified using a 58 mL Q Sepharose column (GE Healthcare). *Pe*AAOx was eluted with a linear NaCl gradient (0–0.6 M over 6 CV) using 10 mM sodium phosphate buffer, pH 5.5. Fractions containing *Pe*AAOx were pooled, concentrated and desalted using HiTrap desalting columns (GE Healthcare) and 10 mM sodium phosphate buffer, pH 5.5. The *Pe*AAOx concentration was calculated based on the absorbance using the molar extinction coefficient of ε_{463} 11,050 M^{-1} cm^{-1}.

Activity assay

The activity of *Pe*AAOx was determined by UV–vis spectroscopy, using an Agilent Cary 60 UV–vis spectrophotometer, following the oxidation of ABTS (ε_{405} = 36,800 M^{-1} cm^{-1}) by horseradish peroxidase (POD) at the expense of hydrogen peroxide. In general, 0.044 μM *Pe*AAOx was used to convert 3 mM of *trans*-2-hex-2-enol. The hydrogen peroxide formed in this reaction was subsequently used to convert 2 mM of ABTS to $ABTS^{\cdot+}$ by an excess of POD (500 U mL^{-1}). The reactions were performed at 30 °C in oxygen-saturated 50 mM KP_i buffer at pH 7.0.

Flow reactor experiments

PFA microreactor coils (750 μm ID) with a volume of 3 and 6 mL were constructed. The reaction mixture was introduced via a syringe pump (Fusion 200, Chemyx), while the pure oxygen flow was controlled by a mass flow controller (EL-FLOW, Bronkhorst), resulting in a segmented flow (Supporting Information File 1, Figure S8). Residence times were taken as the time between the solution entering and exiting the coil and were varied by altering the flow, keeping the ratio of oxygen to liquid at three to one. Samples were collected on ice and as soon as enough volume was collected, extracted with ethyl acetate and analysed by GC (vide infra).

GC analysis

The collected reaction mixtures were extracted into an equal volume of ethyl acetate, dried with magnesium sulphate and analysed on a CP-wax 52 CB GC column (50 m × 0.53 m × 2 μm) (GC method: 60 °C for 3 min; 30 °C/min to 105 °C; 105 °C for 7 min; 30 °C/min to 250 °C; 250 °C for 1 minute). Dodecane (5 mM) was added as standard.

Work-up semi-preparative scale

The reaction mixture was directly collected in deuterated chloroform at the end of the flow reactor followed by recording the NMR spectrum in order to evaluate the conversion (see Supporting Information File 1). The organic mixture was diluted and introduced into a separation funnel and washed with brine. The aqueous phase was backwashed once with DCM. The collected organic phase was dried over $MgSO_4$, filtered and concentrated under reduced pressure. Purification of the isolated mixture was performed by flash chromatography on silica (pure DCM). The final product was obtained as colourless oil (200 mg).

(*E*)-Hex-2-enal

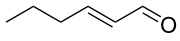

TLC (DCM) R_f 0.9; ^{1}H NMR (399 MHz, $CDCl_3$) δ 9.44 (d, *J* = 7.7 Hz, 1H), 6.78 (dt, *J* = 15.6, 6.8 Hz, 1H), 6.05 (ddq, *J* = 15.5, 7.8, 1.3 Hz, 1H), 2.33–2.18 (m, 2H), 1.48 (h, *J* = 7.4 Hz, 2H), 0.90 (t, *J* = 7.4 Hz, 3H); ^{13}C NMR (101 MHz, $CDCl_3$) δ 194.3, 158.9, 133.3, 34.8, 21.3, 13.8.

Supporting Information

Supporting Information File 1

General information and supporting figures.
[https://www.beilstein-journals.org/bjoc/content/supplementary/1860-5397-14-58-S1.pdf]

Acknowledgements

We thank the Netherlands Organisation for Scientific Research for financial support through a VICI grant (no. 724.014.003).

ORCID® iDs

Gabriele Laudadio - https://orcid.org/0000-0002-2749-8393
Timothy Noël - https://orcid.org/0000-0002-3107-6927
Frank Hollmann - https://orcid.org/0000-0003-4821-756X

References

1. Alshammari, H.; Miedziak, P. J.; Morgan, D. J.; Knight, D. W.; Hutchings, G. J. *Green Chem.* **2013,** *15,* 1244–1254. doi:10.1039/C3GC36828A
2. Turner, N. J. *Chem. Rev.* **2011,** *111,* 4073–4087. doi:10.1021/cr200111v
3. Hollmann, F.; Arends, I. W. C. E.; Buehler, K.; Schallmey, A.; Bühler, B. *Green Chem.* **2011,** *13,* 226–265. doi:10.1039/c0gc00595a
4. Kroutil, W.; Mang, H.; Edegger, K.; Faber, K. *Curr. Opin. Chem. Biol.* **2004,** *8,* 120–126. doi:10.1016/j.cbpa.2004.02.005
5. Pickl, M.; Fuchs, M.; Glueck, S. M.; Faber, K. *Appl. Microbiol. Biotechnol.* **2015,** *99,* 6617–6642. doi:10.1007/s00253-015-6699-6
6. Ni, Y.; Holtmann, D.; Hollmann, F. *ChemCatChem* **2014,** *6,* 930–943. doi:10.1002/cctc.201300976
7. Churakova, E.; Arends, I. W. C. E.; Hollmann, F. *ChemCatChem* **2013,** *5,* 565–568. doi:10.1002/cctc.201200490
8. Bommarius, A. S.; Karau, A. *Biotechnol. Prog.* **2005,** *21,* 1663–1672. doi:10.1021/bp050249q
9. Van Hecke, W.; Ludwig, R.; Dewulf, J.; Auly, M.; Messiaen, T.; Haltrich, D.; Van Langenhove, H. *Biotechnol. Bioeng.* **2009,** *102,* 122–131. doi:10.1002/bit.22042
10. Van Hecke, W.; Bhagwat, A.; Ludwig, R.; Dewulf, J.; Haltrich, D.; Van Langenhove, H. *Biotechnol. Bioeng.* **2009,** *102,* 1475–1482. doi:10.1002/bit.22165
11. Illner, S.; Hofmann, C.; Löb, P.; Kragl, U. *ChemCatChem* **2014,** *6,* 1748–1754. doi:10.1002/cctc.201400028
12. Kaufhold, D.; Kopf, F.; Wolff, C.; Beutel, S.; Hilterhaus, L.; Hoffmann, M.; Scheper, T.; Schlüter, M.; Liese, A. *J. Membr. Sci.* **2012,** *423–424,* 342–347. doi:10.1016/j.memsci.2012.08.035
13. Gemoets, H. P. L.; Su, Y.; Shang, M.; Hessel, V.; Luque, R.; Noël, T. *Chem. Soc. Rev.* **2016,** *45,* 83–117. doi:10.1039/C5CS00447K
14. Plutschack, M. B.; Pieber, B.; Gilmore, K.; Seeberger, P. H. *Chem. Rev.* **2017,** *117,* 11796–11893. doi:10.1021/acs.chemrev.7b00183
15. Kockmann, N.; Thenée, P.; Fleischer-Trebes, C.; Laudadio, G.; Noël, T. *React. Chem. Eng.* **2017,** *2,* 258–280. doi:10.1039/C7RE00021A
16. Gutmann, B.; Cantillo, V.; Kappe, C. O. *Angew. Chem., Int. Ed.* **2015,** *54,* 6688–6728. doi:10.1002/anie.201409318
17. Noël, T.; Su, Y.; Hessel, V. Beyond Organometallic Flow Chemistry: The Principles Behind the Use of Continuous-Flow Reactors for Synthesis. *Organometallic Flow Chemistry;* Topics in Organometallic Chemistry, Vol. 57; Springer, 2016; pp 1–41. doi:10.1007/3418_2015_152
18. Mallia, C. J.; Baxendale, I. R. *Org. Process Res. Dev.* **2016,** *20,* 327–360. doi:10.1021/acs.oprd.5b00222
19. Tamborini, L.; Fernandes, P.; Paradisi, F.; Molinari, F. *Trends Biotechnol.* **2018,** *36,* 73–88. doi:10.1016/j.tibtech.2017.09.005
20. Peris, E.; Okafor, O.; Kulcinskaja, E.; Goodridge, R.; Luis, S. V.; Garcia-Verdugo, E.; O'Reilly, E.; Sans, V. *Green Chem.* **2017,** *19,* 5345–5349. doi:10.1039/C7GC02421E
21. Bolivar, J. M.; Wiesbauer, J.; Nidetzky, B. *Trends Biotechnol.* **2011,** *29,* 333–342. doi:10.1016/j.tibtech.2011.03.005
22. Zor, C.; Reeve, H. A.; Quinson, J.; Thompson, L. A.; Lonsdale, T. H.; Dillon, F.; Grobert, N.; Vincent, K. A. *Chem. Commun.* **2017,** *53,* 9839–9841. doi:10.1039/C7CC04465H
23. Tang, X.; Allemann, R. K.; Wirth, T. *Eur. J. Org. Chem.* **2017,** 414–418. doi:10.1002/ejoc.201601388
24. Tomaszewski, B.; Lloyd, R. C.; Warr, A. J.; Buehler, K.; Schmid, A. *ChemCatChem* **2014,** *6,* 2567–2576. doi:10.1002/cctc.201402354
25. Jones, E.; McClean, K.; Housden, S.; Gasparini, G.; Archer, I. *Chem. Eng. Res. Des.* **2012,** *90,* 726–731. doi:10.1016/j.cherd.2012.01.018
26. Gasparini, G.; Archer, I.; Jones, E.; Ashe, R. *Org. Process Res. Dev.* **2012,** *16,* 1013–1016. doi:10.1021/op2003612
27. Toftgaard Pedersen, A.; de Carvalho, T. M.; Sutherland, E.; Rehn, G.; Ashe, R.; Woodley, J. M. *Biotechnol. Bioeng.* **2017,** *114,* 1222–1230. doi:10.1002/bit.26267
28. Ruiz-Dueñas, F. J.; Ferreira, P.; Martinez, M. J.; Martinez, A. T. *Protein Expression Purif.* **2006,** *45,* 191–199. doi:10.1016/j.pep.2005.06.003
29. Ferreira, P.; Medina, M.; Guillén, F.; Martínez, M. J.; Van Berkel, W. J. H.; Martínez, A. T. *Biochem. J.* **2005,** *389,* 731–738. doi:10.1042/bj20041903
30. Guillén, F.; Martinez, A. T.; Martinez, M. J. *Eur. J. Biochem.* **1992,** *209,* 603–611. doi:10.1111/j.1432-1033.1992.tb17326.x
31. Guillén, F.; Martinez, A. T.; Martínez, M. J. *Appl. Microbiol. Biotechnol.* **1990,** *32,* 465–469. doi:10.1007/bf00903784
32. Bormann, S.; Gomez Baraibar, A.; Ni, Y.; Holtmann, D.; Hollmann, F. *Catal. Sci. Technol.* **2015,** *5,* 2038–2052. doi:10.1039/C4CY01477D
33. Toftgaard Pedersen, A.; Birmingham, W. R.; Rehn, G.; Charnock, S. J.; Turner, N. J.; Woodley, J. M. *Org. Process Res. Dev.* **2015,** *19,* 1580–1589. doi:10.1021/acs.oprd.5b00278
34. Tufvesson, P.; Lima-Ramos, J.; Nordblad, M.; Woodley, J. M. *Org. Process Res. Dev.* **2011,** *15,* 266–274. doi:10.1021/op1002165

License and Terms

The definitive version of this article is the electronic one which can be found at:
doi:10.3762/bjoc.14.58

BEILSTEIN JOURNAL OF ORGANIC CHEMISTRY

Nanoreactors for green catalysis

M. Teresa De Martino[1], Loai K. E. A. Abdelmohsen[1], Floris P. J. T. Rutjes[2] and Jan C. M. van Hest[*1]

Review

Open Access

Address:
[1]Eindhoven University of Technology, P.O. Box 513, 5600 MB Eindhoven, The Netherlands and [2]Radboud University, Institute for Molecules and Materials, Heyendaalseweg 135, 6525 AJ Nijmegen, The Netherlands

Email:
Jan C. M. van Hest[*] - j.c.m.v.hest@tue.nl

* Corresponding author

Keywords:
catalysis; dendrimers; green chemistry; nanogels; nanoreactors; micelles; polymersomes

Beilstein J. Org. Chem. **2018,** *14,* 716–733.
doi:10.3762/bjoc.14.61

Received: 31 October 2017
Accepted: 13 March 2018
Published: 29 March 2018

This article is part of the Thematic Series "Integrated multistep flow synthesis".

Guest Editor: V. Hessel

Abstract

Sustainable and environmentally benign production are key drivers for developments in the chemical industrial sector, as protecting our planet has become a significant element that should be considered for every industrial breakthrough or technological advancement. As a result, the concept of green chemistry has been recently defined to guide chemists towards minimizing any harmful outcome of chemical processes in either industry or research. Towards greener reactions, scientists have developed various approaches in order to decrease environmental risks while attaining chemical sustainability and elegancy. Utilizing catalytic nanoreactors for greener reactions, for facilitating multistep synthetic pathways in one-pot procedures, is imperative with far-reaching implications in the field. This review is focused on the applications of some of the most used nanoreactors in catalysis, namely: (polymer) vesicles, micelles, dendrimers and nanogels. The ability and efficiency of catalytic nanoreactors to carry out organic reactions in water, to perform cascade reaction and their ability to be recycled will be discussed.

Introduction

It is widely acknowledged that “the best solvent is no solvent”; however, running a reaction under neat conditions is very challenging from the points of view of mass transfer and temperature gradients [1,2]. Therefore, sustainable chemical technologies are often related to the use of a green non-harmful solvent [3], water. In principle, green chemistry refers to (1) the employment of raw material (substrates) in an efficient manner, (2) decreasing the resulting waste or undesired byproducts, and (3) using cheap and environment friendly solvents (i.e., water). Generally, using water as a solvent is an acceptable choice for green chemistry [4-6]. Indeed, water is attractive from both economic and environmental points of view, and is not taken

into account when the E-factor (defined as mass ratio of waste to desired product) for a chemical process is determined [7,8]. This is to be true for chemical processes where the utility of water is limited to the work-up at the end of the process and not when used as a reaction medium. However, it should be noted that the utility of water as a reaction medium is the safest, but not the greenest choice. Unfortunately, most organic compounds and catalysts are not soluble in water, limiting its utility for most reactions [9,10]. For this reason, scientists across academia and industry have proposed many solutions in order to maximize the outcome of reactions (i.e., yields, enantioselectivities, etc.) in water and, thereby, harness its utility for further applications. The abovementioned issues are particularly relevant in the field of asymmetric catalysis, which besides overcoming catalyst compatibility also has to deal with cost issues [11,12]. Research on asymmetric catalysis has been mainly focused on performing catalytic reactions with high enantioselectivity and efficiency [13,14]. As a result, a wide range of chiral catalysts have been established [15,16]. Chiral catalysts are, however, not only incompatible with aqueous solutions, but also expensive due to the structural complexity of the ligands used and the usage of transition metals. Finding an approach to utilize chiral catalysts in water while minimizing their cost (i.e., recycling) is still a big challenge. In order to accomplish this, various strategies have been proposed and applied [17-19]. One significant, well-established and widely used strategy, is the use of site-isolated techniques, i.e., creating a separate micro environment [20-22] for catalysts to (1) allow their use in incompatible media, (2) to reduce their costs by recycling them, and (3) avoid any unfavorable environmental influences that might affect reaction yield and output [23,24]. Indeed, such a strategy proved to be advantageous for performing reactions in water and minimizing both reaction waste and cost [25,26].

Attempts to support homogeneous metal complexes onto organic or inorganic surfaces to facilitate their removal/extraction from the reaction mixture has proven to be successful [27,28]. In fact, the utility of catalytic supports has been fundamental to the concept of entrapping catalysts in organic nanodomains and bringing the notion of catalytic nanoreactors to light [29,30]. In recent years the use of nanocontainers/reactors wherein catalysts are entrapped and physically separated in an isolated compartment has appeared to be an excellent facile approach to enhance performance of reactions in water [31-34]. Pioneering examples in this field include small molecule host–guest containers such as cavitands [35-37], and calixarenes [38,39]. Besides these supramolecular cage structures compartmentalization can also be achieved in macromolecular nanoreactors. The advantage of employing these polymeric structures is their improved robustness and loading capacity, which makes recycling and efficient usage of catalytic species more achievable. Nanocompartments such as polymersomes [40], micelles [41], dendrimers [42], and nanogels [43,44] represent smart and compact devices to carry out reactions in aqueous media. Besides, their facile recyclability make them very suitable as nanoreactors for a multitude of applications in synthetic chemistry [24,31]. In a recent study the E-factors for different traditional coupling reactions used in the pharmaceutical industry were reported and compared to those achieved in micellar nanoreactors [45], showing for the latter a decrease of at least an order of magnitude, which underlines their considerable potential in green catalysis (Table 1).

In this review we will focus on the application of polymeric nanoreactors in green catalysis by highlighting their structure and ability to encapsulate and shield catalysts. Four different types of nanoreactors will be described, namely micelles, polymersomes, dendrimers and nanogels. The choice of discussing these nanoreactors stems from their accredited relevance in the field of catalysis and the significant number of examples published in literature. The advantageous aspects of these four classes of nanoreactors over non-supported homogeneous systems include: 1) the site isolation of reactive components (enabling cascade reactions), 2) the ability to convert hydrophobic substrates in water (under green conditions), and 3) the facile catalyst recovery. All these attractive features are covered in this review. Moreover, in this review we have not attempted to be comprehensive, but we rather want to illustrate the application potential of these nanoreactors with some illustrative examples of the most relevant classes of organic reactions (performed in water), which should interest both academia and industry.

Table 1: Representative comparison of E-factors (including the aqueous work-up), of a pharmaceutically relevant synthesis, carried out via a traditional and a micellar process [45].

reaction	E-factors in traditional process	E-factors in micelles
Heck coupling (300 g scale)	136	7.6
Suzuki–Miyaura (302 g scale)	83	8.3
Sonogashira coupling (57 kg scale)	37.9	7.0

Review

1. Homogeneous vs heterogeneous catalysis

Catalysis, in general, is divided into two major types, homogenous and heterogeneous. In homogeneous catalysis catalyst and substrates are both present and molecularly dissolved in the same phase (typically a liquid phase) [46]. Homogeneous catalysis involves the use of biocatalysts (enzymes), organocatalysts and metal catalysts [47]. Catalysis is defined as heterogeneous when catalysts are in an aggregated state, and are thus in a different phase than the reactants [27,48]. Heterogeneous catalysts typically consist of a solid carrier, the so called "support", on which catalytic sites are dispersed [49,50]. Homogeneous catalysis is generally performed under milder operative conditions than heterogeneous catalysis [51]. In fact, heterogeneous catalysts generally possess very high decomposition temperatures (above 100 °C) [52]. The presence of a solid phase often results in the formation of temperature gradients when using high temperatures, which leads to an increase in reactant diffusion and a consequent hampering of mass transfer [53]. Furthermore, the catalytic sites in heterogeneous catalysis are often not as well-defined as in homogeneous catalysis. Therefore, homogeneous catalysis usually results in better selectivity and less byproducts [54].

Although homogenous catalysis ensures high selectivity and a better reaction outcome, yet it is expensive (catalyst recycling is not always an option) and it requires the utility of harmful solvents, yielding high E-factors [53]. In order to lower the E-factor, water should be used in the work-up procedure and separation. It has to be pointed out, however, that the presence of water during the process and its purification afterwards, especially when coming from industrial wastes, poses stringent limitations from an economical and environmental point of view.

A good method for homogeneous catalysts separation and reuse is offered by the use of biphasic liquid–liquid systems. Recycling can be achieved in the reactor when the organic phase is sampled out, while the aqueous phase containing the catalyst is retained into the vessel, enabling for continuous processing. The main issue that has to be solved in such set-up is the tolerability of the catalyst to water (its solubility, its activity, etc.) [55]. A strategy to overcome this problem is the inclusion and confinement of the homogeneous catalysts into a host nano-architecture [56]. Compartmentalization enables catalyst segregation and shielding, and ensures its facile removal from the reaction mixture after the reaction has taken place [34]; this facilitates reactions to be performed in water followed by liquid–liquid separation of products and catalyst [22]. Moreover, shielding and segregation of catalysts in a nanoreactor facilitates one-pot tandem reactions that, in most cases, require two or more incompatible catalysts [22,57]. Catalyst confinement leads to a high local concentration of the substrate at the active site, which results in higher reaction rates and better conversion [9]. In this review we will highlight some typical nanoreactors that are used to accommodate homogeneous catalysts, holding promise in green organic synthesis. A division will be made between self-assembled nanoreactors, section 2, and covalent systems, section 3.

2. Self-assembled nanoreactors

Self-assembled nanoreactors are macromolecular architectures that are non-covalently assembled from their constituent building units [58,59]. Such nanoreactors allow for physical confinement of catalysts, shielding them from their surroundings [60]. Compartmentalization of catalysts in supramolecular nanoreactors is advantageous from kinetic (faster catalytic process) [61] and thermodynamic (lower transition state of reaction) [9] catalysis points of view. Segregation and isolation of catalysts inside nanoreactors guarantee, in most cases, a valuable platform for catalyst recycling [30]. In the following section we will discuss the utility of some of the well-established catalytic nanoreactors towards green(er) chemistry [62].

2.1. Micelles

Micelles are supramolecular architectures that are assembled of amphiphilic molecules [41]. Above the critical micellar concentration (CMC), surfactants with the appropriately designed hydrophilic head (neutral, anionic and cationic) and hydrophobic chain organize themselves in micelles [31]. Micelles have been extensively studied [9,32] and their utility as nanoreactors is well-established [41,58]. Various micellar morphologies can be obtained depending on the 'packing parameter' [56-61], which is defined as $p = v/a_o\, l_c$, where v is the volume, l_c is the length of the hydrophobic chain and a_o is the optimal area of the head groups [62]. As a general rule, if $p \leq 1/3$ spherical micelles are obtained, while cylindrical micelles, or the so-called worm-like micelles, form when $1/3 \leq p \leq 1/2$. A typical micelle acquires a hydrophobic core that is able to accommodate hydrophobic catalysts, providing thermodynamic and kinetic control over chemical reactions [31]. Moreover, carrying out reactions in such a hydrophobic core leads to a concentration effect for hydrophobic substrates, which ensures higher reaction rates than those performed in bulk [63]. Besides, the structure of any micellar catalytic environment is governed by the arrangement of the amphiphilic molecules, creating, in many cases, a regioselective environment (Figure 1) that affects the outcome of some reactions [29].

Non-spherical, high aspect ratio micelles are preferred for catalysis as such structures provide large surface area where reactions could take place [64]. This has been particularly the case

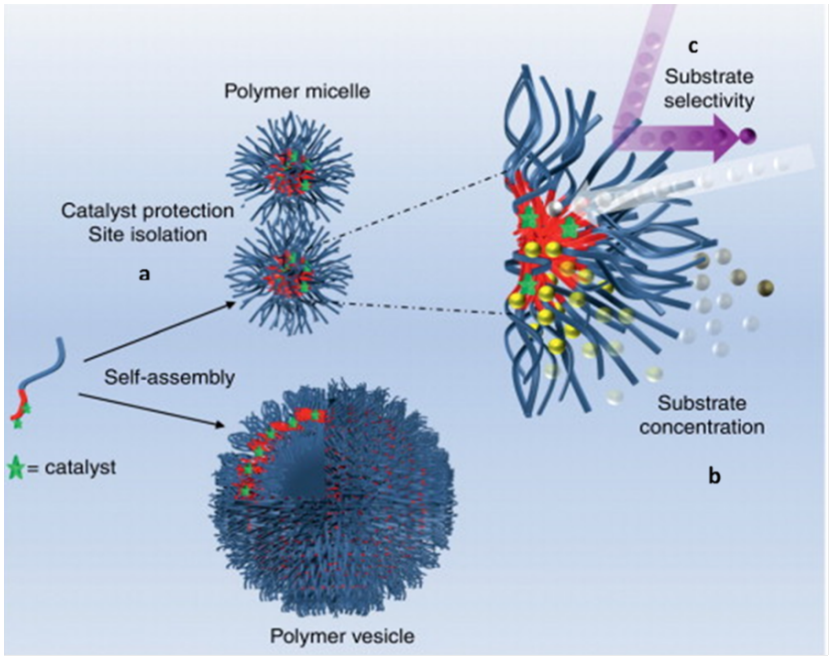

Figure 1: Assembly of catalyst-functionalized amphiphilic block copolymers into polymer micelles and vesicles. Characteristics of a nanoreactor system are shown using the polymer micelles including (a) the catalysts are protected and isolated from each other by the micellar shell, (b) substrates are effectively sequestered by the core from the surrounding environment, creating a highly concentrated environment for confined catalysis, (c) the nanostructure shell may regulate the access of substrates to the catalyst-containing micelle core. Reprinted with permission from reference [29].

for dehydration reactions [24]. Due to the combination of the structures' high aspect ratio and the hydrophobic effect, water could effectively diffuse away from the catalytic site, which enabled the enhanced formation of product. [40].

Catalysis in micelles: Micelles as nanoreactors have been extensively used in organic synthesis [31], allowing reactions in water [65] with better yields and easier catalyst recover [26] than traditional processes.

Lipshutz and co-workers have successfully exploited micelles not only as nanoreactors, but as an outstanding platform for achieving greener organic reactions [26,65,66]. They have shown, for example, C–N cross-coupling reactions between heteroaryl bromides, chlorides or iodides and carbamate, sulfonamide or urea derivatives to be successfully realized in water using palladium-loaded TPGS-750-M (*dl*-α-tocopherol methoxypolyethylene glycol succinate) micelles (Scheme 1). Moreover, this micellar catalytic system allowed for catalyst

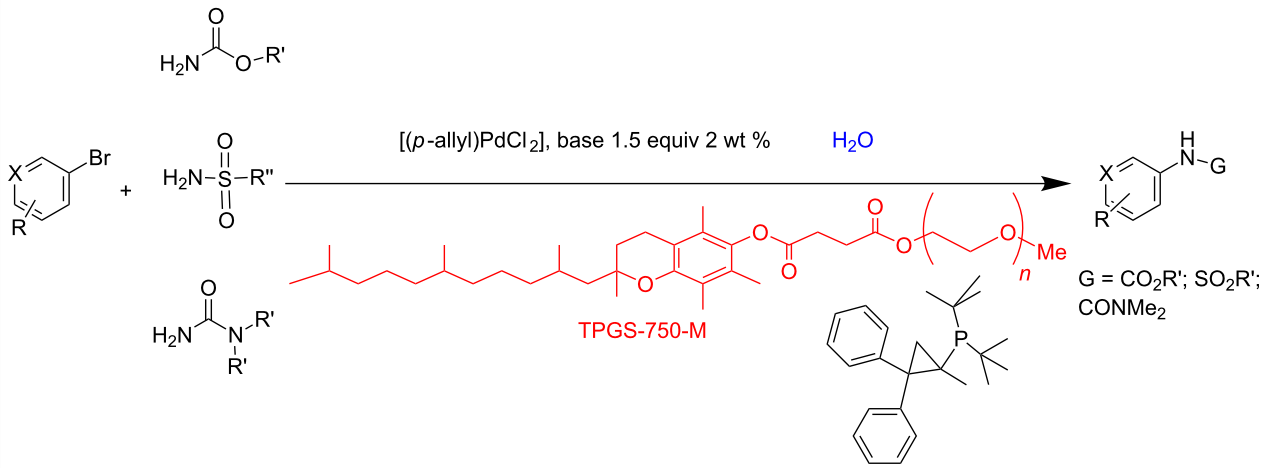

Scheme 1: C–N bond formation under micellar catalyst conditions, no organic solvent involved. Adapted from reference [67].

recycling, minimizing the amount of the used organic solvent and generated waste [67].

The same group reported another interesting catalytic micelle system, which is based on PTS (polyoxyethanyl α-tocopheryl sebacate) [68]. Using PTS-based micelles, they showed the amination of allylic ethers in water (Table 2 and Table 3). The reaction of different ethers with naphthylmethylamine resulted in excellent yields (Table 2). Comparable yields were obtained when different amines reacted with *trans*-cinnamyl phenyl ether (Table 3). In both of the cases micelles were used to protect the very sensitive and unstable $[Pd(allyl)Cl]_2$ intermediate from air.

Micelles were also used to perform cross-coupling between benzyl and aryl halides in water [65]. This reaction is known to result in very limited yields due to the undesired homo-coupling reaction between electron-rich and electron-poor benzyl bromides [69]. This draw-back has been circumvented by using Pd-catalytic micelles, which were assembled in water using TMEDA (tetramethylethylenediamine) as additive. TMEDA was used to stabilize the Pd catalyst by chelation and indeed, presence of TMEDA resulted in higher yield [65]. High catalytic efficiency of these Pd-catalytic micelles was also achieved while catalyzing reactions involving less reactive or sterically hindered species.

Handa et al. described a self-assembled TPGS-750M micelle (shown in Scheme 1), that allowed for copper-catalyzed Suzuki–Myaura coupling of aryl iodides (Scheme 2) [70]. When the reaction was conducted in inert atmosphere, no product was formed. However, the reaction was performed successfully in the presence of air, suggesting that the actual mechanistic pathway involved the formation of a P–(O)–N species on the ligand. The presence of traces of Pd was also needed in this process, as 200 ppm of $Pd(OAc)_2$ worked like a co-catalyst being beneficial either for the reaction rate and the yields, and no product was observed without the Pd source. Furthermore, the recyclability of the catalyst was improved and the experiments could be repeated up to 5 runs with yields >90%. Contrary to the results obtained in bulk, using micelles resulted in higher yields even after catalyst recycling, providing a promising catalytic platform for these coupling reactions [70].

Lee et al. described an approach to perform catalysis in micelles based on rod–coil block copolymers [71]. Micelles were assembled from hydrophilic poly(ethylene oxide) (PEO) and hexa-*p*-

Table 2: Reactions of allylic ethers **1a–e** with naphthylmethylamine[a].

run	ether	time (h)	product	yield (%)
1	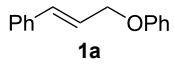 **1a**	20 (min)	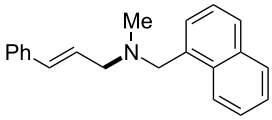	98
2	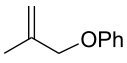 **1b**	1	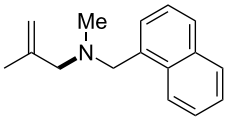	81
3	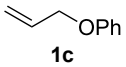 **1c**	5 (min)	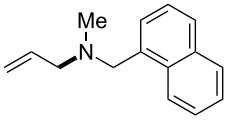	91
4	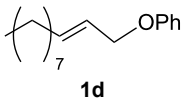 **1d**	1.5	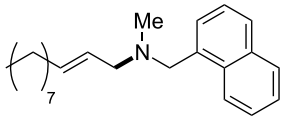 E:Z => 25:1	90
5	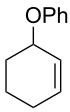 **1e**	5	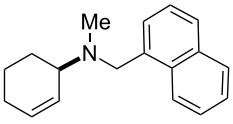	80

[a]Reactions were carried out under air at rt in 2 wt % PTS/water in the presence of $[Pd(allyl)Cl]_2$ (0.5 mol %), bis[(2-diphenylphosphino)phenyl] ether (DPEphos, 1 mol %), ether (1 equiv), naphthylmethylamine (1.5 equiv), K_2CO_3 (1.5 equiv) and HCO_2Me (4 equiv). Adapted from reference [68].

Table 3: Reaction of amines **2a**–**f** with *trans*-cinnamyl phenyl ether[a].

run	amine	time (h)	product	yield[b] (%)
A	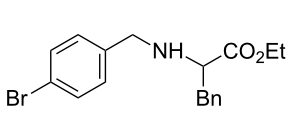 **2a**	7	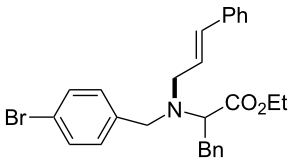	83
B	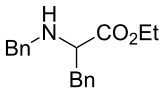 **2b**	2.5	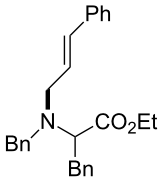	91
C	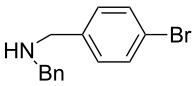 **2c**	14	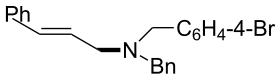	82
D	NH_2-*o*-tol **2d**	2.5	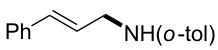	86
E	NH_2-Ph **2e**	2.5	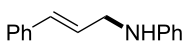	86 (9[c])
F	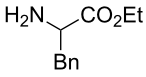 **2f**	2.5	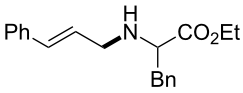	80 (6[c])

[a]Reactions were carried out under air at rt in 2 wt % PTS/water in the presence of $[Pd(allyl)Cl]_2$ (0.5 mol %), DPEphos (1 mol %), *trans*-cinnamyl phenyl ether (1 equiv), amine (1.5 equiv), K_2CO_3 (1.5 equiv) and HCO_2Me (4 equiv). [b]Isolated yields. [c]Doubly allylated product. Adapted from reference [68].

phenylene, providing a platform for Suzuki reactions with the hydrophobic core acting as a suitable pocket for apolar aromatic guests [71,72]. With such a platform, full conversion was achieved at room temperature in water. Almost quantitative yields were observed when aryl chloride coupling was performed with arylboronic acids. This is indeed remarkable as aryl chlorides are generally not as reactive as aryl bromides or aryl iodides.

Lipshutz and Ghorai developed a micellar system called PQS to perform aldol reactions in water [25]. As depicted in Figure 2, PQS (**4a**) has an OH moiety that allows for its linkage to the organocatalyst proline **4b**. Also, PQS has a lipophilic component that acts as a reaction solvent for hydrophobic dienes. The latter feature allows aldol reactions to take place efficiently in water.

The aldol reaction between cyclohexanone and *p*-nitrobenzaldehyde was chosen to verify the performance of this nanoreactor. PQS-proline and the analogous mixed diester derivative of 4-hydroxyproline were prepared and tested in this process. The aldol product was achievable only by using the proline compound **4b**, therefore different substrates were subsequently tested using 10 mol % of this catalyst in water at room temperature. The achievement of this study was not only on the stereoselectivity of the catalysts, but also on the substrate selectivity (Table 4): the preferred substrates are water-insoluble, suggesting that the reaction is occurring in the lipophilic pocket and not in water. The authors also demonstrated the ability of the PQS system to be recycled up to 10 times without loss in its catalytic activity.

Catalytic micelles were also prepared by O'Reilly et al. when a novel amphiphilic Sulfur–Carbon–Sulfur (SCS) pincer Pd catalyst together with a PAA (poly(acrylic acid)) based polymer self-assembled in water [32]. The catalytic activity of the nanostructures was compared to the results achieved with the small molecule analogues of the pincer Pd complex, in a Suzuki–Miyaura coupling. When the reaction of vinyl epoxide with phenylboronic acid was realized with 2% of pincer catalyst, the rate was 100 times higher for the water-based micellar system compared to the same reaction in organic solvent with the unsupported Pd-complex. A 100 times lower amount of catalyst was also loaded (0.02%), and still the reaction rate

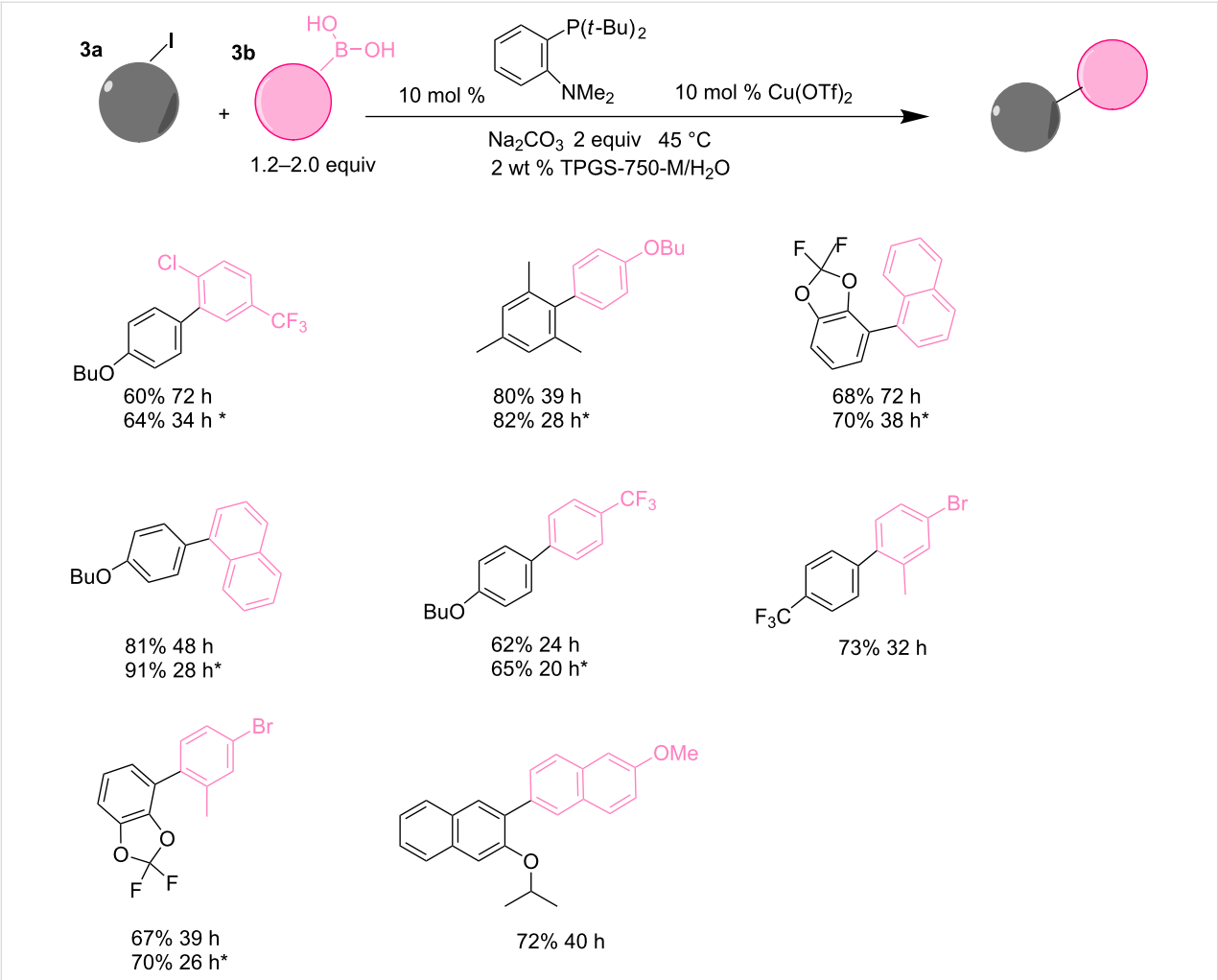

Scheme 2: Suzuki−Miyaura couplings with, or without, ppm Pd. Conditions: ArI 0.5 mmol **3a**, Ar'B(OH)$_2$ (0.75–1.00 mmol, 1.5–2.0 equiv) **3b**, *with 200 ppm of Pd(OAc)$_2$. Adapted from reference [70]. Copyright 2016 American Chemical Society.

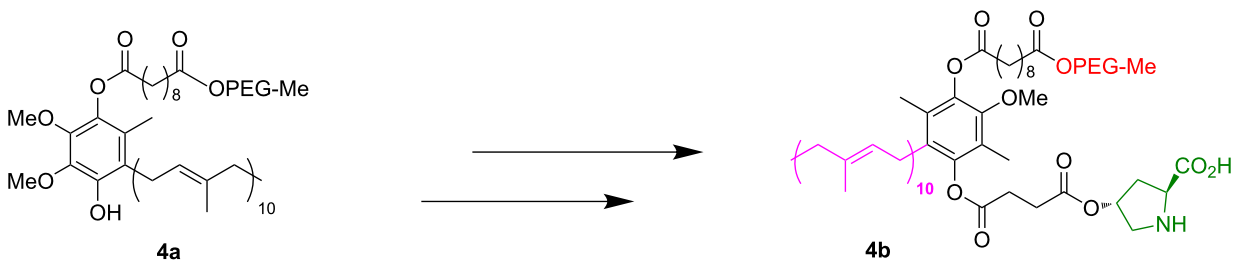

Figure 2: PQS (**4a**), PQS attached proline catalyst **4b**. Adapted from reference [26]. Copyright 2012 American Chemical Society.

achieved was higher than the ones in organic media. This remarkable kinetic effect was attributed to two factors: 1) the small particle radius which increased the nanoreactor's surface area, and 2) the creation of a more hydrophobic local pocket, as the catalyst was facing directly the hydrophobic membrane. Furthermore, the nanosystem also facilitated catalyst recycling by normal extraction.

2.2. Polymeric vesicles

Polymeric vesicles or polymersomes are synthetic bilayered hollow architectures that are self-assembled from amphiphilic block copolymers [73]. The synthetic nature of polymersomes allows for facile tuning of their properties such as size [13,74], membrane permeability [75] and stability [76]. Various copolymers have been reported for polymersome formation such as

Table 4: Representative PQS-proline **4b**-catalyzed reactions[a]:

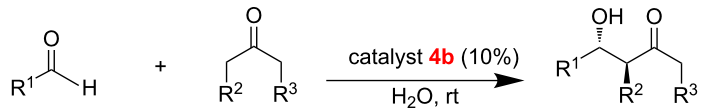

entry	product	time (h)	yield (%)[b]	*anti*:*syn*[c]	ee[d] (%)
1	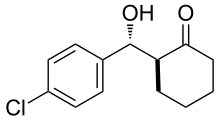	30	88	82:18	90
2	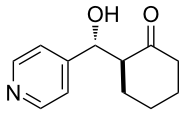	18	90	90:10	90
3	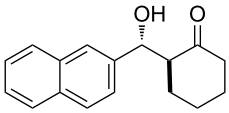	48	74	86:14	92
4	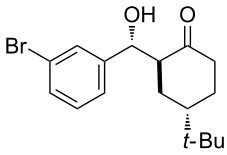	36	80	83:17	91
5	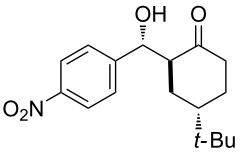	18	85	85:15	79
6	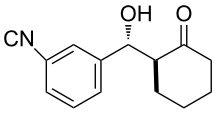	30	80	90:10	97
7	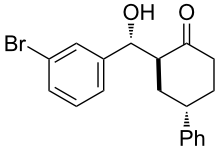	36	82	68:32	86
8	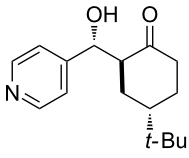	18	85	89:11	75
9	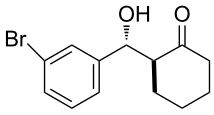	36	82	84:16	86
10	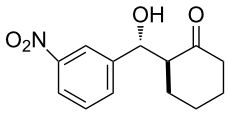	24	90	90:10	91

[a]The reactions were performed with aldehyde (0.01 mmol), ketone (0.5 mmol), and catalyst **4b** (0.01 mmol) at rt. [b]Combined yield of isolated diastereomers. [c]Determined by ^{1}H NMR of the crude product. [d]Determined by chiral-phase HPLC analysis for *anti*-products. Adapted from reference [26]. Copyright 2012 American Chemical Society.

poly(ethylene glycol)-*b*-polystyrene (PEG-*b*-PS) [14,77], polystyrene-*b*-polyisocyanopeptide (PS-*b*-PIAT)[21,22] and poly(*N*-isopropylacrylamide)-*b*-poly(ethylene oxide) (PNIPAM-*b*-PEO) [78]. The term "polymersomes" is derived from liposomes because of the structural resemblance. Compared to liposomes, polymersomes are mechanically robust vesicles and therefore considered to be highly attractive for nanoreactor applications [24,40]. Polymersomes comprise an aqueous lumen and hydrophobic membrane. Such hydrophilic and hydrophobic compartments are capable of accommodating hydrophilic (e.g., enzymes) or hydrophobic catalysts (e.g., metal catalysts) in their lumen or bilayer, respectively [28,79]. In an aqueous environment the hydrophobic membrane attracts hydrophobic substrates and brings them in proximity to the membrane-bound catalyst, leading to faster reaction rates. The presence of multicompartments in one system is interesting from a catalysis point of view as multistep cascades using incompatible catalysts can be achieved in one polymersome nanoreactor [22]. The compositional versatility of polymersomes thus allows for several applications in catalysis by encapsulating in or tethering catalysts to their compartments [33,80]. Polymersomes preserve and protect catalysts in their compartments improving, most of the times, catalytic activity and their performance in incompatible solvents such as water [21,24].

Catalysis in polymersomes: Polymersomes have been most often used as biocatalytic nanoreactors [22,81-83]. Polymersome nanoreactors were also employed in Pickering emulsions [83]. Pickering emulsions are emulsions stabilized by colloidal particles that adsorb at the water–oil interface. They are more stable than classical emulsions and do not require the usage of small molecule surfactants. This is a big advantage in downstream processing and product and catalyst recovery. The enzyme *Candida antarctica* lipase B (CalB) was encapsulated in the lumen of the polymersomes or in the Pickering emulsion water droplet. The esterification reaction of 1-hexanol and hexanoic acid was used to evaluate the catalytic performance of the CalB-loaded Pickering emulsions. Higher enzymatic activity was observed when CalB was encapsulated and the best results were achieved when the enzyme was in the lumen (Figure 3b), highlighting the advantage of enzyme compartmentalization and shielding. The explanation for this improved performance is the enlarged contact area between (hydrophobic) substrate and (water soluble) enzyme. Moreover, the system was recycled for at least 9 times without any loss in enzymatic activity.

Polymersomes have proven to be very useful for the performance of multistep catalytic conversions, in particular with enzymes [81]. Voit et al. studied the use of cross-linked pH sensitive polymersomes for the conversion of glucose in a tandem reaction [82]. The hydrophilic block of their polymersomes was PEG, and the hydrophobic block contained both poly[2-(diethylamino)ethyl methacrylate] (PDEAEM) which is pH responsive, and poly[4-(3,4-dimethylmaleimido)butyl methacrylate] (PDMIBM) as cross-linker. The activity of glucose

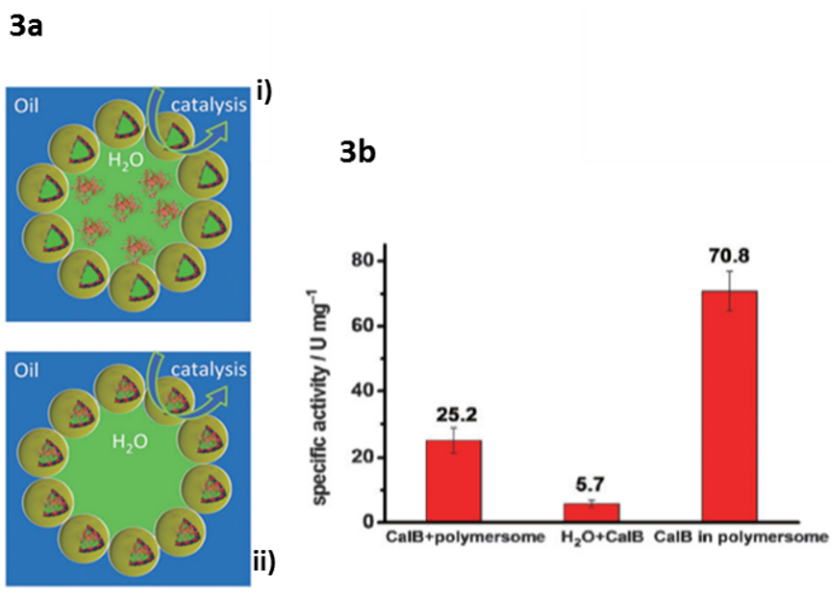

Figure 3: 3a) Schematic representation of a Pickering emulsion with the enzyme in the water phase (i), or with the enzyme inside the polymersome lumen (ii). 3b) Chart of the specific activities of CalB dissolved in the water phase of the polymersome Pickering emulsion (left), CalB in a biphasic water/toluene system (middle,) and CalB encapsulated in the lumen of the polymersome Pickering emulsion (right). Adapted with permission from [79].

oxidase (GOx) to convert glucose into D-glucono-δ-lactone and hydrogen peroxide was the first step of the reaction (Scheme 3A); subsequently, myoglobin (Myo) employed the hydrogen peroxide produced to oxidize guaiacol to quinone and water (Scheme 3B).

When the pH was below 7, the permeability of the cross-linked membrane allowed for substrate/product diffusion, but at basic pH the membrane collapsed and prevented any transport of small molecules. Two different activity tests were performed: 1) GOx and Myo were both entrapped inside the polymersome lumen; 2) GOx and Myo were individually incorporated into the polymersomes and mixed together in solution; in both of the cases the final product formation was monitored by UV–vis spectroscopy. The control over the pH allowed the regulation of the enzymatic cascade (no product was observed at pH 8 in both of the reactive systems), as the diffusion through the membrane was not possible. Moreover, the crosslinking enabled stabilization of the enzymes, which remained active also after 10 days.

Polymersome nanoreactors have also been used to perform many types of non-enzymatic catalytic reactions, such as the proline-catalyzed asymmetric aldol reaction of cyclohexanone and 4-nitrobenzaldehyde [83]. Cross-linked polymersome nanoreactors were also used to perform asymmetric cyclopropanation reactions in water [15]. These products are highly desired intermediates in the preparation of agrochemicals and pharmaceuticals [84-86]. To perform cyclopropanation reactions in polymersomes, the membrane was cross-linked with bisoxazoline (BOX) ligands complexing the copper catalyst. Cyclopropanation reactions were efficiently performed in water, resulting in high yields and enantioselectivities, comparable to those when the reaction was carried out in organic solvent [80] (Figure 4).

As depicted in Table 5, substrate selectivity was observed when catalytic polymersomes were used, reasonably ascribed to a concentration effect, with more hydrophobic substrates leading to an increased local concentration around the catalyst in the hydrophobic membrane and as a consequence a higher reaction rate.

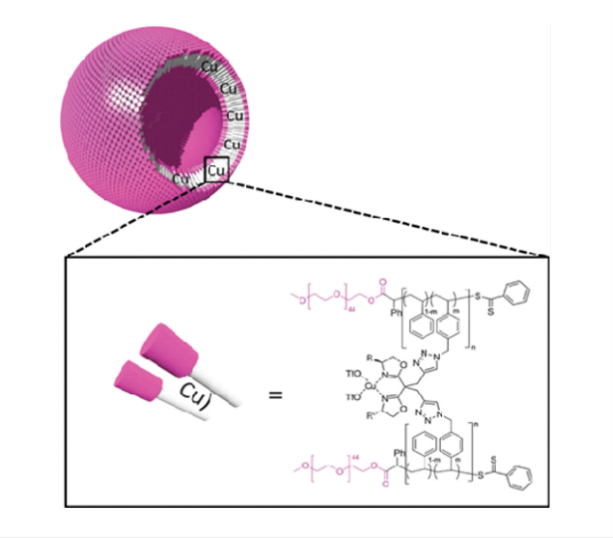

Figure 4: Cross-linked polymersomes with $Cu(OTf)_2$ catalyst. Reprinted with permission from [15].

Dergunov et al. reported on the design of a porous polymeric nanoreactor with a lipid bilayer for coupling reactions [87]. These nanocapsules were loaded with palladium catalysts and successfully used in Suzuki, Sonogashira and Heck cross-coupling reactions. Catalytic activity was compared to the activity of the freshly prepared free catalyst, and the palladium entrapment did not affect either the conversion or the yields of the reaction [28]. The catalyst immobilization also allowed facile Pd removal from the final product and catalyst recycling.

Polymeric nanoreactors were also used to perform ring-opening polymerization (ROP) in water. Nallani et al. reported on the enzymatic polymerization of lactones using CalB, which was immobilized in both the polymersome lumen and bi-layer [21]. Nanoreactors for ROP were prepared from polystyrene-polyisocyanopeptide (PS-PIAT) and CalB was incorporated within either the lumen or polymer membrane (Figure 5).

Scheme 3: Cascade reaction with GOx and Myo. Adapted from reference [82].

Table 5: Asymmetric cyclopropanation reaction of styrene derivatives and ethyl diazoacetate[a].

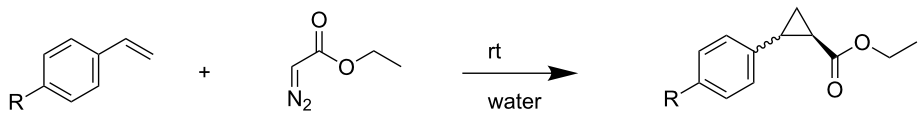

entry	R	time (min)	load[b] (%)	catalyst	conversion[c,d] (%)	*trans*/*cis*[d]	ee *trans*[e] (%)
1	H	120	10	C1	50[f]	73/27	60
2	H	10	10	C1	54	74/26	60
3	H	10	2	C1	12	72/28	60
4	H	10	10	C2	39	68/32	84
5	H	10	10	C3	43	59/41	34[g]
6	OMe	10	10	C2	93[h]	68/32	59[i]
7	Cl	10	10	C2	32[h]	75/25	53[i]
8	tBu	10	10	C2	67[h]	67/33	71

[a]Reactions carried out in 3.0 mL of Milli-Q water with 5.0 equiv of styrene and 1.0 equiv of ethyl diazoacetate. [b]Catalyst loading in mol %. cConversion of ethyl diazoacetate into cyclopropane product. [d]Determined by ^{1}H NMR using triethylene glycol dimethyl ether as an internal standard. eDetermined by chiral GC. [f]Polymersomes started to precipitate after 15 min. [g]Configuration of the product was (1*S*,2*S*). [h]Isolated yields. [i]Determined by chiral HPLC. Adapted from reference [15].

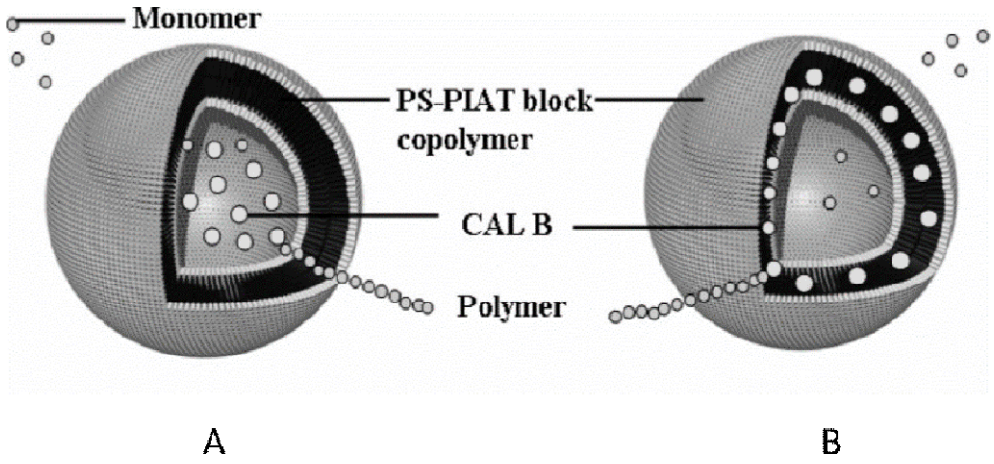

Figure 5: Schematic representation of enzymatic polymerization in polymersomes. (A) CALB in the aqueous compartment (B) CALB embedded in the bilayer. Reprinted with permission from [21]. Copyright 2007 American Chemical Society.

ROP is usually performed in organic solvent so that hydrolysis reactions can be avoided [17]. However, when nanoreactors were used, polymerization proceeded efficiently in water and without formation of any undesired products, providing a platform for aqueous ROP [21].

As shown in this section, polymersomes have been applied as a platform towards greener reactions [22,88], either by allowing reactions to be performed in water [21,83] or by providing a recyclable catalytic system [80]. As they contain both hydrophobic and aqueous compartments, they are especially useful for the immobilization of different catalysts, such as organocatalysts and enzymes that require different microenvironments for their optimal performance.

3. Covalent systems

3.1. Dendrimers

Dendrimers are a class of highly branched molecules with high degree of symmetry [89]. They consist of different generations in which every generation is twice the molecular weight of the previous one. Dendritic architectures comprise three regions: a core, inner shell and outer shell [90]. The properties of dendrimers such as hydrophobicity can be tuned by varying their initial molecular components or the number of genera-

tions they possess [91,92]. They can assemble in a spherical shape, and within the three-dimensional structure, an interior void is present wherein to accommodate other molecules [93].

Catalysis in dendrimers: The controlled synthesis of dendrimers and their applications as nanoreactors and catalyst carriers have been extensively studied over the last decades [94-96]. Fan and co-workers incorporated a bis(oxazoline)-copper(II) complex in the hydrophobic core of a polyether dendrimer [11]. The copper catalytic complex was used to carry out asymmetric Mukaiyama aldol reactions. Although this system did not result in any substantial improvements in yields or enantioselectivities, it allowed for facile catalyst recovery and recycling.

Dendrimers were also used to encapsulate bimetallic catalysts to attain highly selective reactions [95,97]. The first successful attempt was reported by Chung and Rhee, in which they showed the encapsulation of a bimetallic Pt–Pd catalyst in a highly branched PMAM-OH dendrimer corona [93]. These catalytic dendrimers were employed in partial hydrogenation of 1,3-cyclooctadiene into cyclooctene. The utility of these dendrimers in hydrogenation reactions resulted in efficient reactions that proceeded with unprecedented selectivity of 99%. Moreover, this system is one of the first of bimetallic catalytic systems to be used for hydrogenation reactions in water.

Water soluble dendrimer-stabilized nanoparticles (DSN) have been shown to be highly efficient in the catalysis of olefin hydrogenation and in Suzuki coupling reactions [98,99]. Ornelas et al. entrapped a palladium catalyst with dendrimers containing triazole groups (DSN) (Figure 6) [100].

The aim here was to provide a platform to perform hydrogenation in water. By using only 0.01% of palladium at room temperature, the hydrogenation of allyl alcohol was realized [101]. DSNs were recycled for up to 10 times without loss in activity. DSN nanoreactors were later shown to be utilized for catalysing

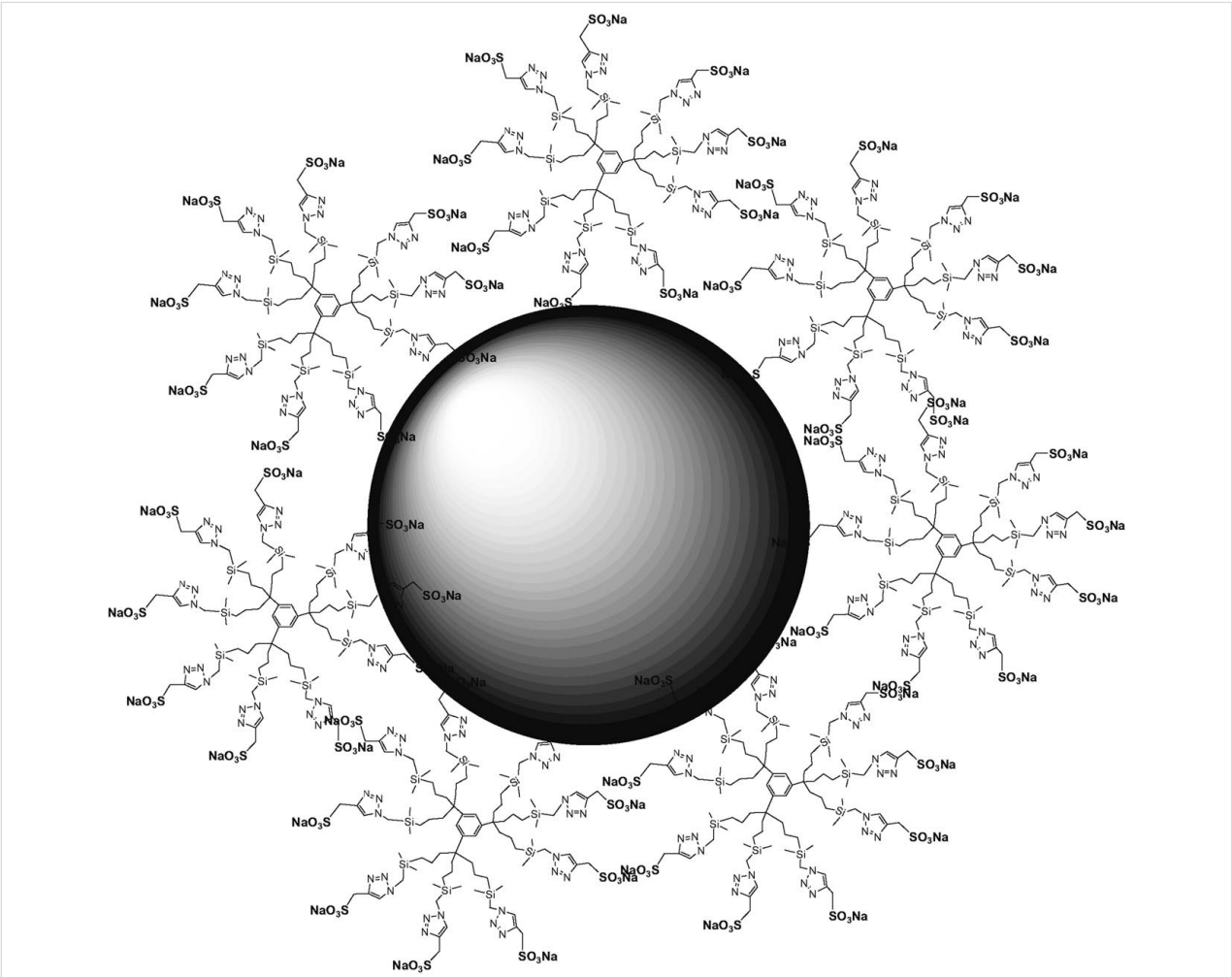

Figure 6: Representation of DSN-G_0. Reprinted with permission from [100].

Suzuki coupling reactions between $PhB(OH)_2$ and PhX (X = I or Br) in water [100].

Other examples of water-soluble dendrimers are peptide- and glycol-based dendrimers [102,103]. As a result of their compositional versatility, they have been reported in many applications for biomedical engineering (e.g., glycopeptide dendrimers for drug delivery [104]).

The ability of peptide dendrimers to perform catalysis in an aqueous environment has also been investigated [105]. Many different libraries of peptide dendrimers have been used for biocatalytic applications, such as hydrolysis and aldolase reactions [105-108], showing their potential in green catalysis.

Peptide dendrimers including aspartate, histidine and serine were utilized by Reymond et al. as catalytic esterase triad. Using fluorogenic 8-acyloxypyrene-1,3,6-trisulfonates as substrate (Figure 7) at the pH optimum of 5.5, triads' activity was successfully demonstrated [107].

A noticeable rate enhancement was observed, related to a large apparent reactivity increase per catalytic site. Such an enhanced activity could be explained by the relatively high hydrophobic

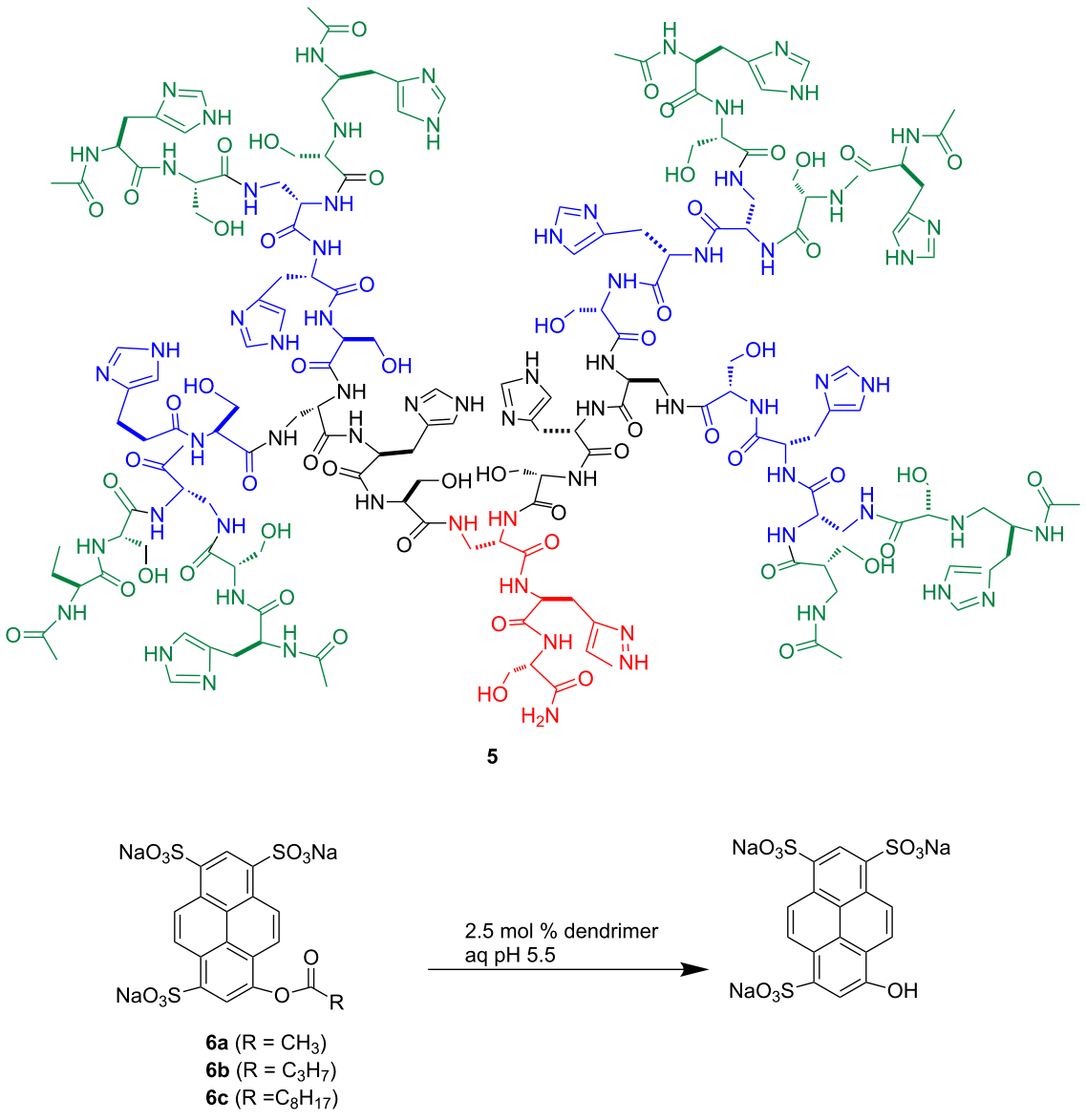

Figure 7: The multivalent esterase dendrimer **5** catalyzes the hydrolysis of 8-acyloxypyrene 1,3,6-trisulfonates **6a**–**c**. Reprinted with permission from [105].

binding of the acyl group and the presence of histidine side chains that act as catalytic groups and as electrostatic substrate binding sites in their basic and acidic forms, respectively.

3.2. Nanogels

Nanogels are hydrophilic polymer networks which can swell in the presence of water [109]. They can be crosslinked by either chemical bonds or physical methods, such as non-covalent interactions, entanglements and crystalline domains. The nanogels display excellent swelling behavior and are shape resistant [43,110]. Due to these unique properties they have mostly been studied as materials in biomedical applications such as controlled drug delivery [111]. Nanogels show promise as nanoreactors as they not only are colloidal stable particle in water but also can be prepared form a wide range of components and in many different sizes and shapes. They have been used for the templated synthesis of metal nanoparticles, via which the shape and size of the nanogel directed the formation of the corresponding particle with similar morphology [56,112]. The metal nanoparticle core is covered by polymeric brushes, the length and the grafting are important factors which can affect the reaction, as discussed in the following paragraph, and the easy manufacturing of metal nanoparticles makes the preparation of these core-brushes nanosystems suitable for many applications [113-115].

Catalysis in nanogels: Nanogels have intrinsic properties that make them well suited for green chemistry [116,117]. Water-compatible gels are usually based on poly(*N*-isopropylacrylamide) (PNIPAM), poly(*N*-vinylcaprolactam) (PVCL) or other water-soluble polymers [109]. For instance, PNIPAM is a thermo-responsive polymer, which has a lower critical solution temperature (LCST) of 32 °C. Above the LCST, individual polymer chains switch from a swollen coil configuration to a collapsed globular one, providing a nano-environment that is suitable for either hydrophobic or hydrophilic substrates [112]. Water forces PNIPAM brushes to become hydrophobic, acting as a suitable environment for most organic reactions [118]; it allows hydrophobic substrates to diffuse towards the encapsulated catalysts, leading to a concentration effect that directly contributes to an efficient aqueous reaction [119].

The preparation of catalytic nanocomposite hydrogels has been widely reviewed [56,114]. Several examples showing their utility as nanoreactors for various reactions such as coupling, oxidation and reduction reactions have been reported [43,114,118]. Wei et al. described a nanogel composed of poly(*N*-isopropylacrylamide) brushes grafted on Pd-NPs (Pd@PNIPAM) to carry out coupling reactions in water under mild conditions [120]. They showed highly efficient coupling of several hydrophobic aryl halides with phenylboronic acid, which in all cases resulted in yields above 70%. Moreover, the Pd@PNIPAM nanoreactors could be easily recycled thanks to the reversible phase-transition of the polymeric brushes [112].

Que et al. reported the synthesis of gold nanoparticles (Au NPs) sheltered in PEG-PS nanogels for the reduction of 4-nitrophenol (4NP) [121]. Thiol functionalized PEG blocks were immobilized on Au NPs. PS segments improved the stability of the system and provided the necessary hydrophobic environment that is required to undertake the reduction reaction in water. The outcome of using Au@PEG-PS as nanoreactors was compared to those resulting from using both uncoated and PEG-coated Au NPs. While Au@PEG-PS resulted in quantitative conversions for 5 subsequent cycles, both uncoated and PEG_{45} coated Au NPs resulted in full and 61% conversions only for the first cycle, respectively. Recycling of uncoated and PEG_{45} coated Au NPs was not possible, highlighting the significance of the nanoreactor design (Figure 8).

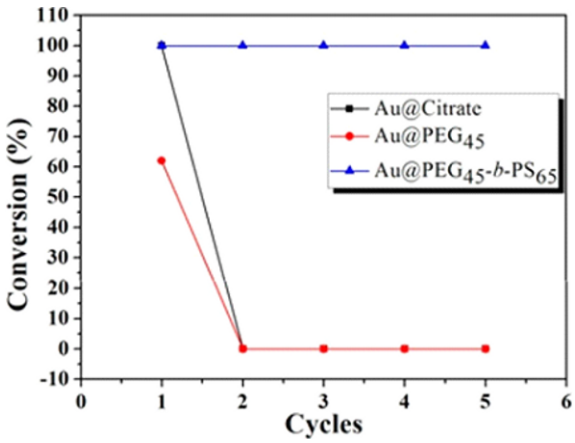

Figure 8: Conversion of 4-NP in five successive cycles of reduction, catalyzed by Au@citrate, Au@PEG and Au@PEG_{45}-*b*-PS_{65}. Reprinted with permission from [121]. Copyright 2015 American Chemical Society.

Superior catalytic activity of Au@PEG-*b*-PS was observed in the reduction reaction of 4-nitrophenol to 4-aminophenol. The catalytic activity increased with the decrease in the chain length of the PS block. In addition, the high stability imparted by the PS layer endowed Au@PEG-*b*-PS with good reusability in catalysis without the loss of catalytic activity, and prevented from electrolyte-induced aggregation, making the system very attractive as nanoreactor.

Following on the previous work, He et al. synthesized cross-linked nanogels that were based on poly(acrylamide-*co*-acryl acid) (poly(AAm-*co*-AAc)) [117]. These nanogels were transformed into their catalytic counterparts by growing silver nano-

particles (Ag NPs) inside the cross-linked polymeric network. These catalytic nanogels were also used to catalyse the reduction of 4-nitrophenol to 4-aminophenol in water. The activity of these nanoreactors was tuned by varying the Ag NPs loading and the cross-linking density; higher activities were achieved by increasing the amount of Ag NPs loaded and decreasing the degree of polymer cross-linking. Such conditions facilitated the diffusion of water and substrates through the hydrogels and increased the probability of the reactant to be in contact with the catalyst (Ag NPs).

Conclusion

In this review we have discussed the utility of supramolecular polymersomes, micelles, dendrimers and nanogels in catalysis. Over the past decades, many groups have demonstrated the specific features which make these nanoreactors an advantageous choice for chemical synthesis. In particular, they combine a high active surface area with a good dispersion in solution and therefore are ideal structures for facile diffusion of reactants. Furthermore, the compartments protect the catalyst from undesired interactions with the environment, which can be either the solvent, specifically water, or other catalytic species. As a result they allow reactions to proceed in water and often at room temperature, with excellent yields and selectivities, which traditionally can only be achieved by performing catalysed reactions in organic media. Moreover, although they are homogenously dispersed in the solvent, the nanoreactors are still large enough to be separated from the reaction mixture using standard filtration protocols. Therefore, they enable a facile purification and catalyst reuse.

This latter feature has potentially both an economic and environmental impact, deriving from a lower consumption of organic solvents, as lowering the E-factor in a process is a must for the modern chemical industry. Despite these many advantages, nanoreactors have not yet found widespread use in industry. A number of reasons can account for this. First of all, the construction of the nanoreactors is not always a cost-efficient process. Scalability and reproducibility in nanoreactor production also are key factors that have to be addressed. The recyclability and cost price should be improved to allow competition with existing heterogeneous and homogeneous processes. Furthermore, in most cases only model reactions have been studied. The improvement of a process that is highly relevant for industry would aid in a further acceptance of this technology by the end users. Another issue is that the specific characteristics of nanoreactors should be employed more effectively. Physical protection and separation of catalytic species will allow the performance of multistep conversions in one-pot reactors. This would then enable continuous flow processing, as intermediate work-up steps and solvent switching procedures can be prevented. Although this requires still much development, it is to be expected that in the near future nanoreactors will be key to a more sustainable production of fine chemicals.

Acknowledgements

The authors acknowledge support from Horizon 2020 FET-Open program 737266 - ONE-FLOW; with regard to the graphical abstract we acknowledge Dennis Vriezema and Pille et al. *Biomacromolecules*, **2017**, *18*, 1302 (https://pubs.acs.org/doi/abs/10.1021%2Facs.biomac.7b00064); further permissions related to the material excerpted should be directed to the ACS.

ORCID® iDs

M. Teresa De Martino - https://orcid.org/0000-0002-7644-0876
Loai K. E. A. Abdelmohsen - https://orcid.org/0000-0002-0094-1893
Floris P. J. T. Rutjes - https://orcid.org/0000-0003-1538-3852
Jan C. M. van Hest - https://orcid.org/0000-0001-7973-2404

References

1. Sheldon, R. A. *Green Chem.* **2005,** *7,* 267–278. doi:10.1039/b418069k
2. Simon, M.-O.; Li, C.-J. *Chem. Soc. Rev.* **2012,** *41,* 1415–1427. doi:10.1039/C1CS15222J
3. Rogers, R. D.; Seddon, K. R. *Science* **2003,** *302,* 792–793. doi:10.1126/science.1090313
4. Clark, J. H. *Green Chem.* **1999,** *1,* 1–8. doi:10.1039/a807961g
5. Mulvihill, M. J.; Beach, E. S.; Zimmerman, J. B.; Anastas, P. T. *Annu. Rev. Environ. Resour.* **2011,** *36,* 271–293. doi:10.1146/annurev-environ-032009-095500
6. Clark, J. H.; Tavener, S. J. *Org. Process Res. Dev.* **2007,** *11,* 149–155. doi:10.1021/op060160g
7. Sheldon, R. A. *Green Chem.* **2007,** *9,* 1273–1283. doi:10.1039/b713736m
8. Sperry, J.; García-Álvarez, J. *Molecules* **2016,** *21,* 1527. doi:10.3390/molecules21111527
9. Lipshutz, B. H.; Ghorai, S.; Leong, W. W. Y.; Taft, B. R.; Krogstad, D. V. *J. Org. Chem.* **2011,** *76,* 5061–5073. doi:10.1021/jo200746y
10. Lu, J.; Lazzaroni, M. J.; Hallett, J. P.; Bommarius, A. S.; Liotta, C. L.; Eckert, C. A. *Ind. Eng. Chem. Res.* **2004,** *43,* 1586–1590. doi:10.1021/ie0303247
11. Yang, B.-Y.; Chen, X.-M.; Deng, G.-J.; Zhang, Y.-L.; Fan, Q.-H. *Tetrahedron Lett.* **2003,** *44,* 3535–3538. doi:10.1016/S0040-4039(03)00680-4
12. Canali, L.; Sherrington, D. C. *Chem. Soc. Rev.* **1999,** *28,* 85–93. doi:10.1039/a806483k
13. Mase, N.; Nakai, Y.; Ohara, N.; Yoda, H.; Takabe, K.; Tanaka, F.; Barbas, C. F. *J. Am. Chem. Soc.* **2006,** *128,* 734–735. doi:10.1021/ja0573312
14. Okino, T.; Takemoto, Y. *Org. Lett.* **2001,** *3,* 1515–1517. doi:10.1021/ol015829c
15. van Oers, M. C. M.; Abdelmohsen, L. K. E. A.; Rutjes, F. P. J. T.; van Hest, J. C. M. *Chem. Commun.* **2014,** *50,* 4040–4043. doi:10.1039/C3CC48865A
16. Wu, Y.; Zhang, Y.; Yu, M.; Zhao, G.; Wang, S. *Org. Lett.* **2006,** *8,* 4417–4420. doi:10.1021/ol061418q

17. Peeters, J. W.; van Leeuwen, O.; Palmans, A. R. A.; Meijer, E. W. *Macromolecules* **2005,** *38,* 5587–5592. doi:10.1021/ma050510j
18. Lee, J.; Kim, S. M.; Lee, I. S. *Nano Today* **2014,** *9,* 631–667. doi:10.1016/j.nantod.2014.09.003
19. Küchler, A.; Yoshimoto, M.; Luginbühl, S.; Mavelli, F.; Walde, P. *Nat. Nanotechnol.* **2016,** *11,* 409–420. doi:10.1038/nnano.2016.54
20. Kleij, A. W.; Reek, J. N. H. *Chem. – Eur. J.* **2006,** *12,* 4218–4227. doi:10.1002/chem.200500875
21. Nallani, M.; de Hoog, H.-P. M.; Cornelissen, J. J. L. M.; Palmans, A. R. A.; van Hest, J. C. M.; Nolte, R. J. M. *Biomacromolecules* **2007,** *8,* 3723–3728. doi:10.1021/bm7005938
22. Peters, R. J. R. W.; Marguet, M.; Marais, S.; Fraaije, M. W.; van Hest, J. C. M.; Lecommandoux, S. *Angew. Chem., Int. Ed.* **2014,** *53,* 146–150. doi:10.1002/anie.201308141
23. Poli, R. *Fundamental and Applied Catalysis Effects of Nanoconfinement on Catalysis;* Springer, 2017.
24. Schoonen, L.; van Hest, J. C. M. *Adv. Mater.* **2015,** *28,* 1109–1128. doi:10.1002/adma.201502389
25. Tu, Y.; Peng, F.; Adawy, A.; Men, Y.; Abdelmohsen, L. K. E. A.; Wilson, D. A. *Chem. Rev.* **2016,** *116,* 2023–2078. doi:10.1021/acs.chemrev.5b00344
26. Lipshutz, B. H.; Ghorai, S. *Org. Lett.* **2012,** *14,* 422–425. doi:10.1021/ol203242r
27. Cole-Hamilton, D. J. *Science* **2003,** *299,* 1702–1706. doi:10.1126/science.1081881
28. Dergunov, S. A.; Khabiyev, A. T.; Shmakov, S. N.; Kim, M. D.; Ehterami, N.; Weiss, M. C.; Birman, V. B.; Pinkhassik, E. *ACS Nano* **2016,** *10,* 11397–11406. doi:10.1021/acsnano.6b06735
29. Lu, A.; O'Reilly, R. K. *Curr. Opin. Biotechnol.* **2013,** *24,* 639–645. doi:10.1016/j.copbio.2012.11.013
30. *Catalyst Separation, Recovery and Recycling;* Cole-Hamilton, D. J.; Tooze, R. P., Eds.; Springer: Dordrecht, 2006; pp 1–247.
31. Dwars, T.; Paetzold, E.; Oehme, G. *Angew. Chem., Int. Ed.* **2005,** *44,* 7174–7199. doi:10.1002/anie.200501365
32. Patterson, J. P.; Cotanda, P.; Kelley, E. G.; Moughton, A. O.; Lu, A.; Epps, T. H., III; O'Reilly, R. K. *Polym. Chem.* **2013,** *4,* 2033–2039. doi:10.1039/c3py21137a
33. Kim, K. T.; Meeuwissen, S. A.; Nolte, R. J. M.; van Hest, J. C. M. *Nanoscale* **2010,** *2,* 844–858. doi:10.1039/b9nr00409b
34. Leenders, S. H. A. M.; Gramage-Doria, R.; de Bruin, B.; Reek, J. N. H. *Chem. Soc. Rev.* **2015,** *44,* 433–448. doi:10.1039/C4CS00192C
35. Abe, H.; Mawatari, Y.; Teraoka, H.; Fujimoto, K.; Inouye, M. *J. Org. Chem.* **2004,** *69,* 495–504. doi:10.1021/jo035188u
36. Zolotukhin, M. G.; Hernández, M. d. C. G.; Lopez, A. M.; Fomina, L.; Cedillo, G.; Nogales, A.; Ezquerra, T.; Rueda, D.; Colquhoun, H. M.; Fromm, K. M.; Ruiz-Treviño, A.; Ree, M. *Macromolecules* **2006,** *39,* 4696–4703. doi:10.1021/ma052148e
37. Djernes, K. E.; Moshe, O.; Mettry, M.; Richards, D. D.; Hooley, R. J. *Org. Lett.* **2012,** *14,* 788–791. doi:10.1021/ol203243j
38. Shimizu, S.; Shirakawa, S.; Suzuki, T.; Sasaki, Y. *Tetrahedron* **2001,** *57,* 6169–6173. doi:10.1016/S0040-4020(01)00572-5
39. Gutsche, C. D.; Alam, I. *Tetrahedron* **1988,** *44,* 4689–4694. doi:10.1016/S0040-4020(01)86171-8
40. Che, H.; van Hest, J. C. M. *J. Mater. Chem. B* **2016,** *4,* 4632–4647. doi:10.1039/C6TB01163B
41. Khullar, P.; Singh, V.; Mahal, A.; Kumar, H.; Kaur, G.; Bakshi, M. S. *J. Phys. Chem. B* **2013,** *117,* 3028–3039. doi:10.1021/jp310507m
42. Vriezema, D. M.; Comellas Aragonès, M.; Elemans, J. A. A. W.; Cornelissen, J. J. L. M.; Rowan, A. E.; Nolte, R. J. M. *Chem. Rev.* **2005,** *105,* 1445–1490. doi:10.1021/cr0300688
43. Thomas,, V.; Namdeo, M.; Mohan, Y. M.; Bajpai, S. K.; Bajpai, M. *J. Macromol. Sci., Part A: Pure Appl. Chem.* **2007,** *45,* 107–119. doi:10.1080/10601320701683470
44. McMorn, P.; Hutchings, G. J. *Chem. Soc. Rev.* **2004,** *33,* 108–122. doi:10.1039/b200387m
45. Lipshutz, B. H.; Isley, N. A.; Fennewald, J. C.; Slack, E. D. *Angew. Chem., Int. Ed.* **2013,** *52,* 10952–10958. doi:10.1002/anie.201302020
46. Tariq, M.; Ali, S.; Khalid, N. *Renewable Sustainable Energy Rev.* **2012,** *16,* 6303–6316. doi:10.1016/j.rser.2012.07.005
47. Ross, J. R. H. *Heterog. Catal.* **2012,** 1–15. doi:10.1016/B978-0-444-53363-0.10001-5
48. Campanati, M.; Fornasari, G.; Vaccari, A. *Catal. Today* **2003,** *77,* 299–314. doi:10.1016/S0920-5861(02)00375-9
49. Rao, R. G.; Blume, R.; Hansen, T. W.; Fuentes, E.; Dreyer, K.; Moldovan, S.; Ersen, O.; Hibbitts, D. D.; Chabal, Y. J.; Schlögl, R.; Tessonnier, J.-P. *Nat. Commun.* **2017,** *8,* No. 340. doi:10.1038/s41467-017-00421-x
50. Buurmans, I. L. C.; Weckhuysen, B. M. *Nat. Chem.* **2012,** *4,* 873–886. doi:10.1038/nchem.1478
51. Pritchard, J.; Filonenko, G. A.; van Putten, R.; Hensen, E. J. M.; Pidko, E. A. *Chem. Soc. Rev.* **2015,** *44,* 3808–3833. doi:10.1039/C5CS00038F
52. Mortreux, A.; Petit, F. In *Industrial Applications of homogeneous catalysis;* Ugo, R.; James, B. R., Eds.; 1988; pp 1–347.
53. Dekker, F. H. M.; Bliek, A.; Kapteijn, F.; Moulijn, J. A. *Chem. Eng. Sci.* **1995,** *50,* 3573–3580. doi:10.1016/0009-2509(95)00210-V
54. Copéret, C.; Chabanas, M.; Petroff Saint-Arroman, R.; Basset, J.-M. *Angew. Chem., Int. Ed.* **2003,** *42,* 156–181. doi:10.1002/anie.200390072
55. Pagliaro, M.; Pandarus, V.; Ciriminna, R.; Béland, F.; DemmaCarà, P. *ChemCatChem* **2012,** *4,* 432–445. doi:10.1002/cctc.201100422
56. Lu, Y.; Spyra, P.; Mei, Y.; Ballauff, M.; Pich, A. *Macromol. Chem. Phys.* **2007,** *208,* 254–261. doi:10.1002/macp.200600534
57. van Oers, M. C. M.; Rutjes, F. P. J. T.; van Hest, J. C. M. *Curr. Opin. Biotechnol.* **2014,** *28,* 10–16. doi:10.1016/j.copbio.2013.10.011
58. Kapishon, V.; Whitney, R. A.; Champagne, P.; Cunningham, M. F.; Neufeld, R. J. *Biomacromolecules* **2015,** *16,* 2040–2048. doi:10.1021/acs.biomac.5b00470
59. van Herrikhuyzen, J.; Portale, G.; Gielen, J. C.; Christianen, P. C. M.; Sommerdijk, N. A. J. M.; Meskers, S. C. J.; Schenning, A. P. H. J. *Chem. Commun.* **2008,** 697–699. doi:10.1039/B715820C
60. Erhardt, R.; Böker, A.; Zettl, H.; Kaya, H.; Pyckhout-Hintzen, W.; Krausch, G.; Abetz, V.; Müller, A. H. E. *Macromolecules* **2001,** *34,* 1069–1075. doi:10.1021/ma000670p
61. Jain, S.; Bates, F. S. *Science* **2003,** *300,* 460–464. doi:10.1126/science.1082193
62. Blanazs, A.; Armes, S. P.; Ryan, A. J. *Macromol. Rapid Commun.* **2009,** *30,* 267–277. doi:10.1002/marc.200800713
63. Wang, L.-M.; Jiao, N.; Qiu, J.; Yu, J.-J.; Liu, J.-Q.; Guo, F.-L.; Liu, Y. *Tetrahedron* **2010,** *66,* 339–343. doi:10.1016/j.tet.2009.10.091
64. Minkler, S. R. K.; Isley, N. A.; Lippincott, D. J.; Krause, N.; Lipshutz, B. H. *Org. Lett.* **2014,** *16,* 724–726. doi:10.1021/ol403402h
65. Duplais, C.; Krasovskiy, A.; Wattenberg, A.; Lipshutz, B. H. *Chem. Commun.* **2010,** *46,* 562–564. doi:10.1039/B922280D
66. Lipshutz, B. H.; Ghorai, S.; Abela, A. R.; Moser, R.; Nishikata, T.; Duplais, C.; Krasovskiy, A.; Gaston, R. D.; Gadwood, R. C. *J. Org. Chem.* **2011,** *76,* 4379–4391. doi:10.1021/jo101974u

67. Isley, N. A.; Dobarco, S.; Lipshutz, B. H. *Green Chem.* **2014,** *16,* 1480–1488. doi:10.1039/c3gc42188k
68. Nishikata, T.; Lipshutz, B. H. *Chem. Commun.* **2009,** 6472–6474. doi:10.1039/b914982a
69. De Graaf, W.; Boersma, J.; Van Koten, G. *Organometallics* **1990,** *9,* 1479–1484. doi:10.1021/om00119a019
70. Handa, S.; Smith, J. D.; Hageman, M. S.; Gonzalez, M.; Lipshutz, B. H. *ACS Catal.* **2016,** *6,* 8179–8183. doi:10.1021/acscatal.6b02809
71. Lee, M.; Jang, C.-J.; Ryu, J.-H. *J. Am. Chem. Soc.* **2004,** *126,* 8082–8083. doi:10.1021/ja048264z
72. Lee, M.; Cho, B.-K.; Zin, W.-C. *Chem. Rev.* **2001,** *101,* 3869–3892. doi:10.1021/cr0001131
73. Discher, B. M.; Won, Y.-Y.; Ege, D. S.; Lee, J. C.-M.; Bates, F. S.; Discher, D. E.; Hammer, D. A. *Science* **1999,** *284,* 1143–1146. doi:10.1126/science.284.5417.1143
74. Sanson, C.; Schatz, C.; Le Meins, J.-F.; Brûlet, A.; Soum, A.; Lecommandoux, S. *Langmuir* **2010,** *26,* 2751–2760. doi:10.1021/la902786t
75. Kim, K. T.; Cornelissen, J. J. L. M.; Nolte, R. J. M.; Van Hest, J. C. M. *Adv. Mater.* **2009,** *21,* 2787–2791. doi:10.1002/adma.200900300
76. Hickey, R. J.; Koski, J.; Meng, X.; Riggleman, R. A.; Zhang, P.; Park, S.-J. *ACS Nano* **2014,** *8,* 495–502. doi:10.1021/nn405012h
77. Gao, C.; Wu, J.; Zhou, H.; Qu, Y.; Li, B.; Zhang, W. *Macromolecules* **2016,** *49,* 4490–4500. doi:10.1021/acs.macromol.6b00771
78. Hong, C.-Y.; You, Y.-Z..; Pan, C.-Y. *J. Polym. Sci., Part A: Polym. Chem.* **2004,** *42,* 4873–4881. doi:10.1002/pola.20248
79. Wang, Z.; van Oers, M. C. M.; Rutjes, F. P. J. T.; van Hest, J. C. M. *Angew. Chem., Int. Ed.* **2012,** *51,* 10746–10750. doi:10.1002/anie.201206555
80. van Oers, M. C. M. *Asymmetric Catalysis in Polymersome Nanoreactors*. Randboud Universiteit : Nijmegen, 2015; http://hdl.handle.net/2066/140662.
81. Kuiper, S. M.; Nallani, M.; Vriezema, D. M.; Cornelissen, J. J. L. M.; van Hest, J. C. M.; Nolte, R. J. M.; Rowan, A. E. *Org. Biomol. Chem.* **2008,** *6,* 4315–4318. doi:10.1039/b811196k
82. Gräfe, D.; Gaitzsch, J.; Appelhans, D.; Voit, B. *Nanoscale* **2014,** *6,* 10752–10761. doi:10.1039/C4NR02155J
83. van Oers, M. C. M.; Veldmate, W. S.; van Hest, J. C. M.; Rutjes, F. P. J. T. *Polym. Chem.* **2015,** *6,* 5358–5361. doi:10.1039/C5PY00872G
84. Alcón, M. J.; Corma, A.; Iglesias, M.; Sánchez, F. *J. Mol. Catal. A: Chem.* **1999,** *144,* 337–346. doi:10.1016/S1381-1169(98)00385-9
85. Sharma, V. B.; Jain, S. L.; Sain, B. *Catal. Lett.* **2004,** *94,* 57–59. doi:10.1023/B:CATL.0000019331.06455.0f
86. Lee, H. M.; Bianchini, C.; Jia, G.; Barbaro, P. *Organometallics* **1999,** *18,* 1961–1966. doi:10.1021/om9900667
87. Dergunov, S. A.; Kesterson, K.; Li, W.; Wang, Z.; Pinkhassik, E. *Macromolecules* **2010,** *43,* 7785–7792. doi:10.1021/ma1012418
88. Van Dongen, S. F. M.; Nallani, M.; Cornelissen, J. J. L. M.; Nolte, R. J. M.; Van Hest, J. C. M. *Chem. – Eur. J.* **2009,** *15,* 1107–1114. doi:10.1002/chem.200802114
89. Tomalia, D. A.; Fréchet, J. M. *Prog. Polym. Sci.* **2005,** *30,* 217–219. doi:10.1016/j.progpolymsci.2005.03.003
90. Bronstein, L. M.; Shifrina, Z. B. *Nanotechnol. Russ.* **2009,** *4,* 576–608. doi:10.1134/S1995078009090031
91. Tomalia, D. A.; Majoros, I. *J. Macromol. Sci., Polym. Rev.* **2003,** *43,* 411–477. doi:10.1081/MC-120023912
92. Cheng, Y.; Zhao, L.; Li, Y.; Xu, T. *Chem. Soc. Rev.* **2011,** *40,* 2673–2703. doi:10.1039/c0cs00097c
93. Chung, Y.-M.; Rhee, H.-K. *Catal. Lett.* **2003,** *85,* 159–164. doi:10.1023/A:1022181327349
94. Peng, X.; Pan, Q.; Rempel, G. L. *Chem. Soc. Rev.* **2008,** *37,* 1619–1628. doi:10.1039/b716441f
95. Scott, R. W. J.; Wilson, O. M.; Oh, S.-K.; Kenik, E. A.; Crooks, R. M. *J. Am. Chem. Soc.* **2004,** *126,* 15583–15591. doi:10.1021/ja0475860
96. Scott, R. W. J.; Sivadinarayana, C.; Wilson, O. M.; Yan, Z.; Goodman, D. W.; Crooks, R. M. *J. Am. Chem. Soc.* **2005,** *127,* 1380–1381. doi:10.1021/ja044446h
97. Lang, H.; Maldonado, S.; Stevenson, K. J.; Chandler, B. D. *J. Am. Chem. Soc.* **2004,** *126,* 12949–12956. doi:10.1021/ja046542o
98. Ornelas, C.; Aranzaes, J. R.; Salmon, L.; Astruc, D. *Chem. – Eur. J.* **2008,** *14,* 50–64. doi:10.1002/chem.200701410
99. Ornelas, C.; Salmon, L.; Aranzaes, J. R.; Astruc, D. *Chem. Commun.* **2007,** 4946–4948. doi:10.1039/b710925c
100. Ornelas, C.; Ruiz, J.; Salmon, L.; Astruc, D. *Adv. Synth. Catal.* **2008,** *350,* 837–845. doi:10.1002/adsc.200700584
101. Wilson, O. M.; Knecht, M. R.; Garcia-Martinez, J. C.; Crooks, R. M. *J. Am. Chem. Soc.* **2006,** *128,* 4510–4511. doi:10.1021/ja058217m
102. Lim, J.; Simanek, E. E. *Org. Lett.* **2008,** *10,* 201–204. doi:10.1021/ol7024907
103. Agrawal, P.; Gupta, U.; Jain, N. K. *Biomaterials* **2007,** *28,* 3349–3359. doi:10.1016/j.biomaterials.2007.04.004
104. Dewey, D. C.; Strulson, C.; Cacace, D. N.; Bevilacqua, P. C.; Keating, C. D. *Nat. Commun.* **2014,** *5,* No. 4670. doi:10.1038/ncomms5670
105. Reymond, J.-L.; Darbre, T. *Org. Biomol. Chem.* **2012,** *10,* 1483–1492. doi:10.1039/c2ob06938e
106. Sommer, P.; Uhlich, N. A.; Reymond, J.-L.; Darbre, T. *ChemBioChem* **2008,** *9,* 689–693. doi:10.1002/cbic.200700606
107. Biswas, R.; Maillard, N.; Kofoed, J.; Reymond, J.-L. *Chem. Commun.* **2010,** *46,* 8746–8748. doi:10.1039/c0cc02700f
108. Clouet, A.; Darbre, T.; Reymond, J.-L. *Angew. Chem., Int. Ed.* **2004,** *43,* 4612–4615. doi:10.1002/anie.200460177
109. Klouda, L. *Eur. J. Pharm. Biopharm.* **2015,** *97,* 338–349. doi:10.1016/j.ejpb.2015.05.017
110. Seliktar, D. *Science* **2012,** *336,* 1124–1128. doi:10.1126/science.1214804
111. Ratner, B. D.; Hoffman, A. S. *ACS Symp. Ser.* **1976,** *31,* 1–36. doi:10.1021/bk-1976-0031.ch001
112. Varma, S.; Bureau, L.; Débarre, D. *Langmuir* **2016,** *32,* 3152–3163. doi:10.1021/acs.langmuir.6b00138
113. Neamtu, I.; Rusu, A. G.; Diaconu, A.; Nita, L. E.; Chiriac, A. P. *Drug Delivery* **2017,** *24,* 539–557. doi:10.1080/10717544.2016.1276232
114. Molina, M.; Asadian-Birjand, M.; Balach, J.; Bergueiro, J.; Miceli, E.; Calderón, M. *Chem. Soc. Rev.* **2015,** *44,* 6161–6186. doi:10.1039/C5CS00199D
115. Sasaki, Y.; Akiyoshi, K. *Chem. Rec.* **2010,** *10,* 366–376. doi:10.1002/tcr.201000008
116. Lu, A.; Smart, T. P.; Epps, T. H.; Longbottom, D. A.; O'Reilly, R. K. *Macromolecules* **2011,** *44,* 7233–7241. doi:10.1021/ma201256m
117. He, Y.; Huang, G.; Pan, Z.; Liu, Y.; Gong, Q.; Yao, C.; Gao, J. *Mater. Res. Bull.* **2015,** *70,* 263–271. doi:10.1016/j.materresbull.2015.04.028
118. Zhang, J.; Zhang, M.; Tang, K.; Verpoort, F.; Sun, T. *Small* **2014,** *10,* 32–46. doi:10.1002/smll.201300287

119. Tokareva, I.; Minko, S.; Fendler, J. H.; Hutter, E. *J. Am. Chem. Soc.* **2004,** *126,* 15950–15951. doi:10.1021/ja044575y
120. Wei, G.; Zhang, W.; Wen, F.; Wang, Y.; Zhang, M. *J. Phys. Chem. C* **2008,** *112,* 10827–10832. doi:10.1021/jp800741t
121. Que, Y.; Feng, C.; Zhang, S.; Huang, X. *J. Phys. Chem. C* **2015,** *119,* 1960–1970. doi:10.1021/jp511850v

License and Terms

BEILSTEIN JOURNAL OF ORGANIC CHEMISTRY

Assessing the possibilities of designing a unified multistep continuous flow synthesis platform

Mrityunjay K. Sharma[‡1,2], Roopashri B. Acharya[‡2], Chinmay A. Shukla[‡1,2] and Amol A. Kulkarni[*1,2,§]

Review

Open Access

Address:
[1]Academy of Scientific and Innovative Research (AcSIR), CSIR-National Chemical Laboratory (NCL) Campus, Pune 411008, India and [2]Chem. Eng. & Proc. Dev. Div., CSIR-National Chemical Laboratory, Dr. Homi Bhaba Road, Pashan, Pune 411008, India

Email:
Amol A. Kulkarni[*] - aa.kulkarni@ncl.res.in

* Corresponding author ‡ Equal contributors
§ Tel: +91 20 25902153

Keywords:
automation; continuous flow synthesis; cybernetics; multistep flow synthesis; unified platforms

Beilstein J. Org. Chem. **2018,** *14,* 1917–1936.
doi:10.3762/bjoc.14.166

Received: 22 January 2018
Accepted: 22 June 2018
Published: 26 July 2018

This article is part of the Thematic Series "Integrated multistep flow synthesis".

Guest Editor: V. Hessel

Abstract

The multistep flow synthesis of complex molecules has gained momentum over the last few years. A wide range of reaction types and conditions have been integrated seamlessly on a single platform including in-line separation as well as monitoring. Beyond merely getting considered as ‘flow version’ of conventional ‘one-pot synthesis’, multistep flow synthesis has become the next generation tool for creating libraries of new molecules. Here we give a more ‘engineering’ look at the possibility of developing a ‘unified multistep flow synthesis platform’. A detailed analysis of various scenarios is presented considering 4 different classes of drugs already reported in the literature. The possible complexities that an automated and controlled platform needs to handle are also discussed in detail. Three different design approaches are proposed: (i) one molecule at a time, (ii) many molecules at a time and (iii) cybernetic approach. Each approach would lead to the effortless integration of different synthesis stages and also at different synthesis scales. While one may expect such a platform to operate like a ‘driverless car’ or a ‘robo chemist’ or a ‘transformer’, in reality, such an envisaged system would be much more complex than these examples.

Review

Introduction

Flow chemistry is now seen as a reliable approach for the synthesis of simple organic compounds [1-6], complex large molecular weight medicinal drugs [7-12], polymeric materials [13-15], nanomaterials (metallic, bimetallic, composites, metal oxides, etc.) [16-18], catalysts [7,19], etc. In the recent times, the applicability of this tool has been extended for the synthesis of high value drugs involving multiple reaction steps including separation protocols [8,9,20]. A vast range of useful molecules

that are synthesized in flow has also helped integrate the complex synthesis with fine engineering to make the systems completely automated [9,20]. Flow chemistry gains its benefits from excellent heat and mass transfer rates and rapid mixing which is not possible in the case of conventional synthesis modes [21]. In general, the continuous flow synthesis aims at conducting the reactions at intrinsic kinetics. This helps to have reactors having smaller volumes making them inherently safer. Due to low processing volumes and reactions at intrinsic rates without much of human intervention it is possible to carry out hazardous reactions and a reaction at much higher temperature which is not possible with conventional methods [22,23]. An automated flow synthesis approach also reduces the labor costs significantly and operation can go on for a long time without any interruptions or significant downtime for the maintenance [9,20]. Many reactions have been performed in flow synthesis and are shown to be better than conventional synthesis [24-27]. A few examples of experimental set-ups of successfully demonstrated multistep flow synthesis encompassing various kinds of reactions from the literature are given in Table 1.

Table 1: Reactions and corresponding flow synthesis set-up from the literature.

reaction name and flow set-up
Grignard reaction [28] 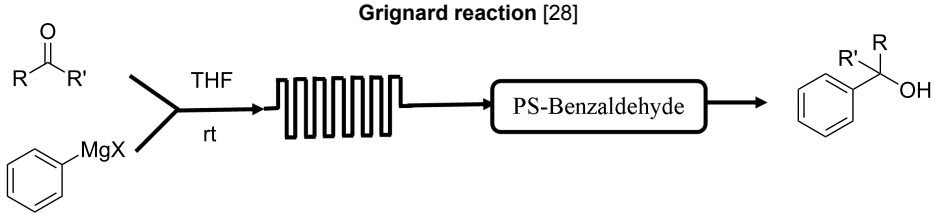
Curtius rearrangement [29] 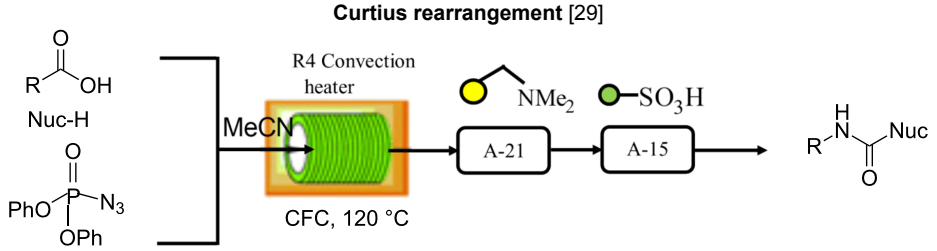
Heck reaction [30] 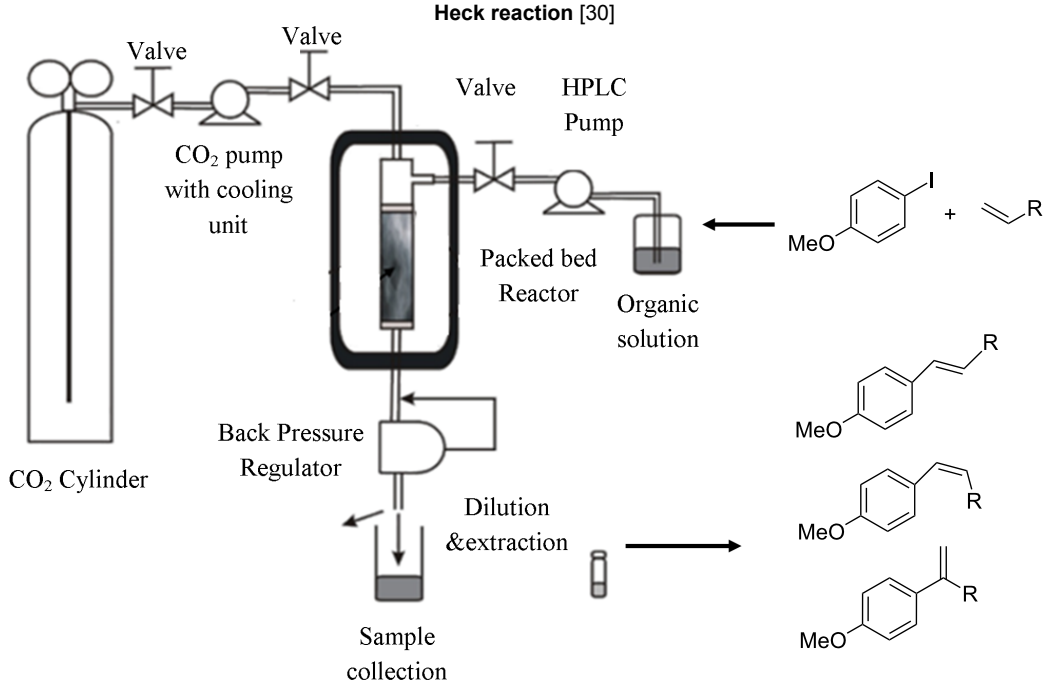

Table 1: Reactions and corresponding flow synthesis set-up from the literature. (continued)

Cannizzaro oxidation reaction [31]

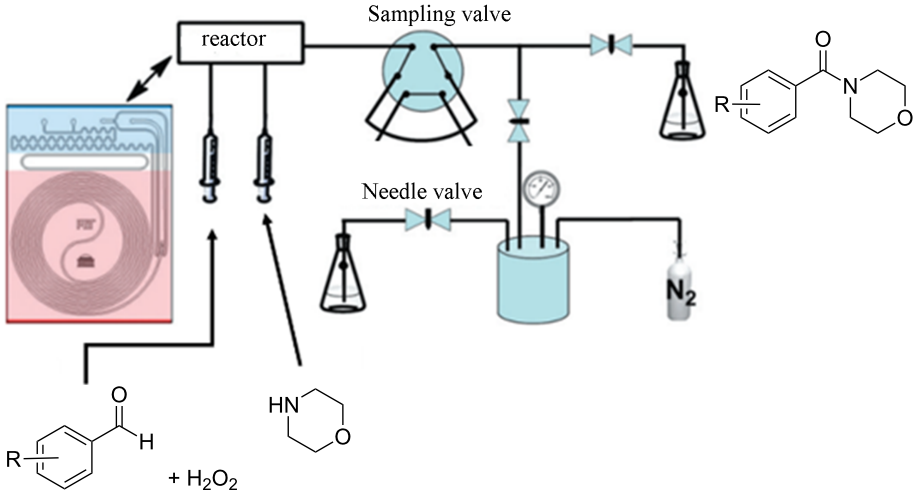

Biginelli reaction [32]

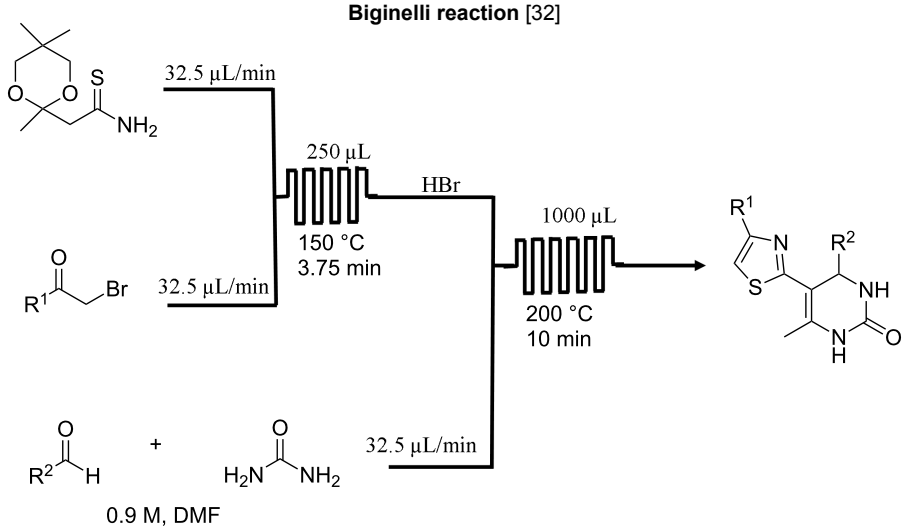

Single step approaches were useful in terms of evaluating the concepts in continuous flow synthesis. However, since synthesis of any fine chemical or medicinal drug or agrochemical compound involves a sequence of reactions as well as several unit operations, by making only one process step continuous does not make much impact in terms of overall efficiency, economics and operation time. Thus the flow synthesis made its mark in terms of improving the product quality and reducing the environmental impact, albeit only for single reactions. This also helped to understand the safety related issues of flow synthesis and even helped to study the effect of operating parameters (viz. flow rates, temperature, pressure, pH, etc.) and design parameters (viz. mixing, heat transfer, mass transfer, dispersion, etc.), which together helped in developing reactor selection protocols and safer intensification window for its continuous operation. Over the time even the process control structures also got evolved for specific kind of experimental set-ups and even automated self-optimizing platforms were also tested [33]. The natural evolution was an archetype for the multistep flow synthesis. The integration of in-line separation has taken the confidence of the synthesis community one step ahead [21,34,35]. In parallel to this, in-line analytical techniques have also been used for on-line measurement and characterization [36-38]. Multistep flow synthesis is a significant milestone in practice of organic synthesis. In the recent time, there has been a visible surge in the number of publications on multistep flow synthesis with specific target molecules [26,39]. Table 2 shows a few drugs which are synthesized using multistep flow synthesis. Multistep flow synthesis approach has the capability of replacing the conventional synthesis methods. It involves many unit operations also made to operate continuously to truly harness the benefits of flow chemistry which is not an easy task.

Table 2: A few important drug molecules synthesized in multistep continuous flow.

molecules and reaction/separation steps	end product	remarks
olanzapine (Zyprexa) [11] • 4 reaction steps • 2 separation steps	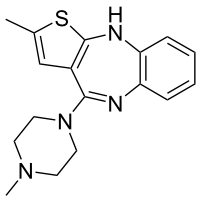	• antipsychotic drug • inductive heating was used • starting materials used: aryl iodide, aminothiazole Pd_2dba_3, xantphos, Bu_4NOAc, Et_3SiH, HCl, piperazine
tamoxifen [12] • 5 reaction steps	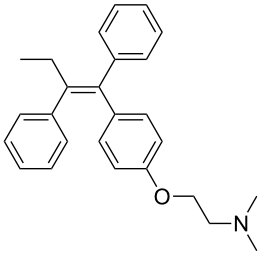	• breast cancer drug • telescope synthesis • moisture sensitive reagents were used • starting materials used: Weinreb amide, PhMgBr, aryl bromide, *n*-BuLi, aq HCl, TFAA, Et_3N
amitriptyline [10] • 6 reaction steps	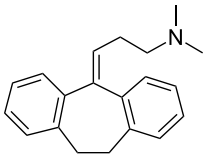	• antidepressant drug • moisture sensitive reagents were used • tube-in-tube reactor was used • inductive heating was used • starting materials used: benzyl bromide, *n*-BuLi, CO_2, Grignard reagent, EtOH
rufinamide [40] • 3 reaction steps	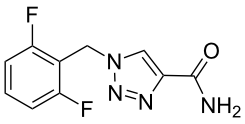	• anticonvulsant drug • telescope synthesis • copper tubing was used as reactor and catalyst • starting materials used: aryl bromide, NaN_3, methyl propiolate, aq NH_3
artemisinin [41] • 3 reaction steps • 4 separation steps	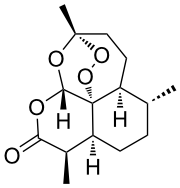	• antimalarial drug • the pressure was monitored to avoid unsafe backpressure due to clogging • starting materials used: dihydroartemisinic acid, TFA, toluene, O_2, TMOF/TEOF/succinic anhydride
telemisartan [42] • 3 reaction steps	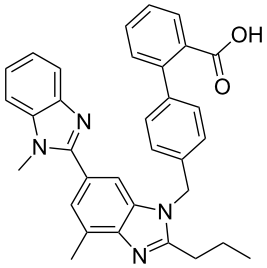	• hypertension drug • telescope synthesis • starting materials used: benzimidazole derivative, *t*-BuOK, bromide derivative, aq KOH, bromobenzimidazole
ibuprofen [43] • 3 reaction steps • 1 separation step	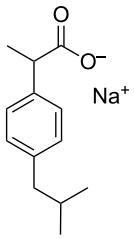	• nonsteroidal anti-inflammatory drug • three minutes residence time • starting materials used: isobutylbenzene, propionyl chloride, $AlCl_3$, TMOF, ICl, NaOH, 2-mercaptoethanol

Table 2: A few important drug molecules synthesized in multistep continuous flow. (continued)

(*S*)-rolipram [7] • 4 reaction steps	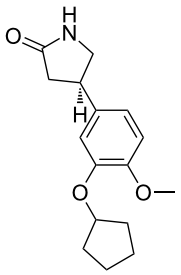	• anti-inflammatory drug and selective phosphodiesterase 4 (PDE4) inhibitor • heterogeneous catalysts • starting materials used: aldehyde derivative, nitromethane, malonate, Et_3N, H_2, water and *o*-xylene
(±)-pregabalin [44] • 3 reaction steps	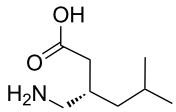	• used as a therapeutic agent for nervous system disorders such as epilepsy, anxiety disorder, and neuropathic pain • heterogeneous catalysts • starting materials used: isovaleraldehyde, methyl malonate, nitromethane, 1-PrOH, H_2, HCl, NaOH

The utilization of the same approach for the synthesis of a wide range of products is very challenging since each product in the chemical synthesis involves different synthesis procedures, different conditions, different phases and different isolation protocols. However, the approaches adopted for several multistep flow synthesis still lack from seamless extrapolation to other synthesis platforms, including the non-availability of specific unit operation in continuous mode at the throughputs suitable for laboratory scale. Though, the multistep continuous flow synthesis approach is very promising for the synthesis of important chemicals having applications as medicinal drugs, agrochemicals, perfumery compounds etc., in general, the components/equipment in a flow synthesis platform are almost identical and this paves the way to think of developing a unified flow synthesis platform that can facilitate multistep synthesis involving a wider range of reactions over a varied range of conditions. Such a platform would help to reduce the time in planning of experimental set-ups for individual reaction(s) or sequences and will also help to do a seamless integration of experimental conditions with smaller laboratory footprint. In addition to the most obvious purpose of having such a platform that will facilitate the synthesis of any molecule including several intermediate stages, it will help in terms of the following:

1. **End-to-end synthesis:** Total synthesis of various molecules involving multiple chemical transformations (homogeneous or reactions involving multiple phases) at various optimal conditions including work-up/purification in continuous mode.
2. **Screening:** Rapid screening of operating conditions and development of a library of molecules from similar initial substrates.
3. **Convenience:** Selection of the specific parts of the set-up for a given synthesis step or for selecting a sequence of reaction steps reduces the time to disassemble and re-assemble the set-up for different products. So, operating the set-up and deciding the parameters for each step becomes convenient using a unified platform.
4. **Modularity in true sense:** Making the reaction platform having plug-and-play approach would make it modular in true sense.
5. **Adaptability:** Having components with multiple functions will reduce the overall number of equipment/instruments on the synthesis platform.
6. **Automation:** Reduced human intervention facilitated by in-line measurements, automated optimization programs and continuous operation for a controlled set of conditions will be the unique features that will make such platforms attractive and efficient.
7. **Reproducibility:** Development of individual reaction steps and their optimization at various locations of an organization can become reproducible upon integration through such platforms.

While the concept of a unified synthesis platform looks fascinating and useful to reach the targets like ‘Dial-a-molecule’ [45], in reality, it can be very challenging. Some of the challenges are as follows:

1. **A varied range of conditions:** A multistep synthesis platform developed for one target molecule cannot always be utilized for different products since each product either requires different chemistry or a different set of unit operations or unit operation sequences. In some cases, synthesis and chemistries can be very different

such that totally different set of flow reactors (including material of construction) and operating conditions has to be employed, e.g., flow chemistry literature shows the use of a wide variety of flow reactors, e.g., tube-in-tube gas permeable membrane reactors [46-48], high-pressure reactors utilizing back pressure regulators [49-51], reactors with different heating and cooling modes (e.g., inductive heating [11,52], microwave [53-55] etc.) and many more, also very special reactors [56] with other difficulties that need to be taken care. Also reactions are varied in terms of conditions such as the utilization of novel process windows [57-59] where high temperature and pressure is utilized which needs special attention in terms of safety and other criteria compared to the reactions requiring ambient conditions and low to moderate temperatures.

2. **Matching of time scales:** Residence time associated with a specific operating condition in each reactor and in a separation protocol (i.e., unit operation) in sequence has to be matched properly to get the desired final product which needs to be optimized every time if the throughput in the start or anywhere else gets changed in the sequence. This is very important for synthesis steps where downstream processing is also in sequence. Usually time scales for work-up procedures like extraction, crystallization, solvent switch etc. are longer compared to the main reaction and for any particular reaction in sequence the time scale for all other steps has to be either fixed or it gets fixed based on the initial step. One option is to have more pumps and collect the reaction mass at some point to change the flow rate for matching of time scale [7-9,20]. However, such an arrangement is complex and makes it very difficult to vary for each new scenario which requires special skill set or modification in chemical step.
3. **Suitability of control structure and sensitivity:** A multistep flow synthesis approach possesses challenges in terms of controls where a slight change anywhere in the process sequence can hamper the product output or will require very different kind of control strategies in the subsequent steps. For example, the reaction can be sensitive towards mixing, mass transfer/flow regime, temperature, etc. Slight variation in pump flow rate or coolant flow rate/temperature can change the relative time scales of the process affecting its selectivity. For such cases, the control system should quickly bring the process to steady state to maintain the desired selectivity. Shukla and Kulkarni have reported a control structure for a few synthetically important drug molecules and discussed challenges involved in developing such a control process [60].
4. **Monitoring:** Utilization of in-line analysis techniques and constant monitoring of the product also requires specialized equipment to be used and relative 'analysis time' in the whole process sequence is much greater compared to the reaction time. During utilization of such in-line techniques like HPLC, UV and IR etc. where analysis time is greater than reaction, provision has to be provided for intermittent sampling to monitor the reaction progress. In those instances it is the analysis time that dictates the control structure and parameters to be varied in case of any disturbance at/during any stage of operation [38,61].
5. **Optimization:** In continuation to the first point above, since every reaction step would have a different set of optimal conditions, the availability of a varied range of utility (i.e., the heating or cooling systems) and their suitability for integration on a single platform would be challenging for configuring the entire platform. Moreover, even after realizing such a platform, optimal conditions for each step would be different this might need significant reconfiguration for making a real 'plug-and-play' kind of system. This means that the unified synthesis platform should have a number of utility variations as low as possible.
6. **Compatibility:** The material of construction or make of the process components may not be always suitable for a given set of reactants/products/solvents/byproducts. Even the change in the sequence should be adaptable such a system can be very expensive as well.
7. **Skills:** With the advent of many flow synthesis tools available in the market much of the above issues may be taken care of. However, the automation in multistep synthesis needs careful selection. In general, setting-up of a multistep flow synthesis platform is very time consuming and needs multidisciplinary skills or a bigger team as it gets reflected in a few excellent works from the literature [8,9,20,62].

Motivation

In view of the above introduction, in rest of this manuscript, we have explored the feasibility of having a unified multistep flow synthesis platform which can help to do almost any flow synthesis. Such a platform, if developed would resolve most of the above-stated challenges and will reduce the time and other resources whenever new chemistry has to be developed in continuous flow manner. The proposed platform will contain all the necessary components of a multistep synthesis unit that will be sufficient to perform a number of chemical syntheses with wide variation in synthesis steps. With the developed platform it will be very easy to do a screening of different chemistries and save a lot of time for beginner chemists in terms of locating and

assembling the setup. The proposed approaches are more as a guideline and will need elaborate engineering analysis before actually building them. However, we have also given specific recommendations in that direction. Before presenting and evaluating various approaches for building a unified multistep synthesis platform in Table 3 we have given definitions of a few terms used throughout the manuscript and their relevance.

Design complexity

A general flow chemistry setup requires some basic equipment like pumps, reactors (usually a flow reactor tube of required length and diameter or a microchannel reactor having various geometries or a static mixer) or a continuous stirred tank reactor or a fixed bed reactor or other intensified process equipment viz. spinning disc reactor, impinging jet reactor etc.) and a thermostat which will maintain the reaction temperature and components viz. valves, measurement devices and so on. As mentioned earlier, a list of various terms used in this article is given in Table 3. The functionality and nature of the setup can change with the chemistry under investigation and the experience of an individual involved in handling simple to complex synthesis containing a large number of stages and components. This demands more attention to address a few important aspects of such a unified synthesis platform.

Component selection: Component selection is the most important task for designing any synthesis set-up that targets a specific product. For a typical multistep flow synthesis involving several reaction stages, the system will require several components, reactors, and equipment. One can definitely identify some class of reaction where the same kind and number of components can be utilized but a slight change in synthesis route/chemistry will require a new component to be added extra or for the same component the suitable material of construction might be different than before. This can lead to a bulky system having a complex flow path.

Choice of parameters: Choice of a range of operating conditions/parameters is a very crucial aspect while designing a unified synthesis platform. In a multistep synthesis route, each stage will have its own set of operating conditions for getting the optimum yield. A set of reactors and components designed for a specific reaction would require optimization in terms of operating conditions to match the throughput or residence time when used for another reaction. Moreover, once the system or synthesis platform is built, any minor variation needed at one stage due to possible variation in the purity of reactants will require manipulation at each stage in the sequence.

Number of steps: The number of reaction steps and subsequent downstream processing for the synthesis of any final drug molecule or an agrochemical is usually different. Therefore the components needed for a specific synthesis protocol will also vary. Thus a unified multistep flow synthesis platform may not be adequate and cannot be complete for the synthesis of any and every molecule. For example, a few synthesis steps need very specific type of equipment (viz. ozonolysis), which is not needed in every routine synthesis.

Sequencing of components: For a unified synthesis platform to become adaptive to any kind of reaction sequence (reaction followed by separation and purification) is one of the most important design challenges. As the component in a platform would be fixed, for every synthesis either some components must be

Table 3: Definition of the specific terms used in the article.

terms as used in this article	meaning/relevance
1. reactor	the section of the platform used for carrying out reactions. Usually, reactors are followed by separators (for extraction, distillation, chromatographic separation, crystallization, etc.).
2. instrument	wireless or cabled electronic unit that interfaces with the reactor and separator to facilitate monitoring and/or measurement and/or control.
3. equipment	an electronic unit that facilitates dosing of gas, liquid and solid.
4. component	connecting joints between reactor(s), instruments and equipment. These will include fittings, connectors, valves, etc.
5. module	an assembly of all the above segments to facilitate flow synthesis along with monitoring and control (1–4).
6. variables and parameter	set of conditions (set points or variables) that are used for optimizing a specific reaction section or the entire sequence of reactions.
7. stage	individual unit operations (viz. pre-heating, mixing, reaction, quenching, separation, etc.).
8. number of steps	number of reactions (chemical transformations) in a sequence to obtain the final product.
9. synthesis sequence	a sequence of reactions and unit operations (stages) in the synthesis path for the specific final product.

bypassed or connected in a loop, which would increase the dead volume in the overall system. This would enhance the residence time, demand more safety features and also need more inventory. A larger dead volume has its own challenges.

Control strategy: Devising a control strategy for a unified synthesis platform itself will be the most complex task. The complexity will originate from the varied control structures needed for individual synthesis sequence. For every reaction sequence verification of the sensitivity bounds on the specific control, strategy has to be developed for optimum performance of the setup.

Scale of operation: Throughput for any targeted molecule may vary based on the user requirement. Choosing a component to be operated in up-scaling and down-scaling mode at several throughputs with a wide range of operating conditions is very difficult. More than the effect of residence time, the hydrodynamics for the same reactor would vary depending upon the throughput and will affect the performance severely. In such a case, the plug-and-play mode might work provided the change of component is limited and absolutely necessary.

Troubleshooting: As a unified platform will involve lots of components for a chosen multistep synthesis flow path, the standard protocols for start-up, operation and shut-down will vary depending upon the reaction sequence. Thus, the interlocks and control structure should be updated accordingly. For example, among the presently available automated flow synthesis platforms, the limitation always comes from non-availability of troubleshooting protocols.

Simultaneous use for synthesis of different molecules: Having a unified platform will serve the purpose only if all the units on the platform are utilized all the time which may not be the case always. Utilizing all the components simultaneously for different synthesis sequence will need isolation of one flow path from the other and since the whole system is integrated, this will introduce complex operational challenges.

Utility optimization: The operating conditions for individual reactions in a sequence are usually different and the reaction temperature can vary from −78 °C < T < 200 °C. In such a situation, it cannot be a viable option to have a different utility for individual reaction steps.

The above mentioned specific points need to be taken into account while planning for a unified synthesis platform for flow synthesis. Thus, depending upon the set of targeted molecules or functional group transformations it is possible to propose several design/assembly options. In rest of this article, we bring out a few different ways in which it would be possible to design a unified flow synthesis platform. A few case studies from the literature on multistep flow synthesis of very specific drug molecules are used to explore and evaluate the design approach for building a single synthesis platform that can help produce all of those drug molecules, each having a very different synthesis route.

How do we use it for drug synthesis?

The proposed options of a unified synthesis platform will serve as a convenient tool at lab scale. Many new chemistries that are parts of a multistep flow synthesis route are to be performed with slight changes in the component/layout. The platform will serve as a single destination for the multistep flow synthesis whenever a reaction has to be optimized or new screening has to be done. It is expected that with slight modifications, a user will be able to 'choose' a multistep synthesis flow path in the unified platform.

Approach

For designing such a system we have analyzed the literature on multistep flow synthesis of API's through complex chemistry. We have shortlisted the papers which contained different equipment's used in the pharmaceutical manufacturing to cover most of the functional groups which can be organized on the single platform and can be utilized for a number of chemical syntheses.

After identification of specific molecules to be used for developing a unified synthesis platform we have identified the number of components associated with a synthesis and then optimized the number of component which will be sufficient to do all the identified reactions. Once the components were chosen the optimal sequencing which will be efficient to do the reactions without much difficulty has been developed and sequencing was done. In order to evaluate the feasibility of the above concept, we have considered different multistep syntheses as case studies. Number of steps, starting material and other conditions are listed in Table 4.

For these few cases we have evaluated three different approaches that can be used for developing a single synthesis platform. Every approach is based on a different logic of making a unified multistep flow synthesis platform. Figure 1 shows a comparison between the different approaches.

Approach 1: Unimolecular synthesis (one at a time)

The first approach towards development of a unified flow synthesis platform mainly aims at minimizing the number of components and to perform the reactions in a single system without much change of components (Figure 2). Here the components

Table 4: Multistep synthesis case studies selected for the article.

multistep synthesis of (*S*)-rolipram [7]

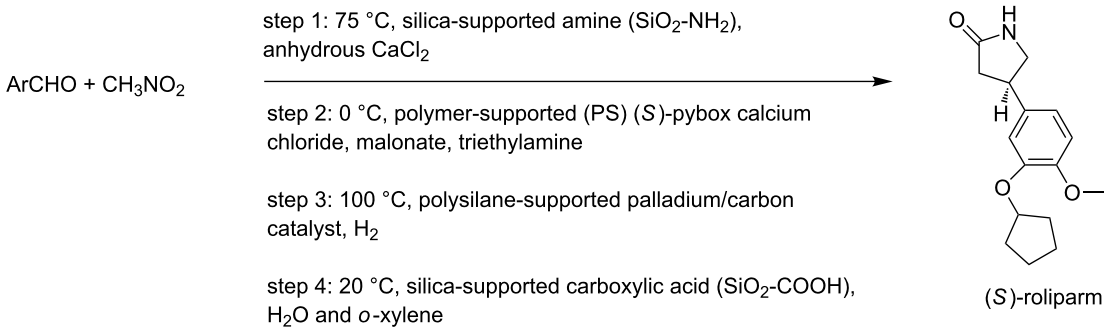

multistep synthesis of ribociclib [63]

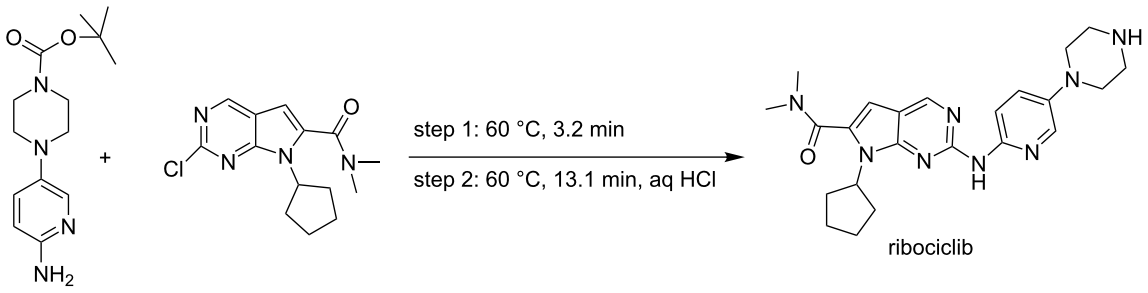

multistep synthesis of prexasertib monolactate monohydrate [8]

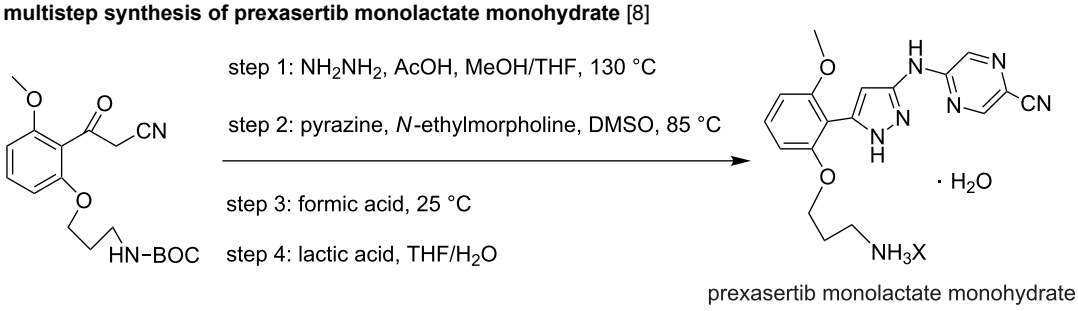

multistep synthesis of lidocaine hydrochloride [9]

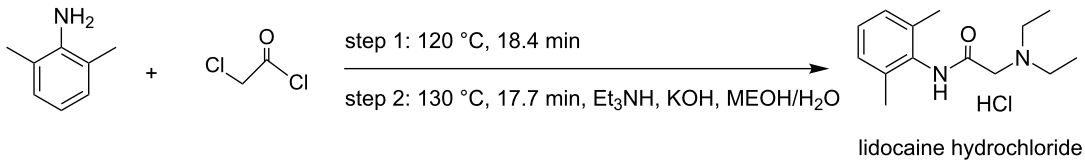

multistep synthesis of fluoxetine hydrochloride [9]

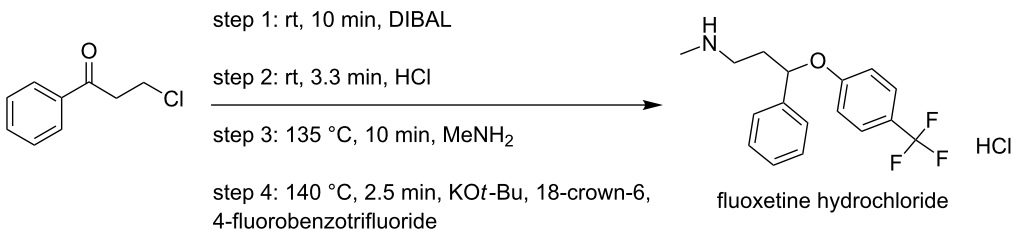

Table 4: Multistep synthesis case studies selected for the article. (continued)

multistep synthesis of diphenhydramine hydrochloride [9]

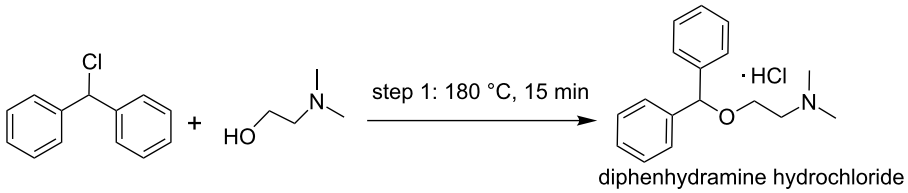

diphenhydramine hydrochloride

multistep synthesis of diazepam [9]

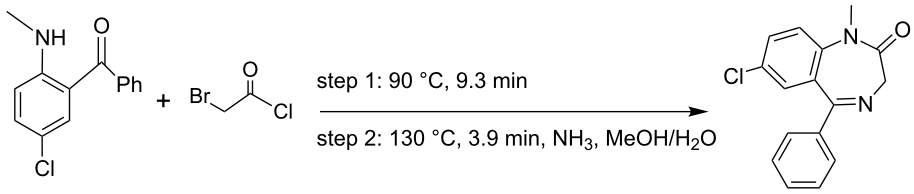

diazepam

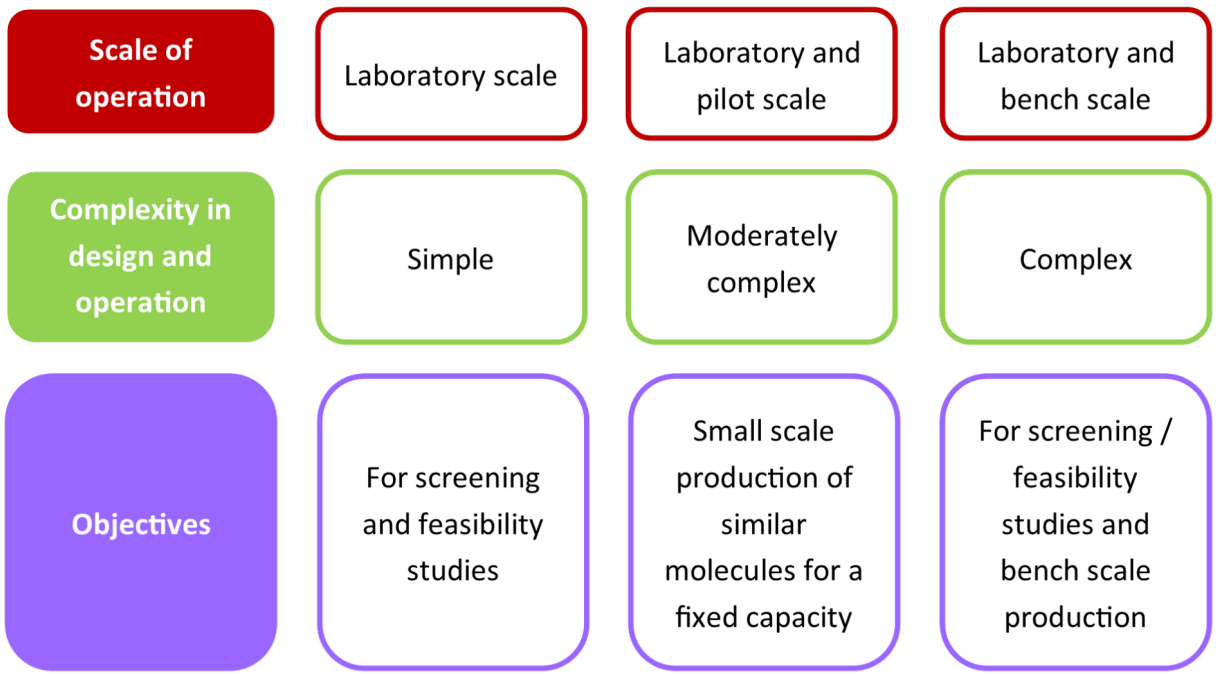

Figure 1: Key features of different approaches for unified multistep synthesis platform.

are fixed on one platform and the synthesis of a specific compound is carried out by choosing the path which is required for the reaction and other paths are blocked by using automated valves. This approach is good for relatively simple reactions and for some complicated reactions the number of components increases that lead to a large number of connections and a complex control structure. Table 5 shows the path for the synthesis of different products based on approach 1, Table 6 shows a list of components required for the synthesis of the above products using approach 1.

Figure 2 involves the platform for the synthesis of API's listed in Table 5. One example has chosen from Table 5 to explain approach 1. The description for the synthesis of prexasertib monolactate monohydrates based on approach 1 in Figure 2 is explained as follows: The synthesis of Prexasertib monolactate

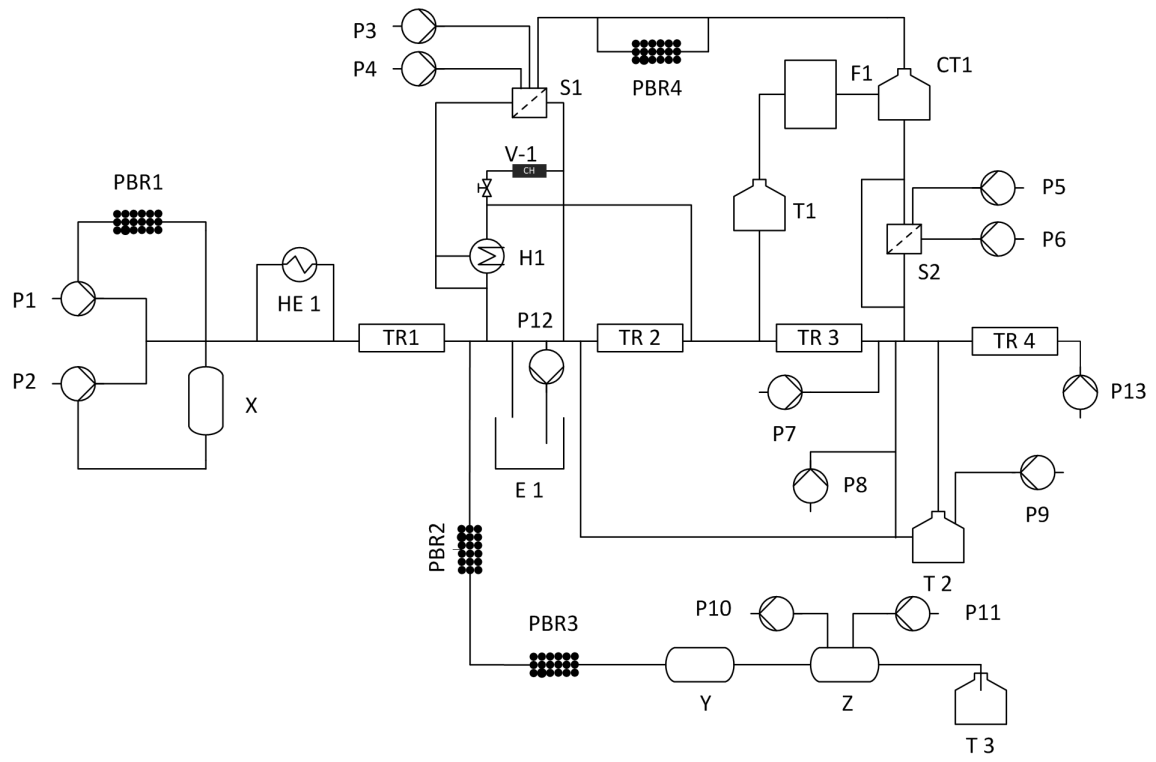

Figure 2: Schematic representation of a unified platform for the flow synthesis (P1–P14 pumps, PBR packed bed reactor, HE1 heat exchanger, H1 heater, S1 and S2 separator, E1 extractor, TR1–TR4 tubular reactor, CH charcoal, CT1 crystallization tank, T1–T3 tanks, F1 filtration).

Table 5: Conventional path for the synthesis of different intermediates based on approach 1.

intermediate	multistep synthesis flow path
prexasertib monolactate monohydrate	P1+P2→HE1→TR1→E1→TR2→TR3→RE1→T2→TR4→F1→T1
aliskiren hemifumatate	P1+P2→R1→S1→S2→TR4→S1→PBC→C1→S2→T2
diphenhydramine hydrochloride	P1+P2→R1→H1→BPR→CH→S1
lidocaine hydrochloride	P1+P2→R1→R2→BPR→CH→S1
diazepam	P1+P2→R1→R2→BPR→CH→S1
fluoxetine hydrochloride	P1+P2→R1→R2→S1→S2→R3→S1→H1→R2→T1
ricociclib	P1+P2→R1→R2→S1→R4→T1
rolipram	P1+P2→PBR1→X→TR1→PBR2→PBR3→Y→Z→T3

Table 6: Components required for the synthesis of the above API's [pumps (P), reactor (R), heat exchanger (HEx), heater (H), back pressure regulator (BPR), packed/fixed bed reactor (PBR/FBR), separator (S), charcoal adsorption cartridge (CA), liquid–liquid extractor (LLEx)]

name of API's	P	R	HEx	H	BPR	PBR/FBR	S	CA	LLEx
diphenhydramine hydrochloride	4	1	–	1	1	–	1	1	–
lidocaine hydrochloride	5	2	–	–	1	1	1	–	–
diazepam	4	2	–	–	1	1	1	1	–
fluoxetine hydrochloride	11	4	–	1	4	–	4	–	–
aliskiren hemifumarate	14	2	–	–	–	1	5	–	–
ricociclib	4	2	–	–	–	–	2	–	2
rolipram	7	1				5			
prexasertib monolactate monohydrate	20	3	1		–	–	1	–	2

monohydrates involves four steps a) condensation b) aromatic nucleophilic substitution reaction, c) deprotection and d) formation of lactate salt. Details of the same are given below:

- **Condensation:** Condensation takes place in a first reactor TR1 between the nitrile and hydrazine at high temperature and under pressure. Here, the nitrile was dissolved in a THF and hydrazine was dissolved in a mixture of solvents such as methanol, acetone, and water. The nitrile was pumped using pump P1 and hydrazine was pumped through P2 into the tubular reactor TR1 maintained at a temperature of 130 °C at residence time of 60 minutes to obtain the pyrazole. The impurities of the pyrazole were removed by passing it to the continuous countercurrent extraction E1. Here a solvent exchange process takes place between toluene and water. The pyrazole was then concentrated using automated rotary evaporator RE1. The concentrated product was diluted with DMSO using pump P13.
- **Aromatic nucleophilic substitution:** The nucleophilic substitution reaction takes place between the pyrazole and *N*-ethylmorpholine. Pyrazole of step 1 in the extractor was pumped through P13 and *N*-ethylmorpholine through P3 into the reactor TR2 to form the arylated product of the pyrazole. Here the reactor was maintained at a temperature of 70–100 °C for 1–3 hours. The product was crystallized in CT1 with the anti-solvent methanol pumped through P4 into the crystallization tank. The crystallized product was filtered and separated in S2.
- **Deprotection:** The second-stage product from the separator enters into the tubular reactor TR3 at a temperature of 20–40 °C with a residence time of 4 hours. Into this reactor nitrogen gas was pumped through peristaltic pump P7 and formic acid using pump P8. In TR3 gas–liquid reaction takes place.
- **Formation of the lactate salt:** In step four, lactic acid was pumped through pump P3 to form the final lactate salt of the product. Here the excess of formic acid and lactic acid was removed by the rotary evaporator RE1, then passes through TR4 into the crystallization tank CT1. The solid product formed was filtered in F1 and stored in a tank T1.

Challenges in performing multiple reactions in a single platform as given above: The number of valves needed to select the desired set of equipment is much higher. The reactions which take place only in a packed bed reactor and do not involve a separator, filter, crystallizer, etc. The path required for the synthesis is the same as that of synthesizing it individually so that the number of components required will remain unchanged and it is the same as that of an individual synthesis.

Approach 2: multimolecular operation (more than 1 molecule at a time)

This approach consists of identifying and optimizing a minimum number of components for performing flow synthesis of different molecules. The developed platform will contain all the necessary components for synthesis (flow reactors, packed columns etc.) to the downstream processing (extractor, separator, crystallizers, dilution tank etc.). Some of these components can be used for different chemistries just by changing the flow rates or the operating conditions specific to the chemistry. The components will be arranged on a platform where the order of arrangement can be varied in terms of processing needed for chemical synthesis just by connecting the components via tubes. The designed platform will be provided with some accessories which will include at least one component of all types on the platform (of different or same volume, or suitable to the different operational parameters) with an exactly same dimension which will make replacement of a component easy in case of failure or whenever needed. This platform will be a plug-and-play kind of system where the user will just have to choose the specific order of the component arrangement and to select the operating parameters before starting any experiment. The platform can be used for a specific synthesis step optimization or for performing an optimized multistep synthesis. The plug-and-play approach makes it very useful in the sense that if some or any component on the platform is not being utilized for any synthesis that component can be removed and used for another purpose or simultaneous synthesis of different molecules can be done using components which are not being utilized for the ongoing synthesis. The components like dilution tanks, crystallization tanks, and gravity based liquid–liquid separators can serve different purposes if planned properly before the experiment so that the same component can be used interchangeably with different chemistries reducing the need for different components still further.

Figure 3 shows the unified platform based on the approach 2 which contains the optimum component based details extracted from the literature of selected case studies. The sequence of components was arranged according to the described setup in the case studies selected. Figure 4 depicts 4 processes in one chart and the components in blue color are the common components, which will take part in the synthesis of any or every molecule chosen from the case studies. That reduces the quantity of the same kind of components by 4 times. The number of components for each unit operation is quite large, however, that helps to carry out the synthesis of all the identified products in the chart.

To have a view of the platform as in approach 2 one example of diphenhydramine hydrochloride is covered here from the case

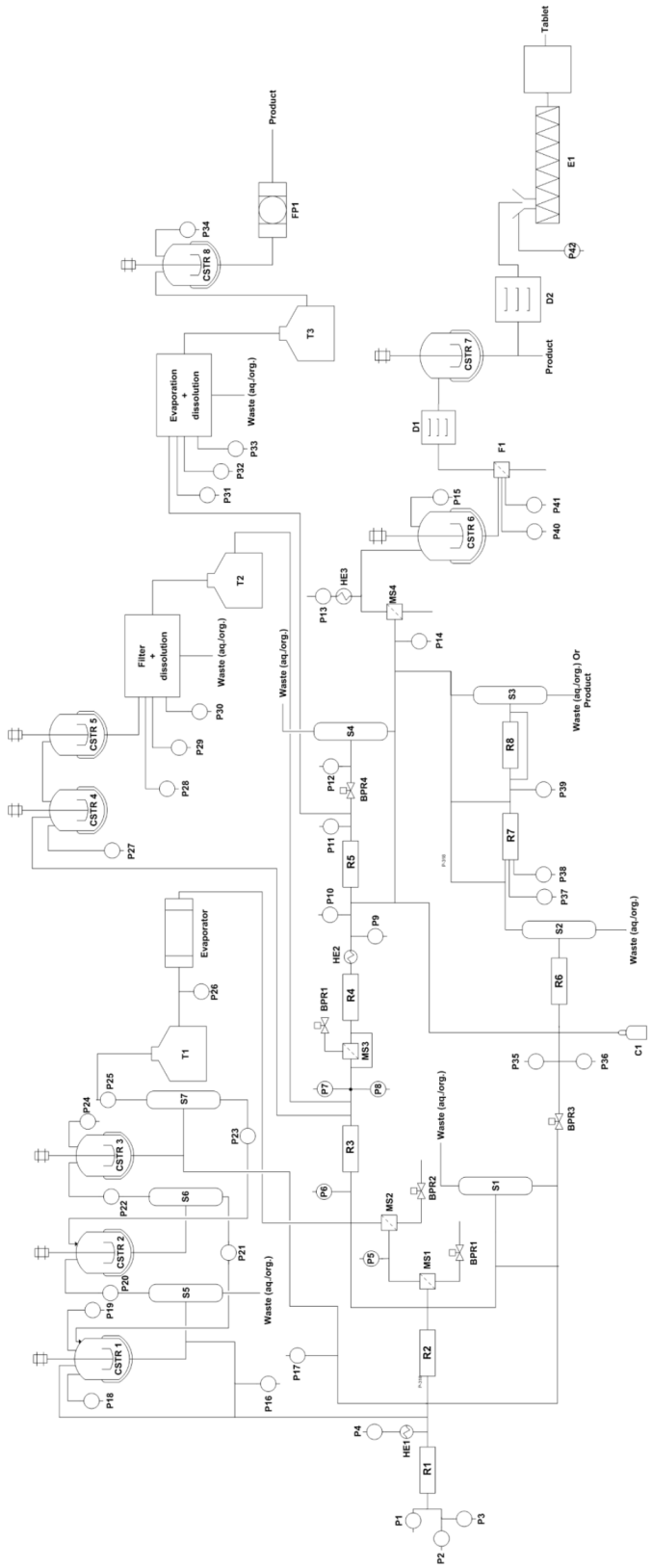

Figure 3: Layout of a unified synthesis platform (including all the component) for multiple drug molecules (approach 2) R – coil reactor/packed bed reactor/scavenger, P – pump, HE – heat exchanger, CSTR – stirred tank reactor/crystallizer/dilution tank, T – storage tank, F – filter, S – gravity-based separator, D – dryer, FP – filter press, MS – membrane separator, E – extruder, BPR – back pressure regulator.

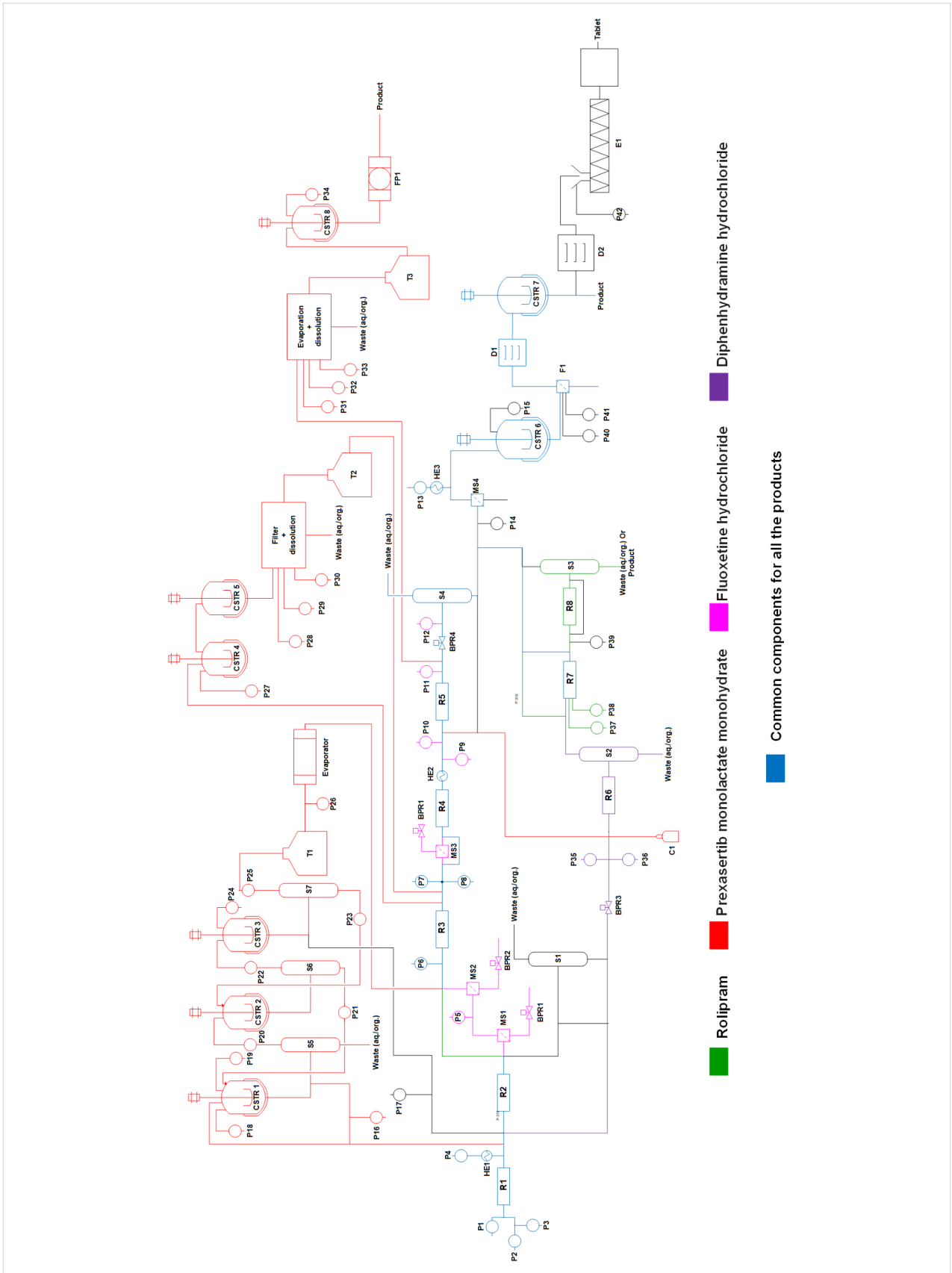

Figure 4: Layout for synthesis of 4 molecules on a single platform (approach 2).

studies, where two reactants 2-dimethylaminoethanol and neat chlorodiphenylmethan is being pumped from P1 and P2 to reactor R1 where it is getting heated at a temperature of 180 °C at a pressure of 1.7 MPa. The molten salt which comes out of reactor R1 is then treated with aqueous NaOH through pump P4 which is heated to 140 °C through HE1. In-line extraction and purification happen in packed bed column reactor R6 by water and hexane which are pumped through pump P35 and P36. The resulting biphasic solution passes through gravity operated liquid–liquid separator S2 with automatic level control. In the downstream section the API was precipitated with HCL through pump P14 and the precipitate is dissolved in ethanol and crystallized in CSTR6 maintaining temperature at 5 °C. After the crystals are being filtered through F1 and dried in D1, the final product was dissolved in water in CSTR7. The final product diphenhydramine hydrochloride is collected in the form of a solution. The overall process follows the path as shown in the sequence of Scheme 1.

With this approach, it is very easy to reduce the number of components significantly to perform a number of different chemical steps of varying nature (except very different chemistries where very specific equipment is required). The platform developed using this approach will have the following key features:

1. **Useful for a limited number of molecules:** This approach will be very useful if a similar set of chemical transformation is to be performed which will reduce the number of components significantly, however, the approach discussed above is not unique since everyone can come up with an optimum number of components based on the chemistries involved and the level of expertise.

2. **Volume of each component:** Choosing the right component volume plays a very critical role here since that is going to fix the residence time and the overall throughput. For the same synthesis route, the volume of a component will vary if the throughput is going to increase or decrease. It becomes very important before designing such a platform to define the scale of operation and the type of chemistry that will be used since much of the selection criteria will depend on the aforesaid two parameters.

3. **A number of components:** As components can be interchanged and reused, defining the number of components is not critical but one has to take this into account since this will depict the overall costs of building such a platform. Though one can have a large number of accessories, adding each one on the synthesis platform will increase the cost.

4. **Connection for components:** Connecting the components in proper sequence is required for success in any multistep flow synthesis including work-up. Making a connection before and after each operation will add an extra volume to the existing process volume, which needs to be taken care off. In this approach, the connection is not fixed rather the plug-and-play kind of approach can bring the components close to each other reducing the need for intermediate heating/cooling or the requirement of an additional utility to maintain the reaction temperature in the tubes.

5. **Instrumentation:** Here, we have not explicitly considered any instrumentation (other than in-line analysis or measurements for monitoring a given reaction/purification) but that can be added at the specific steps wherever needed.

6. **Utility:** At this point of time it is assumed that for each reaction step the heating or cooling arrangement (also referred as 'utility' in the chemical process engineering and plant operation) is arranged individually.

Approach 3: a cybernetic approach

The third approach can be based on the need for a versatile and extremely flexible system. Figure 5 shows the concept of a unified platform (Approach 3) for multistep synthesis in a continuous flow. The platform can have three basic modules which are interconnected.

The first, reactor module includes different reactors types that are commonly used in the synthesis of APIs viz. tubular reactor (R1–R4), packed bed reactor (R5–R8) and stirred tank reactor (R9). The reactors are equipped with a jacket for maintaining the reaction temperatures. Additionally, multiple temperature zones can also be provided if required. The reactor module also includes mixers (M1–M9) that are commonly used in flow

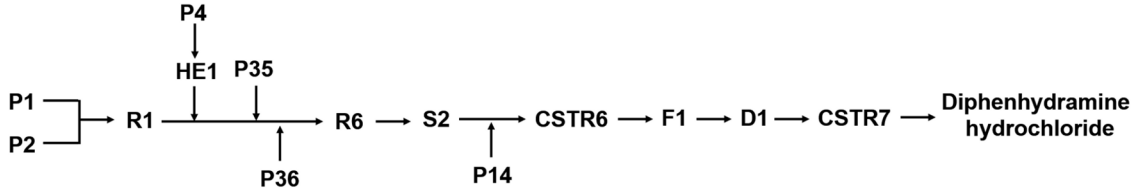

Scheme 1: The overall process for the synthesis of diphenhydramine hydrochloride.

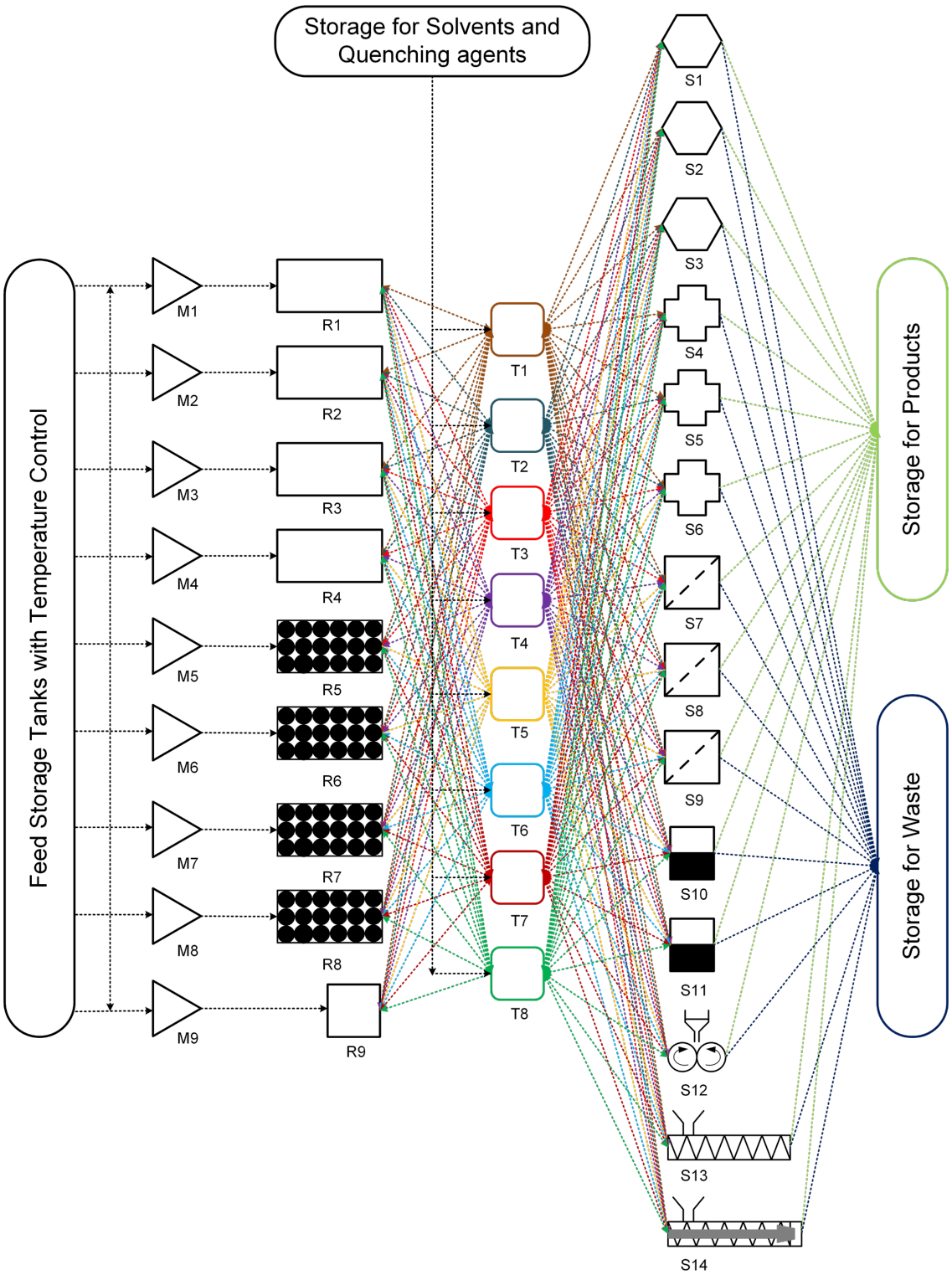

Figure 5: Approach 3 for a unified platform for multistep synthesis. M1–M9 = mixers, R1–R4 = tubular reactors, R5–R8 = packed bed reactor, R9 = stirred tank reactor, T1–T8 = Intermediate storage tanks, S1–S3 = adsorption columns, S4–S6 = extraction columns/gravity-based separator, S7–S9 = membrane separator/Filter, S10–S11 = evaporator, S12 = rotary drum dryer, S13 = vacuum screw dryer, S14 = extruder.

chemistry [64,65]. The continuous flow reactor can also be equipped with in-line static mixing elements [63].

The second module includes the intermediate storage tanks (T1–T8) with an agitator and a jacket for maintaining the temperature. The intermediate storage tanks can be used for multiple purposes viz. preheating/precooling any reaction intermediate, mixing reagents, quenching the reaction, dilution, crystallization, reaction and can be operated in batch or continuous mode (CSTRs). Preheating and precooling are essential for getting reproducible and reliable experimental data.

The third and final module includes separators viz. membrane separators/filters, scavengers or adsorption column (packed column), extractors/gravity separators, dryers, extruders, etc. These three modules can be fixed in a 3D space on a skid. However, the tubings, valves and back pressure regulators need not be fixed and can remain connected to individual module units as per process requirements. Avoiding the tubing will add more flexibility to the unified platform similar to pipeless plants [66]. The entire platform has separate tanks for storing the feed, product, solvent/buffer solution for extraction and waste collection. The feed storage tanks will be equipped with temperature control for preheating or precooling of any reagent before mixing. Moreover, the unified platform can be integrated into any commercial separation and analytical system. This approach is analogous to cybernetics [67].

Table 7 shows the process components required and the sequence of unit operations for producing various pharmaceutical products using approach 3. These unit modules can be connected in the desired sequence by connecting the tubing. Additionally, valves and back pressure regulators can be used whenever required. The unit operations which are not required for the process under consideration will not be connected. This approach allows connecting any unit operation in any desired sequence making it a unified platform for multistep synthesis. Such a platform can be integrated with chromatography purification systems, in-line analytical instruments, a mold for tablet making and various commercial instruments.

As suggested, a priory information should be known regarding kinetics of various processes (reaction/drying/crystallization/adsorption/desorption), solubility data (extraction/crystallization), etc. This approach is useful for testing proof of the concept for a continuous process of various drugs which are in clinical trials. However, this approach may not be feasible for pilot or production scale as the scale of operation is different and reactors and separators should be designed accordingly. The ideal use of this platform is to evaluate the possibility of the synthesis concept of various processes along with automation having a variety of unit operations and operating conditions and collect useful data for further plant design or for using it for a specific period of time to meet the production needs and then switch to another molecule, making it a flexible production platform. Eventually, at the pilot or production scale, it will be analogous to approach 2. Key features of this approach can be given as follows: (i) truly unified multistep flow synthesis platform, (ii) intermediate tanks can be used for preheating/precooling, isolating different pressure zones and intermediate storage, (iii) the system will have all the necessary components like back pressure regulator, check valve, control valve, temperature and

Table 7: Sequence of unit operations for various pharmaceutical products by approach 3.

reference	product	reactors/equipment/components (number)	sequence of unit operations as per approach 3 (see Figure 5)
Tsubogo et al. [7]	(*R*)- and (*S*)-rolipram	• packed bed reactors (4) • adsorption columns (3)	M5→R5→T5→S1→M6→R6→T6→M7→R7→T7→S2→T8→S3→R8
Pellegatti et al. [63]	ribociclib	• flow reactors (2) • stirred tank reactor (1)	M1→R1→M2→R2→S4→T1→M3→R3→S5→R9
Cole et al. [8]	prexasertib monolactate monohydrate	• flow reactors (4)	M1→R1→T1→S4→T2→S5→T3→S6→T4→S10→M2→R2→T5→T6→S7→S8→T7
Adamo et al. [9]	fluoxetine hydrochloride	• flow reactors (4)	M1→R1→T1→S7→T2→S8→R2→T3→S10→A1→T4→R3→T5→S4→downstream
	diazepam	• flow reactors (2)	M1→R1→M2→R2→T1→R5→S4→S1→T2→S5→ downstream
	lidocaine hydrochloride	• flow reactors (2)	M1→R1→N2→R2→T1→R5→S4→downstream
	diphenhydramine hydrochloride	• flow reactor (1)	M1→R1→T1→R5→S4→S1→downstream
Mascia et al. [20]	aliskiren hemifumarate	• flow reactors (2) • crystallizers + tanks (6)	M1→R1→T1→S4→T2→T3→S7→T4→M2→R2→T5→S5→S8→S1→T6→T7→S9→T8→S12→S13→S14→moulding machine

pressure sensors, etc., (iv) the stirred tank reactor can be used for the reaction and also for crystallization, (v) the reactor jacket can have multiple temperature zones to offer more flexibility, (vi) the fixed bed/packed columns can be used as reactors as well as scavenging columns depending on the requirement or even as a mixer if the packing is inert.

While such a unified platform would offer enormous flexibility in operation, it would be challenging to develop such a platform. A few challenges can be given as follows: (i) too many connections, (ii) arrangement of various components in 3D space is critical, (iii) needs very complex control strategy, (iv) minimizing the pipeline length during component assembly is challenging to optimize the residence time variation and will handle more chemicals than conventional systems, (v) relatively large amount feed material will be required when compared (to compensate dead volume) to a single dedicated experimental setup and (vi) automation will be complex as well as expensive.

Simultaneous synthesis of (*S*)-rolipram and ribociclib by approach 3

The aldehyde and nitromethane are dissolved in toluene separately and kept in the feed storage tanks for preheating (see Figure 5). The reagents can be pumped with a suitable pump (viz., peristaltic pump, piston pump, diaphragm pump, etc.) into the mixer M5 and subsequently to reactor R5 which is packed with SiO_2-NH_2 and $CaCl_2$. The intermediate nitroalkane obtained is cooled to 0 °C in the intermediate storage tank T5. The reaction mixture can pass through separator S1 (adsorption column) which is packed with MS 4 Å to remove the byproduct water. A solution of malonate and triethylamine in toluene are precooled to 0 °C in feed storage tanks and pumped to mixer M6 where it is mixed with the nitroalkane stream. The reaction stream can then be passed through reactor R6 which is packed with polymer-supported (*S*)-pybox–calcium chloride and maintained at 0 °C. The reaction stream can be further passed to intermediate tank T6 where it can be preheated to 100 °C. The reaction stream containing Michael addition product is mixed with hydrogen gas (from H_2 cylinder) in mixer M7. The resulting two-phase mixture can be passed to reactor R7 packed with Pd/DMPSi-C catalyst and maintained at 100 °C. The reaction stream can then be passed in intermediate tank T7 where unreacted hydrogen gas is vented and recycled and the liquid stream is preheated to 120 °C. The liquid stream then can pass through separator S2 (adsorption column) packed with Amberlyst-15 Dry to remove impurities. Water and *o*-xylene can be preheated and pumped from the feed storage tanks into intermediate storage tank T8 where it is mixed with the reaction mixture. The process stream can be further passed through separator S3 (adsorption column) packed with Celite. The reaction mixture can pass through reactor R8 packed with silica-supported carboxylic acid and maintained at 120 °C to obtain the product (*S*)-rolipram. In the above example, intermediate storage tanks T1–T4 can also be used instead of T5–T8 as every unit module (reactors, intermediate storage tanks, and separators) can be connected in any desired sequence by simple tube fittings. However, the choice of unit modules should be done on the basis of a lower tubing volume.

Chloropyrimidine and aminopyridine derivatives are dissolved in THF and can be preheated to 60 °C in the feed storage tank. LiHMDS solution in THF also can be preheated to 60 °C in the feed storage tank. Both the solutions can be pumped with suitable pumps in the mixer M1 and then through reactor R1 which is maintained at 60 °C. The product stream can be mixed with preheated HCl in mixer M2 and then passed through reactor R2 which is also maintained at 60 °C. The reaction mixture can then be passed to separator S4 (extractor) to separate the aqueous and organic phases. The organic waste can be collected in the waste storage and the aqueous phase is mixed with sodium hydroxide in intermediate storage tank T1 to quench the HCl. The reaction mixture can be mixed with THF in mixer M3 and passed through reactor R3. The process stream can be further passed to separator S5 (extractor) to separate the aqueous waste and organic phase. The organic phase can be further passed to reactor 9 (stirred tank) where it can be mixed with succinic acid for further batch crystallization to obtain the product ribociclib.

In this way, we can operate two synthetic processes simultaneously in the unified platform (approach 3). However, many unit modules still remain unused (viz., M4, R4, T2–T4, and S6–S14). Table 7 shows the unit module sequences for various products for approach 3.

Conclusion

For the multistep flow synthesis approach, the next evolution is obviously towards a combination of automation, monitoring, screening, optimization, artificial intelligence and instrumentation. It has changed the conventional synthesis approaches through significant improvement in the product quality, efficiency, and smaller environmental foot print. Utilizing the benefits of multistep flow synthesis is not easy and it requires experienced professionals and ready-to-use tools for effortless integration of different synthesis stages. Developing the unified platform which will reduce the effort in setting up the experiments and integration of different component which will definitely help to speed up the overall process to truly harness the advantages of flow synthesis. Based on different objectives viz. reaction screening, library generation, bench/pilot scale synthesis for various molecules we have shown three approaches to

make a unified multistep flow synthesis platform which can be made keeping the interest of individual or organization for future. These approaches show the unique and promising ways to make the unified platform to realize the concepts like dial a molecule. Realising the concept of a unified flow synthesis platform possesses some challenges but those can be taken care based on the need and planning beforehand. Once this platform is built it will act as 'driverless car' or a 'robot chemist' where an only instruction has to be given and platform will take care of the synthesis of the desired molecule based on the specific chosen flow path. The next level of such a platform can only go in the direction of self-regulated automatic 3D configurable synthesis platforms, just like an advanced version of 'Transformers'. With growing machine intelligence, it is expected that the synthesis platforms would harness big data sets as a source of knowledge, artificial intelligence for decision-making abilities at various levels and self-optimization. Developing such a unified integrated multistep flow synthesis platform will be the new thing for organic synthesis to explore the unexplored chemistry.

ORCID® iDs

Amol A. Kulkarni - https://orcid.org/0000-0001-6146-1255

References

1. Baumann, M.; Garcia, A. M. R.; Baxendale, I. R. *Org. Biomol. Chem.* **2015,** *13,* 4231–4239. doi:10.1039/C5OB00245A
2. Webb, D.; Jamison, T. F. *Org. Lett.* **2012,** *14,* 2465–2467. doi:10.1021/ol300722e
3. Shu, W.; Pellegatti, L.; Oberli, M. A.; Buchwald, S. L. *Angew. Chem.* **2011,** *123,* 10853–10857. doi:10.1002/ange.201105223
4. Noël, T.; Kuhn, S.; Musacchio, A. J.; Jensen, K. F.; Buchwald, S. L. *Angew. Chem.* **2011,** *123,* 6065–6068. doi:10.1002/ange.201101480
5. Poh, J.-S.; Browne, D. L.; Ley, S. V. *React. Chem. Eng.* **2016,** *1,* 101–105. doi:10.1039/C5RE00082C
6. Nagaki, A.; Kim, H.; Yoshida, J.-i. *Angew. Chem.* **2009,** *121,* 8207–8209. doi:10.1002/ange.200904316
7. Tsubogo, T.; Oyamada, H.; Kobayashi, S. *Nature* **2015,** *520,* 329–332. doi:10.1038/nature14343
8. Cole, K. P.; Groh, J. M.; Johnson, M. D.; Burcham, C. L.; Campbell, B. M.; Diseroad, W. D.; Heller, M. R.; Howell, J. R.; Kallman, N. J.; Koenig, T. M.; May, S. A.; Miller, R. D.; Mitchell, D.; Myers, D. P.; Myers, S. S.; Phillips, J. L.; Polster, C. S.; White, T. D.; Cashman, J.; Hurley, D.; Moylan, R.; Sheehan, P.; Spencer, R. D.; Desmond, K.; Desmond, P.; Gowran, O. *Science* **2017,** *356,* 1144–1150. doi:10.1126/science.aan0745
9. Adamo, A.; Beingessner, R. L.; Behnam, M.; Chen, J.; Jamison, T. F.; Jensen, K. F.; Monbaliu, J.-C. M.; Myerson, A. S.; Revalor, E. M.; Snead, D. R.; Stelzer, T.; Weeranoppanant, N.; Wong, S. Y.; Zhang, P. *Science* **2016,** *352,* 61–67. doi:10.1126/science.aaf1337
10. Kupracz, L.; Kirschning, A. *Adv. Synth. Catal.* **2013,** *355,* 3375–3380. doi:10.1002/adsc.201300614
11. Hartwig, J.; Ceylan, S.; Kupracz, L.; Coutable, L.; Kirschning, A. *Angew. Chem., Int. Ed.* **2013,** *52,* 9813–9817. doi:10.1002/anie.201302239
12. Murray, P. R. D.; Browne, D. L.; Pastre, J. C.; Butters, C.; Guthrie, D.; Ley, S. V. *Org. Process Res. Dev.* **2013,** *17,* 1192–1208. doi:10.1021/op4001548
13. Iwasaki, T.; Yoshida, J.-i. *Macromolecules* **2005,** *38,* 1159–1163. doi:10.1021/ma048369m
14. Nagaki, A.; Tomida, Y.; Miyazaki, A.; Yoshida, J.-i. *Macromolecules* **2009,** *42,* 4384–4387. doi:10.1021/ma900551a
15. Nagaki, A.; Tomida, Y.; Yoshida, J.-i. *Macromolecules* **2008,** *41,* 6322–6330. doi:10.1021/ma800769n
16. Chou, K.-S.; Hsu, C.-Y.; Liu, B.-T. *RSC Adv.* **2015,** *5,* 29872–29877. doi:10.1039/C5RA00320B
17. Lin, X. Z.; Terepka, A. D.; Yang, H. *Nano Lett.* **2004,** *4,* 2227–2232. doi:10.1021/nl0485859
18. Hemmati, S.; Barkey, D. P.; Eggleston, L.; Zukas, B.; Gupta, N.; Harris, M. *ECS J. Solid State Sci. Technol.* **2017,** *6,* P144–P149. doi:10.1149/2.0171704jss
19. Kupracz, L.; Hartwig, J.; Wegner, J.; Ceylan, S.; Kirschning, A. *Beilstein J. Org. Chem.* **2011,** *7,* 1441–1448. doi:10.3762/bjoc.7.168
20. Mascia, S.; Heider, P. L.; Zhang, H.; Lakerveld, R.; Benyahia, B.; Barton, P. I.; Braatz, R. D.; Cooney, C. L.; Evans, J. M. B.; Jamison, T. F.; Jensen, K. F.; Myerson, A. S.; Trout, B. L. *Angew. Chem., Int. Ed.* **2013,** *52,* 12359–12363. doi:10.1002/anie.201305429
21. Hartman, R. L.; Naber, J. R.; Buchwald, S. L.; Jensen, K. F. *Angew. Chem., Int. Ed.* **2010,** *49,* 899–903. doi:10.1002/anie.200904634
22. Deadman, B. J.; Collins, S. G.; Maguire, A. R. *Chem. – Eur. J.* **2015,** *21,* 2298–2308. doi:10.1002/chem.201404348
23. Movsisyan, M.; Delbeke, E. I. P.; Berton, J. K. E. T.; Battilocchio, C.; Ley, S. V.; Stevens, C. V. *Chem. Soc. Rev.* **2016,** *45,* 4892–4928. doi:10.1039/C5CS00902B
24. McQuade, D. T.; Seeberger, P. H. *J. Org. Chem.* **2013,** *78,* 6384–6389. doi:10.1021/jo400583m
25. Pastre, J. C.; Browne, D. L.; Ley, S. V. *Chem. Soc. Rev.* **2013,** *42,* 8849–8869. doi:10.1039/c3cs60246j
26. Webb, D.; Jamison, T. F. *Chem. Sci.* **2010,** *1,* 675–680. doi:10.1039/c0sc00381f
27. Wegner, J.; Ceylan, S.; Kirschning, A. *Adv. Synth. Catal.* **2012,** *354,* 17–57. doi:10.1002/adsc.201100584
28. Riva, E.; Gagliardi, S.; Martinelli, M.; Passarella, D.; Vigo, D.; Rencurosi, A. *Tetrahedron* **2010,** *66,* 3242–3247. doi:10.1016/j.tet.2010.02.078
29. Baumann, M.; Baxendale, I. R.; Ley, S. V.; Nikbin, N.; Smith, C. D.; Tierney, J. P. *Org. Biomol. Chem.* **2008,** *6,* 1577–1586. doi:10.1039/b801631n
30. Lau, P. L.; Allen, R. W. K.; Styring, P. *Beilstein J. Org. Chem.* **2013,** *9,* 2886–2897. doi:10.3762/bjoc.9.325
31. Liu, X.; Jensen, K. F. *Green Chem.* **2012,** *14,* 1471–1474. doi:10.1039/C2GC35078E
32. Pagano, N.; Herath, A.; Cosford, N. D. P. *J. Flow Chem.* **2011,** *1,* 28–31. doi:10.1556/jfchem.2011.00001
33. Fabry, D. C.; Sugiono, E.; Rueping, M. *React. Chem. Eng.* **2016,** *1,* 129–133. doi:10.1039/C5RE00038F
34. Ghislieri, D.; Gilmore, K.; Seeberger, P. H. *Angew. Chem., Int. Ed.* **2015,** *54,* 678–682. doi:10.1002/anie.201409765
35. Borukhova, S.; Noël, T.; Hessel, V. *ChemSusChem* **2016,** *9,* 67–74. doi:10.1002/cssc.201501367
36. Koos, P.; Gross, U.; Polyzos, A.; O'Brien, M.; Baxendale, I.; Ley, S. V. *Org. Biomol. Chem.* **2011,** *9,* 6903–6908. doi:10.1039/c1ob06017a

37. Hopkin, M. D.; Baxendale, I. R.; Ley, S. V. *Chem. Commun.* **2010,** *46,* 2450–2452. doi:10.1039/c001550d
38. McMullen, J. P.; Jensen, K. F. *Annu. Rev. Anal. Chem.* **2010,** *3,* 19–42. doi:10.1146/annurev.anchem.111808.073718
39. Porta, R.; Benaglia, M.; Puglisi, A. *Org. Process Res. Dev.* **2016,** *20,* 2–25. doi:10.1021/acs.oprd.5b00325
40. Zhang, P.; Russell, M. G.; Jamison, T. F. *Org. Process Res. Dev.* **2014,** *18,* 1567–1570. doi:10.1021/op500166n
41. Gilmore, K.; Kopetzki, D.; Lee, J. W.; Horváth, Z.; McQuade, D. T.; Seidel-Morgenstern, A.; Seeberger, P. H. *Chem. Commun.* **2014,** *50,* 12652–12655. doi:10.1039/C4CC05098C
42. Martin, A. D.; Siamaki, A. R.; Belecki, K.; Gupton, B. F. *J. Flow Chem.* **2015,** *5,* 145–147. doi:10.1556/JFC-D-15-00002
43. Snead, D. R.; Jamison, T. F. *Angew. Chem.* **2015,** *127,* 997–1001. doi:10.1002/ange.201409093
44. Ishitani, H.; Kanai, K.; Saito, Y.; Tsubogo, T.; Kobayashi, S. *Eur. J. Org. Chem.* **2017,** 6491–6494. doi:10.1002/ejoc.201700998
45. http://generic.wordpress.soton.ac.uk/dial-a-molecule/ (accessed Jan 22, 2018).
46. Brzozowski, M.; O'Brien, M.; Ley, S. V.; Polyzos, A. *Acc. Chem. Res.* **2015,** *48,* 349–362. doi:10.1021/ar500359m
47. Polyzos, A.; O'Brien, M.; Petersen, T. P.; Baxendale, I. R.; Ley, S. V. *Angew. Chem., Int. Ed.* **2011,** *50,* 1190–1193. doi:10.1002/anie.201006618
48. Cranwell, P. B.; O'Brien, M.; Browne, D. L.; Koos, P.; Polyzos, A.; Peña-López, M.; Ley, S. V. *Org. Biomol. Chem.* **2012,** *10,* 5774–5779. doi:10.1039/c2ob25407g
49. Razzaq, T.; Glasnov, T. N.; Kappe, C. O. *Eur. J. Org. Chem.* **2009,** 1321–1325. doi:10.1002/ejoc.200900077
50. Razzaq, T.; Kappe, C. O. *Chem. – Asian J.* **2010,** *5,* 1274–1289. doi:10.1002/asia.201000010
51. Murphy, E. R.; Martinelli, J. R.; Zaborenko, N.; Buchwald, S. L.; Jensen, K. F. *Angew. Chem., Int. Ed.* **2007,** *46,* 1734–1737. doi:10.1002/anie.200604175
52. Ceylan, S.; Coutable, L.; Wegner, J.; Kirschning, A. *Chem. – Eur. J.* **2011,** *17,* 1884–1893. doi:10.1002/chem.201002291
53. Baxendale, I. R.; Pitts, M. R. *Chim. Oggi* **2006,** *24,* 41–45.
54. Glasnov, T. N.; Kappe, C. O. *Chem. – Eur. J.* **2011,** *17,* 11956–11968. doi:10.1002/chem.201102065
55. Nikam, A. V.; Kulkarni, A. A.; Prasad, B. L. V. *Cryst. Growth Des.* **2017,** *17,* 5163–5169. doi:10.1021/acs.cgd.7b00639
56. Jähnisch, K.; Hessel, V.; Löwe, H.; Baerns, M. *Angew. Chem., Int. Ed.* **2004,** *43,* 406–446. doi:10.1002/anie.200300577
57. Hessel, V. *Chem. Eng. Technol.* **2009,** *32,* 1655–1681. doi:10.1002/ceat.200900474
58. Illg, T.; Löb, P.; Hessel, V. *Bioorg. Med. Chem.* **2010,** *18,* 3707–3719. doi:10.1016/j.bmc.2010.03.073
59. Hessel, V.; Cortese, B.; de Croon, M. H. J. M. *Chem. Eng. Sci.* **2011,** *66,* 1426–1448. doi:10.1016/j.ces.2010.08.018
60. Shukla, C. A.; Kulkarni, A. A. *Beilstein J. Org. Chem.* **2017,** *13,* 960–987. doi:10.3762/bjoc.13.97
61. Yue, J.; Schouten, J. C.; Nijhuis, T. A. *Ind. Eng. Chem. Res.* **2012,** *51,* 14583–14609. doi:10.1021/ie301258j
62. Heider, P. L.; Born, S. C.; Basak, S.; Benyahia, B.; Lakerveld, R.; Zhang, H.; Hogan, R.; Buchbinder, L.; Wolfe, A.; Mascia, S.; Evans, J. M. B.; Jamison, T. F.; Jensen, K. F. *Org. Process Res. Dev.* **2014,** *18,* 402–409. doi:10.1021/op400294z
63. Pellegatti, L.; Hafner, A.; Sedelmeier, J. *J. Flow Chem.* **2016,** *6,* 198–201. doi:10.1556/1846.2016.00017
64. Hessel, V.; Löwe, H.; Schönfeld, F. *Chem. Eng. Sci.* **2005,** *60,* 2479–2501. doi:10.1016/j.ces.2004.11.033
65. Falk, L.; Commenge, J.-M. *Chem. Eng. Sci.* **2010,** *65,* 405–411. doi:10.1016/j.ces.2009.05.045
66. Realff, M.; Shah, N.; Pantelides, C. C. *Comput. Chem. Eng.* **1996,** *20,* 869–883. doi:10.1016/0098-1354(95)00181-6
67. Kafarov, V. *Cybernetic Methods in Chemistry and Chemical Engineering [in Russian];* Khimiya: Moscow, 1976; pp 102–110.

License and Terms

BEILSTEIN JOURNAL OF ORGANIC CHEMISTRY

A general and atom-efficient continuous-flow approach to prepare amines, amides and imines via reactive *N*-chloramines

Katherine E. Jolley[1], Michael R. Chapman[1] and A. John Blacker[*1,2]

Full Research Paper

Open Access

Address:
[1]School of Chemistry, Institute of Process Research and Development, University of Leeds, Leeds, LS2 9JT, United Kingdom and [2]School of Chemical and Process Engineering, University of Leeds, Leeds, LS2 9JT, United Kingdom

Email:
A. John Blacker[*] - j.blacker@leeds.ac.uk

* Corresponding author

Keywords:
continuous flow; CSTR; *N*-chloramine; synthetic methods; telescoping

Beilstein J. Org. Chem. **2018,** *14,* 2220–2228.
doi:10.3762/bjoc.14.196

Received: 16 April 2018
Accepted: 10 August 2018
Published: 24 August 2018

This article is part of the Thematic Series "Integrated multistep flow synthesis".

Guest Editor: V. Hessel

Abstract

Chloramines are an important class of reagents, providing a convenient source of chlorine or electrophilic nitrogen. However, the instability of these compounds is a problem which makes their isolation and handling difficult. To overcome these hazards, a continuous-flow approach is reported which generates and immediately reacts *N*-chloramines directly, avoiding purification and isolation steps. 2-Chloramines were produced from the reaction of styrenes with *N*-alkyl-*N*-sulfonyl-*N*-chloramines, whilst *N*-alkyl or *N,N'*-dialkyl-*N*-chloramines reacted with anisaldehyde in the presence of *t*-BuO_2H oxidant to afford amides. Primary and secondary imines were produced under continuous conditions from the reaction of *N*-chloramines with base, with one example subsequently reduced under asymmetric conditions to produce a chiral amine in 94% ee.

Introduction

N-Chloramines are versatile reagents, however, their availability is restricted by their stability, so useful would be in situ methods to produce and use them [1,2]. The continuous-flow methodology is useful in this context, enabling control over reaction exotherms and improved measures for containment. To evaluate the use of *N*-chloramines in the laboratory requires multiphase flow methods, and until recently these have been limited by the availability of suitable equipment. Microreactors have been used for mixing biphases and employ either static mixers or shaped chambers and channels that repeatedly split and mix the liquids [3-5]. These rely on flow rates within the mixing zone that are sufficient to overcome phase separation [6]. Actively mixed, multistage and variable residence time (t_{res}) continuous stirred tank reactors (CSTRs) allow much

lower flow rates and therefore longer t_{res} for slow reactions [7,8]. The use of CSTRs to carry out sequential or multistep reactions has been exploited by Ley and others [9-11]. The strategy is useful, since it has the potential to eliminate time-consuming and costly product isolations. In these systems, the reactants and products are fluids which are contacted with solid-supported reagents that after some time require regeneration, which is not convenient within chemical manufacture.

Chloramine itself is unstable, though has been produced safely at large scale using continuous-flow methods; in fact, chloramine has been used as an intermediate in the manufacture of hydrazine using the Raschig process [12,13]. *N*-Alkyl-*N*-chloramines are equally unstable, yet have only been prepared in batch via reaction of a primary or secondary amine with Cl_2 gas, *N*-chlorosuccinimide, chloramine-T or hypochlorite salts [14,15]. Whilst Cl_2 gas is atom efficient it is difficult to handle, with associated toxicity, and the acid byproduct which leads to *N*-chloramine hydrolysis [16]. On the other hand, *N*-chlorosuccinimide or chloramine-T are commonly employed, being commercially available, stable and straightforward to handle, though both exhibit poor atom economy [17-21]. Sodium hypochlorite (NaOCl) solutions are less widely used, yet readily available, economic and provide an atom efficient reagent for *N*-chloramine formation [22-24].

A continuous-flow process for the oxidation of alcohols using NaOCl as a phase-transfer catalyst was recently reported [25]. We have published a communication that describes the continuous mixing of aqueous NaOCl and an organic solution of secondary amine, using either a tubular reactor with in-line static mixers or a single stage CSTR [26]. The reactor was selected to provide a t_{res} for optimal conversion. This was achieved according to reaction kinetics and hydrophobicity of the amine, which affects its partition between phases. Herein, we report improvements to this process and the use of *N*-alkyl-*N*-chloramine in subsequent continuous-flow reactions (Figure 1).

These reagents can be used as electrophilic or radical amination agents in a wide range of reactions [14]. In the present study, we opted to evaluate the addition of *N*-alkyl-*N*-chloramines with (a) alkenes to produce amines, (b) aldehydes to give amides, (c) reaction with a base to afford imines. Several alkenes are known to react with *N*-haloamines to form aziridines and other *N*-heterocycles. Typically, the reactions require a catalyst (e.g., Cu, I_2) [17,18,27], whilst more active reagents such as chloramine-T with osmate catalysts have been used to make 1,2-aminoalcohols and diamines [28-33]. Improved methods for the formation of amides remain an important goal for the pharma industry. In this regard, the reaction of *N*-chloramine with aldehydes, *t*-BuO_2H and iron or copper catalysts to give secondary and tertiary amides was reported in batch recently [33,34], though safety concerns upon scale-up makes this a useful reaction to translate to flow. Likewise, imines are an important class of compounds and are increasingly used as precursors to optically active amines [35-39]. Whilst normally prepared via a corresponding carbonyl compound, final dehydration can be problematic. The oxidation of a racemic amine and subsequent chiral reduction may offer a valuable alternative if coupled into a sequential flow protocol. There are reports on the formation of imines from *N*-chloramines using bases (e.g., NaOMe, KO*t*-Bu, NEt_3 and NaOH) [40-45], with one specific study using this technique to racemise and resolve enantiopure tetrahydroquinolines [46,47], and another accessing an intermediate to the drug telaprevir [45]. Our study complements these findings, by supplying a continuous-flow oxidation–reduction sequence which telescopes both *N*-chloramine and imine intermediates to produce chiral amines.

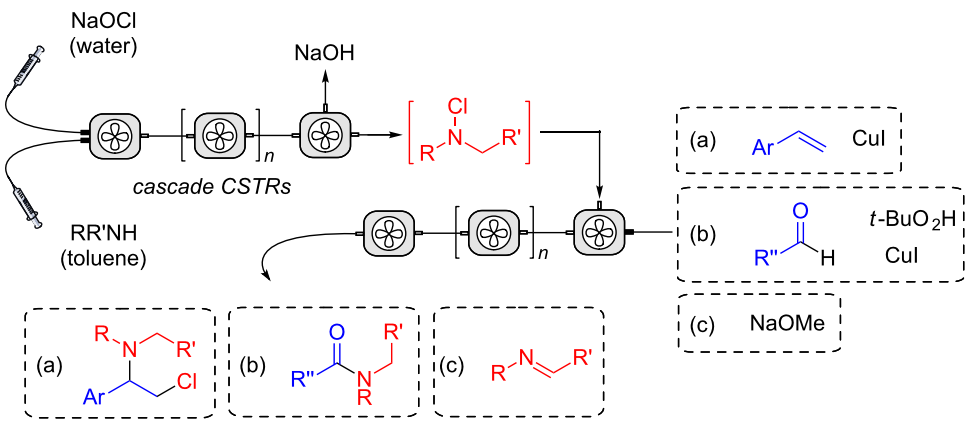

Figure 1: Continuous-flow process to produce and react *N*-chloramines.

Results and Discussion

N-Chloramine formation

N-(Di)alkyl-*N*-chloramines have been prepared in continuous organic–aqueous biphasic flow using either static mixers or a single-stage CSTR [26]. The choice of reactor and definition of t_{res} for this reaction is governed by both the thermodynamic phase partition parameter of reactants and mixing efficiency which control mass transfer between each phase (and thus, reaction rate). We decided to exploit a multi-stage cascade CSTR developed by our group recently [8], which enables efficient mixing over long t_{res} (Figure 2).

Using a 5-stage variant, various unsymmetrical *N*-chloramines were produced with unprecedented productivities (Table 1).

The rapid nature of this chlorination step makes in situ generation and consumption feasible in flow mode. Comparing Table 1, entries 1 and 3, the 5-stage CSTR, with one fifth the

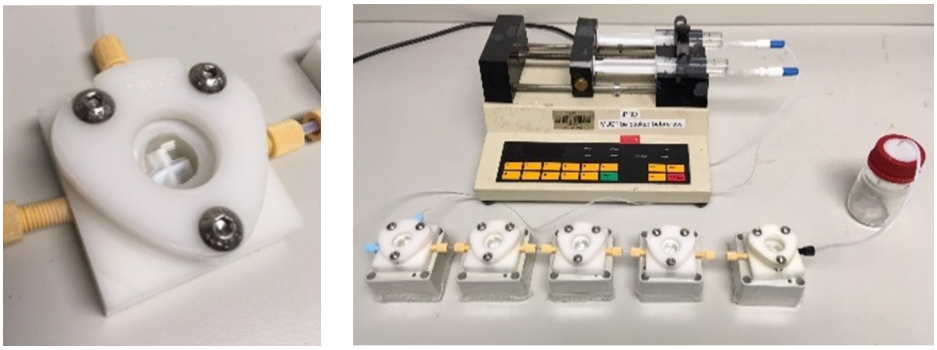

Figure 2: Left: Laboratory scale CSTR developed by our group [8]. Right: 5-stage CSTR configuration using co-feeds of amine in toluene and aqueous NaOCl.

Table 1: Continuous *N*-chloramine formation.

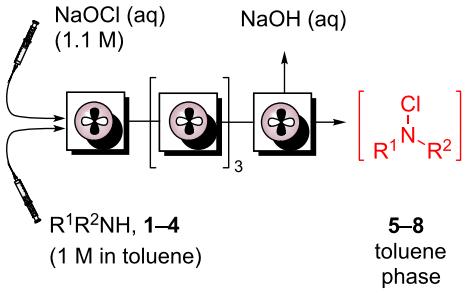

1,**5**: R^1 = Me, R^2 = Bn
2,**6**: R^1 = H, R^2 = -CH(Me)Ph
3,**7**: R^1 = Me, R^2 = -CH(Me)Ph
4,**8**: R^1,R^2 = -CH(Me)$(CH_2)_4$-

entry	starting material	product	reactor[a] (vol/mL)	t_{res} (min)	conversion (%)[b]	productivity (mol L^{-1} h^{-1})
1	**1**	**5**	SM (6)	20	89	1.3
2	**1**	**5**	CSTR[c] (50)	25	100	1.2
3	**1**	**5**	CSTR[d] (10)	5	94	5.6
4	**2**	**6**	CSTR[d] (10)	10	92	2.8
5	**3**	**7**	CSTR[d] (10)	30	93	0.9
6	**4**	**8**	CSTR[d] (10)	10	100	3.0

[a]SM = static mixer. [b]Determined by ^{1}H NMR spectroscopy. [c]1-Stage CSTR. [d]5-Stage CSTR.

volume of that in Table 1, entry 2, provides a much shorter t_{res} than the in-line static mixer (SM) with comparable conversion of *N*-benzyl-*N*-methylamine (**1**) to the *N*-alkyl-*N*-chloramine **5** at steady state, representing a productivity value of 5.6 mol L^{-1} h^{-1}. The same reactor geometry was used to chlorinate primary, secondary acyclic and cyclic amines **2**–**4** in conversions between 92–100%, with productivities ranging between 0.9–3 mol L^{-1} h^{-1} (Table 1, entries 4–6). In each case, separation of the product-rich toluene phase avoided *N*-chloramine isolation and allowed direct deployment in further reactions.

Reaction of *N*-chloramine with alkene

Initially our study tested the reaction of *N*-chloromorpholine (**16**) to styrene (**13**) varying Cu catalyst loading and a range of temperatures. The anti-Markovnikov addition product was observed with 10% CuI catalyst loading, at ambient temperature. However, it required 24 hours (see Supporting Information File 1, S1), and this slow reaction prevents sensible translation of the process into continuous flow. Despite trying alternative catalysts or other conditions no improvement was found. Instead, the more electron-poor *N*-chloro-*N*-methyl-*p*-toluenesulfonamide (**11**) was investigated as substrate. Differential scanning calorimetry (DSC) was used to assess the thermal stability of **11**, which melts at 78 °C and decomposes between 160–200 °C. This profile peaks at 188 °C, corresponding to an enthalpy of decomposition of −84.7 kJ mol^{-1} (see Supporting Information File 1, S2). A maximum safe operating temperature of 110 °C was implemented to avoid thermal decomposition and thermal runaway.

The direct reaction of *N*-chloramine **11**, or the benzyl-substituted variant **12**, led to a single regioisomer of the amine product in a lower reaction time than the analogous reaction using **16** (15 minutes vs 24 hours in batch mode; Supporting Information File 1, Table S1, entry 2 and Table 2, entries 1–5. The products **14** and **15**, prepared in batch, were isolated in 78 and 68% yield, respectively, and characterized (see Supporting Information File 1, S4). These standards enabled monitoring of the steady-state conversion in continuous flow by ^{1}H NMR.

Following an optimization study, it was found that the Cu catalyst could be omitted when operating at 100 °C for 1 hour reaction time in batch, providing quantitative conversion to product (Table 2, entry 4). Conducting the same reaction under an atmosphere of air or in the presence of TEMPO, suppressed all product formation (Table 2, entry 5). Due to the safety concerns of scaling-up such a batch reaction, a heated single-stage CSTR was evaluated to immediately quench the *N*-chloramine. Flowing an aqueous solution of in situ generated **11** or **12** into a

Table 2: Batch vs flow study of reaction of *N*-chloramine with styrene.

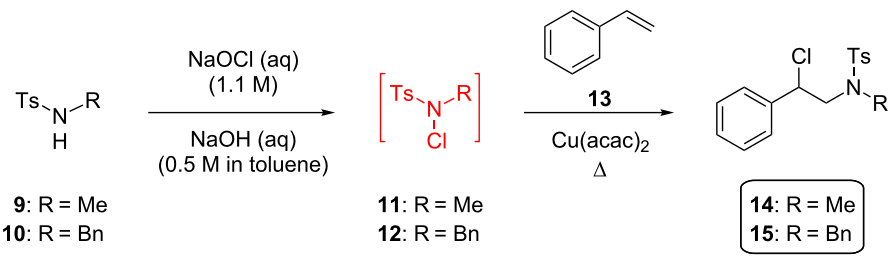

9: R = Me
10: R = Bn

11: R = Me
12: R = Bn

14: R = Me
15: R = Bn

entry	mode/substrate	catalyst (mol %)	temperature (°C)	time (min)	product	conversion (%)[a]
1	batch/**9**	2	100	15	**14**	62
2	batch/**9**	2	80	15	**14**	98
3	batch/**9**	2	rt	60	**14**	50
4	batch/**9**	0	100	60	**14**	100
5[b]	batch/**9**	0	100	60	**14**	0
6	batch/**10**	2	110	60	**15**	100
7[c]	CSTR/**9**	0	100	30 60 75	**14**	12 73 76
8[c]	CSTR/**10**	0	100	30 60 120	**15**	67 77 77

[a]Conversion measured by ^{1}H NMR spectroscopy. [b]Reaction carried out in either air or presence of TEMPO (1 equiv) led to the same result. [c]1-Stage CSTR, co-feed with styrene in toluene and substrate in toluene/diglyme 3:1.

stream of toluene containing styrene (**13**) enabled the continuous production of alkylated amine products **14** and **15** (Table 2, entries 7 and 8, respectively). In each case the t_{res} was comparable with batch (reaction of **11** = 75 minutes, **12** = 60 minutes), with steady-state conversions or 76 and 77% observed, respectively.

Reaction of *N*-chloramine with aldehyde

Reaction of *N*-chloramines with aromatic and aliphatic aldehydes to form amides has been reported by Porcheddu [34]. Under these literature conditions, $FeCl_3$ catalyst (0.15 mol %), *t*-BuO_2H oxidant (3.6 equiv) and excess aldehyde **17** (5 equiv) were employed to react with dilute *N*-chloramine **16** (0.064 M in MeCN), delivering amide **18** in 77% conversion and 54% isolated yield. Our interests were to improve the productivity of this system, by exploiting higher concentrations of *N*-chloramine produced in flow mode (200 mM). Table 3 summarizes a comparative study between batch and continuous flow for this reaction.

Initial tests involving 200 mM substrate concentration afforded amide **18** in 60% conversion (Table 3, entry 2). Increasing the catalyst loading to 15 mol % led to a quantitative conversion of **18** within 1 hour reaction time. Unexpectedly, a control reaction omitting the $FeCl_3$ catalyst resulted in 90% conversion following a two-hour reaction time (Table 3, entry 4). Removing the *t*-BuO_2H oxidant reduced the reaction rate significantly, leading to 10% conversion under otherwise identical conditions (Table 3, entry 5), whilst fewer equivalents of aldehyde **17** led to 30% product formation (Table 3, entry 6). Notably, other oxidants such as H_2O_2 and NaOCl failed to produce any amide product. Likewise, attempts to couple morpholine in place of its *N*-chloro derivative reached only 19% conversion.

Following the investigation of the batch reaction, it was transferred to a CSTR. Feeding 200 mM *N*-chloramine to meet a separate solution of aldehyde **17** (5 equiv) and *t*-BuO_2H (5 equiv), a t_{res} of 100 minutes afforded amide **18** in 70% conversion at steady state. Under analogous conditions, $FeCl_3$ (5 mol %) was included in the oxidant stream to give 96% steady-state conversion to **18** (Figure 3). This data represents productivities of 19 and 26 g L^{-1} h^{-1} for the uncatalysed and $FeCl_3$-catalyzed amide formation, respectively (Supporting Information File 1, S4).

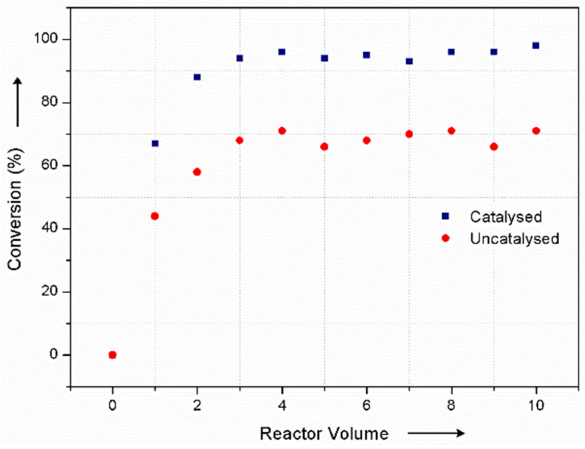

Figure 3: Continuous-flow amide **18** formation using 1-stage CSTR. Blue squares: $FeCl_3$ included; red circles: $FeCl_3$ not included.

Table 3: Batch vs flow study of reaction of *N*-chloramine with an aldehyde.

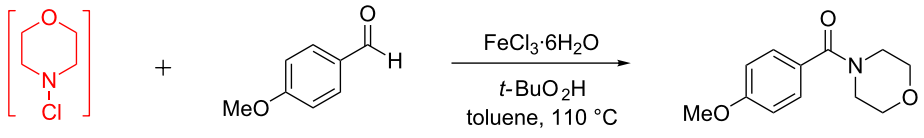

16, 200 mM **17** **18**

entry	mode	$FeCl_3$ (mol %)	equiv **17**/*t*-BuO_2H	time (min)	conversion/yield (%)[a]
1[b]	batch	0.15	5/3.6	300	77/54
2[c]	batch	0.15	5/3.6	300	60
3	batch	15	5/3.6	60	100
4	batch	0	5/3.6	120	90
5	batch	15	5/0	120	10
6	batch	0	1/3.6	120	30
7	CSTR	0	5/5	100	70[d]
8	CSTR	5	5/5	100	96[d]

[a]Conversion measured by gas chromatography as the average of three runs. [b]Literature conditions quoted as 88% [34]. [c][**16**] = 200 mM. [d]Conversion recorded at steady state.

Reaction of *N*-chloramine with base

The base-induced dehydrochlorination of *N*-chloramines is a facile route to imines, which may be used for further functionalization. Our study began by examining a host of bases to convert *N*-chloramine **5** to benzylidene(methyl)amine (**19**) as a model reaction system (Table 4).

To achieve a complete conversion, NEt_3 was required in large excess (5 equiv) over 42 hours, which proved unsuitable for continuous flow (Table 4, entry 1). Whilst KO*t*-Bu and NaOMe bases allowed rapid imine formation (Table 4, entries 2–6), though their low solubility in MeOH or toluene would require slurry pumping in flow mode which is undesirable. In addition, the isolation procedure is not straightforward, requiring multiple unit operations. To avoid this, a phase-transfer catalyst (TBAB) was used along with NaOH (Table 4, entries 7–9). This reagent, in a toluene/water mixture, promoted full conversion to imine **19** (Table 4, entry 8). The separation of the toluene phase provided the imine product, which may be deployed directly in further reactions.

To validate the batch protocol *N*-chloramines **5** and **7** underwent smooth dehydrochlorination to produce imines **19** and **20** in 83 and 100% conversion after 1 hour (Table 5, entries 1 and 2). The cyclic *N*-chloramine **8** was converted in batch mode to the corresponding imine **21**, though required 18 hours to reach 84% conversion (Table 5, entry 3). The rapid nature of the imine formation prompted us to investigate a fully continuous protocol to both *N*-chlorinate and subsequently dehydrochlorinate amines, which would represent a mild and atom-efficient alternative method of amine oxidation. A 5-stage cascade CSTR was employed to link *N*-chloramine generation with base-promoted imine formation. A 1 M stream of *N*-chloramine **5** in toluene was mixed in the first CSTR with separate flows of aqueous NaOH and TBAB (10 mol % relative to substrate) and t_{res} was adjusted by changing the number of subsequent CSTR chambers (n) (Table 5, entry 1). It is noteworthy that attempts to mix NaOH and TBAB solutions via a T-piece prior to the mixing chamber were not successful, as a precipitate forms from the mixture leading to reactor blockage. A quantitative conversion of **5** to imine **19** was realized using the NaOH/TBAB protocol with a t_{res} of 2 hours with good productivity (0.25 mol L^{-1} h^{-1}, Table 5, entry 1). Under analogous conditions, *N*-chloramine **7** was converted to imine **20** in 88% conversion, which could be improved to 99% conversion by extending t_{res} to 3 hours (Table 5, entry 2). However, the same conditions proved only able to convert 19% of the *N*-chloramine **8** at steady state with t_{res} of 2 h (Table 5, entry 3). To achieve a higher conversion an impractical t_{res} would be required if the same batch conditions were used. In this regard, the use of heated CSTRs would be useful to explore.

The formation of both imines **20** and **21** are of interest as an asymmetric reduction would give an optically pure amine. To demonstrate this, imine **20**, formed in situ, underwent asymmetric-transfer hydrogenation in both batch and flow modes, using $[IrCp^*Cl_2]_2$ as catalyst with the ligand (*R,R*)-TsDPEN, using the hydrogen-donor reagent formic acid/triethylamine (Scheme 1).

Table 4: Batch optimization study of the dehydrochlorination of *N*-chloramines.

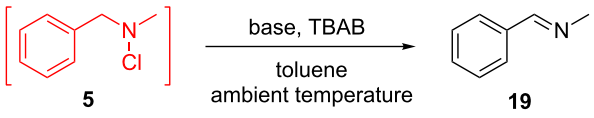

5 **19**

entry	base	catalyst	solvent	time (h)	conversion (%)[a]
1	NEt_3 (5 equiv)	none	toluene	42	92
2	KO*t*-Bu (5 equiv)	none	MeOH	15	90
3	NaOMe (2 equiv)	none	toluene/MeOH 1:1	2	100
4	NaOMe (10 equiv)	none	toluene/MeOH 1:1	1	100
5	NaOMe (1 equiv)	none	toluene/MeOH 1:1	1	47
6	NaOMe (5 equiv)	none	toluene	1	100
7	NaOH 25% aq	TBAB[b]	toluene/water 1:1	1	83
8	NaOH 25% aq	TBAB[b]	toluene/water 1:1	3	100
9	NaOH 40% aq	TBAB[b]	toluene/water 1:1	1	50
10	NaOH 25% aq	none	toluene/MeOH (1%)	19	0
11	NaOH 25% aq	none	toluene/MeOH (20%)	19	0

[a]Measured by ^{1}H NMR spectroscopy. [b]Reaction temperature = 60 °C.

Table 5: Batch vs flow study of the dehydrochlorination step.

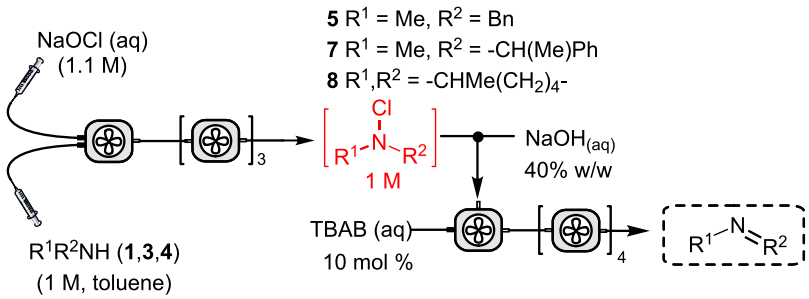

1 R^1 = Me, R^2 = Bn
3 R^1 = Me, R^2 = -CH(Me)Ph
4 R^1,R^2 = -CH(Me)$(CH_2)_4$-

19 R^1 = Me, R^2 = CH-Ph
20 R^1 = Me, R^2 = C(Me)Ph
21 R^1,R^2 = C(Me)$(CH_2)_4$-

entry	product	mode	t_{res} (h)	conversion (%)[a]
1	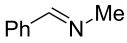 **19**	batch flow	1 2	83 100
2	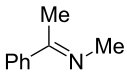 **20**	batch flow flow	1 2 3	100 88 99
3	 **21**	batch flow	18 2	84 19

[a]Measured by ^{1}H NMR spectroscopy.

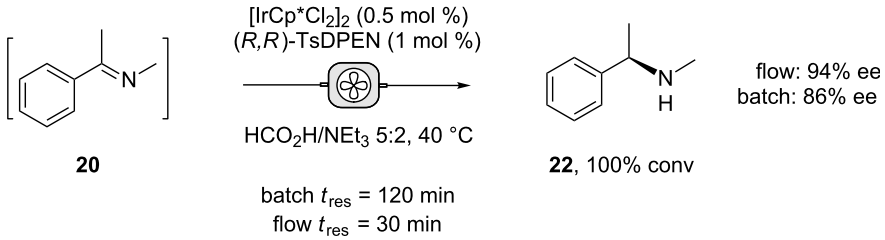

20

22, 100% conv

Scheme 1: Continuous-flow transfer hydrogenation of in situ generated imines.

Under batch conditions, a t_{res} of 120 minutes gave quantitative reduction of the imine, affording the *R*-isomer in 86% ee. Translating the procedure to continuous flow, a fresh solution of imine **20** and catalyst mixture were pumped into a heated CSTR over a 30-minutes t_{res}, affording chiral amine **22** in 94% ee with complete conversion. It is unclear why a higher optical activity was seen using continuous flow. However, it is known that $[IrCp^*Cl_2]_2$ can slowly racemise this amine which may be more of a problem in batch with the longer reaction time [48].

Conclusion

A continuous-flow approach to prepare and handle unstable *N*-chloramines is reported. The method exploits the superior mixing of a CSTR compared with classical batch, to enable fast *N*-chlorination of amines under biphasic conditions. By virtue of a flowing solution, the in situ generated chloramines may be transferred directly into new reaction media, with examples of (i) addition to an alkene to form a new C–N and C–Cl bond, (ii) reaction with aldehyde to produce amides, and (iii) dehy-

drochlorination with a base to afford imines reported within our study. Of these examples, the latter was further explored by immediate asymmetric-transfer hydrogenation of an in situ formed imine under continuous-flow conditions, as a potentially productive route to chiral amines.

Supporting Information

Supporting Information File 1

Details of reactor assembly, NaOCl titration and NMR spectra.
[https://www.beilstein-journals.org/bjoc/content/supplementary/1860-5397-14-196-S1.pdf]

Acknowledgements

The research for this work has received funding from the Innovative Medicines Initiative joint undertaking project Chem21 under *grant agreement* n°115360, resources of which are composed of financial contribution from the European Union's Seventh Framework Programme (FP7/2007-2013) and EFPIA companies in kind contribution.

ORCID® iDs

Katherine E. Jolley - https://orcid.org/0000-0001-6223-9808
A. John Blacker - https://orcid.org/0000-0003-4898-2712

References

1. Urben, P. In *Bretherick's Handbook of Reactive Chemical Hazards,* 7th ed.; Bretherick, L., Ed.; Academic Press: Oxford, 2007; pp 15–20.
2. Antelo, J. M.; Arce, F.; Parajo, M. *J. Phys. Org. Chem.* **1996,** *9,* 447–454. doi:10.1002/(SICI)1099-1395(199607)9:7<447::AID-POC778>3.0.CO;2-X
3. Wiles, C.; Watts, P. *Eur. J. Org. Chem.* **2008,** 1655–1671. doi:10.1002/ejoc.200701041
4. Zhang, Y.; Born, S. C.; Jensen, K. F. *Org. Process Res. Dev.* **2014,** *18,* 1476–1481. doi:10.1021/op500158h
5. Wiles, C.; Watts, P. *Green Chem.* **2012,** *14,* 38–54. doi:10.1039/C1GC16022B
6. Nagy, K. D.; Shen, B.; Jamison, T. F.; Jensen, K. F. *Org. Process Res. Dev.* **2012,** *16,* 976–981. doi:10.1021/op200349f
7. Mo, Y.; Jensen, K. F. *React. Chem. Eng.* **2016,** *1,* 501–507. doi:10.1039/C6RE00132G
8. Chapman, M. R.; Kwan, M. H. T.; King, G.; Jolley, K. E.; Hussain, M.; Hussain, S.; Salama, I. E.; González Niño, C.; Thompson, L. A.; Bayana, M. E.; Clayton, A. D.; Nguyen, B. N.; Turner, N. J.; Kapur, N.; Blacker, A. J. *Org. Process Res. Dev.* **2017,** *21,* 1294–1301. doi:10.1021/acs.oprd.7b00173
9. Pastre, J. C.; Browne, D. L.; Ley, S. V. *Chem. Soc. Rev.* **2013,** *42,* 8849–8869. doi:10.1039/c3cs60246j
10. Ley, S. V. *Chem. Rec.* **2012,** *12,* 378–390. doi:10.1002/tcr.201100041
11. Wegner, J. C.; Ceylan, S.; Kirschning, A. *Adv. Synth. Catal.* **2012,** *354,* 17–57. doi:10.1002/adsc.201100584
12. Worley, S. D.; Wojtowicz, J. A. *Kirk-Othmer Encyclopedia of Chemical Technology;* John Wiley & Sons Inc., 2000.
13. Rothgery, E. F. *Kirk-Othmer Encyclopedia of Chemical Technology;* John Wiley & Sons Inc., 2000.
14. Kovacic, P.; Lowery, M. K.; Field, K. W. *Chem. Rev.* **1970,** *70,* 639–665. doi:10.1021/cr60268a002
15. Wille, U. In *Science of Synthesis;* Enders, D.; Schaumann, E., Eds.; Thieme: Stuttgart, 2009; Vol. 40b, pp 846–847.
16. Seppelt, K.; Sundermeyer, W. *Z. Naturforsch., B: Anorg. Chem., Org. Chem., Biochem., Biophys., Bio l.* **1969,** *24,* 774–775. doi:10.1515/znb-1969-0622
17. Lyalin, B. V.; Petrosyan, V. A. *Russ. J. Electrochem.* **2000,** *36,* 164–169. doi:10.1007/bf02756901
18. Heuger, G.; Kalsow, S.; Göttlich, R. *Eur. J. Org. Chem.* **2002,** 1848–1854. doi:10.1002/1099-0690(200206)2002:11<1848::AID-EJOC1848>3.0.CO;2-V
19. Grandl, J.; Sakr, E.; Kotzyba-Hibert, F.; Krieger, F.; Bertrand, S.; Bertrand, D.; Vogel, H.; Goeldner, M.; Hovius, R. *Angew. Chem., Int. Ed.* **2007,** *46,* 3505–3508. doi:10.1002/anie.200604807
20. Kostyanovsky, R. G.; Gella, I. M.; Markov, V. I.; Samojlova, Z. E. *Tetrahedron* **1974,** *30,* 39–45. doi:10.1016/S0040-4020(01)97214-X
21. Campbell, M. M.; Johnson, G. *Chem. Rev.* **1978,** *78,* 65–79. doi:10.1021/cr60311a005
22. Lindsay-Smith, J. R.; McKeer, L. C.; Taylor, J. M. *Org. Synth.* **1989,** *67,* 222–228. doi:10.15227/orgsyn.067.0222
23. Larionov, O. V.; Kozhushkov, S. I.; de Meijere, A. *Synthesis* **2003,** 1916–1919. doi:10.1055/s-2003-41037
24. Zhong, Y.-L.; Zhou, H.; Gauthier, D. R.; Lee, J.; Askin, D.; Dolling, U. H.; Volante, R. P. *Tetrahedron Lett.* **2005,** *46,* 1099–1101. doi:10.1016/j.tetlet.2004.12.088
25. Vanoye, L.; Yehouenou, L.; Philippe, R.; de Bellefon, C.; Fongarland, P.; Favre-Réguillon, A. *React. Chem. Eng.* **2018,** *3,* 188–194. doi:10.1039/C7RE00155J
26. Blacker, A. J.; Jolley, K. E. *Beilstein J. Org. Chem.* **2015,** *11,* 2408–2417. doi:10.3762/bjoc.11.262
27. Thakur, V. V.; Talluri, S. K.; Sudalai, A. *Org. Lett.* **2003,** *5,* 861–864. doi:10.1021/ol027530f
28. Sharpless, K. B.; Chong, A. O.; Oshima, K. *J. Org. Chem.* **1976,** *41,* 177–179. doi:10.1021/jo00863a052
29. Ando, T.; Kano, D.; Minakata, S.; Ryu, I.; Komatsu, M. *Tetrahedron* **1998,** *54,* 13485–13494. doi:10.1016/S0040-4020(98)00827-8
30. Chemler, S. R.; Bovino, M. T. *ACS Catal.* **2013,** *3,* 1076–1091. doi:10.1021/cs400138b
31. Göttlich, R. *Synthesis* **2000,** 1561–1564. doi:10.1055/s-2000-7605
32. Noack, M.; Göttlich, R. *Eur. J. Org. Chem.* **2002,** 3171–3178. doi:10.1002/1099-0690(200209)2002:18<3171::AID-EJOC3171>3.0.CO;2-L
33. Cadoni, R.; Porcheddu, A.; Giacomelli, G.; de Luca, L. *Org. Lett.* **2012,** *14,* 5014–5017. doi:10.1021/ol302175v
34. Porcheddu, A.; De Luca, L. *Adv. Synth. Catal.* **2012,** *354,* 2949–2953. doi:10.1002/adsc.201200659
35. Grogan, G.; Turner, N. J. *Chem. – Eur. J.* **2016,** *22,* 1900–1907. doi:10.1002/chem.201503954
36. Hussain, S.; Leipold, F.; Man, H.; Wells, E.; France, S. P.; Mullholland, K. R.; Grogan, G.; Turner, N. J. *ChemCatChem* **2015,** *7,* 579–583. doi:10.1002/cctc.201402797

37. Wakchaure, V. N.; Kaib, P. S. J.; Leutzsch, M.; List, B. *Angew. Chem., Int. Ed.* **2015,** *54,* 11852–11856. doi:10.1002/anie.201504052
38. Spindler, F.; Blaser, H.-U. In *The Handbook of Homogenous Hydrogenation;* de Vries, J. G.; Elsevier, J., Eds.; Wiley-VCH, 2008; pp 1193–1214.
39. Blacker, A. J. In *The Handbook of Homogenous Hydrogenation;* de Vries, J. G.; Elsevier, C. J., Eds.; Wiley-VCH, 2008; pp 1215–1244.
40. Wills, M. In *Topics in Current Chemistry;* Guinella, G., Ed.; Springer International Publishing: Switzerland, 2016; Vol. 14, pp 1–36.
41. Bartsch, R. A.; Cho, B. R. *J. Am. Chem. Soc.* **1979,** *101,* 3587–3591. doi:10.1021/ja00507a025
42. Cho, B. R.; Namgoong, S. K.; Bartsch, R. A. *J. Org. Chem.* **1986,** *51,* 1320–1324. doi:10.1021/jo00358a030
43. Cho, B. R.; Namgoong, S. K.; Kim, T. R. *J. Chem. Soc., Perkin Trans. 2* **1987,** 853–856. doi:10.1039/P29870000853
44. Zhu, R.; Xu, Z.; Ding, W.; Liu, S.; Shi, X.; Lu, X. *Chin. J. Chem.* **2014,** *32,* 1039–1048. doi:10.1002/cjoc.201400471
45. Liu, L.-W.; Wang, F.-Y.; Tian, F.; Peng, L.; Wang, L.-X. *Org. Process Res. Dev.* **2016,** *20,* 320–324. doi:10.1021/acs.oprd.5b00345
46. Scott, J. D.; Willams, R. M. *Chem. Rev.* **2002,** *102,* 1669–1730. doi:10.1021/cr010212u
47. Zhang, Y.; Feng, J.; Jia, Y.; Wang, X.; Zhang, L.; Liu, C.; Fang, H.; Xu, W. *J. Med. Chem.* **2011,** *54,* 2823–2838. doi:10.1021/jm101605z
48. Blacker, A. J.; Stirling, M. J.; Page, M. I. *Org. Process Res. Dev.* **2007,** *11,* 642–648. doi:10.1021/op060233w

License and Terms